DOCTORAL THESIS

Application of Chemical Additives in Minerals Beneficiation

Implications on Grinding and Flotation Performance

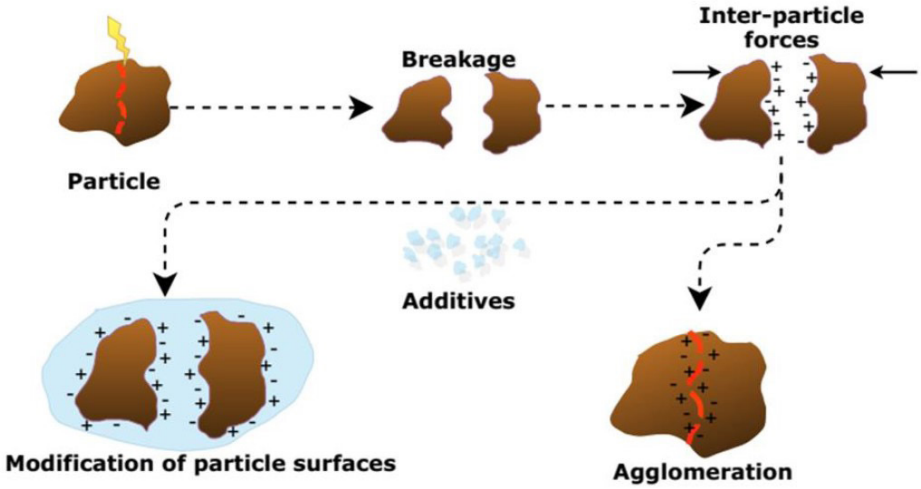

Vitalis Chipakwe

Mineral Processing

LULEÅ UNIVERSITY OF TECHNOLOGY

LULEÅ UNIVERSITY OF TECHNOLOGY

Application of Chemical Additives in Minerals Beneficiation

Implications on Grinding and Flotation Performance

Vitalis Chipakwe

Division of Minerals and Metallurgical Engineering

Department of Civil, Environmental and Natural Resources Engineering

Luleå University of Technology

SE-971 87, Luleå

Sweden

February 2023

Cover photo: Schematic illustration of the effect of grinding additives on particle surfaces (Chipakwe, 2021).

ABSTRACT

The application of chemical additives, known as grinding aids (GAs), dates to 1930 in the cement industry. Unlike the cement industry, where the use of GAs is in the final processing step, it could be one of the first processing steps in ore beneficiation. Further to grinding performance, the successful application of GAs requires understanding the effect on ground products and possible interaction of the GAs in view of downstream processes. Understanding and controlling any GA-separation reagent interactions is critical to ensure that the required downstream process efficiency and integrity of the entire value chain are maintained. In this thesis, the effect of selected chemical additives on dry grinding performance and product properties is investigated. Second, the effect of the additives on surface properties and pulp chemistry, together with the resulting behavior in subsequent froth flotation separation, is investigated.

The use of environmentally benign and sustainable alternatives to conventional surfactants is growing within mineral processing. To this end, a polysaccharide-based grinding aid (PGA) (natural polymer) together with a polyacrylic acid-based grinding aid (AAG) (synthetic polymer) were used as grinding aids. The effect of PGA and AAG at varying concentrations was investigated with respect to energy consumption, particle size distribution, BET surface area, roughness, and rheology. The resulting grinding parameters were correlated with the measured rheology indices from the automated FT4 powder rheometer. Moreover, the effect of the GAs on the flotation of quartz from magnetite was investigated using an artificial mixture ore. Zeta potentials, stability measurement, adsorption test, and FTIR analyzes were performed to understand the mechanisms of surface interaction and adsorption.

The grinding results indicated that the application of GAs reduced energy consumption by up to 31.1 % and gave a finer-uniform product size, higher specific surface area, and increased surface roughness compared to grinding without. Further studies on powder rheology indicated that the GAs used resulted in improved material flowability compared to grinding without additives. There was a strong correlation ($r > 0.93$) between the grinding and the flow parameters. Flotation tests on pure samples illustrated that PGA has beneficial effects on magnetite depression (with negligible impact on quartz floatability) through reverse flotation separation. The benefits were further confirmed by the flotation of the artificial mixture in the presence of PGA. The PGA adsorption mechanism was mainly through physical interaction based on UV-Vis spectra, zeta potential tests, Fourier transform infrared spectroscopy (FT-IR), and stability analyses. Additionally, single mineral flotation tests indicated that AAG enhanced quartz collection with minimal effect on magnetite. Mixed mineral flotation revealed that, by using AAG, comparable metallurgical performance

could be achieved at a lower collector dosage. The zeta potentials and stability measurements showed that AAG shifts the potential, thus improving the stability and dispersion of the suspension. Adsorption tests revealed that AAG adsorbed on both quartz and magnetite, with the former having a higher capacity. Fourier transform infrared spectroscopy showed that the interaction between AAG and the minerals occurs via a physical interaction.

The findings illustrate that GAs improved grinding efficacy at optimum dosage and enhanced product properties. Furthermore, the predominant mechanism of GAs is based on the alteration of rheological properties. Importantly, the feasibility of using GAs to improve grinding performance has been demonstrated with secondary beneficial effects on flotation.

Keywords: Energy; Grinding aid; Flowability; Dry grinding; FT4 Powder Rheometer; Surface properties; Rheology; Flotation; Polymers; Surface chemistry; Green Chemistry.

"Two things we have total control of in our lives are our ATTITUDE and our EFFORT"

ACKNOWLEDGEMENTS

First, I would like to give honor and thanks to the almighty God for his overarching grace.

I would like to express my sincere gratitude to my supervisor, Associate Professor Saeed Chehreh Chelgani, for giving me this wonderful opportunity to pursue my studies and for his encouragement and guidance.

I would also like to appreciate my co-supervisors, Professor Jan Rosenkranz and Dr. Tommy Karlkvist, for their encouragement, guidance, and invaluable discussion and comments on my work.

My sincere acknowledgment also goes to Dr. Chris Hulme-Smith from KTH University for the fruitful collaboration and discussion on powder rheometry studies. Sincere gratitude to Dr. Andras Gorzsas from Umeå University for assistance with FTIR analysis and Vimbainashe Dzimbanhete for assistance with SEM analysis and their fruitful discussions. I am also indebted to Nick Irons from Solenis for the support and discussions on grinding aid formulations.

I wish to convey my many thanks to my friends and colleagues in the mineral processing group and a special mention to Malin Johansson, Dr. Bertil Pålsson, Associate Professor Mehdi Parian, and Dr. Parisa Semsari for their patience and help in laboratory setups. I wish to thank my colleagues at Process Technology, Boliden Mines for their support and encouragement.

I would also like to express my gratitude for the financial support from the KolArctic CBC programme (SEESIMA) and the Center of Advanced Mining and Metallurgy (CAMM^2) that ensured the success of this research work. The work was also supported financially by Ellen, Walter och Lennart Hesselmans stiftelse.

I am deeply indebted to my family for their selfless love, support, and belief in all my endeavors.

Last and certainly not least, I would like to thank my wife, Rumbidzaishe, for her continuous love, patience, and unconditional support and encouragement.

Luleå, February 2023

Vitalis Chipakwe

PUBLICATIONS

This thesis is based on the following papers

I. **V. Chipakwe,** P. Semsari, T. Karlkvist, J. Rosenkranz, S. Chehreh Chelgani. A critical review on the mechanisms of chemical additives used in grinding and their effects on the downstream processes. *Journal of Materials Research and Technology*, 9:4, 2020, pp 8148-8162. https://doi.org/10.1016/j.jmrt.2020.05.080.

II. **V. Chipakwe,** P. Semsari, T. Karlkvist, J. Rosenkranz, S Chehreh Chelgani. A comparative study on the effect of chemical additives on dry grinding of magnetite ore. *South African Journal of Chemical Engineering*, 34, 2020, pp 135-141. https://doi.org/10.1016/j.sajce.2020.07.011.

III. **V. Chipakwe,** C. Hulme-Smith, T. Karlkvist, J. Rosenkranz, S Chehreh Chelgani. Effects of chemical additives on rheological properties of dry ground ore - a comparative study. *Mineral Processing And Extractive Metallurgy Review*, 43:3, 2021 pp 380-389. https://doi.org/10.1080/08827508.2021.1890591

IV. **V. Chipakwe,** T. Karlkvist, J. Rosenkranz and S. Chehreh Chelgani. Beneficial effects of a polysaccharide-based grinding aid on magnetite flotation: a green approach. *Scientific reports*, *12*:6502, 2022, pp XXX. https://doi.org/10.1038/s41598-022-10304-x

V. **V. Chipakwe**, T. Karlkvist, J. Rosenkranz and S. Chehreh Chelgani. Exploring the effect of a polyacrylic acid-based grinding aid on magnetite-quartz flotation separation. *Separation and Purification Technology, 305:*122530, 2022, pp XXX https://doi.org/10.1016/j.seppur.2022.122530

Author's Contribution

Paper I: *A critical review on the mechanisms of chemical additives used in grinding and their effects on the downstream processes.*

VC & SCC composed the initial conceptualization and scope of investigations. VC, PS & SCC were responsible for the literature survey. VC, PS & SCC performed the formal literature analysis and wrote the original manuscript draft. TK & JR provided supervision and reviewed and edited the manuscript. SCC & JR provided supervision and resources.

Paper II: *A comparative study on the effect of chemical additives on dry grinding of magnetite ore.*

VC & SCC composed the initial conceptualization and theoretical investigations. VC & SCC formulated the experimental design. VC & PS were responsible for conducting the experimental work and formal measurement data analysis. VC & SCC performed formal data analysis and data curation and wrote the original draft of the manuscript. TK & JR provided supervision and reviewed and edited the manuscript. SCC & JR provided supervision and resources.

Paper III: *Effects of chemical additives on rheological properties of dry ground ore - a comparative study*

VC & SCC composed the initial conceptualization and theoretical investigations. VC, CHS & SCC formulated the experimental design. VC & CHS were responsible for conducting the experimental work and formal analysis of the measurement data. VC & SCC performed the formal analysis of data and data curation and wrote the original draft of the manuscript. TK, CHS & JR reviewed and edited the manuscript. SCC & JR provided supervision and resources.

Paper IV: *Beneficial effects of a polysaccharide-based grinding aid on magnetite flotation: a green approach*

VC & SCC composed the initial conceptualization and theoretical investigations. VC & SCC formulated the experimental design. VC was responsible for conducting the experimental work and formal analysis of the measurement data. VC & SCC performed the formal analysis of data and data curation and wrote the original draft of the manuscript. TK & JR provided supervision and reviewed and edited the manuscript. SCC & JR provided supervision and resources.

Paper V: *Exploring the effect of a polyacrylic acid-based grinding aid on magnetite-quartz flotation separation*

VC & SCC composed the initial conceptualization and theoretical investigations. VC & SCC formulated the experimental design. VC was responsible for conducting the experimental work and formal analysis of the measurement data. VC & SCC

performed the formal analysis of data and data curation and wrote the original draft of the manuscript. TK & JR provided supervision and reviewed and edited the manuscript. SCC & JR provided supervision and resources.

Other publications not included in this thesis

I. **V. Chipakwe,** R. Jolsterå, and S. Chehreh Chelgani, Nanobubble-Assisted Flotation of Apatite Tailings: Insights on Beneficiation Options. *ACS Omega*. 2021. https://doi.org/10.1021/acsomega.1c01551

II. **V. Chipakwe,** A. Sand, and S. Chehreh Chelgani. Nanobubble assisted flotation separation of complex Pb–Cu–Zn sulfide ore–assessment of process readiness. *Separation Science and Technology*, 57(8), pp.1351-1358. 2022. https://doi.org/10.1080/01496395.2021.1981942

III. Ann Bazar, J., Rahimi, M., Fathinia, S., Jafari, M., **Chipakwe, V**. and Chehreh Chelgani, S. Talc Flotation—An Overview. *Minerals*, 11(7), p.662, 2021. https://doi.org/10.3390/min11070662

IV. Saeed, M., De Souza, C.V., **Chipakwe, V.** and Chehreh Chelgani, S. Influence of hydrodynamic variables on scaling up of mechanical flotation cells. *Arabian Journal of Geosciences* 15, 1606 (2022). https://doi.org/10.1007/s12517-022-10908-7

Conference papers

I. **V. Chipakwe*,** T. Karlkvist, J. Rosenkranz, S. Chehreh Chelgani. Study on effects of additives on dry grinding performance of magnetite. *In proceedings of Conference in Minerals Engineering 2020*, Luleå, Sweden, 4-5 February 2020

II. **V. Chipakwe*,** T. Karlkvist, J. Rosenkranz, S Chehreh Chelgani. On rationalization of energy consumption in dry grinding process: Role of grinding aids. *In proceedings of International Plaksin Readings,* Online, 21-25 September 2020.

III. **V. Chipakwe*,** S. Chehreh Chelgani. Assessment of Nanobubble Assisted Flotation Readiness. *In proceedings of Conference in Minerals Engineering 2022*, Luleå, Sweden, 8-9 February 2022

CONTENTS

NOTATION

GA	Grinding aid	
PGA	Polysaccharide-based grinding aid	
AAG	Polyacrylic acid-based grinding aid	
SSA	Specific surface area	$[m^2/g]$
BFE	Basic flow energy	[mJ]
SI	Stability index	[-]
SE	Specific energy	[mJ/g]
AE	Aerated energy	[mJ]
ABFE	Aerated basic flow energy	[mJ]
FRI	Flow rate index	[-]
TE	Total energy	[mJ]
BET	Brunauer–Emmett–Teller	
W_i	Work index of material used in Bond's law	[kWh/t]
E_C	Energy consumption	
F_{80}	Particle size, which 80% of the mill feed, in µm	
P_{80}	Particle size, which 80% of the mill product, in µm	
D_{50}	Particle size which d0% of the mill product, in µm	
A_B	BET surface area measurement,	$[m^2/g]$

ρ	Bulk density of solid	$[g/cm^3]$
D	Average particle diameter	[μm]
R_s	Surface roughness described in Jaycock & Parfitt's equation	[-]
FTIR	Fourier transform infrared	
ICP-OES	Inductively coupled plasma optical emission spectrometry	
SEM	Scanning electron microscope	
XRD	X-ray diffraction	
CRMs	Critical raw materials	
TSI	Turbiscan stability index	[-]

PART I – SUMMARY

1. INTRODUCTION

This chapter presents the context of the thesis work and the importance of mineral processing in the green transition that is highly dependent on raw materials. This chapter briefly describes the current challenges in sourcing raw materials coupled with the ever-declining ore grades. To deal with some of these challenges, the use of chemical additives (grinding aids) is introduced. The chapter concludes with the aim and objectives of this research.

1.1. Background

The world is seized by the urgent need to decarbonize society and the economy by reducing and ultimately eliminating the use of fossils evident to global climate change. Among many set targets, the reduction of global greenhouse gas emissions by replacing fossil-based energy sources with greener and renewable ones such as solar, wind and water is key (Beylot et al., 2019; Chazel et al., 2020; Pommeret et al., 2022; Valero et al., 2018). However, this green transition requires material and metals, which require more mining to source these much needed raw materials (Chazel et al., 2020; Valero et al., 2018). In other words, the mining industry is now faced with the challenge of securing these materials. Despite the increased demand for critical raw materials, ore grades have declined over time, and maintaining or increasing metal production means more volumes must be processed. According to Mudd (2009), this will also translate into more energy and water use per metal produced from these lean ores, Figure 1. In addition to lean ores and high demand, environmental guidelines are becoming stricter and stricter for better use of resources. All this presents a greater challenge to the primary resource production and even recycling industries, threatening the supply of critical raw materials (CRMs).

Within the mining value chain for the production of CRMs, grinding is central in mineral processing to achieve particle size reduction and mineral liberation, which is highly energy intensive. It accounts for 50% of the power consumption in a concentrator plant (Singh et al., 2018; Somani et al., 2017). Grinding generally has poor energy efficiency and accounts for about 2-3% of the world's generated electricity (Napier-Munn, 2015). As a result of the depleting resources, the processing of more complex and finely disseminated ores is becoming common. Such processes require fine grinding or ultrafine grinding to liberate the valuable minerals from the gangue material; thus increasing energy requirements (Chipakwe et al., 2020a; Singh et al., 2018). Within mineral processing, wet grinding is preferred to dry grinding due to the ease of material handling and higher energy efficiency (Chelgani et al., 2019; Feng and Aldrich, 2000). However, water scarcity is a major threat to mining activities, especially in arid regions such as South Africa, Australia, Chile, and China. In these regions, high levels of water consumption have pronounced negative environmental impacts (Franks et al., 2015; Gunson et al., 2012; Kökkiliç et al., 2015; Nguyen et al., 2014; Rivas-Perez et al., 2017). In addition to arid areas, countries such as Sweden have established guidelines that highlight the need to conserve and recycle water in mining operations for better resource utilization and environmental benefits (Ranängen and Lindman, 2017; SIP STRIM, 2019). These two aspects (energy and water usage) continue to be

pertinent within the mineral beneficiation industry and are key to achieving sustainability targets (Gunson et al., 2012; Jeswiet and Szekeres, 2016).

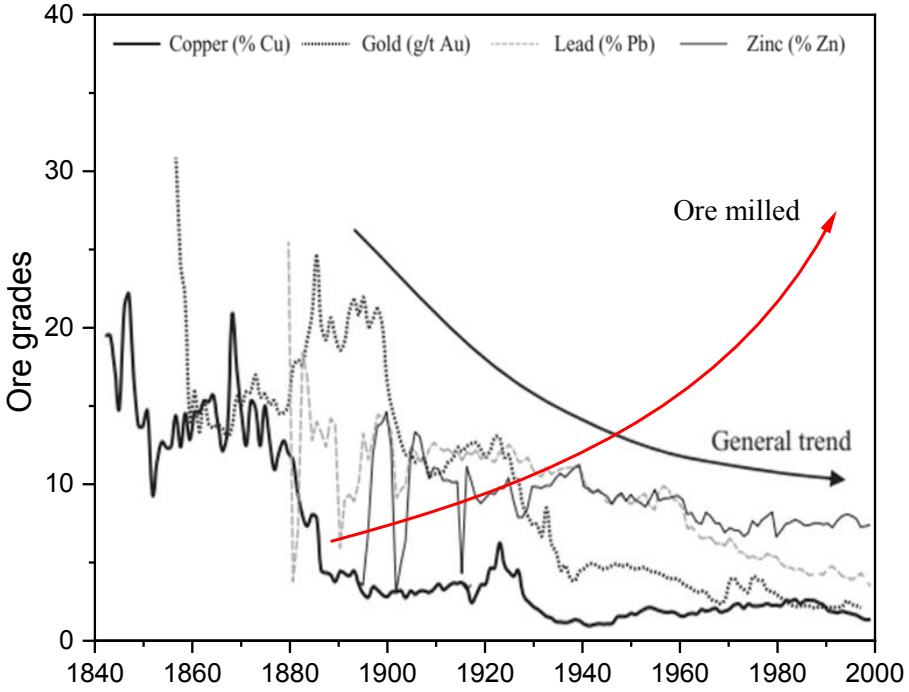

Figure 1. Average ore grades for commodities and an anticipated corresponding increase in milled tonnages. Modified after (Mudd, 2009) **Mudd, (2009).**

Current efforts to address the high energy consumption and poor energy efficiency associated with grinding in the minerals industry can be divided into three strategies (Napier-Munn, 2015; Przwara et al., 2018a): (i) development of alternative equipment, (ii) development of alternative flowsheet configuration, (iii) alteration of material properties of ores. Considerable investments have been made in the development of alternative equipment. The use of stirred media mills and high pressure grinding rolls (HPGR) improves grinding efficiencies compared to conventional tumbling mills, ball mills and rod mills (Morrell, 2009; Przwara et al., 2018c; Xiao et al., 2012). The development of new approaches to mineral processing, such as the geometallurgical approach, which provides a holistic and integrated mine to mill view, has made strides in addressing these challenges (Napier-Munn, 2015). Investigations have shown the potential to improve grinding efficiencies by exploiting the material properties of the ore, such as thermal, electrical, magnetic, microwave and bulk and surface properties (Adewuyi et al., 2020; Singh et al., 2018; Somani et al., 2017). The authors summarize the application of various pretreatment processes that exploit these material properties, such as microwave treatment, shock wave treatment, ultrasonic treatment, electrical disintegration, thermal treatment, and chemical additive treatment. However, little has been discussed about the industrial application of chemical additives for mineral processing despite the empirical evidence presented in the

cement industry (El-Shall and Somasundaran, 1984a; Hao et al., 2017; Weibel and Mishra, 2014a).

Grinding aid (GA) refers to any substance added to the mill (amount should not exceed 0.25 wt.% of the material), which increases grinding efficiency and energy consumption reduction during grinding (Fuerstenau, 1995; Klimpel and Manfroy, 1978). Studies have shown that GAs can also improve mill throughput (Csoke et al., 2010; Gokcen et al., 2015; Noaparast and Rafiei, 2003). The reduction in energy consumption is explained by the reduction in agglomeration and improved rheology in the mill (Choi et al., 2009; Prziwara et al., 2018c). It was reported that the narrow particle size distribution of products in the presence of GAs could help minimize energy consumption in downstream processes such as classification (Kotake et al., 2011). However, there has been little discussion on applying GAs in dry mineral processing that addresses some of the shortcomings mentioned above. The application of GAs goes back to 1930 in the cement industry. Despite the evident benefits of GAs in the literature, there is a lack of scientific understanding of the mechanism behind the effect on grinding processes. Surprisingly, the aspect of energy expended to characterize the effects is neglected, which is the basis for their application in the industry. Properties such as zeta potential, surface tension, pH, ionic strength, temperature, and chemical composition to address these gaps. Another approach is required to look at machine characteristics such as mill speed, size, stress loading mechanism, and mill filling. Unlike the cement industry, where chemical additives are used in grinding in the final process step, grinding is one of the first processing steps in ore beneficiation. This further requires a better understanding of the properties of the effects of GA on the grinding product and downstream separation processes.

Despite the lack of understanding of the mechanism of the effect of these GAs, there is a consensus that adsorption of these chemical additives is a prerequisite for their applications (Chipakwe et al., 2020b; Prziwara and Kwade, 2020). It can be postulated that these chemicals will remain on the surface of the particles after milling. Grinding as a step prior to the flotation separation process influences the surface properties of the particles, the solution/pulp chemistry the surface chemistry, and even the crystal structure (Bruckard et al., 2011; Bulejko et al., 2022; Chelgani et al., 2019; Grano, 2009; Tong et al., 2021). Froth flotation remains the most versatile separation technique, yet very complex, using differences in natural or imparted wettability of the mineral surface (Farrokhpay et al., 2020; Mesa and Brito-Parada, 2019; Zhang et al., 2021). In flotation, solution and surface chemistry are important in understanding the physicochemical processes occurring at the solid-water and the air-water interface (Sun et al., 2022; Xie et al., 2021). A better understanding of these aspects will pave the way for the application of GAs as an energy-efficient technology, ultimately reducing environmental impacts.

1.2. Research aims and hypothesis

This research aims to understand how chemical additives used as grinding aids affect the grinding process and how the resulting products affect downstream processes. Consequently, this should provide the knowledge of the formulation, synthesis, and optimization of GAs for the size reduction process. The main hypothesis is that the use of chemical additives as grinding aids addresses some of the challenges associated

with dry grinding without adversely affecting downstream separation processes such as flotation. Various materials and process conditions are also believed to respond differently to grinding aid types and dosages, indicating that each application needs to be tailor-made. This hypothesis forms the basis of this research, in which the objectives are to:

- Review the existing literature on the application of grinding aids in mineral processing
- Evaluate and compare the performance of a natural polymer and a synthetic polymer
- Compare grinding characteristics and products from grinding with and without grinding aids.
- Investigate the influence of grinding aids on powder rheology as a probable mechanism of effect.
- Investigate the effect of the grinding aids on surface and solution chemistry in the context of froth flotation
- Investigate the overall effect of the grinding aids on the reverse flotation of quartz from magnetite

2. LITERATURE REVIEW

This chapter aims to present the state of art to better understand the challenges and limitations of size reduction units, especially in dry grinding systems. In addition, an overview of the use and mechanisms of chemical additives (grinding aids) is presented, which highlights knowledge gaps within the area. A brief introduction to the importance and growing trend in the use of sustainable reagents in mineral processing is discussed. The chapter ends with a presentation of the research questions and a clarification of the scope of the research undertaken.

2.1. Grinding and grinding environments (dry vs. wet)

Although mining is not the largest consumer of fresh water in the world (about 1%), the specific situation around the location of mining operations may result in high consumption on a local scale (Kinnunen et al., 2021). For example, in Chile, the Antofagasta mining region accounts for 65 % of the country's water consumption (Donoso et al., 2013). In addition to looking for alternative water sources such as seawater, efforts are being made to recycle process water, and importantly reduce usage (Gunson et al., 2012; Moran et al., 2014). Among efforts, a balance of water intake and effluent volume and quality is a common practice (Kinnunen et al., 2021). This has also led to the use of dry methods such as filtered and stacked tailings, considering that tailings account for 50 % of water loss in a processing plant (Donoso et al., 2013). In some cases, ore sorting can also help reduce the amount of material to be comminuted by removing gangue materials (Kinnunen et al., 2021). In the case of comminution, dry grinding has been investigated as a possible way to reduce water usage; however, there is an extensive gap in our knowledge about improving its efficiency, especially in terms of energy use (Chelgani et al., 2019; Gunson et al., 2012; Kökkiliç et al., 2015). To address the high energy consumption in dry grinding and the scarcity of potable water for mineral processing, chemical additives employed as grinding aids have become a promising alternative.

In mineral beneficiation, wet grinding is much preferred compared to dry grinding, but the growing scarcity of water poses a threat to mining activities, especially in arid regions. Sweden, as the largest iron ore producer in Europe, has set goals to improve resource efficiency and reduce water use in mining activities through dry beneficiation and look for possible strategies (SIP STRIM, 2019). Among other drawbacks, high energy consumption remains the main problem for dry grinding; see Figure 2. This necessitates the need for energy-efficient technologies and strategies.

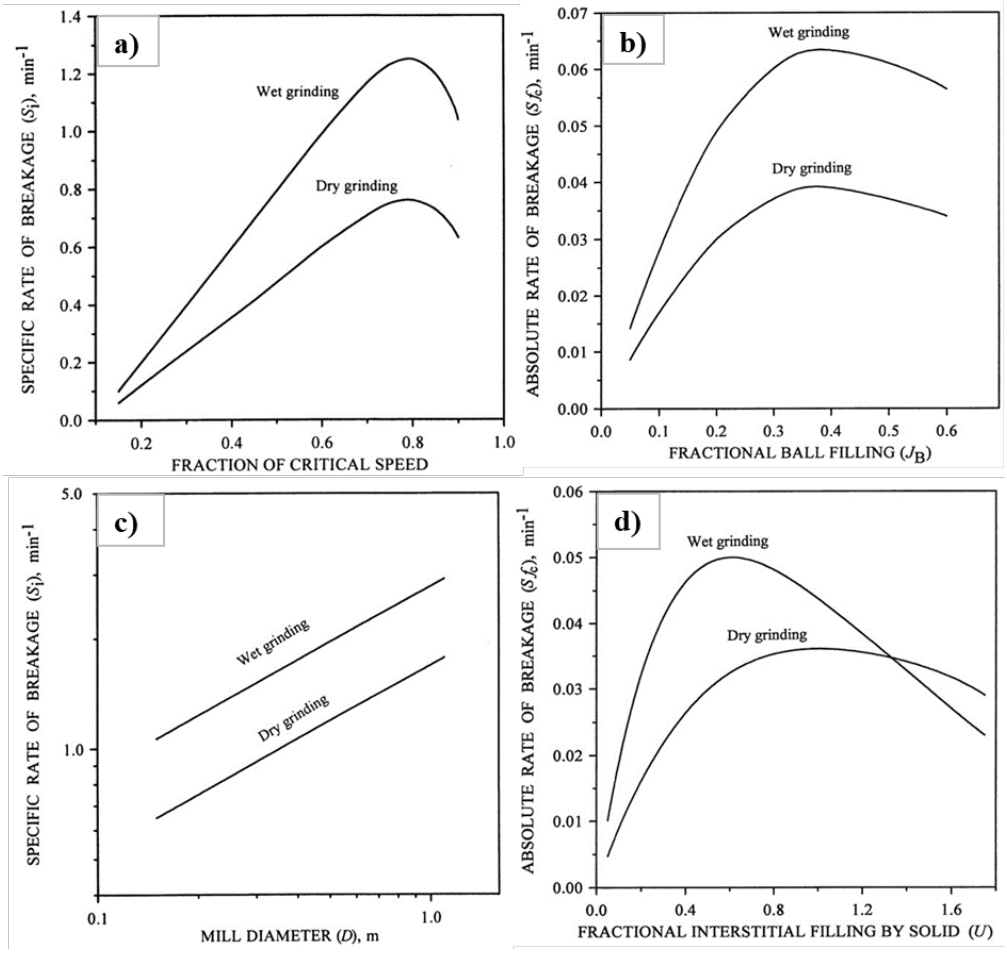

Figure 2. Comparison of dry and wet grinding breakage rates with varying a) mill critical speed, b) mill ball load, c) mill diameter, and d) mill interstitial filling after (Ozkan et al., 2009). *Reused with permission from Elsevier. Copyright © 2022.*

Due to the current processing of finely disseminated ores, grinding is a prerequisite to ensure size reduction and mineral liberation before any subsequent separation stage. As such, for any dry beneficiation technique such as classification, sorting, magnetic separation, gravity, or electrostatic separation, an efficient dry grinding process is required. Dry grinding has many merits, such as less wear of the grinding media compared to wet grinding, smaller fractions of fine products (gives a higher proportion of middlings and coarser material +100 μm), and the potential for improving the efficiency of downstream processes (Bruckard et al., 2011; Kanda et al., 1988; Koleini et al., 2012; Ogonowski et al., 2018; Routray and Swain, 2019). However, one of the main drawbacks of dry grinding is the high energy consumption (Figure 2), that is, approximately 20%-25 % higher compared to wet grinding (Bruckard et al., 2011; Feng and Aldrich, 2000; Kanda et al., 1988; Ogonowski et al., 2018). Furthermore, dry grinding is characterized by low material transport in the pneumatic pumping

system, resulting in lower throughputs (Feng and Aldrich, 2000; Kanda et al., 1988; Ogonowski et al., 2018). Bruckard et al. (2011) reported that particle agglomeration increases in dry grinding, which affects the downstream separation process. From any operational point of view, dry grinding has the risk of high noise and dust pollution (Kanda et al., 1988; Ogonowski et al., 2018). Considerable work has been done to reduce energy consumption; however, few of them examined GAs as one of the promising alternatives to address the limitations of dry grinding (Fuerstenau, 1995; Prziwara et al., 2018c). The use of chemical additives (grinding aids) in mineral processing can be considered a promising alternative to reduce energy consumption. Chemicals that can be used as GAs range from organic (such as polyols, alcohols, esters, and amines) to inorganic (such as calcium oxide, sodium silicate, sodium carbonate, and sodium chloride). They could also be used as modifiers, flocculants, surfactants, and dispersants in downstream processes.

2.2. Grinding aids and associated mechanisms

Although GAs date to 1930 (National Materials Advisory Board - Commission on Sociotechnical Systems, 1981), no agreed mechanism for their effect exists (Fuerstenau, 1995; Hao et al., 2017; Weibel and Mishra, 2014a). Some mechanisms have been proposed for the effect of GAs, which are mainly based on two principles, namely (i) the chemical-physical effect on individual particles, such as the surface energy reduction (Rehbinder and Kalinkovaskaya, 1932) and (ii) the effect on the particle arrangement and material flow properties Figure 3 (Klimpel and Manfroy, 1978; Locher and Seebach, 1972). Although it is difficult to determine the mechanism of adsorption experimentally, it was reported that for all these proposed mechanisms, the adsorption of the GA onto the particle surface is a prerequisite (Snow and Luckie, 1974). This adsorption has been agreed to occur in the following ways; hydrogen bonding, especially for particles with near-neutral surface charges, chelating bonding with metal ions, hydrophobic bonding through the hydrocarbon tail, and electrostatic bonding (Klimpel, 1999; Mishra et al., 2017).

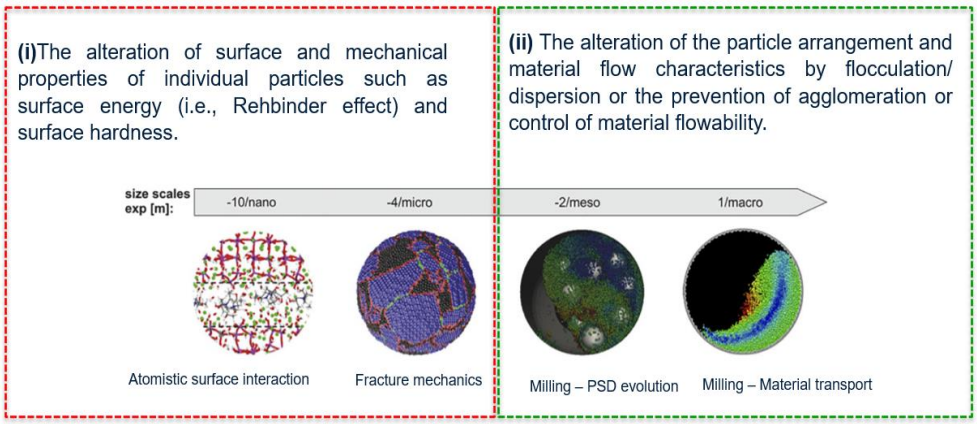

Figure 3. Effect of grinding additives on particle surfaces (Mishra et al., 2015). *Reused with permission from Taylor & Taylor & Francis Group. Copyright © 2022*

In general, the impact of GAs on rheology is accepted as the main mechanism; however, no scientific knowledge substantiates this. During grinding, the material flow plays a pivotal role in the product particles' properties (El-Shall and Somasundaran, 1984a; He et al., 2004). To understand the mechanism of effectiveness of GA, the grinding process can be simply described as a process that simultaneously involves the transportation and capture of particles in the grinding zone and the application of mechanical stress to produce breakage (El-Shall and Somasundaran, 1984a; Prziwara et al., 2018c; Routray and Swain, 2019). All of these scenarios have emphasized the importance of flow characterization studies when GAs are considered. The application of grinding aids has indicated that an optimum dosage exists for given conditions, which depend on both the material properties and the processing conditions. This shows the complexity of the process, which could be due to the dynamic nature of the grinding process (Prziwara et al., 2018b, 2018c).

During grinding, mass flow plays a pivotal role in particles' movement to and from the grinding zone (El-Shall and Somasundaran, 1984b; Fuerstenau, 1995; He et al., 2004). Although quite complex, estimating the flow properties during grinding provides a better understanding of the mill charge's material movement. The flow behavior of cohesive powders depends on; (i) intrinsic properties such as porosity, particle size, density, shape, and roughness, (ii) bulk properties such as particle size distribution (PSD), bulk density, and cohesive/adhesive forces, and (iii) environmental factors such as state of compaction, bed void humidity, and temperature Figure 4 (Divya and Ganesh, 2019; Leturia et al., 2014).

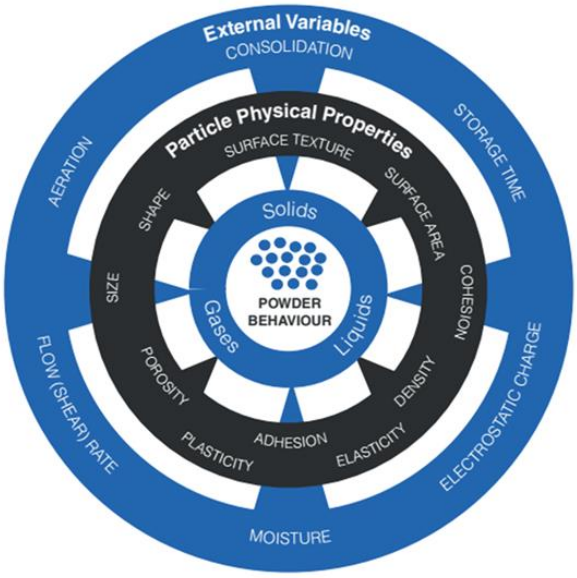

Figure 4. Physical and external variables affecting powder flow behavior after (Freeman and Technology, 2007).

There are several empirical techniques available to analyze flow characteristics, such as shear cell testers, angle of repose, bulk density, uniaxial compression test,

Hall/Carnell method, tapped density, and bed collapse (Divya and Ganesh, 2019; Hare et al., 2015; Leturia et al., 2014). These empirical techniques have poor reproducibility and sensitivity and are largely user-dependent. Previous studies on the influence of GAs on flow behavior have been carried out using empirical techniques (Csoke et al., 2010; Prziwara et al., 2018b; Rajendran Nair and Paramasivam, 1999). Recent advances in automated powder rheometers have addressed these limitations and provide a correlation between the different empirical tests and the dynamic, shear, and bulk properties (Freeman, 2007; Hare et al., 2015; Leturia et al., 2014). Shi et al. (2018) highlighted the importance of carefully interpreting these results from automated powder rheometers. The FT4 powder rheometer is an advanced system that can measure flow behavior while the powder is in motion (more representative of the process conditions) and can fill the gap. In general, considering that flowability is not an inherent property and that a single characteristic is inadequate Figure 4. Therefore, a multivariate method that correlates the results of different empirical tests, such as the FT4 powder rheometer, is needed. The stability and variable flow rate test method of the FT4 powder rheometer measures flow properties in a dynamic, constrained forced flow environment that closely simulates a grinding process in a tumbling mill.

2.3. Effect of grinding aids on the grinding process

To date, some studies on the effect of GAs on efficiency in regard to power consumption (Table 1), grindability, reduction ratio, and mill operating parameters such as mill filling have been performed (Choi et al., 2010; Diler, 2018; Noaparast and Rafiei, 2003; Prziwara et al., 2018b). Prziwara et al. (2018b) investigated their effects on bulk properties such as particle size distribution, specific surface area, powder flowability, specific surface energy, and product fineness. GAs have been applied to address the problem of over-grinding and under-grinding (selective grinding) associated with polymetallic sulfide ores due to their effect on producing a narrow particle size distribution (Enustun et al., 1987; Ma et al., 2010). Several investigations reported improved material fluidity, which allowed grinding at high solid concentrations (reducing the amount of processing water) (Han et al., 2010; Ma et al., 2010; Rajendran and Paramasivam, 1999; Zheng et al., 1996). Yusupov and Kirillova (2010) reported that the use of GA decreased the amount of slime in the flotation feed compared to grinding without GA, which is beneficial for flotation performance (Feng and Aldrich, 2000). Reducing excess fines by using GA can also improve the dewatering processes such as thickening, decanting, filtration, and tailings storage facility (TSF) draining and help in water recycling (Mwale et al., 2005). Moreover, using GAs reduces energy consumption in downstream processes such as dewatering, classification, and pumping due to improved flow properties (Kotake et al., 2011; Melorie and Raj Kaushal, 2018).

Table 1. Effect of GAs on energy consumption

Grinding aid	Material	Reduction in power consumed (%)	Reference
Triethylamine (TEA)	Limestone	98.5	(Csoke et al., 2010)
BMA-1923™ (Amine based)	Feldspar	60.0	(Gokcen et al., 2015)
TIPA	Cement	20.6	(Altun et al., 2015)
Propylene glycol	Clinker	10.0	(Noaparast and Rafiei, 2003)
Sodium polyphosphate	Copper ore	15.7	(Noaparast and Rafiei, 2003)
Alcohol	Coal	2.37	(Noaparast and Rafiei, 2003)
Diethylamine (DEA)	Coal	1.05	(Noaparast and Rafiei, 2003)
Sodium polyphosphate	Talc	33.7	(Diler, 2018)
Sodium polycarboxylic acid	Talc	20.7	(Diler, 2018)
Polyacrylic acid	Calcite	37.2	(Choi et al., 2010)
Triethylamine (TEA)	Cement	17.34	(Toprak et al., 2014)
Polyacrylic acid	Limestone	100	(Zheng et al., 1996)
Aluminum chloride	Coal	25.0	(Enustun et al., 1987)
Sodium silicate	Chromite	4.67	(Routray and Swain, 2019)

2.4. Effect of grinding aids on downstream processes

Grinding as a step before the flotation separation process influences the surface properties of the particles, the solution/pulp chemistry, surface chemistry, and even the crystal structure (Bruckard et al., 2011; Bulejko et al., 2022; Chelgani et al., 2019; Tong et al., 2021). Although understanding the mechanism of the effect of these GAs remains unsatisfactory, there is consensus that the adsorption of these chemical additives is a prerequisite for their applications (Chipakwe et al., 2020a; Prziwara and Kwade, 2020). It can be postulated that these chemicals will remain on the surface of the particles after milling. Ersoy et al. (2022) investigated the effect of triethanolamine (TEA) and monoethyl glycol (MEG) (the most typical GAs) on the surface of calcium carbonate. Both GAs have been reported to adsorb on particle surfaces, resulting in changes in product properties such as rheology, dispersion, and color properties (Ersoy et al., 2022). Bulejko et al. (2022) examined the effect of 0.1 wt. % TEA in ultrafine wet grinding of corundum. TEA affected zeta potentials, turbidity, viscosity, and improved grinding performance. They considered only one concentration of TEA (0.1

wt.%) and reported relatively unstable suspensions based on zeta potentials and turbidity measurements (Bulejko et al., 2022). Although several studies have discussed the effects of GAs on the final product (centered on the cement and aggregate industry, where grinding is usually the final step), few investigations addressed their effects on products in view of downstream processes such as flotation (Chipakwe et al., 2020a; Mao et al., 2022; Prziwara and Kwade, 2020). In addition to the change in the properties of the product during grinding, froth flotation involves the use of surfactants that can potentially interact with these grinding aids. The opposing effects of grinding aids have been reported in the literature without actual understanding Table 2.

Table 2. Downstream effects of grinding aids

Grinding Aid	Effects	Reference
Triethanolamine (TEA)	2.13 % increase in quartz recovery in flotation.	(Mao et al., 2022)
Triisopropanolamine (TIPA)	2.63 % increase in quartz recovery in flotation.	(Mao et al., 2022)
Calcium Oxide	2.9 % increase in dense media separation efficiency of magnetite (65.0 - 67.9%)	(Bhima. Rao et al., 1991)
ZALTA™	4 % increase in copper recovery through flotation by maintaining high throughput without comprising the mineral liberation	(Solenis, 2016)
Benzyl arsenic acid	6.4 % increase in flotation recovery of cassiterite (51.6 – 58%)	(Yang, 1994)
Sodium hexa-metaphosphate	42 % decrease in flotation recovery of cassiterite (51.6 – 9.6%)	(Yang, 1994)
Hydroxylamine based GA	7% reduction in recycled fines in an air classifier underflow (22.6-15.5 %)	(Toprak et al., 2014)
Ammonium chloride	Increased dissolution of chromite in HCl	(Anoshin et al., 1994)
Potassium ethyl xanthate (PEX)	6% increase in recovery of chromite ore	(Camalan and Hoşten, 2019)

2.5. Sustainable reagents in mineral processing

To address current environmental issues, a few investigations have been conducted on the use of sustainable and eco-friendly benign materials as a surfactant in mineral processing. Sustainable reagents can be defined as materials derived from renewable, waste or recycled material or their combinations, which are also biodegradable or recyclable at the end of life (Mohanty et al., 2022; Zhu et al., 2016). Among such reagents, natural biopolymers have become popular, namely starch, cellulose, lignin, chitins, lipids, and their derivatives (Lapointe and Barbeau, 2020; Mohanty et al., 2022). Despite being environmentally friendly, the application of biopolymers remains limited due to several drawbacks. The dosage tends to be higher than that of synthetic polymers, coupled with a low efficiency and less productive synthesis route. Such drawbacks have led to the trade-off of modification and blending with some synthetic polymers, reducing their biodegradability (Lapointe and Barbeau, 2020; Mohanty et al., 2022; Zhu et al., 2016). Biopolymers are advantageous because of their low cost, abundance, and nontoxicity. The design and selection of GAs are based almost exclusively on their grinding performance with little focus on creating sustainable chemistries. Within the cement industry, many chemicals have been used as GAs, ranging from pure chemicals such as triethanolamine (TEA) to, more recently, high-charge polymers (Cheng et al., 2019; Chipakwe et al., 2020a; Fuerstenau, 1995; Weibel and Mishra, 2014b). These are mainly based on ethylene glycol, propylene glycol, triisopropanol amine (TIPA), triethanolamine (TEA), and tetraethylenepentamine (TEPA) (Chipakwe et al., 2020a; El-Shall and Somasundaran, 1984b; Fuerstenau, 1995). Some of these GAs, such as TEPA (amine-based), are not biodegradable and raise environmental concerns (Ervanne and Hakanen, 2007). Waste streams containing alkanolamines can increase the concentration of ammonia, nitrite, and nitrate, which could infiltrate the subsoils and water sources (Ervanne and Hakanen, 2007).

In addition to the demonstrated merits of natural polymers, some investigations on chemical additives have explored the utilization of waste streams from other industries, such as waste cooking oil, glycerine, lignin and cane molasses as GAs (Gao et al., 2011; Zhang et al., 2016). This has also been motivated by the high cost of triethanolamine-based GAs and the concepts of 'circular economy', which are emerging in the production of raw materials to reduce waste generation and reuse 'waste' from other processes. Zhang et al., (2016) demonstrated that a mixture of lignin, cane molasses, and waste glycerine could be used as GAs in cement production. Polysaccharide-based chemistries are a promising alternative to less toxic and cheaper reagent development options (Lapointe and Barbeau, 2020; Nuorivaara and Serna-Guerrero, 2020). Since low environmental impact practices are in high demand within the mineral processing value chain (Aznar-Sánchez et al., 2019; Nuorivaara and Serna-Guerrero, 2020), the best scenario would be the development of chemicals that improve grinding performance and ensure that they do not have adverse impacts on downstream processes. Some studies have focused on the mineral industry, with further discussion of downstream effects (Bhima. Rao et al., 1991; Yang, 1994); however, they were not in-depth. Understanding and controlling any GA-separation reagent interactions is critical to ensure that the required downstream process efficiency and integrity of the entire value chain are maintained.

2.6. Research questions and limitations of the work

In this thesis, limitations are reported concerning the commercial reagents utilized in the study. Limited information was available due to confidentiality and intellectual property on proprietary ingredients and/or formulations. Therefore, limited knowledge is available about the molecular structure or chemical composition of commercial reagents. However, the thesis focuses on the application of the reagents and analyses of the resulting effects. From the concise literature review, the following questions were identified, which form the scope of this thesis and can be formulated as follows.

RQ1: How effective are grinding aids in reducing energy consumption during dry grinding? **– Paper I & II**

RQ2: What is the relationship between particle arrangement (dispersion/ flowability) and milling rate during dry grinding with grinding aids? **– Paper I & III**

RQ3: What are the differences and similarities between dry ground products with and without grinding aids? **– Paper II & III**

RQ4: What are the changes in the surface and solution chemistry with and without grinding aids? **– Paper IV & V**

RQ5: How do these changes, if any, affect overall flotation performance? **– Paper IV & V.**

3. EXPERIMENTAL METHODOLOGY

This chapter aims to introduce the methodological approach applied in the work summarized in Table 6. Experimental work focuses mainly on grinding and flotation experiments. Further analyzes were carried out on the different samples/streams around the tests. The material, characterization, and equipment, instrumentation and analysis performed in the work are presented. Further statistical analysis was applied in the analysis of the data.

3.1. Materials

Two polymers were used as GAs, namely, Zalta™ GR20-587 (synthetic polymer) and Zalta™ VM1122 (natural polymer) from Solenis (Sweden) were considered for the experiments (Table 3). Polyacrylic-based polymer (Zalta™ GR20-587: AAG) with a typical chemical structure and a medium-molecular weight polysaccharide (Zalta™ VM1122: PGA) that mainly comprises dextran, shown in Figure 5. Other reagents used in the study as collector and depressant are presented in Table 4.

Table 3. Chemical and physical properties of grinding aids

Chemical and physical properties	**Zalta™ GR20-587 (AAG)**	**Zalta™ VM1122 (PGA)**
Description	Grinding aid	Grinding aid
Classification	Polyacrylic acid-based	Polysaccharide-based
Charge	Anionic	Non-ionic
pH	8	4-7
Appearance	Aqueous solution	Liquid
Color	Yellow	White
Boiling point °C	100	98.9 – 103.3
Flashpoint °C	-	207
Water solubility	Soluble	-
Dynamic viscosity (mPa·s)	150	2.0-3.0
Density at 20°C (g/cm^3)	1.20	1.06

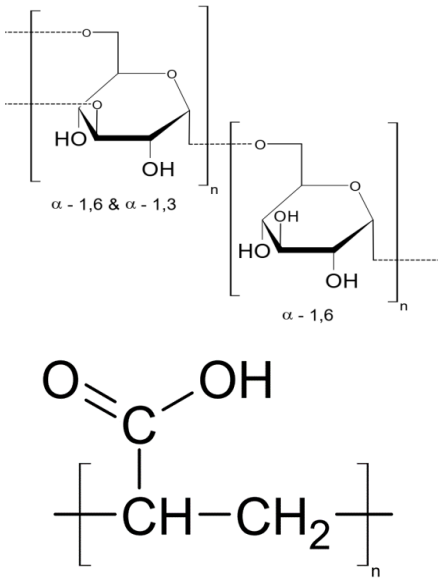

Figure 5. Typical chemical structure of dextran (top) and polyacrylic acid (bottom).

Table 4. Chemical properties of other reagents used

Chemical	Description	Classification	Charge	Source
Lilaflot 822M	Collector	Ether diamine	Cationic	Nouryon
Starch	Depressant	Corn starch	-	Merck
Sodium hydroxide	pH modifier	Alkaline	Neutral	Merck
Hydrochloric acid	pH modifier	Acidic	Neutral	Merck

For the study, samples of pure quartz (99.9 % SiO_2) and magnetite (96.0 % Fe_3O_4) were obtained from VWR, Sweden. Magnetite ore from a mine in Malmberget, north of Sweden, was received from LKAB (Luossavaara Kiirunavaara Aktiebolag). X-ray diffraction (XRD) analysis was performed using a D/MAX-2500 pc powder diffractometer equipped with Co-Kα (λ = 1.54) for mineral identification. (Figure 6).

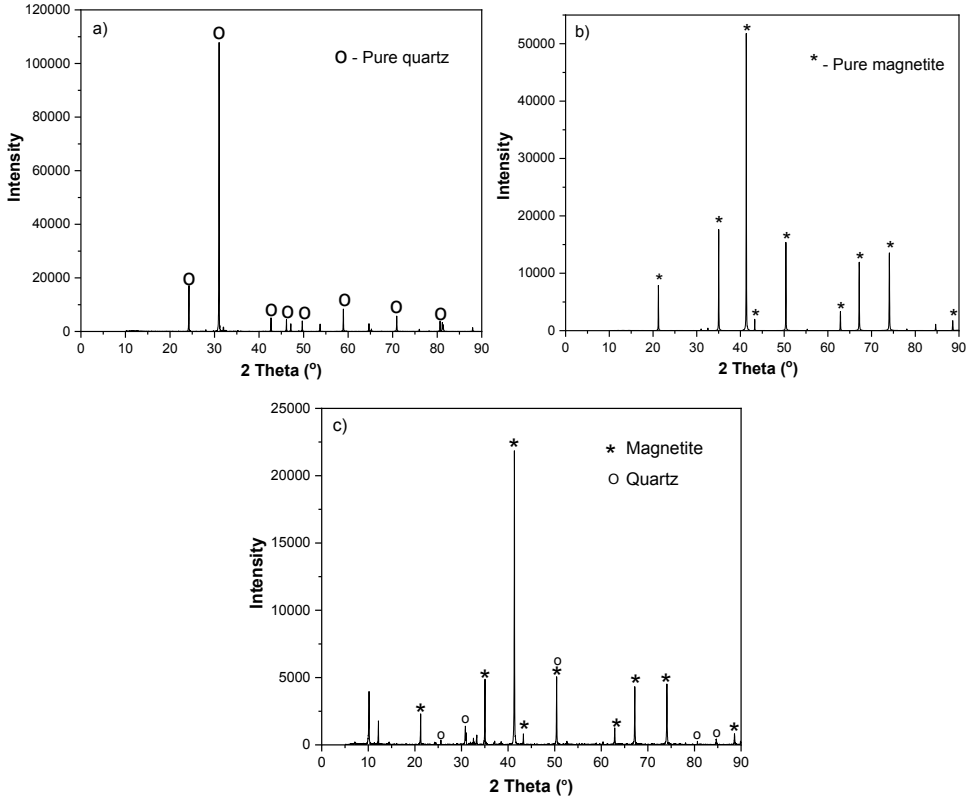

Figure 6. X-ray diffraction pattern of the a) pure quartz, b) pure magnetite, and c) magnetite ore.

3.2. Grinding test protocol

A laboratory scale ball mill (CAPCO, UK) (Figure 7) was used for the grinding experiments with the parameters summarized in Table 5. The feed (magnetite ore) had a top size of 2.8 mm and an F_{80} of 2594 µm. The mill conditions were kept constant for all runs. For the first run, the ball mill was run with the ore for 30 minutes, and the energy was read from an energy meter before and after the operation. The same conditions were applied through the grinding process with GAs.

Table 5. Grinding parameters were considered for the experiments.

CAPCO Jar mill	Ø 115 x 132 mm
Grinding media	Steel balls (graded 10 – 36 mm), 19 vol.% filling
Mill speed	114 rpm, 91 % of critical speed
Mass of sample	220g, Ore: Ball ratio – 0.16 w/w, top size < 2.8 mm
Grinding time	30 minutes

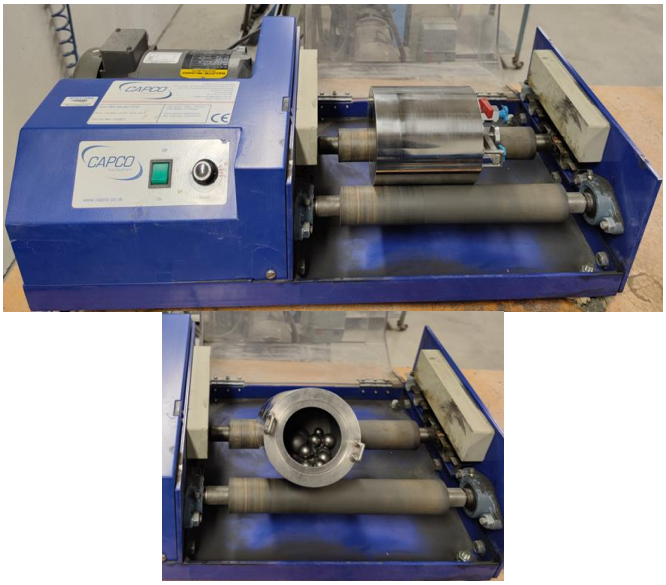

Figure 7. The CAPCO variable speed mill used in the experiments

The GAs were added in the supplied form (no solutions were prepared) just before the grinding procedure. No pretreatment was done to represent the industrial-scale mill conditions for adsorbing GAs during grinding. The grinding products were subjected to particle size distribution (PSD). The grinding energy was determined using the work index according to Equation 1.

$$W = 10.W_i \left(\frac{1}{\sqrt{P}} - \frac{1}{\sqrt{F}}\right) \quad (1)$$

where: Wi: work index (kWh/t), W: specific grinding energy (kWh/t), P: 80% passing size of the mill product, in µm, F: 80% passing size of the mill feed, in µm (Bond, 1961). The ground material was collected after grinding and analyzed for particle size distribution. The particle size was determined using a combination of dry and wet sieve analysis, from which the P_{80} was determined.

3.3. Powder Flow & Bulk Properties measurements

The flowability of the ground material was measured using an FT4 powder rheometer (Figure 8) (Freeman Technology Ltd, UK, now part of Micromeritics, USA). The instrument comprises a twisted blade, piston, or shear head that can rotate and moved axially in the sample while measuring the rotational and axial force. There are different measurement modes: *stability and variable flow rate* test, shear test (rotational) and *aeration* test based on force, velocity, and torque. A 40 cm^3 volume of each ground sample was measured and preconditioned to homogenize the sample for rheometry. All tests were carried out in 25 mm diameter glass vessels: a 25 cm^3 vessel for the *stability and variable flow rate* test, a 10 cm^3 vessel for the shear test and a 35 cm^3 vessel for the *aeration* test (although the sample volume for the aeration tests was 25 cm^3), following the operating procedures (Leturia et al., 2014).

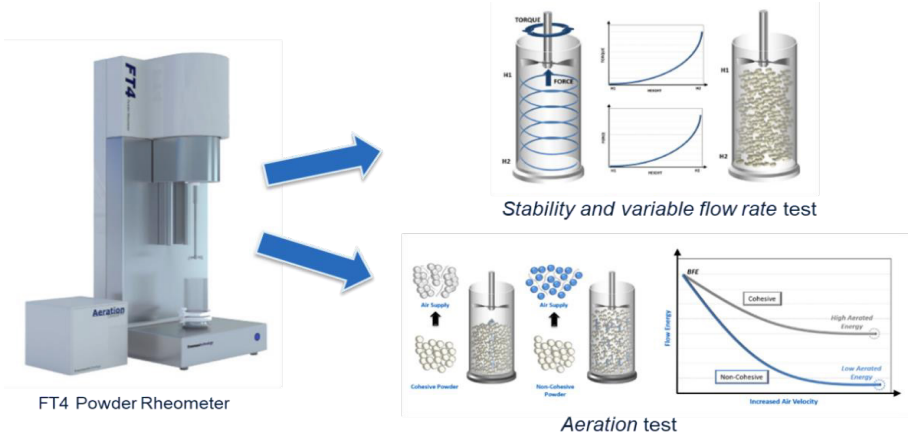

Figure 8. The FT4 Powder Rheometer was used in the experiments. Modified after (Freeman and Technology, 2007)

3.3.1 Stability and variable flow rate tests

The test procedure involves lowering the rotating blade into the powder at a defined axial and rotational speed and then, bringing it up out of the powder at the same speed, measuring the torque and axial force at all times. The first seven test cycles use an axial speed of 100 mm/s at the tip of the blade to assess the constant resistance to blade motion. The remaining four cycles use decreasing axial speeds, starting at 100 mm/s and then 70, 40, and 10 mm/s, to measure the resistance dependence on blade speed. In between each test cycle, the powder is conditioned (the blade moves through it in a predefined way) to remove the effect of the previous test and restore it to a consistent starting condition. During both downward and upward movement, the torque and axial force required to move the powder bed were measured and used for different calculations. This standard test produces data that are then used to determine:

- Basic Flowability Energy, BFE (energy required to move the blade downwards during the seventh test cycle),
- Specific Energy, SE (the energy required to move the blade out of the powder during the seventh cycle divided by the mass of the sample),
- Stability Index, SI (the ratio of the total energy consumed by the seventh test cycle to that consumed during the first test cycle), and
- Flow Rate Index, FRI (the ratio of the energy consumed during the cycle at a blade speed of 100 mm/s to that at 10 mm/s).

3.3.2 Aerated tests

An *aeration* test was also conducted on the different mixtures to assess the flow behavior in an aerated environment. Different airflow rates (0, 2, 4, 6, and 10 mm/s) from the cell bottom. The torque and axial force were recorded during the downward movement (tip speed = 100 mm/s) to give the total energy consumption (TE). The successive increase in the airflow rate reduces the energy to give a minimum, which implies total fluidization of the bed. The corresponding total energy (TE) value gives the aerated energy (AE), while the reduction in energy as the airflow increases gives

the aeration ratio (AR) (the ratio of the energy consumed during the test cycle without airflow to the aeration energy). The basic flow energy in the aerated environment (A-BFE) is also determined.

3.4. Surface morphology

For each product ground with and without GAs, the Micromeritics Flowsorb II 2300 instrument measured the BET-specific area. Furthermore, the density of the selected materials was measured using an automated Micromeritics AccuPyc II 1340 gas pycnometer. The specific surface area (area per unit mass or volume) is a useful measurement for particle characterization and roughness. When a solid surface is exposed to a gas, e.g. nitrogen, the gas molecules are attracted and adsorbed on the surface to form adsorbed layers. Under fixed conditions assuming a monolayer of molecules, the amount of adsorbed gas is proportional to the total surface area of the solid, which increases with increasing roughness (Allen, 1997). The BET technique measured the particle surface area, which can be used to characterize the surface roughness of the particles. The surface roughness (R_S) values (dimensionless) was calculated using the following Equation 2 described by Jaycock and Parfitt (1981).

$$R_S = A_B \rho \left(\frac{D}{6}\right) \quad (2)$$

where: A_B is the BET surface area measurement, ρ is the solid density, and D is the average particle diameter. Surface morphology under different grinding conditions was also characterized using scanning electron microscopy (SEM). Secondary imaging (SE) was performed using the Zeiss Sigma 300 VP instrument (QanTmin).

3.5. Flotation tests protocol

3.5.1 Single mineral flotation tests

Single mineral flotation for pure magnetite and pure quartz was performed using a mini flotation cell (Clausthal cell). In each flotation, 7.5 g of the sample (-106 + 38 µm) was added together with deionized water to the 150 cm^3 capacity. Before the flotation stage, the slurry was agitated with a predetermined amount of PGA for 10 min to allow adsorption on the particle surface. The predetermined amount of reagents (depressant and collector) were added to the slurry and conditioned, adjusting pH and reagent doses for (5+5) - 10 min, Figure 9. Caustic starch was used as a depressant. For each set of experiments, a fresh 1% alkaline starch solution was prepared in 1: 4 ratio. A cationic ether diamine collector, Lilaflot 822M, was recommended and supplied by Nouryon (Sweden). The pH was adjusted by adding 1.0M NaOH or 1.0M HCl. The flotation was conducted for 2 min scraping every 10 s. The froth products and tails were collected, weighed, and dried, and recovery was calculated based on the dry weight. Each experiment was performed in duplicate and the average was reported.

3.5.2 Mixed mineral flotation

The mini mixed mineral flotation of the model ore was also performed using a Clausthal cell. The model ore consisted of 5.0 g magnetite and 2.5 g quartz (ratio 2:1). For each test, 7.5 g of the mixture (-106 + 38 µm) was used together with deionized water. Before the flotation stage, the slurry was agitated with a predetermined amount

of GA for 10 min to allow adsorption on the surface of the particle. For PGA, the collector was fixed at 300 g/t, and the depressant was varied together with GA. While for AAG the depressant was fixed at 1000 g/t and the collector was varied. Conditioning was performed for 10 min, followed by flotation for 2 min. The froth products and tails were collected, weighed, dried, and recovery was calculated based on dry weight and chemical analyses using induction plasma (ICP OES). Each experiment was performed in duplicate, and the average was reported. A further evaluation of the selectivity of the process was calculated using Equation 3.

$$S = R_1 - R_2 \quad (3)$$

Where R_1 is the recovery of magnetite and R_2 is the recovery of quartz. A higher selectivity index S extrapolates better selectivity for flotation separation (Chipakwe et al., 2021; FAN et al., 2010). To better assess the observed effect of GA on the separation of quartz from magnetite, surface analysis of the mineral surfaces was considered.

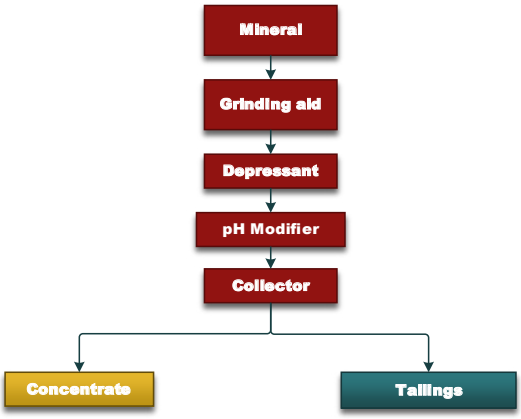

Figure 9. Schematic flowsheet for the flotation tests.

3.6. Zeta potential measurements

The zeta potential measurements for the ground samples were performed using a CAD ZetaCompact instrument. The instrument's principle is based on microelectrophoresis, i.e., the observation of particle motion under an electric field using a CCD camera. Image analysis is performed by Zeta4 software based on the Smoluchowski equation to evaluate electrophoretic mobility data (Forbes et al., 2014). The suspension was prepared by adding 30 mg of a pure sample with samples of -5 µm samples (obtained by ultrasound bath sieving) mixed with various GAs concentrations and flotation reagents and 10^{-2} M KCl solution as the electrolyte. The suspension was stirred uniformly in a beaker to form a suspension containing 0.01 wt.%. The reported values are the calculated mean measurements.

3.7. Adsorption measurements

Adsorption measurements to determine the amount of adsorbed GA were performed using the solution depletion method on the UV-VIS spectrometer (DU Series 730 – Beckman Coulter, USA). Standard solutions with GA concentrations ranging from 0 to 5 mg/ml and 0 to 100 mg/l for PGA and AAG respectively were used to obtain the

calibration curve Figure 10. 1.0 g of the sample (-106 +38 µm) with 40 ml and the predetermined reagent concentration were added to a 100 ml flask. The suspension was stirred for 2 hours at pH 10 and 20±1 °C to ensure maximum adsorption. After vacuum filtration, the solution was passed through a 0.22 µm millipore membrane and the concentration of the remaining GA in the solution was analyzed using UV absorbance at wavelengths of 220 and 210 nm for PGA and AAG, respectively. Measurements were corrected for blanks and performed in triplicate. The concentration that was depleted from the solution was assumed to be adsorbed onto the surface of the sample particle. The adsorption density was calculated using Equation 4;

$$Q_e = \frac{(C_1 - C_0)V}{m} \quad (4)$$

Where Q_e is the amount of GA (mg/g) adsorbed on the sample particle surface, C_0 and C_1 are the initial and final concentrations, i.e., before and after adsorption (mg/L), respectively, m is the mass (g) of the sample, and V is the volume (L) of the GA solution. Furthermore, the experimental data for the adsorption isotherms were fitted to the Langmuir (Equation 5) and Freundlich (Equation 6) models.

$$Q_e = \frac{K_L C_e Q_0}{1 + K_L C_e} \quad (5)$$

$$Q_e = K_F C_e^{\frac{1}{n}} \quad (6)$$

Where Q_e is the amount of GA (mg/g) adsorbed, C_e is the equilibrium concentration of GA. Q_m and K_L are Langmuir constants whilst K_F and $^1/_n$ are the Freundlich constants related to the maximum monolayer adsorption capacity and energy of adsorption, respectively (Zhang et al., 2018).

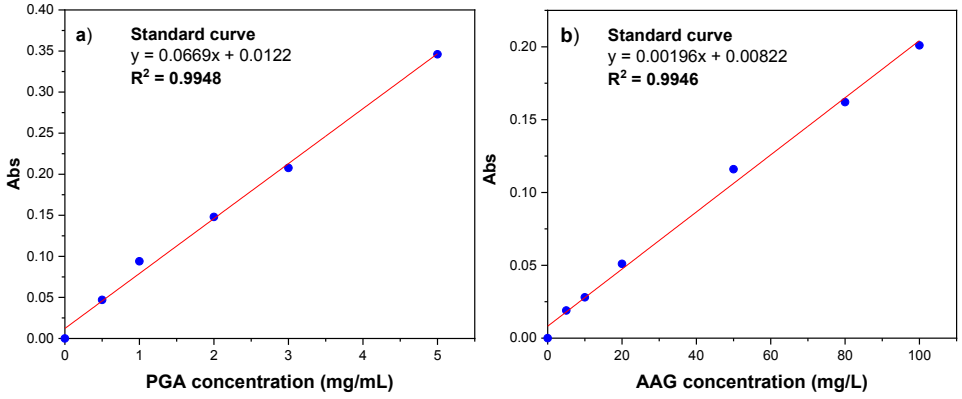

Figure 10. Standard curve of a) PGA and b) AAG adsorption

3.8. Stability measurements

The suspension stability measurements were performed using Turbiscan LAB Expert (Formulaction, France). Measurements were carried out to determine the behavior of coagulation and dispersion in the presence and absence of GA. 50 mg of quartz and

magnetite particles were added separately to 40 ml of deionized water. A predetermined amount of reagents was then added and stirred for 20 min at pH 10. 20 ml of suspension was transferred to a measuring vial and scanned at a height of 40 mm at 30 ° C. The suspension stability was scanned over 100 times in 60 min at 30 s intervals. Transmission intensities (T) and backscattering (BS) of pulsed near-infrared light (λ = 880 nm) were recorded as a function of time. The data was then analyzed using TLab EXPERT 1.13 and Turbiscan Easy Soft software to calculate the Turbiscan Stability Index (TSI) Equation 7. The values of the TSI coefficients vary from 0 to 100, that is, from extremely stable to an unstable system (Ataie et al., 2020; Bastrzyk and Feder-Kubis, 2018).

$$TSI = \sqrt{\frac{\sum_{i=1}^{n}(x_i - X_{BS})^2}{n-1}} \quad (7)$$

Where x_i is the average backscattering for a minute of measurement, x_{BS} is the average x_i, and n is the number of scans.

3.9. FT-IR spectroscopy measurements

The samples were ground to approximately -2 μm using an agate mortar and pestle. A 2.0 g aliquot was treated with predetermined reagents and conditioned for 40 min at pH 10. The solid samples were thoroughly washed using deionized water. After washing and vacuum drying at 35 °C for 24 hours, the samples were subjected to FTIR analysis. The samples were analyzed by diffuse reflectance (DR) and attenuated total reflectance (ATR) FTIR spectroscopy, using an IFS 66V/S instrument and a Vertex 80v instrument, respectively (Bruker Optics, Ettlingen, Germany) under vacuum conditions (below 7 mbar), according to the protocol by András and Björn (2014).

3.9.1 Diffuse reflectance - IR

For diffuse reflectance measurements, powder from dry samples (approx. 10 mg) was mixed with infrared spectroscopy grade potassium bromide (KBr, Merck/Sigma-Aldrich, ca. 390 mg) and manually ground using an agate mortar and pestle until a homogeneous mixture was achieved. Spectra were recorded in the range of 400-4000 cm^{-1} at 4 cm^{-1} spectral resolution, and 128 scans were co-added, using pure KBr as the background under the same parameters. Spectra were processed using the built-in functions of OPUS (version 7, Bruker Optics, Ettlingen, Germany). The spectra were the first baseline corrected (64-point rubberband) over the entire spectral range, then vector normalized, and finally offset corrected. After these steps, no smoothing, derivatization, or other processing was applied.

3.9.2 Attenuated total reflectance - IR

ATR measurements were performed using a Bruker platinum accessory with a diamond internal reflection element. Spectra were recorded in the range of 400-4000 cm^{-1} at 4 cm^{-1} spectral resolution, and 100 scans were co-added, using the empty diamond crystal as the background under the same parameters. The spectra were processed using the built-in functions of OPUS (version 7, Bruker Optics, Ettlingen, Germany) in the same way as the DR spectra.

3.10. Statistical analysis

All measurements were performed in duplicate and were based on a series of different batches and mean values were reported. Statistical analyzes were performed using analysis of variance (ANOVA) at a 95 % significance level using Origin Pro 9.0 (OriginLab, USA). The association between the parameters was assessed using Pearson's correlation analysis '*r*'. '*r*' is a linear factor that determines the relationships among variables to show their dependence. It ranges from -1 to +1. The sign of the *r*-value indicates the magnitude of a relationship, and its absolute value shows its strength.

Table 6. Overview of the analytical and experimental procedures

Method	Paper I	Paper II	Paper III	Paper IV	Paper V
Literature survey	X	X	X	X	X
Particle size distribution		X	X	X	X
Grinding		X	X	X	X
Powder rheology and bulk properties			X		
Surface area (BET - method)		X		X	X
Microscopy (SEM)					X
Flotation				X	X
Zeta potentials		X		X	X
Adsorption test				X	X
Stability test				X	X
Spectroscopy				X	X

4. RESULTS & DISCUSSION

This chapter summarizes, discusses, and presents the results of the work. The findings of the application of grinding aids are discussed, highlighting the implications on grinding and flotation performance. The effect of grinding aids on product properties, rheology, surface chemistry, and slurry chemistry is presented. The results are also discussed on how the knowledge gained in the work helps in the general understanding and application of grinding aids in mineral processing.

4.1. Grinding

4.1.1 Energy consumption

Work index calculations (Figure 11) indicate that the GAs reduce energy consumption for all the additives compared to the reference test (reference line). The extent of energy reduction is affected by both the type of grinding aid and the dosage. In terms of GA type, PGA and AAG had a 31.1 and 26.6% reduction, respectively, compared to the reference test. The difference in the work index of the selected GAs can be attributed to the change in the material flowability. As the flowability increases to an optimum, the energy is transferred more efficiently to allow for the successful breakage of all particles, after which the efficiency drops again.

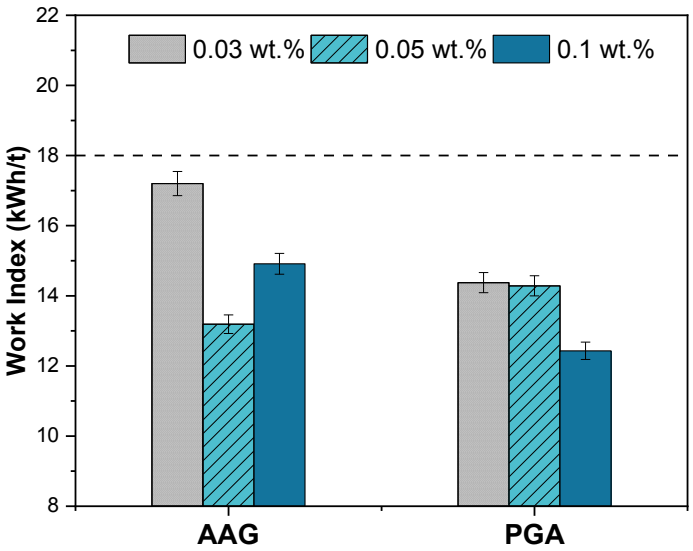

Figure 11. Effect of grinding aids on work index.

Compared to the reference test, the work index drops off when using AAG and, interestingly, begins to increase with dosage increments. This sudden increase in the work index after 0.05 wt.% dosage implies that an optimal flowability improvement exists, allowing for effective particle breakage. High powder flowability affects particle capture, with particles more easily pushed out of the active grinding zone, resulting in

poor size reduction (Prziwara et al., 2018c; Schönert, 1996). Accordingly, less mass is captured in the case of high flowability (above optimum), resulting in less effective reduction in particle size for the given energy and higher amounts of energy consumption per given mass.

4.1.2 Product fineness

The effect of GA types and their dosage on the product fineness was analyzed using a combination of dry and wet sieving, as well as specific surface area measurements. GAs resulted in an increase in product fineness, expressed by P_{80}, compared to dry grinding without additive (reference line) (Figure 12). Thus, both the type of GA and the dosage affect the fineness of the product. The finest product size was achieved from the investigated dosage ranges by grinding with PGA and, lastly, AAG. A decrease in product fineness for AAG was achieved, which is more drastic at high dosages. These results correspond to those of Gamal (2017) during the wet grinding of quartz separately conditioned with various GA, namely sodium silicate, isoamyl alcohol, and ethylene glycol ether in a ball mill. As observed for the work index, a similar trend can be seen for the increase in fineness when the dosage reaches a maximum, which follows a sudden decrease in fineness for AAG.

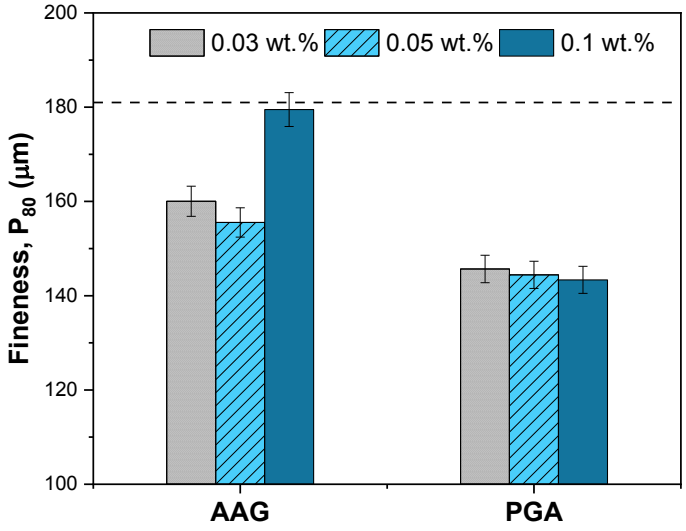

Figure 12. Effect of grinding aids on product fineness.

4.1.3 Particle size distribution

The results (Figure 13) indicate that the middling size fraction (+38 -150 µm) has the highest frequency within the particle size distribution of dry ground samples, which can be considered an optimum condition for downstream separation processes such as flotation. Grinding in the presence of PGA produces particle size distributions of 23.2; 58.8; and 18.5 %, while the reference test results in 24.9; 53.2 and 21.9 % for the size fractions of -38, +38 -150, and +150 µm size fractions, respectively, that is, the use of GA reduces the production of fine particles (-38 µm). This corroborates the findings of Zhao et al. (2015) on the grinding of ultrafine fly ash in a ball mill using a mixture of triethanolamine and ethylene glycol. The resulting narrow particle size distribution

can be attributed to the improvement in flowability as a result of the use of GAs. This allows all particles to be ground under the optimum particle bed thickness. Differences in particle size distribution between GAs can be attributed to differences in material flowability. Differences in flowability result in various captured masses, which consequently has a selective impact on particle breakage behavior within a particle bed (Prziwara et al., 2018c). In the case of high captured mass and comparatively low stress intensity, the particle breakage will be poor and will lead to excessive fines generation. Therefore, it strengthens the position that the best GA balances the captured mass and the stress intensity, resulting in a narrow particle size distribution – with no under or overgrinding.

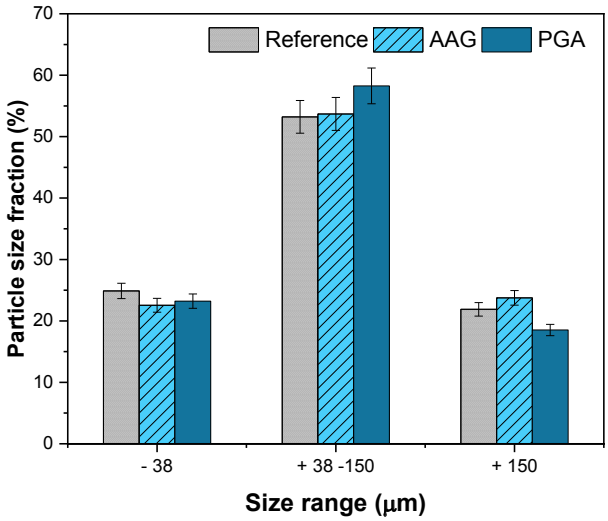

Figure 13. Particle size distribution of products for different grinding aids at 0.1 wt.% dosage

This can be explained using the mass-capturing concept by Schönert (1996). Some scholars believe that the grinding aid performance is influenced by the number of polar groups and the length and structure of the nonpolar groups (Yang et al., 2019, 2022; Yoshioka et al., 1997). In addition to this, some studies found no correlation between the functional group and grinding performance (Prziwara et al., 2019; Weibel and Mishra, 2014b). Also, to the different functional groups (hydroxyl for PGA and carboxyl for AAG), findings suggest that the carbon chain and the anionicity of the GA play a role. Huang et al. 2019 investigated the effect of anionicity, nonpolar chain, and polar part on grinding efficiency. It was found that there exists an optimum molar ratio of the polar head: nonpolar chain and that shorter chains were more desirable than longer ones (Yang et al., 2019, 2022). The difference in the performance of the GAs can thus be attributed to the probable mechanism of stabilization (reduction in interparticle forces). Stabilization of the particle-particle interaction can be described as electrostatic, steric, or electrosteric (Mende et al., 2003). The nature of the GAs could explain the difference in performance with PGA (non-ionic), it can be inferred that it is mainly via steric stabilization while AAG (anionic) would be electrosteric.

4.2. Powder Flow & Bulk Properties

Flow characterization of different GAs and dosages was performed using *stability and variable flow rate* and *aeration* tests. The application of GAs generally improves flowability, as shown in Figure 14. Stability and variable flow rate and aeration tests show that flowability increases with increasing GA dosage for the examined range.

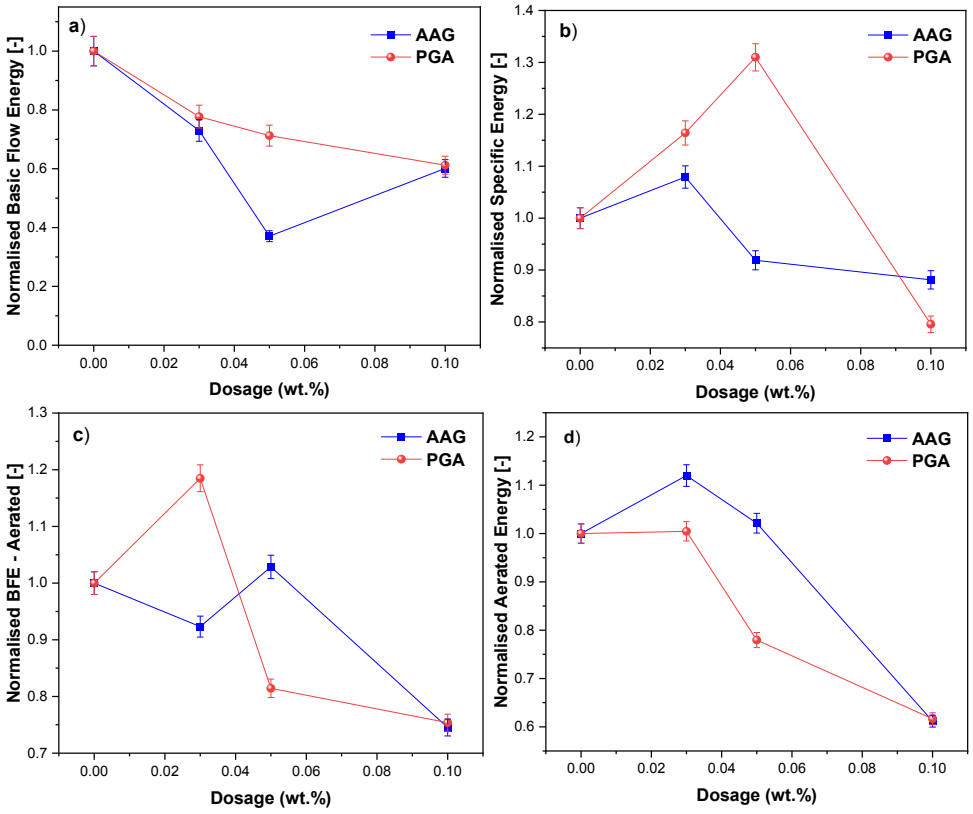

Figure 14. Effect of GAs on normalized flow indexes a) Basic flow rate, b) Specific energy, c) Aerated basic flow energy, and d) Aerated energy

4.2.1 Basic flow energy (BFE) and stability indices (SI)

The experimental results show that all grinding aids significantly reduce BFE, indicating improved flowability in the presence of GA of varying magnitude depending on the type and dosage (Figure 15). The higher BFE for the reference test (indicated by dashed lines) compared to the tests that included GAs indicates that the high resistance to flow is inherent in the ore powder. The BFE data for the different GAs with varying dosages show that AAG has an initial decrease in BFE followed by a sudden increase after 0.05 wt.%. On the contrary, increasing the concentration of PGA results in even lower basic flow energy for the investigated ranges. AAG reduces the flow energy requirement by 62.9 % at 0.05 wt.% dosage, whereas PGA has a 38.8 % reduction at 0.1 wt.%.

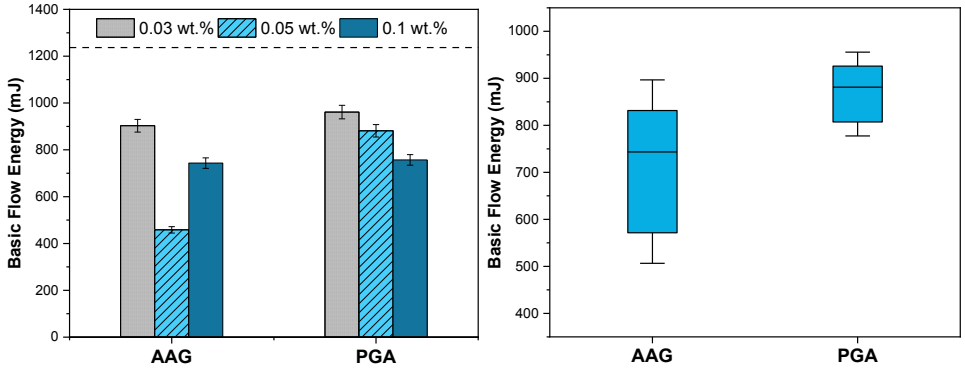

Figure 15. The basic flow energies for different GAs at varying concentrations

4.2.2 Specific energy

Specific energy (SE) measures the powder flowability when it is unconfined or at low-stress levels (i.e., the blade lifting the powder during its upward movement). SE is an accurate measurement for assessing the influence of cohesive/adhesive forces on interparticle interactions, as opposed to the compressibility of the BFE. Both BFE and SE depend on physical properties such as particle size, shape, and texture (Gnagne et al., 2017; Nan et al., 2017). Exploring the effect of GAs and their different concentrations on SE values shows that the reference test gives a value of 8.02 mJ/g, indicating that it has moderate cohesion forces (Figure 16). PGA demonstrated the lowest SE at 0.1 wt.% (6.38 mJ/g). The magnitude of cohesion is only reduced at certain concentrations and is greater than the reference test for some concentrations. While AAG decreases SE with increasing concentration, PGA increases at low concentrations but then decreases with increasing dosage. The fact that the SE decreases with an increase in the GA concentration agrees with the finding that GAs reduce interparticle forces, decrease the degree of cohesion, and improve flowability. These trends agree with the results reported by other investigations, which documented a decrease in SE when reduced cohesion (Katsioti et al., 2009; Prziwara et al., 2018b).

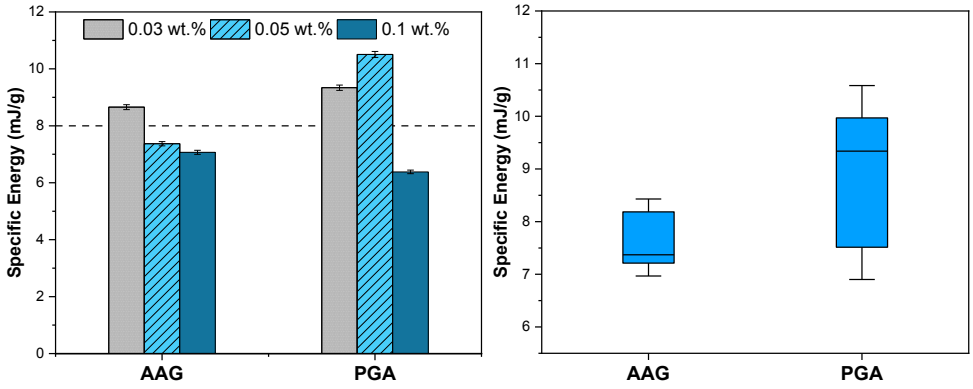

Figure 16. Influence of GAs on specific energy in different conditions.

4.2.3 *Aerated tests*

Since grinding is a dynamic process and, on an industrial scale, the dry milling process is air flow-assisted, the *aeration* test is considered adequate and informative to explore the potential effects of GA (Zhang et al., 2019). Generally, the GA experiments' A-BFE measurements are low compared to the reference test (except for PGA - 0.03 wt.%). This shows that the use of GAs can improve powder fluidization and facilitate transportation (Figure 17). Like the other energy measurements, A-BFE depends on cohesion, particle shape, texture, and density. In general, particles with more cohesive forces are difficult to fluidize (low AR and higher AE). For all GAs, 2 < AR < 20, which implies an average sensitivity to aeration, is typical for powders with moderate cohesion (Freeman and Technology, 2013). (Table 7).

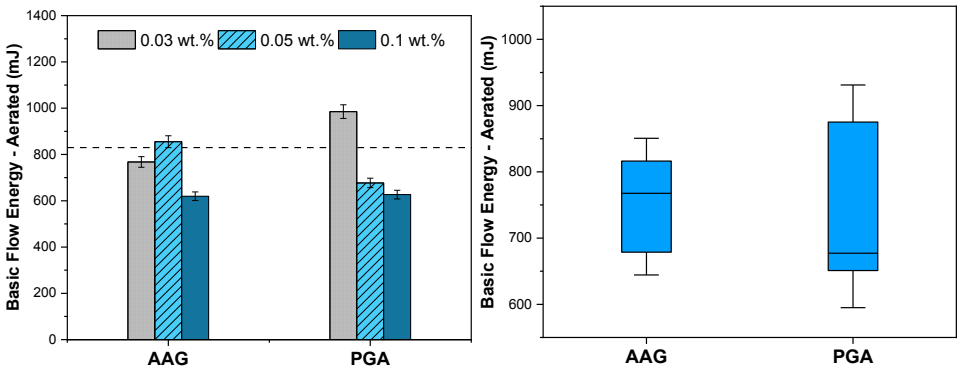

Figure 17. Influence of GAs on the aerated basic flow energy in different dosages.

Several studies have concluded that material transport (flowability) plays an important role in mill throughput and energy consumption in ball milling (He et al., 2004; Orumwense and Forssberg, 1992). As the particle size decreases during grinding, surface forces become more significant, leading to agglomeration and coating of grinding media, which reduces impact (Hasegawa et al., 2000; Prziwara et al., 2018b; Sohoni et al., 1991). The grinding process can be improved by improving the grinding rate or reducing the agglomeration rate. The influence of grinding aids on BFE, SE, A-BFE, and AE has been illustrated, which are a measure of surface forces and are known to retard size reduction in comminution (Kojima and Elliott, 2014, 2012; Prziwara et al., 2018a). However, an upper limit exists in terms of the GA concentration for each additive. This result agrees with the established knowledge of grinding performance that there is an optimum dosage for each GA. It shows that an optimum amount of GA molecules is required to adsorb on the particle surface to ensure the stabilization/neutralization of electrostatic charges.

Consequently, GA molecules continue to be beneficial as long as interparticle forces exist, after which negative effects begin to appear (Liu et al., 1989). It appears that excess GA results in less compressibility at higher dosages, creating a large flow zone, an increased volume fraction, and consequently, a high flow energy. On a mesoscopic scale, it can be concluded that grinding aids reduce particle-particle interactions via stabilization, thus aiding flowability. This phenomenon confirms the difficulties in determining the optimum GA dose as it depends on GA type, process conditions, and

particle surface properties, which are equally complex as determining bulk flow properties. These facts generate a need for a particle-scale-based study investigating the influence on breakage mechanisms. The study's findings support the conceptual premise that the main mechanism of grinding aids is based on the material arrangement properties, although inconclusive, to disprove other mechanisms. This term is supported by the good correlation between grinding efficiency (energy consumption and fineness) and flow indices (BFE, SE, A-BFE and AE). The grinding efficiency increases when the flowability to a maximum, after which it starts to decrease.

Table 7: Aeration test results for various conditions in the presence and absence of GAs.

Type of grinding aid	Dosage (wt.%)	Aerated energy (AR)(mJ)	Aeration ratio
Reference	0	106.7	7.6
AAG	0.03	119.5	6.4
	0.05	109.0	7.9
	0.1	65.3	9.6
PGA	0.03	107.2	9.4
	0.05	83.2	8.1
	0.1	65.8	9.6

Generally, powders with a stability index between 0.9 and 1.1 can be considered normal stable powders (Bian et al., 2015). All experiments show SI values outside this range, except for the tests using PGA at 0.05 wt.% (SI = 0.95) Table 8. In general, all experiments with AAG have low stability, indicating high chances of segregation or disintegrating during flow Table 8 (Freeman and Technology, 2007). However, the samples that contained PGA (0.95-1.35) indicated the minimum deviation from the SI range, suggesting a low tendency to agglomerate compared to the other GAs examined. The observed phenomena can be attributed to factors such as PSD, particle shape, and bulk density (Y. Liu et al., 2017). The different mixtures in addition to the PSD varied with GA and resulted in a narrower PSD compared to the reference test (Figure 13). Liu et al. (2017) used coal powders with different PSDs and showed that a small difference could significantly affect the flowability of the material. The wide PSD has a high isostatic tensile strength (a measure of cohesion) and compressibility, giving a denseer packing than a narrow PSD. Moreover, the high packing density implies efficient packing of the bed, which means that high values of BFE will be needed to move the bed. In the *stability and variable flow rate* testing, compressibility influences the measurements due to the flow zone, which depends on the material bed. The narrow PSD (better uniform particle size) in GA-containing samples may be related to improved flowability (Yun et al., 2018). From these results, it can be concluded that powders with GA require less energy compared to grinding without GA, resulting in improved flowability.

Table 8. Summary of the effects of grinding aids on the grinding parameters and flow indices

		Grinding parameters					Flow indices				
Condition	Dosage	Work index	Fineness	Size range, µm			BFE	SE	SI	A-BFE	AE
	wt.%	kWh/t	P_{80} µm	+150	-150+38	-38	mJ	mJ/g	[-]	mJ	mJ
Reference	0	18.0	181	21.9	53.2	24.9	1237	8.0	1.3	831	106.7
AAG	0.03	17.2	160	23.4	55.8	20.8	903	8.7	1.3	768	119.5
	0.05	13.2	156	25.0	53.6	21.4	458	7.4	0.4	855	109.0
	0.1	14.9	180	22.5	53.7	23.8	743	7.1	1.2	620	65.3
PGA	0.03	14.4	146	24.7	56.7	18.6	961	9.3	1.1	985	107.2
	0.05	14.3	144	25.3	56.3	18.4	881	10.5	0.9	677	83.2
	0.1	12.4	143	23.2	58.3	18.5	757	6.4	1.4	627	65.8

4.3. Correlating the flow properties and grinding parameters

As discussed, all GAs reduce the work index and increase product fineness during grinding; however, the value varies depending on the type and dosage of the GA. Table 8 shows a summary of the grinding parameters and flow indices of different blends. Although the flow properties depend on several factors and are not intrinsic properties, some correlations have been established between the grinding parameters and the flow indices. Pearson's correlation evaluations show that all sample work indexes correlate well with BFE and SE when $r > 0.70$ (Figure 18 & Figure 19). These indices reflect the ease of material movement (flowability) as the GAs reduce the cohesive forces. The linear correlation between the work index and BFE suggests that low BFE values would lower energy consumption. The SE also has a considerable correlation with the work index. This relationship implies that high SE values would result in lower energy consumption and finer particle size. These findings illustrate that too high flowability affects the size reduction efficacy. Taking into account the aeration test indices, significant correlations can be observed between the work index and fineness and the A-BFE and AE results, especially for the PGA case. This relation implies that the increase in fluidization results in improved transport, which also affects the grindability.

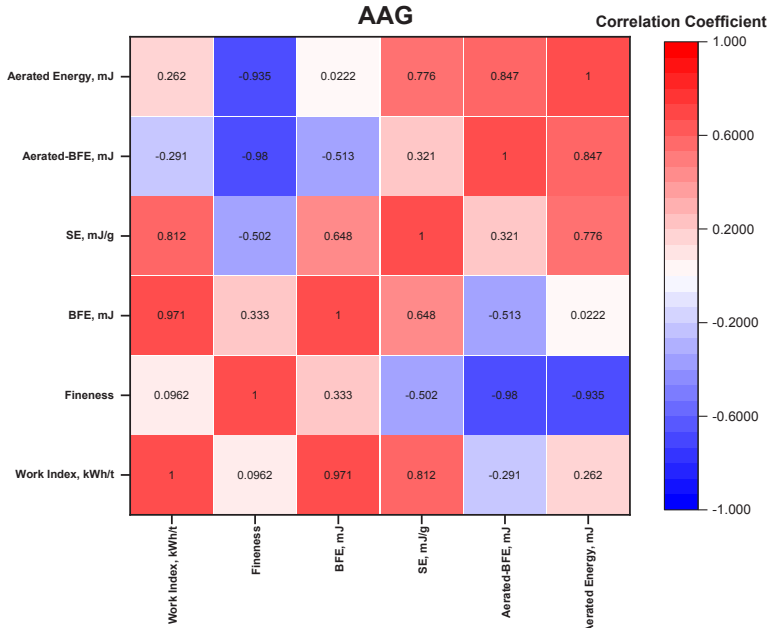

Figure 18. Pearson correlation of grinding parameters and flow indices for AAG

The results show that the use of an optimal grinding aid dosage reduces energy consumption and increases product fineness. The observed phenomena point to an optimum dosage; thus, flowability controls effective particle breakage. High dosages of GA result in high flowability, which affects particle capture. The particles are easily pushed out of the active grinding zone, resulting in a poor grinding efficiency illustrated in Figure 20. A significant correlation was found between grinding

efficiency (including work index) and flow indices. Grinding aids increase grinding efficiency by altering the flow properties, that is, reducing the flow energy and cohesive forces. In this regard, the main mechanism of GAs is based on the properties of the particle arrangement, although it is not conclusive to disprove other mechanisms. The predominant GA mechanism is based on the alteration of rheological properties.

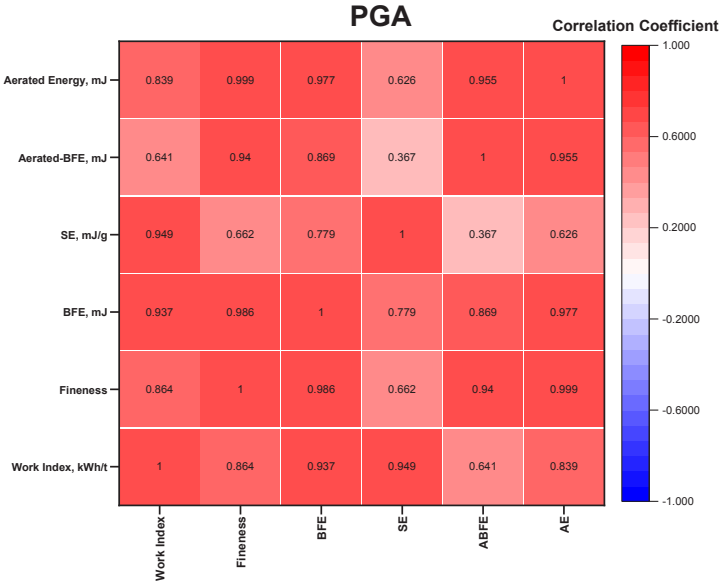

Figure 19. Pearson correlation of grinding parameters and flow indices for PGA

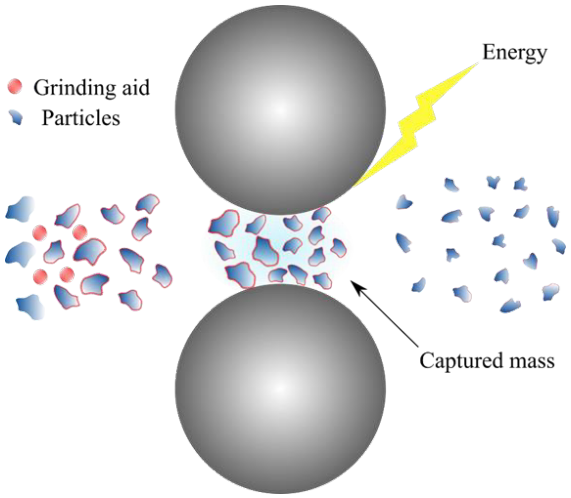

Figure 20. A schematic illustration of the particle-capturing concept concerning material flowability

4.4. Surface area and morphology

The effect of GAs on the specific surface area (SSA) was investigated using BET methods at 0.1 wt.% dosages Figure 21. For all size fractions, GAs generally increase the SSA which also increases with a decrease in particle size as expected. When comparing the two GAs, PGA has superior performance compared to AAG in all size fractions. The superior surface area with the application of grinding aids compared to blank conditions has been widely reported in the literature (Chipakwe et al., 2020a; Kapeluszna and Kotwica, 2022; Liu et al., 2021). Liu et al. (2021), during cobalt aluminate using sodium polyacrylate, the specific surface area was greater (39.56 m^2/g) compared to the blank condition (20.18 m^2/g). The observed increase in SSA supports the improved grinding performance with the generation of new surfaces (higher SSA) according to Rittinger's law (Wills and Finch, 2016). The increase in the SSA at a given energy is attributed to the reduced particle-particle interaction as a result of the enhanced stabilization and neutralization of surface charges.

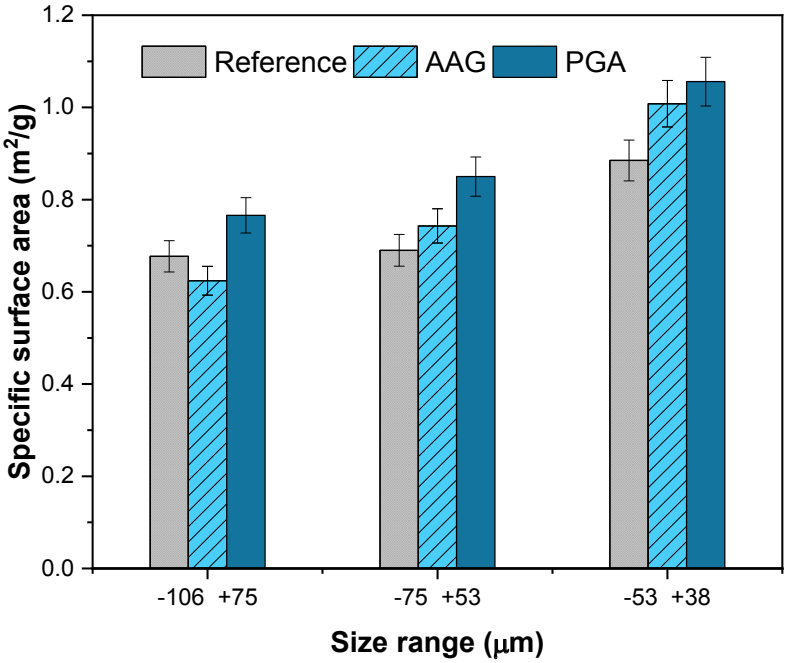

Figure 21. Variation of specific surface area with and without GAs at 0.1 wt.% dosage

The surface roughness of magnetite ore with different GAs was quantitatively determined from BET surface area measurements, bulk density, and mean particle size using Equation 2. GAs result in high surface roughness compared to the reference test, except for AAG at coarser size fraction, Table 9. The increase in surface area can explain the differences in surface roughness for various GAs compared to the reference sample of each size fraction. The surface morphology affects hydrophobicity, ultimately affecting downstream separation processes, especially flotation separation (Zhang et al., 2020). The resulting high surface roughness from using GAs improves the flotation

kinetics due to improved particle-bubble attachment (Ahmed, 2010; Feng and Aldrich, 2000; Hicyilmaz et al., 2006; Ulusoy and Yekeler, 2005).

Table 9. Specific surface area and roughness of ground magnetite ore under different conditions

Size fraction (µm)	Arithmetic mean size (µm)	Sample type	Specific surface area (A_B) (m^2/g)	Surface roughness (R_S)
-106 +75	90.5	Reference	0.677	45.667
		AAG	0.624	42.092
		PGA	0.766	51.671
-75 +53	64.0	Reference	0.690	32.915
		AAG	0.743	35.444
		PGA	0.850	40.548
-53 +38	45.5	Reference	0.885	30.014
		AAG	1.008	34.185
		PGA	1.056	35.813

SEM images were analyzed to further characterize the effect of GAs on morphological features. Figure 22 shows differences in the particle surface of the reference ground sample (Figure 22a) compared to the ground in the presence of GAs at 0.1 wt.% (Figure 22b and Figure 22c), with the latter showing roughening of the surfaces. The reference particle shows smoother surfaces with some fragmented smaller particles on the surface. Smaller particles on the surface suggest an attraction that points to agglomeration tendencies in the absence of GA. Cayirli (2022a) reported similar findings were reported by Cayirli, (2022a) on the effect of different grinding aids on the fine dry grinding of calcite. SEM analysis of ground samples showed more agglomerates in the blank compared to particles with grinding aids (Cayirli, 2022a). Certain grinding mechanisms, such as abrasion and impact, have been reported to influence particle shape and roughness (Semsari Parapari et al., 2020; Tong et al., 2021). The observed roughening for the GAs is consistent with the calculated roughness and the measured SSA, which are superior to the reference. The observed roughening could be attributed to the reduced contribution of abrasion as a result of the improved flowability with the introduction of GAs. Looking closely at the zoomed-out images, the GAs generally resulted in a more uniform and finer particle size distribution than the reference, consistent with the particle production (Figure 13).

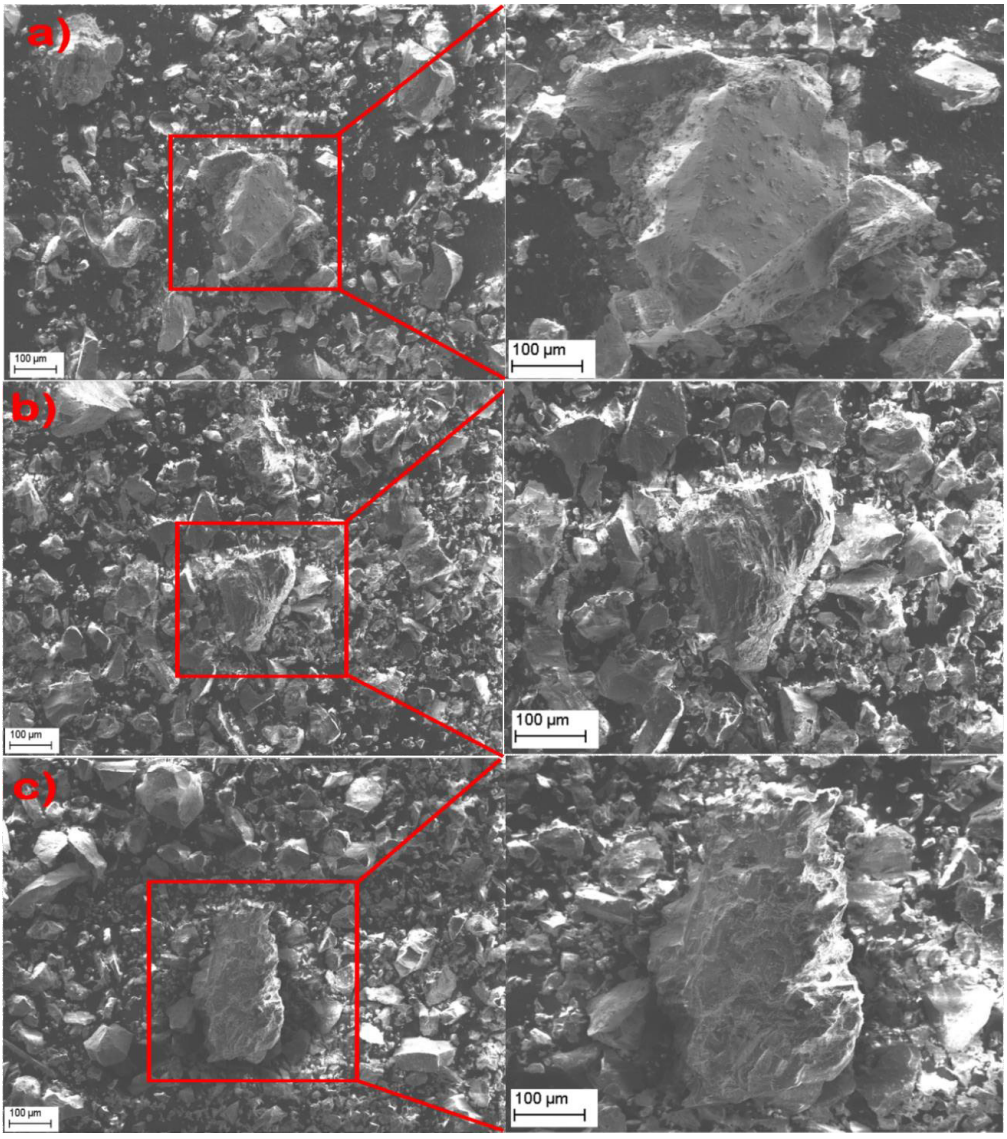

Figure 22. SEM images showing the effect of GAs on the ground product a) reference b) AAG and c) PGA at 0.1 wt.%.

4.5. Effect of Polysaccharide-based grinding aid (PGA) on flotation

4.5.1 Single mineral flotation

Single mineral flotation experiments were carried out to assess the effect of Lilaflot 822M (collector) and starch (depressant) in the absence and presence of PGA (fixed dosage at 100 mg/L). Figure 23a presents the single mineral flotation performance for magnetite and quartz as a function of the collector. With an increase in the Lilaflot

822M concentration, the recoveries of magnetite and quartz increased. As expected, the floatability of quartz under both conditions with and without PGA was markedly enhanced by increasing collector dosages (Lilaflot 822M is a silicate collector). In general, the floatability of quartz is comparable, although the presence of PGA resulted in lower floatability at lower collector concentrations. However, at high Lilaflot 822M concentrations, PGA significantly decreased magnetite floatability compared to quartz. In other words, these findings suggested that PGA has a depressive effect on magnetite, which may be beneficial considering that magnetite depression is the key to reverse flotation separation. To further explore the impacts of PGA through additional experiments, the Lilaflot 822M concentration (collector) was fixed at 50 mg/L, where quartz showed its highest floatability (recovery).

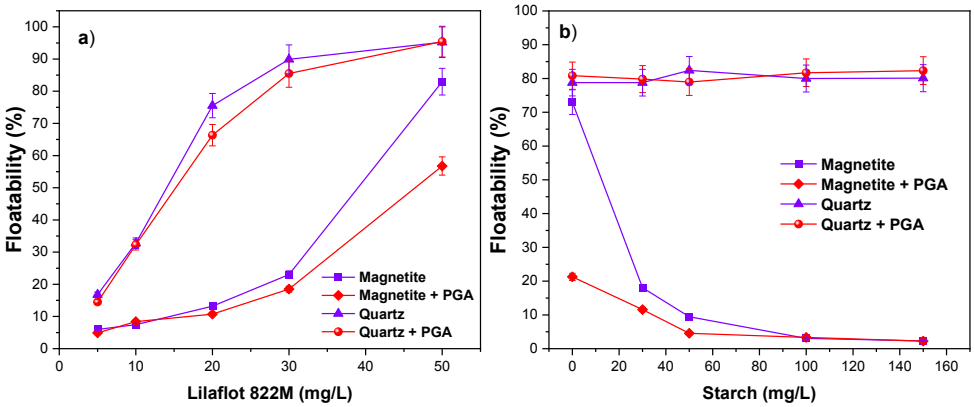

Figure 23. Floatability of magnetite and quartz as a function of a) collector concentration in the presence and absence of 100 mg/L PGA at pH 10 and b) depressant concentration in the presence and absence of 100 mg/L PGA at pH 10 and collector concentration of 50 mg/L.

Furthermore, the floatability of magnetite and quartz as depressant functions with fixed collector and PGA doses was investigated (Figure 23b). As expected, starch and PGA do not affect the floatability of quartz. The floatability of magnetite decreased significantly with increasing starch concentration, confirming the effectiveness of starch as a depressant. For the reference test, the floatability of magnetite continued to decrease with starch addition to a minimum of 2.3 % at 100 mg/L. The depressing impact of PGA and its floatability could be detected (Figure 23b). A significant decrease in magnetite recovery to 21.3 % without starch compared to 73.0 % for the reference test could confirm the depressing effect of PGA. It can also be seen that the maximum depression effect of starch was observed at 100 mg/L, while with the addition of PGA, a comparable depression effect was achieved at 50 mg/L. Generally, single-mineral flotation tests indicated that increasing PGA has a favorable outcome in magnetite depression without changing quartz floatability.

4.5.2 Mixed mineral flotation

Subsequently, mixed mineral flotation experiments were carried out to assess the effect of PGA on the model ore (magnetite: quartz 2:1 mass ratio) Figure 24. Based on the results of the single mineral flotation, 30 mg/L (which translates to 300 g/t) were

considered for the dosages of starch and PGA dosages varied at pH 10. The variation in magnetite metallurgical recovery (as Fe) as a function of PGA and starch dosage is presented in Figure 24a. The results indicated that the recovery of Fe (magnetite hydrophilicity as sinks) improved with increasing the PGA dosage without starch. However, the improvement was negligible after 300 g/t PGA. In the presence of starch, recovery variations were not significant. Higher grades of Fe without starch were reported, although recovery is generally lower (Figure 24b). In other words, no obvious changes could be achieved by increasing the starch concentration from 500 to 1000 g/t. It could be translated as PGA that improves grinding performance and further reduces depressant consumption.

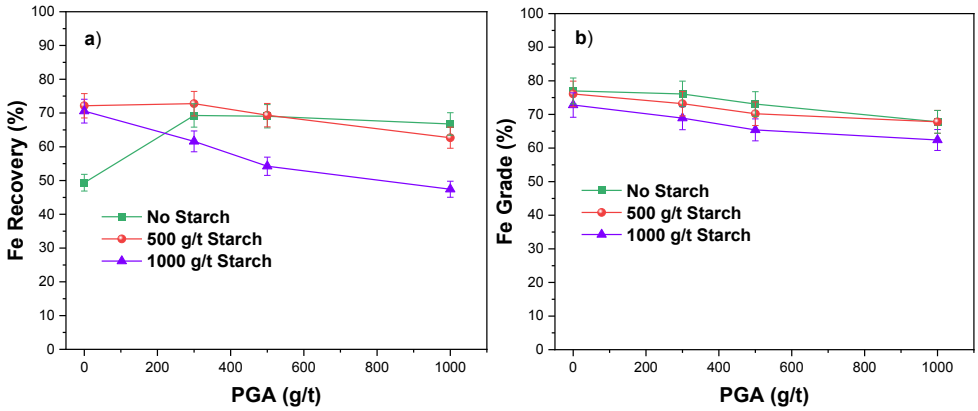

Figure 24. Effect of PGA and starch on magnetite flotation at a fixed amount of collector (300 g/t) at pH 10.

Furthermore, the selectivity of the process was calculated using Equation 3 to better understand the interaction of PGA and starch and their resulting synergistic effects on separation (Figure 25). The flotation results indicated that PGA dosages below 300 g/t could improve selectivity with/without starch. In the absence of PGA starch dosage above 500 g/t is required for better process selectivity. The results also suggest that PGA can give an acceptable selectivity (> 64 %) without starch. It can be observed that high doses of both PGA and starch were not desirable. The highest selectivity can be observed when starch and PGA were 500 and 300 g/t, respectively. The observed improvements in flotation separation corroborate findings reported elsewhere on the beneficial effects of a narrow particle size distribution (Cayirli, 2022b; Prziwara et al., 2019) and surface roughness (Tong et al., 2021; Zhu et al., 2020). In addition to the superior properties observed from the use of PGA, surface analyses were considered to assess the interaction of PGA with mineral surfaces.

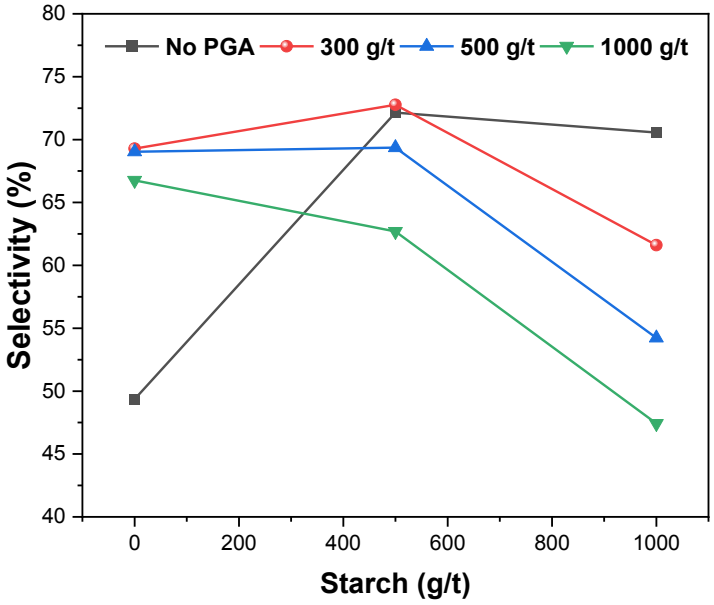

Figure 25. Effect of PGA on selectivity with varying depressant concentration.

4.5.3 Zeta potential measurements

Zeta potential measurements were performed to further explore the interaction mechanism between PGA, Lilaflot 822M, and mineral particles to understand the observed flotation behavior. It is important to assess how these surfactants change the surface properties that affect flotation behavior. The zeta potential indicated (Figure 26) that the addition of PGA slightly affects the electrical charge on the surface of quartz and magnetite, implying a change in the solution, the surface chemistry, or both. These negligible effects could be due to the non-ionic composition of the PGA. The zeta potentials for quartz decreased (absolute value) after PGA treatment. Evaluations illustrated that the zeta potentials decreased sharply from 0 to 15 mg/L (PGA concentration) for both minerals, with quartz changing from -59.5 to -51.6 mV ($\Delta\zeta \sim +7.9$ mV) while magnetite changed from -44.9 to -35.6 mV ($\Delta\zeta \sim +9.3$ mV). The ζ measurements demonstrated that the addition of PGA to both minerals above 30 mg/L has almost no further effect in the investigated ranges. Adding Lilaflot 822M to the system gives more positive zeta potentials, especially for quartz. This illustrated that PGA had an insignificant effect on quartz, evident from the marked effect of Lilaflot 822M adsorption on the surface as a collector. A similar behavior could be observed with the addition of PGA, where the zeta potentials decreased with increasing PGA concentration. The relatively smaller change in magnetite zeta potentials compared to quartz after Lilaflot 822M indicated that the presence of PGA reduced the interaction between Lilaflot 822M and magnetite. This highlighted that PGA adsorbed on magnetite rather than on the quartz surface based on the impact of the collector.

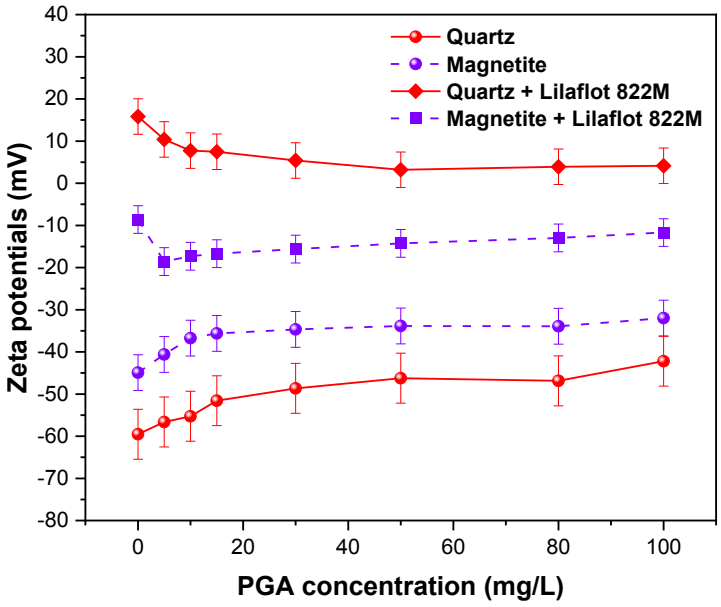

Figure 26. Zeta potentials at varying PGA concentrations with fixed Lilaflot 822M (50 mg/L) and pH

4.5.4 Stability measurements

The Turbiscan stability index (TSI) evaluations (Figure 27) showed that treatment of both particle surfaces results in decreased stability compared to the reference (without PGA treatment). Observations are expected for any suspension since destabilization illustrated the effect of flocculation, coagulation, sedimentation, coalescence, and even a combination (Ataie et al., 2020; Bastrzyk and Feder-Kubis, 2018). Figure 27 shows the destabilization kinetics of magnetite and quartz suspensions as a function of time. TSI values demonstrated that a relatively stable system was in agreement with the zeta potential results (Figure 26) for both quartz and magnetite, which are all below -30 mV at pH 10, showing high stability (Tucker et al., 2015; Uskoković, 2012). The TSI values for magnetite are higher than those for quartz and generally show less stability. After PGA treatment, the stability variation was more pronounced for magnetite compared to quartz for the total investigated time of 60 min. In other words, these results suggested that the destabilizing effect of PGA was more pronounced on magnetite than on quartz, pointing to increased adsorption. This is consistent with the zeta potentials, which showed a higher absolute value for quartz relative to magnetite, indicating better suspension stability. When magnetite particles, the increase in TSI values (reduced dispersion) could help explain the depression effect of PGA, which might be due to aggregation/flocculation, thus hindering flotation. Similar observations have been reported in which polysaccharides interact with iron oxides from aggregations (Engwayu and Pawlik, 2020; Tohry et al., 2021).

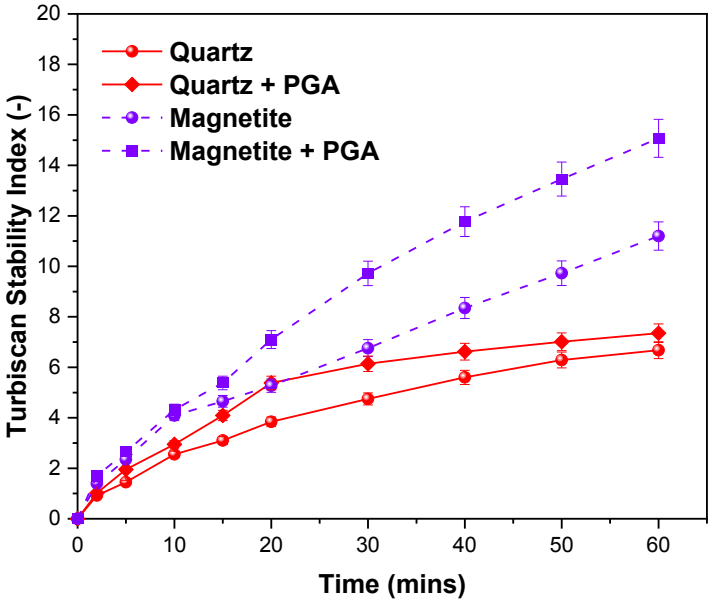

Figure 27. Stability of magnetite and quartz suspensions in the absence and presence of PGA (100 mg/L and pH 10).

4.5.5 Adsorption measurements

Figure 28 shows an increase in adsorbed PGA per unit mass of magnetite and quartz. Furthermore, it could be observed that the adsorption capacity of magnetite was more than double that of quartz. For magnetite, a trend of continued increase can be demonstrated based on the still high slope beyond 3 mg/ml, while for quartz, the curve started plateauing after 2 mg/ml. The results of the adsorption isotherms using the depletion method were fitted to the Langmuir and Freundlich models and are summarized in Table 10. The Langmuir model gave the best fit with R^2 of 0.9651 and 0.9721, while the Freundlich model had R^2 of 0.9085 and 0.8506 for magnetite and quartz, respectively. The trends observed in Figure 27 were also supported by the calculated parameters of the Langmuir and Freundlich models (Table 10). The obtained values of the parameters n and Q_m (which highlighted the strength and capacity of adsorption, respectively) were higher for magnetite than those of quartz, which suggested that the adsorption of PGA on magnetite was much stronger. The findings from the adsorption studies showed that PGA fairly adsorbs on both magnetite and quartz, further confirming the effect of PGA on single-mineral flotation, possibly reducing the surface areas available for collector adsorption, especially for magnetite. These results corroborated the zeta potentials and stability measurement findings that magnetite had a higher and stronger adsorption capability for PGA than quartz.

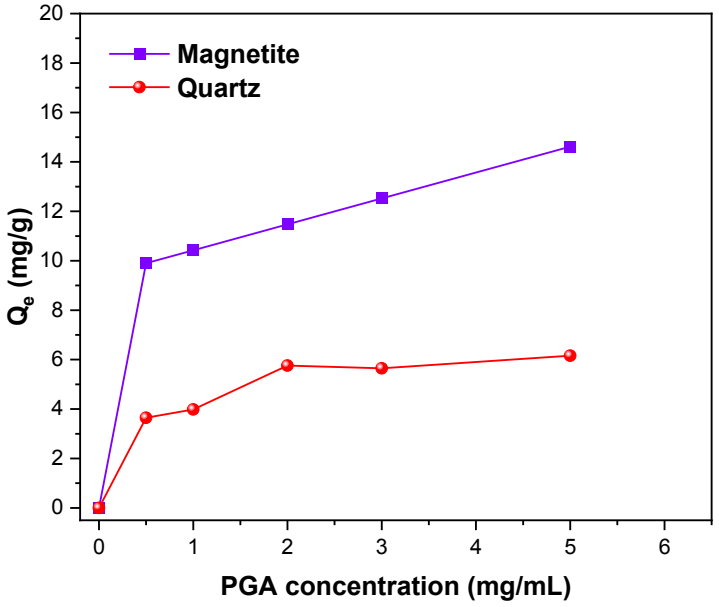

Figure 28. Adsorption of PGA as a function of initial concentration at pH 10

Table 10. Langmuir and Freundlich parameters for PGA adsorption on magnetite and quartz

Particles	Langmuir equation			Freundlich equation		
	Q_m	K_L	R^2	n	K_F	R^2
Magnetite	12.10	9×10^{-1}	0.9651	6.00	3.43	0.9085
Quartz	5.85	6.6×10^{-3}	0.9721	5.18	1.25	0.8506

4.5.6 FTIR Spectra Analysis

The adsorption mechanism of PGA was investigated together with the collector on both magnetite and quartz surfaces. Figure 29a shows the spectra for pure quartz, quartz + PGA, quartz + PGA + Lilaflot 822M, together with the respective pure reagents. For PGA, the main characteristic peaks showed a broad peak between 3000 and 3600 cm^{-1}, demonstrating a hydroxyl group (İspirli et al., 2019; Yilmaz et al., 2021) - OH stretching vibration and appearing at 3308 cm^{-1}. A distinct characteristic peak appeared at 2928 cm^{-1}, related to the C-H stretch vibration (Kavitake et al., 2016; Yilmaz et al., 2021). Furthermore, the C-O stretching vibration was illustrated at 1643 cm^{-1} (Wang et al., 2010). A peak emerged at 1346 cm^{-1} that could be assigned to the symmetric CH_3 bending (İspirli et al., 2019). Strong characteristic peaks emerged at 1006 cm^{-1} and 918 cm^{-1} in the region 950-1100 cm^{-1}, which was attributed to the C-O-C and C-O groups of polysaccharides (İspirli et al., 2019). The peak in the region 950-1100 cm^{-1} was due to the presence of the (1→6)- and (1→3)-linked α-D-glucose units, respectively (Das and Goyal, 2014; Miao et al., 2014). For Lilaflot 822M, characteristic peaks emerged at 2964 cm^{-1} and 2869 cm^{-1}, which were attributed to the CH_2 stretching

bond of the acyclic compounds (X. Liu et al., 2017). The peak at 1587, 1464, and 653 cm^{-1} could be attributed to the bending of the NH_2 or NH bonds (Huang et al., 2014; Liu et al., 2016; X. Liu et al., 2017). It is evident from Figure 29a that the presence or absence of PGA on the quartz surface had no effect, as there is no observable change in the spectra. After treatment with Lilaflot 822M, a characteristic peak was observed on the quartz surface. After treatment of quartz with Lilaflot 822M, the characteristic peak of OH at 2964 cm^{-1} shifted to 2960 cm^{-1} as observed in quartz + PGA + Lilaflot 822M, which was consistent with the findings reported by (X. Liu et al., 2017). Furthermore, the characteristic stretching of CH at 2869 cm^{-1} also changed to 2856 cm^{-1} after treatment. This indicated that Lilaflot 822M was adsorbed on the quartz surface through the OH and CH bonds. Compared to Lilaflot 822M, PGA did not show a characteristic peak, given the water washing in the procedure, which meant that Lilaflot 822M was chemically adsorbed and collaborated with the finding documented by (Huang et al., 2014) and (X. Liu et al., 2017) on the adsorption of amines on the quartz surface. In contrast, the absence of a characteristic PGA peak on the quartz surface suggested that PGA did not chemically adsorb on the quartz surface. This points to the slightly weak physisorption of PGA on the quartz surface.

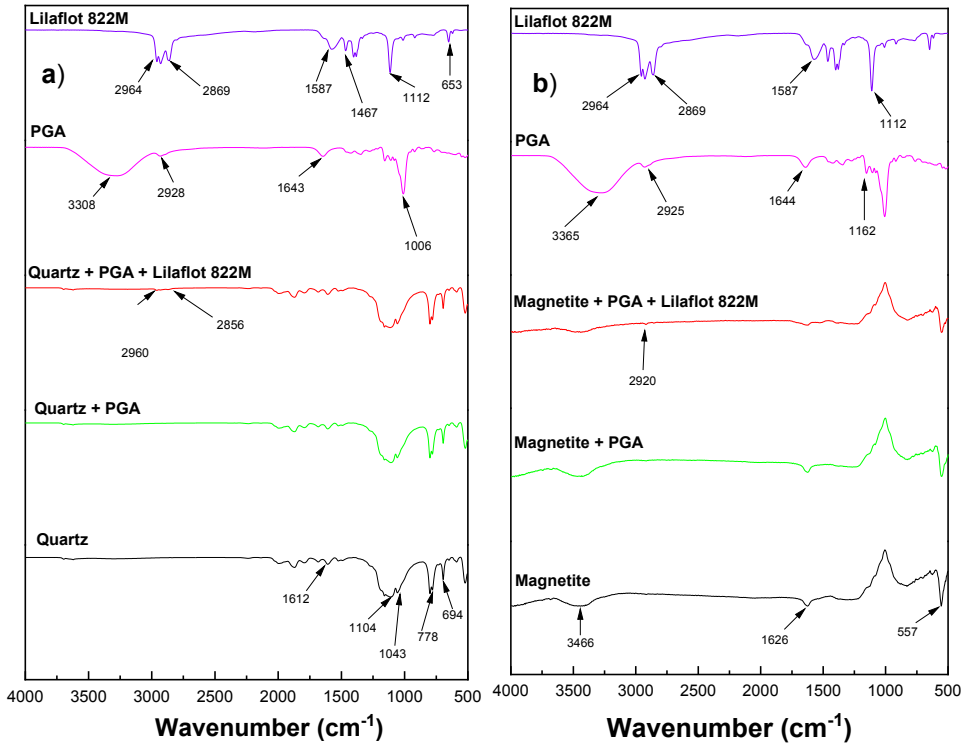

Figure 29. FTIR spectra of a) quartz and b) magnetite in the presence and absence of PGA and Lilaflot 822M (at 100 mg/L).

FTIR spectra for magnetite in the presence and absence of PGA and Lilaflot 822M (Figure 29b) indicated that there was no characteristic peak in magnetite treated with PGA, and therefore there was no impact from PGA. Furthermore, Lilaflot 822M had a

negligible impact on the magnetite surface, as evidenced by the relatively weak characteristic shifted peak at 2920 cm^{-1}. Negligible characteristic peaks on magnetite meant weak adsorption, especially compared to Lilaflot 822M adsorption on the quartz surface. The absence of a characteristic peak on magnetite in the presence of PGA suggested that PGA did not adsorb chemically but possibly had a physical interaction. From the IR analysis, it can be said that the interaction mechanism was not chemical for both quartz and magnetite with PGA. However, considering that the particles were subjected to a thorough washing with water before analysis, the interaction could be physical, probably due to hydrogen bonding. Shrimali and Miller (2016), in their concise review of the interaction of polysaccharides and iron ores, outline that polysaccharide adsorption may be due to hydrogen bonding, hydrophobic interaction, or chemical complexing (acid-base reaction). The hydrophobic interaction might play a major role in reducing the surface charge, allowing flocculation/aggregation of the particles, thus leading to magnetite depression. This is consistent with observations suggesting that the mechanism of nonionic polymer adsorption would be due to the hydrophobic chain interaction leading to the bridging and/or charge neutralization (Chimonyo et al., 2020; Filippov et al., 1997; Hanumantha Rao and Forssberg, 1997).

4.6. Effect of Polyacrylic-based grinding aid (AAG) on flotation

4.6.1 Single mineral flotation

The flotation experiments were conducted on single minerals to study the effect of AAG in the ether-amine (Lilaflot 822M) system for quartz and magnetite at pH 10 (Figure 30a). The results demonstrated that by increasing the Lilaflot 822M concentrate as a collector, both the quartz and magnetite recoveries increase, in addition to the absence or presence of AAG. Further analyzes reveal that the addition of AAG increases the floatability of quartz and magnetite (Figure 30a). The observed increase in the floatability of quartz in the presence of Lilaflot 822M (an ether amine) corroborates the literature findings showing the efficacy at pH 10 (Tohry et al., 2021; Vieira and Peres, 2007). Quartz recovery reached a maximum of 90 % at 20 mg/L of the collector in the absence of AAG, while it would be 92 % at 10 mg/L of the collector in the presence of AAG. In other words, higher recoveries were achieved in the presence of AAG at a lower collector concentration. Similar behavior is observed for magnetite floatability, which at 20 mg/L collectors, its recovery increases from 15 to 80 % in the absence and presence of AAG, respectively. Generally, in both scenarios, the presence of AAG enhances the floatability of both quartz and magnetite.

In addition to the system, the effect of AAG on the flotation behavior of quartz and magnetite in the presence of a depressant was investigated. Starch was utilized as a depressant to address the undesirable floatability of magnetite in the reverse flotation setup. The floatability was investigated as a function of starch concentration at a fixed collector concentration of 20 mg/L and pH 10. As expected, a minimum effect was observed on quartz floatability with some decreases at concentrations above 80 mg/L (Figure 30b). For the reference sample, starch was effective in depressing magnetite, giving the lowest floatability of 3 % at 50 mg/L. In the presence of AAG, magnetite floatability was found to be quite high, with the lowest floatability of 2 % achieved only at 100 mg/L starch concentration. Evidently, the presence of AAG results in

increased starch dosages. The single mineral flotation test showed that the application of AAG improved the collection of quartz and magnetite even at a lower collector dose. However, it was also observed that the addition of AAG increases the amount of depressant to counteract the improved magnetite collection. Artificial mixtures were used in subsequent flotation tests to gain a complete understanding of the behaviors observed in single-mineral flotation.

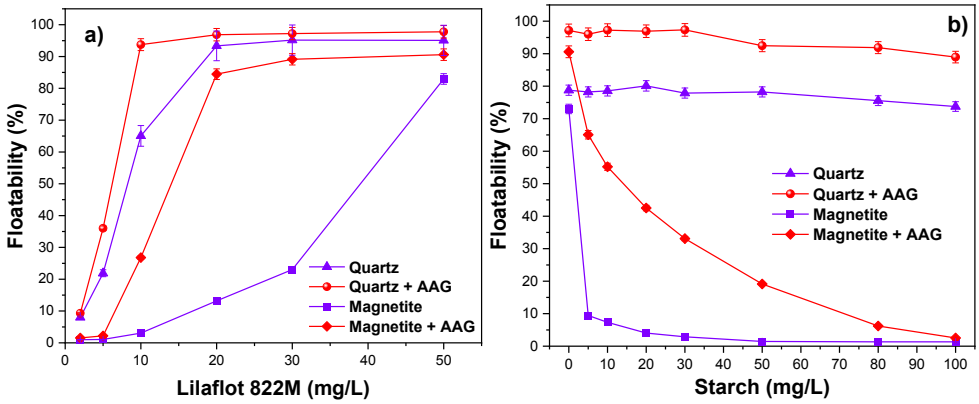

Figure 30. Single mineral flotation of magnetite and quartz as a function of a) varying collector concentration and b) varying depressant concentration in the presence and absence of 100 mg/L AAG at pH 10 and collector concentration of 50 mg/L.

4.6.2 Mixed mineral flotation

Mixed mineral flotation of magnetite and quartz mixture with a mass ratio of 2:1 to determine the effect of improved separation of quartz from magnetite. As shown in Figure 31, the addition of AAG influences both recovery and grade. The result of the reference sample test shows that the recovery initially increases with increasing collector concentration to a maximum of 93.3 % at 200 g/t, which starts to decrease. The addition of AAG improves recovery, especially at lower collector doses, supporting the findings of single-mineral flotation. At 500 g/t of AAG, a comparable maximum recovery of 92.1 % is achieved at a collector dose of 100 g/t. Adding AAG to all investigated collector concentrations, less than 200 g/t, results in higher recoveries than the reference sample. Figure 30b agrees with the findings on the grades that increase with increasing collector and AAG concentrations. As in reverse flotation, the observed increase in grade is accompanied by a decrease in the mass recovery, thus ultimately decreasing the metallurgical recovery. The results indicate that AAG enhances the collection of quartz and, to a lesser extent, the collection of magnetite.

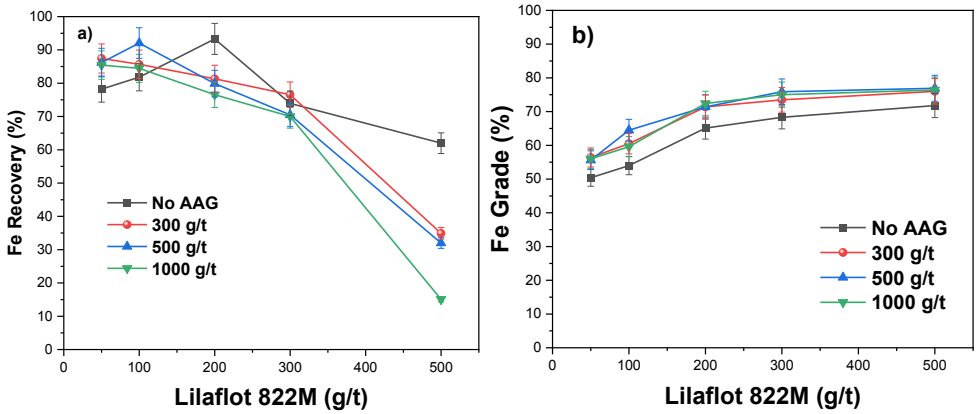

Figure 31. Flotation results of the mixture in the presence and absence of AAG and varying collector dosage at pH 10

Further evaluation of the selectivity of the process based on Equation 3 is presented in Figure 32. It can be observed that at lower collector dosages (below 300 g/t) the presence of AAG increases the process selectivity. However, it should be noted that, above 300 g/t collector, the presence of AAG becomes detrimental to the process selectivity. For all scenarios, the best selectivity is reported between 200 and 300 g/t collector with a maximum of 76.2 % at 300 g/t AAG and 200 g/t collector. The results indicate that AAG enhances the collection of quartz and, to a lesser extent, the collection of magnetite. The selectivity variations at different AAG and collector dosages suggest synergistic interactions in the system. To better assess the observed effect of AAG on the separation of quartz from magnetite, surface analysis of the mineral surfaces was considered.

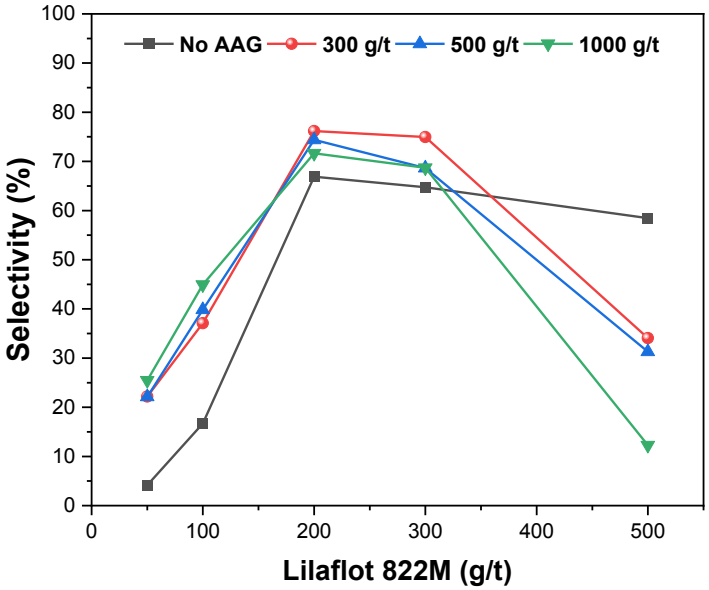

Figure 32. Effect of AAG on selectivity with varying collector concentration.

4.6.3 *Zeta potential measurements*

The effect of AAG on the colloidal stability of quartz and magnetite particles was carried out using zeta potentials from electrophoresis measurements. The change in zeta potential as a function of AAG concentration at pH 10 and 50 mg/L Lilaflot 822M is presented in Figure 33. For all conditions, it can be observed that the zeta potentials decreased (more negative and increase in magnitude) when the AAG concentration was increased. For the reference test, quartz and magnetite have zeta potentials of -43.2 and -46.5 mV compared to -83.5 and -74.6 mV at 100 mg/L AAG respectively. The trend shows that the presence of AAG enhances the stability of the suspension regardless of the type of mineral. A similar shift in the zeta potentials is observed for both minerals as Lilaflot 822M (a collector); however, the results show a more pronounced change for quartz, indicating increased adsorption of Lilaflot 822M as a collector on its surface. From these observations, it could be considered that the addition of AAG results in an increased negative charge, especially on quartz, which could promote the interaction with the collector and improve its floatability.

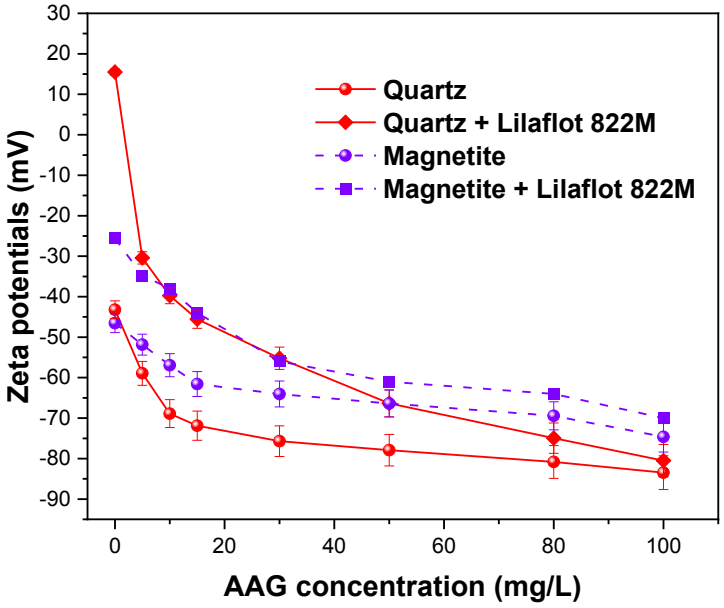

Figure 33. Variation of zeta potentials as a function of AAG concentration at pH 10

4.6.4 *Stability measurements*

To further understand the effect of AAG on mineral suspensions, stability studies were conducted based on the Turbiscan stability index. The variation in the Turbiscan stability index as a function of AAG in quartz and magnetite suspensions is presented in Figure 34. A similar behavior can be observed as the presence of AAG results in stabilization of the suspension (reduction in TSI), which corroborates the findings from the zeta potentials. The change is more pronounced for quartz surfaces than for magnetite surfaces. These findings corroborate the claim in the literature that PAA-derived polymers impart stability as a dispersant (Wu et al., 2010). The observed

decrease in stability also points to increased dispersibility with the introduction of AAG, which can also increase the quartz recovery.

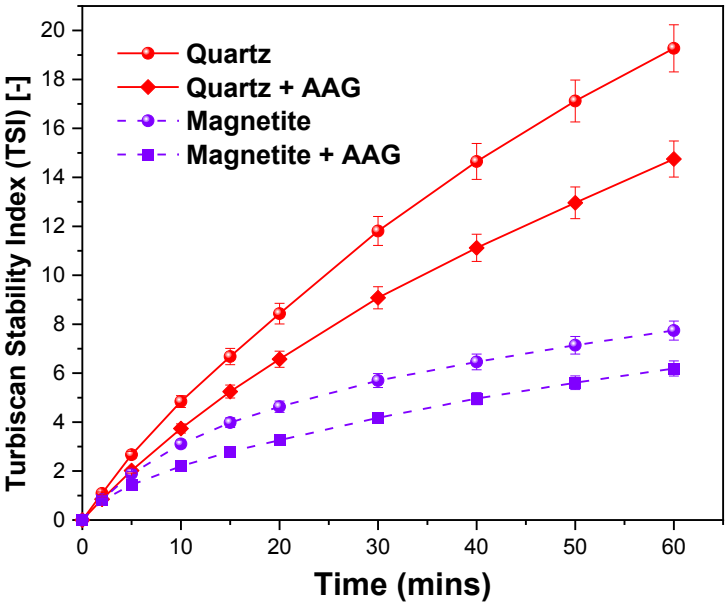

Figure 34. Stability of quartz and magnetite suspensions in the absence and presence of AAG (100 mg/L and pH 10).

4.6.5 Adsorption measurements

The flotation and suspension stability results showed a pronounced effect of AAG on quartz relative to magnetite. To better understand the phenomenon, adsorption measurements were performed on both mineral surfaces after treatment with varying concentrations of AAG at pH 10. Figure 35 shows how the amount of AAG adsorbed per unit of mass increases with the AAG concentration. It is evident that quartz has a high adsorption capacity with respect to magnetite in the investigated concentration. Furthermore, the adsorption isotherms are fitted to the Langmuir and Freundlich models (Table 11). From the Langmuir model, the adsorption capacity (Q_m) is higher for quartz compared to magnetite, with 3.45 and 3.19, respectively. Similarly, the Freundlich model shows stronger adsorption (n) for quartz compared to magnetite, with 5.20 and 4.72, respectively. The Langmuir model gave the best fit with R^2 of 0.9711 and 0.9701, while the Freundlich model had R^2 of 0.8851 and 0.8365 for quartz and magnetite, respectively. These findings show that AAG adsorbs on both quartz and magnetite, supporting the observed effects on the flotation behavior. The superior adsorption of AAG on quartz in comparison to magnetite particles further explains its pronounced effect.

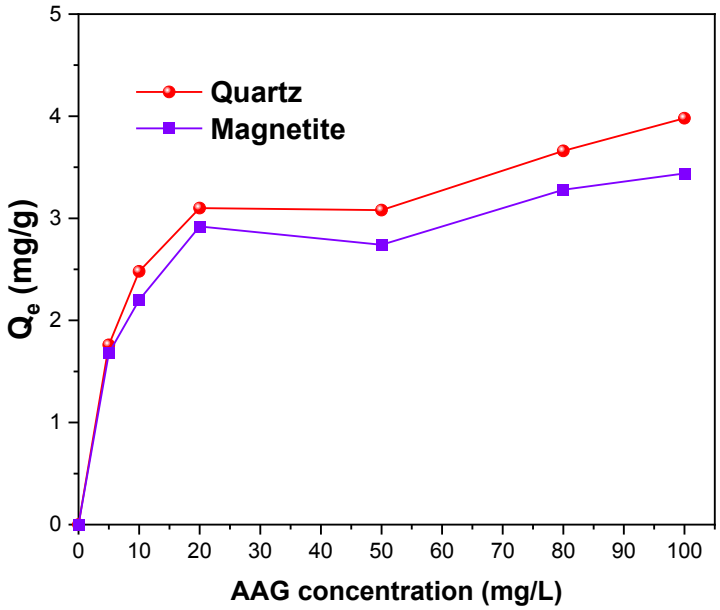

Figure 35. Adsorption of AAG as a function of initial concentration at pH 10

Table 11. Langmuir and Freundlich parameters for AAG adsorption on quartz and magnetite.

Particles	Langmuir equation			Freundlich equation		
	Q_m	K_L	R^2	n	K_F	R^2
Quartz	3.45	0.718	0.9711	5.20	1.70	0.8851
Magnetite	3.19	0.315	0.9701	4.72	1.33	0.8365

4.6.6 FTIR Spectra Analysis

The adsorption results showed that AAG has stronger adsorption on quartz surfaces than on magnetite surfaces. Fourier transform infrared (FTIR) spectra were performed to better understand the adsorption mechanism. Figure 36a shows the spectra for pure quartz, quartz + AAG, quartz + AAG + Lilaflot 822M, together with the respective pure reagents. For Lilaflot 822M, characteristic peaks emerge at 2964 cm^{-1} and 2869 cm^{-1}, which are attributed to the CH_2 stretching bond of the acyclic compounds (X. Liu et al., 2017). The peak at 1587, 1464, and 653 cm^{-1} can be attributed to the bending of the NH_2 or NH bonds (Huang et al., 2014; Liu et al., 2016; X. Liu et al., 2017). A characteristic peak is observed at 1548 cm^{-1} and 1168 cm^{-1} for AAG, which could be due to the deprotonated C=O and C-O bond, respectively, since this was at pH 10 (Zhu et al., 2022). It is evident from Figure 36a that the introduction of AAG on the quartz surface has no new effect since no observable functional group is generated. After treatment with Lilaflot 822M, a characteristic peak is observed on the quartz surface.

The characteristic peak of OH at 2964 cm^{-1}, changes to 2960 cm^{-1} as observed in quartz + AAG + Lilaflot 822M, which is consistent with the findings in the literature (Liu et al., 2016). A similar effect is observed for magnetite + AAG + Lilaflot 822M with a characteristic peak from the introduction of the collector Figure 35b. Furthermore, the characteristic stretching of CH at 2869 cm^{-1} also changes to 2856 cm^{-1} and 2920 cm^{-1} for quartz and magnetite, respectively, after treatment. The spectra suggest a weaker Lilaflot 822M-magnetite interaction than the Lilaflot 822M-quartz interaction. The absence of a characteristic peak after treatment with AAG on both minerals implies that the interaction between AAG and the minerals is not chemical and thus physical adsorption.

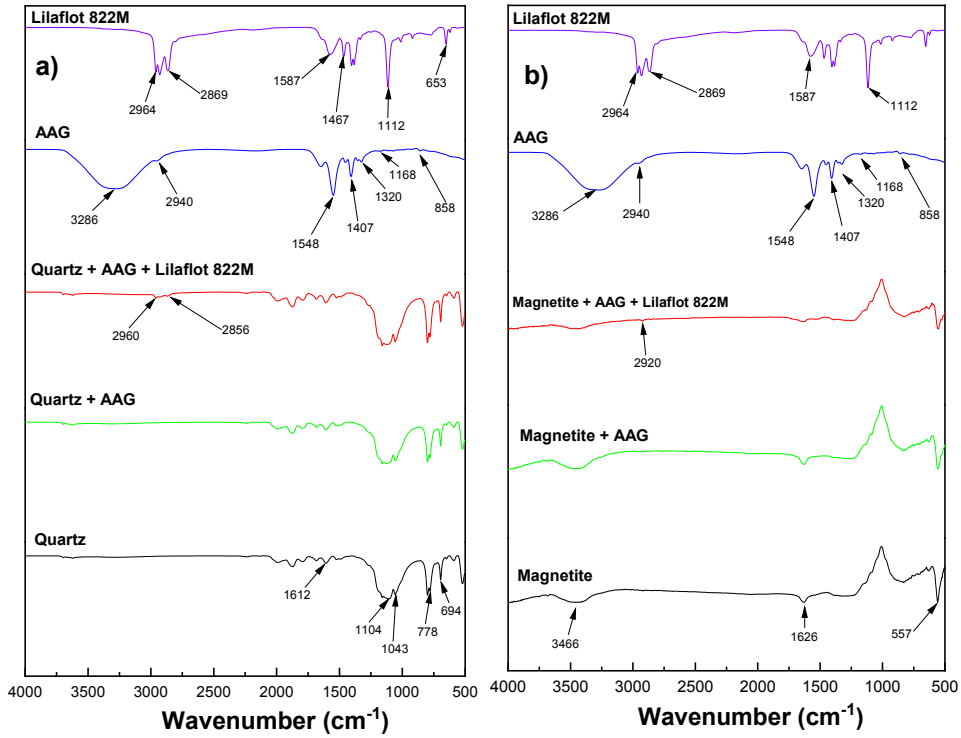

Figure 36. FTIR spectra of a) quartz and b) magnetite in the presence and absence of AAG and Lilaflot 822M (at 100 mg/L).

Some interactions are evident from the observed behavior when AAG is added to both quartz and magnetite. The introduction of AAG markedly enhances the floatability of quartz with a minimal effect on magnetite. Mixed mineral flotation showed that at 500 g/t of AAG, a comparable maximum recovery of 92.1 % is achieved at a collector dosage of 100 g/t. Surface analyzes revealed that AAG adsorbs on mineral surfaces, increases the zeta potential (more negative), and increases the suspension stability. This is consistent with observations reported elsewhere suggesting that AAG increases dispersion and anionicity due to its anionic nature, thus increasing collector adsorption and ultimately improving flotation (Somasundaran and Lee, 1981; Zhu et al., 2022).

5. CONCLUSIONS & FUTURE WORK

The main hypothesis of this research work was that the use of chemical additives as grinding aids could address the drawbacks associated with dry grinding without adverse effects on downstream processes. The research work carried out can be divided into the investigation of grinding performance, the characterization of the mill product, and the effects on flotation separation. The conclusions of the present study are presented together with recommendations for future work.

In general, grinding aids have some additional benefits, in addition to reducing energy consumption, such as improving grinding efficiency, improving material flowability, and narrowing the particle size distribution. These effects can mainly improve the grinding efficiency under selected conditions. The results showed that such additives address the shortcomings of dry grinding in size reduction units. These results highlighted that the selection of suitable grinding aids (ecofriendly) could potentially reduce energy consumption (thereby reducing CO_2 emissions) and improve the distribution of suitable particles for downstream processes, without negative chemical impacts (even positive effects) on subsequent separation stages.

5.1. Answers to Research Questions

RQ1: How effective are grinding aids at reducing energy consumption during dry grinding?

Work index calculations indicate that using the GAs reduces the energy consumption for all the additives compared to the reference test. The extent of energy reduction is affected by both the type of grinding aid and the dosage. In terms of type of GA, PGA and AAG had a reduction of 31.1% and 26.6%, respectively, compared to the reference. Grinding tests showed that PGA resulted in the highest energy reduction. The effect of GA types and their dosage on the product fineness was analyzed using a combination of dry and wet sieving, as well as specific surface area measurements. All GAs used GAs resulted in an increased product fineness, expressed by the P_{80}, compared to dry grinding without additives. Thus, both the type of GA and the dosage affect the fineness of the product.

RQ2: What is the relationship between particle arrangement (dispersion/ flowability) and the milling rate during dry grinding with grinding aids?

The results indicate that all chemical additives are satisfactorily effective grinding aids and improve material flowability compared to grinding without additives (within the examined dosage range). There is an upper limit for the dosage at which GAs benefit from each additive. PGA results in a maximum reduction of the basic flow energy (BFE), a 20.4% reduction of the specific energy (SE), a 24.6% reduction of the aerated basic flow energy (A-BFE), and a 38.3% reduction of the aerated energy (AE). A significant correlation was found between grinding efficiency (including work index) and flow indices. Grinding aids increase grinding efficiency by altering the flow

properties, that is, reducing the flow energy and cohesive forces. The predominant GA mechanism is based on the alteration of rheological properties.

RQ3: What are the differences and similarities between dry ground products with and without grinding aids?

Grinding tests showed that GAS resulted in a narrower particle size distribution, and rough surfaces. In general, the calculations from the BET measurements showed that GAs results in rougher surfaces compared to the reference sample.

RQ4: What are the changes in the surface and solution chemistry with and without grinding aids?

Both GAs influenced the surface chemistry in combination with the solution chemistry in comparison to that of the reference. PGA had minimal effect on the zeta potentials, while AAG resulted in more negative zeta potentials. The zeta potential measurement results showed a large negative shift for both quartz and magnetite; the former was more pronounced in the presence of AAG. For PGA, the zeta potentials decreased (absolute value) after treatment. The suspension stability test revealed that both GAs change the system compared to the reference. AAG results in a more stable suspension with improved dispersion than in the reference test. In contrast, PGA results in a less stable colloid system, suggesting the onset of flocculation, coagulation, sedimentation, coalescence, and even a combination. On the basis of UV-vis spectra, zeta potential tests, Fourier transform infrared (FT-IR) spectroscopy, and stability measurements, the adsorption mechanism for both GAs is mainly via physical interaction. The adsorption results showed superior adsorption of AAG on the quartz surface and PGA on magnetite.

RQ5: How do these changes, if any, affect overall flotation performance?

- According to single-mineral flotation tests, PGA has a depressing effect (positive effects) on magnetite particles with a negligible effect on quartz particles. Through mixed mineral flotation separation (magnetite + quartz at 2:1), comparable results of 86 % recovery and Fe grade of 62 % could be achieved using PGA only without starch. For the best balance in recovery, grade, and separation efficiency, 500 g/t starch and 300 g/t PGA could be recommended.
- For AAG, single mineral flotation indicated that AAG could enhance the quartz collection, thus improving its floatability. The results of artificial mixture flotation revealed that under specific conditions of 500 g/t AAG, pH 10, 1000 g/t starch Fe recovery of 92.1% and 64.5 % could be achieved with 100 g/t Lilaflot 822M compared to the reference with 93.0% recover and 65.1% grade at 200 g/t Lilaflot 822M.

In general, the feasibility of using PGA, a natural green polymer, was beneficial for the grinding and reverse flotation separation performance. These findings highlighted that the selection of suitable grinding aids (ecofriendly) could potentially reduce energy consumption (decrease CO_2 emissions), improve the distribution of suitable particles for downstream processes, and has no negative chemical impacts (even positive effects) on the separation stages. In general, these results have addressed the long-standing question of the effect of polyacrylic-based grinding aids on the resulting products and subsequent flotation separation processes. The presence of AAG not only

improved grinding efficiency, but could potentially decrease the amount of collector required to achieve comparable metallurgical performance. Both cases show that GAs and flotation reagents have synergistic interactions rather than competitive adsorption. This paves the way for future research on the application of grinding aids in mineral processing with the approach of having grinding aids with a secondary beneficial function in view of downstream processes.

5.2. Recommendation & Future work

Despite the obvious advantages of GAs in the grinding and downstream separation processes, further work is still required to address some limitations. Lack of complete understanding of the dominant mechanism of effect limits the control of the process and the development of new grinding aid chemistries. Findings from the current work help to approve that the predominant GA mechanism is based on the alteration of rheological properties on a meso-scale and macroscale. However, this work does not exclusively disprove the mechanisms suggested on the Rehbinder effect. Rather further work is required on the nano and micro-scale to study the influence of GAs on fracture mechanics. There is still a gap in the selection and design of GAs and optimum dosages, which remains empirical. Future use of new methods, such as molecular simulations, could help to understand the effects of additive molecules on the microscale. To address the question of the lack of correlation between GA effectiveness and the functional group, an understanding of the role of the functional group (polar part) together with the hydrocarbon chain (nonpolar part) is needed for better designing and application of GAs.

List of Tables

List of Figures

REFERENCES

Adewuyi, S.O., Ahmed, H.A.M., Ahmed, H.M.A., 2020. Methods of ore pretreatment for comminution energy reduction. Minerals 10. https://doi.org/10.3390/min10050423

Ahmed, M.M., 2010. Effect of comminution on particle shape and surface roughness and their relation to flotation process. Int. J. Miner. Process. 94, 180–191. https://doi.org/10.1016/j.minpro.2010.02.007

Allen, T., 1997. Powder sampling and particle size measurement (Vol. 1). Chapman Hall.

Altun, O., Benzer, H., Toprak, A., Enderle, U., 2015. Utilization of grinding aids in dry horizontal stirred milling. Powder Technol. 286, 610–615. https://doi.org/10.1016/j.powtec.2015.09.001

András, G., Björn, S., 2014. Chemical Fingerprinting of Arabidopsis Using Fourier Transform Infrared (FT-IR) Spectroscopic Approaches, in: Sanchez-Serrano J., S.J. (Ed.), Arabidopsis Protocols. Methods in Molecular Biology (Methods and Protocols). New York, pp. 317–352. https://doi.org/https://doi.org/10.1007/978-1-62703-580-4_18

Anoshin, G.., Yusupov, T.., Razvorotneva, L.., Tsimbalist, V.., Solotchina, E.., 1994. Effect of additives of inorganic salts during superfine grinding on physicochemical and structural properties of chromite. Phys. Chem. bases Conc. 84–87.

Ataie, M., Sutherland, K., Pakzad, L., Fatehi, P., 2020. Experimental and modeling analysis of lignin derived polymer in flocculating aluminium oxide particles. Sep. Purif. Technol. 247, 116944. https://doi.org/10.1016/j.seppur.2020.116944

Aznar-Sánchez, J.A., Velasco-Muñoz, J.F., Belmonte-Ureña, L.J., Manzano-Agugliaro, F., 2019. Innovation and technology for sustainable mining activity: A worldwide research assessment. J. Clean. Prod. 221, 38–54. https://doi.org/10.1016/j.jclepro.2019.02.243

Bastrzyk, A., Feder-Kubis, J., 2018. Pyrrolidinium and morpholinium ionic liquids as a novel effective destabilising agent of mineral suspension. Colloids Surfaces A Physicochem. Eng. Asp. 557, 58–65. https://doi.org/10.1016/j.colsurfa.2018.05.002

Beylot, A., Guyonnet, D., Muller, S., Vaxelaire, S., Villeneuve, J., 2019. Mineral raw material requirements and associated climate-change impacts of the French energy transition by 2050. J. Clean. Prod. 208, 1198–1205. https://doi.org/10.1016/j.jclepro.2018.10.154

Bhima. Rao, R., Narasimhan, K.S., Rao, T.C., 1991. Effect of additives on grinding of magnetite ore. Miner. Metall. Process. 8, 144–151.

Bian, Q., Sittipod, S., Garg, A., Ambrose, R.P.K., 2015. Bulk flow properties of hard and soft wheat flours. J. Cereal Sci. 63, 88–94. https://doi.org/10.1016/j.jcs.2015.03.010

Bond, F.C., 1961. Crushing and Grinding Calculations. Br. Chem. Eng.

Bruckard, W.J., Sparrow, G.J., Woodcock, J.T., 2011. A review of the effects of the grinding environment on the flotation of copper sulphides. Int. J. Miner. Process. 100, 1–13. https://doi.org/10.1016/j.minpro.2011.04.001

Bulejko, P., Šuleková, N., Vlasák, J., Tuunila, R., Kinnarinen, T., Svěrák, T., Häkkinen, A., 2022. Ultrafine wet grinding of corundum in the presence of triethanolamine. Powder Technol. 395, 556–561. https://doi.org/10.1016/j.powtec.2021.09.079

Camalan, M., Hoşten, Ç., 2019. Assessment of grinding additives for promoting chromite liberation. Miner. Eng. 136, 18–35. https://doi.org/10.1016/j.mineng.2019.03.004

Cayirli, S., 2022a. Analysis of grinding aid performance effects on dry fine milling of calcite. Adv. Powder Technol. 33, 103446. https://doi.org/10.1016/j.apt.2022.103446

Cayirli, S., 2022b. Analysis of grinding aid performance effects on dry fine milling of calcite. Adv. Powder Technol. 33, 103446. https://doi.org/10.1016/j.apt.2022.103446

Chazel, S., Benchekroun, H., Canada, B., 2020. Energy Transition Under Mineral Constraints and Recycling.

Chelgani, S.., Parian, M., Parapari, P.S., Ghorbani, Y., Rosenkranz, J., 2019. A comparative study on the effects of dry and wet grinding on mineral flotation separation–a review. J. Mater. Res. Technol. 1–8. https://doi.org/10.1016/j.jmrt.2019.07.053

Cheng, F., Feng, Y., Su, Q., Wei, D., Wang, B., Huang, Y., 2019. Practical strategy to produce ultrafine ceramic glaze: Introducing a polycarboxylate grinding aid to the grinding process. Adv. Powder Technol. 30, 1655–1663. https://doi.org/10.1016/j.apt.2019.05.014

Chimonyo, W., Fletcher, B., Peng, Y., 2020. Starch chemical modification for selective flotation of copper sulphide minerals from carbonaceous material: A critical review. Miner. Eng. 156, 106522. https://doi.org/10.1016/j.mineng.2020.106522

Chipakwe, V., 2021. Comparative Study of Chemical Additives Effects on Dry Grinding Performance. Luleå University of Technology. https://doi.org/ISBN: 978-91-7790-883-8

Chipakwe, V., Jolsterå, R., Chelgani, S.C., 2021. Nanobubble-Assisted Flotation of Apatite Tailings: Insights on Beneficiation Options. ACS Omega. https://doi.org/10.1021/acsomega.1c01551

Chipakwe, V., Semsari, P., Karlkvist, T., Rosenkranz, J., Chelgani, S.C., 2020a. A critical review on the mechanisms of chemical additives used in grinding and their effects on the downstream processes. J. Mater. Res. Technol. 9, 8148–8162. https://doi.org/10.1016/j.jmrt.2020.05.080

Chipakwe, V., Semsari, P., Karlkvist, T., Rosenkranz, J., Chelgani, S.C., 2020b. A critical review on the mechanisms of chemical additives used in grinding and their effects on the downstream processes. J. Mater. Res. Technol. 9, 8148–8162. https://doi.org/10.1016/j.jmrt.2020.05.080

Choi, H., Lee, W., Kim, D.U., Kumar, S., Kim, S.S., Chung, H.S., Kim, J.H., Ahn, Y.C., 2010. Effect of grinding aids on the grinding energy consumed during grinding of calcite in a stirred ball mill. Miner. Eng. 23, 54–57. https://doi.org/10.1016/j.mineng.2009.09.011

Choi, H., Lee, W., Kim, S., 2009. Effect of grinding aids on the kinetics of fine grinding energy consumed of calcite powders by a stirred ball mill. Adv. Powder Technol. 20, 350–354. https://doi.org/10.1016/j.apt.2009.01.002

Csoke, B., Racz, A., Mucsi, G., 2010. Grinding and flowing investigation on dry stirred ball milling in order to determine the influence of grinding aids, in: XXV International Mineral Processing Congress 2010, (IMPC) 2010 Proceedings Brisbane, QLD, Australia. pp. 629–636.

Das, D., Goyal, A., 2014. Characterization and biocompatibility of glucan: A safe food additive from probiotic Lactobacillus plantarum DM5. J. Sci. Food Agric. 94, 683–690. https://doi.org/10.1002/jsfa.6305

Diler, K.-B., 2018. The effect of additives on stirred media milling of talc. Powder Technol. 5, 36–39. https://doi.org/10.1016/S0032-5910(96)03236-6

Divya, S., Ganesh, G.N.., 2019. Characterization of Powder Flowability Using FT4-Powder Rheometer. J. Pharm. Sci. Res. 11, 25–29. https://doi.org/10.3390/ecps2012-00825

Donoso, M., Robles, P.A., Gálvez, E.D., Cisternas, L.A., 2013. Particle size effect on the efficient use of water and energy in mineral concentration processes. Ind. Eng. Chem. Res. 52, 17686–17690. https://doi.org/10.1021/ie402099n

El-Shall, H., Somasundaran, P., 1984a. Physico-chemical aspects of grinding: a review of use of additives. Powder Technol. 38, 275–293. https://doi.org/10.1016/0032-5910(84)85009-3

El-Shall, H., Somasundaran, P., 1984b. Mechanisms of grinding modification by chemical additives: organic reagents. Powder Technol. 38, 267–273.

https://doi.org/10.1016/0032-5910(84)85008-1

Engwayu, J., Pawlik, M., 2020. Adsorption of anionic polymers on hematite – a study of zeta potential distributions. Miner. Eng. 148, 106225. https://doi.org/10.1016/j.mineng.2020.106225

Enustun, B. V., Liu, D.C., Markuszewski, R., Lin, K.L., 1987. Use of a Surfactant as a Coal Grinding Additive. Coal Prep. 4, 193–207. https://doi.org/10.1080/07349348708945532

Ersoy, O., Güler, D., Rençberoğlu, M., 2022. Effects of Grinding Aids Used in Grinding Calcium Carbonate (CACO3) Filler on the Properties of Water-Based Interior Paints. Coatings 12. https://doi.org/10.3390/coatings12010044

Ervanne, H., Hakanen, M., 2007. Analysis of Cement Superplasticizers and Grinding Aids A Literature Survey, POSIVA.

FAN, M., TAO, D., HONAKER, R., LUO, Z., 2010. Nanobubble generation and its applications in froth flotation (part II): fundamental study and theoretical analysis. Min. Sci. Technol. 20, 159–177. https://doi.org/10.1016/S1674-5264(09)60179-4

Farrokhpay, S., Filippov, L., Fornasiero, D., 2020. Flotation of Fine Particles: A Review. Miner. Process. Extr. Metall. Rev. 00, 1–11. https://doi.org/10.1080/08827508.2020.1793140

Feng, D., Aldrich, C., 2000. A comparison of the flotation of ore from the Merensky Reef after wet and dry grinding. Int. J. Miner. Process. 60, 115–129. https://doi.org/10.1016/S0301-7516(00)00010-7

Filippov, L.O., Houot, R., Joussemet, R., 1997. Physicochemical mechanisms and ion flotation possibilities using columns for Cr6+ recovery from sulphuric solutions. Int. J. Miner. Process. 51, 229–239. https://doi.org/10.1016/s0301-7516(97)00024-0

Forbes, E., Davey, K.J., Smith, L., 2014. Decoupling rehology and slime coatings effect on the natural flotability of chalcopyrite in a clay-rich flotation pulp. Miner. Eng. 56, 136–144. https://doi.org/10.1016/j.mineng.2013.11.012

Franks, G. V., Forbes, E., Oshitani, J., Batterham, R.J., 2015. Economic, water and energy evaluation of early rejection of gangue from copper ores using a dry sand fluidised bed separator. Int. J. Miner. Process. 137, 43–51. https://doi.org/10.1016/j.minpro.2015.03.001

Freeman, R., 2007. Measuring the flow properties of consolidated, conditioned and aerated powders - A comparative study using a powder rheometer and a rotational shear cell. Powder Technol. 174, 25–33. https://doi.org/10.1016/j.powtec.2006.10.016

Freeman, Technology, 2013. Aeration Method.

Freeman, Technology, 2007. Stability & Variable Flow Rate Method. Work Instr.

Fuerstenau, D.W., 1995. Grinding Aids. KONA Powder Part. J. 13, 5–18. https://doi.org/10.14356/kona.1995006

Gamal, S.A., 2017. Rationalization of energy consumption in the grinding of some ores by using additives. Mater. Test. 59, 395–401.

Gao, X., Yang, Y., Deng, H., 2011. Utilization of beet molasses as a grinding aid in blended cements. Constr. Build. Mater. 25, 3782–3789. https://doi.org/10.1016/j.conbuildmat.2011.04.041

Gnagne, E.H., Petit, J., Gaiani, C., Scher, J., Amani, G.N., 2017. Characterisation of flow properties of foutou and foufou flours, staple foods in West Africa, using the FT4 powder rheometer. J. Food Meas. Charact. 11, 1128–1136. https://doi.org/10.1007/s11694-017-9489-2

Gokcen, H.S., Cayirli, S., Ucbas, Y., Kayaci, K., 2015. The effect of grinding aids on dry micro fine grinding of feldspar. Int. J. Miner. Process. 136, 42–44. https://doi.org/10.1016/j.minpro.2014.10.001

Grano, S., 2009. The critical importance of the grinding environment on fine particle recovery in flotation. Miner. Eng. 22, 386–394. https://doi.org/10.1016/j.mineng.2008.10.008

Gunson, A.J., Klein, B., Veiga, M., Dunbar, S., 2012. Reducing mine water requirements. J. Clean. Prod. 21, 71–82. https://doi.org/10.1016/j.jclepro.2011.08.020

Han, Y., Zhu, Y., Wang, Z., Tian, Y., 2010. Effects of DA as a grinding aid on selective grinding of Low-Grade bauxite, in: XXV International Mineral Processing Congress 2010, (IMPC) 2010 Proceedings Brisbane, QLD, Australia. pp. 781–789.

Hanumantha Rao, K., Forssberg, K.S.E., 1997. Mixed collector systems in flotation. Int. J. Miner. Process. 51, 67–79. https://doi.org/10.1016/s0301-7516(97)00039-2

Hao, S., Liu, B., Yan, X., 2017. Review on research of cement grinding AIDS and certain problems. Key Eng. Mater. 753 KEM, 295–299. https://doi.org/10.4028/www.scientific.net/KEM.753.295

Hare, C., Zafar, U., Ghadiri, M., Freeman, T., Clayton, J., Murtagh, M.J., 2015. Analysis of the dynamics of the FT4 powder rheometer. Powder Technol. 285, 123–127. https://doi.org/10.1016/j.powtec.2015.04.039

Hasegawa, M., Kimata, M., Shimane, M., Shoji, T., Tsuruta, M., 2000. The effect of liquid additives on dry ultrafine grinding of quartz. Powder Technol. 114, 145–151. https://doi.org/10.1016/S0032-5910(00)00290-4

He, M., Wang, Y., Forssberg, E., 2004. Slurry rheology in wet ultrafine grinding of industrial minerals: A review. Powder Technol. 147, 94–112. https://doi.org/10.1016/j.powtec.2004.09.032

Hicyilmaz, C., Ulusoy, U., Bilgen, S., Yekeler, M., Akdogan, G., 2006. Response of rough and acute surfaces of pyrite with 3-D approach to the flotation. J. Min. Sci. 42, 393–402.

Huang, Z., Zhong, H., Wang, S., Xia, L., Zou, W., Liu, G., 2014. Investigations on reverse cationic flotation of iron ore by using a Gemini surfactant: Ethane-1,2-bis(dimethyl-dodecyl-ammonium bromide). Chem. Eng. J. 257, 218–228. https://doi.org/10.1016/j.cej.2014.07.057

İspirli, H., Yüzer, M.O., Skory, C., Colquhoun, I.J., Sağdıç, O., Dertli, E., 2019. Characterization of a glucansucrase from Lactobacillus reuteri E81 and production of malto-oligosaccharides. Biocatal. Biotransformation 37, 421–430. https://doi.org/10.1080/10242422.2019.1593969

Jaycock, M.J., Parfitt, G.D., 1981. The study of liquid interfaces. Chem. Interfaces 38–132.

Jeswiet, J., Szekeres, A., 2016. Energy Consumption in Mining Comminution, in: Procedia CIRP. Elsevier B.V., pp. 140–145. https://doi.org/10.1016/j.procir.2016.03.250

Kanda, Y., Abe, Y., Yamaguchi, M., Endo, C., 1988. A Fundamental Study of Dry and Wet Grinding from The Viewpoint of Breaking Strength. Powder Technol. 56, 57–62. https://doi.org/10.5188/ijsmer.7.195

Kapeluszna, E., Kotwica, Ł., 2022. The Effect of Various Grinding Aids on the Properties of Cement and Its Compatibility with Acrylate-Based Superplasticizer. Materials (Basel). 15. https://doi.org/10.3390/ma15020614

Katsioti, M., Tsakiridis, P.E., Giannatos, P., Tsibouki, Z., Marinos, J., 2009. Characterization of various cement grinding aids and their impact on grindability and cement performance. Constr. Build. Mater. 23, 1954–1959. https://doi.org/10.1016/j.conbuildmat.2008.09.003

Kavitake, D., Devi, P.B., Singh, S.P., Shetty, P.H., 2016. Characterization of a novel galactan produced by Weissella confusa KR780676 from an acidic fermented food. Int. J. Biol. Macromol. 86, 681–689. https://doi.org/10.1016/j.ijbiomac.2016.01.099

Kinnunen, P., Obenaus-Emler, R., Raatikainen, J., Guignot, S., Guimerà, J., Ciroth, A., Heiskanen, K., 2021. Review of closed water loops with ore sorting and tailings valorisation for a more sustainable mining industry. J. Clean. Prod. 278. https://doi.org/10.1016/j.jclepro.2020.123237

Klimpel, R.R., 1999. The selection of wet grinding chemical additives based on slurry

rheology control. Powder Technol. 105, 430–435. https://doi.org/10.1016/S0032-5910(99)00169-2

Klimpel, R.R., Manfroy, W., 1978. Chemical Grinding Aids for Increasing Throughput in the Wet Grinding of Ores. Ind. Eng. Chem. Process Des. Dev. 17, 518–523. https://doi.org/10.1021/i260068a022

Kojima, T., Elliott, J.A., 2014. A semi-empirical model relating flow properties to particle contacts in fine binary powder mixtures. Powder Technol. 268, 191–202. https://doi.org/10.1016/j.powtec.2014.08.013

Kojima, T., Elliott, J.A., 2012. Incipient flow properties of two-component fine powder systems and their relationships with bulk density and particle contacts. Powder Technol. 228, 359–370. https://doi.org/10.1016/j.powtec.2012.05.052

Kökkiliç, O., Langlois, R., Waters, K.E., 2015. A design of experiments investigation into dry separation using a Knelson Concentrator. Miner. Eng. 72, 73–86. https://doi.org/10.1016/j.mineng.2014.09.025

Koleini, S.M.J., Abdollahy, M., Soltani, F., 2012. Wet and dry grinding methods effect on the flotation of taknar Cu-Zn sulphide ore using a mixed collector. 26th Int. Miner. Process. Congr. IMPC 2012 Innov. Process. Sustain. Growth - Conf. Proc. 5113–5119.

Kotake, N., Kuboki, M., Kiya, S., Kanda, Y., 2011. Influence of dry and wet grinding conditions on fineness and shape of particle size distribution of product in a ball mill. Adv. Powder Technol. 22, 86–92. https://doi.org/10.1016/j.apt.2010.03.015

Lapointe, M., Barbeau, B., 2020. Understanding the roles and characterizing the intrinsic properties of synthetic vs. natural polymers to improve clarification through interparticle Bridging: A review. Sep. Purif. Technol. 231, 115893. https://doi.org/10.1016/j.seppur.2019.115893

Leturia, M., Benali, M., Lagarde, S., Ronga, I., Saleh, K., 2014. Characterization of flow properties of cohesive powders: A comparative study of traditional and new testing methods. Powder Technol. 253, 406–423. https://doi.org/10.1016/j.powtec.2013.11.045

Liu, D.H., Birlingmair, D.H., Burkhart, L.E., Markuszewski, R., 1989. Attrition grinding of coal in the presence of polymeric additives. Coal Prep. 6, 195–206. https://doi.org/10.1080/07349348908960529

Liu, Wenbao, Liu, Wengang, Wang, X., Wei, D., Wang, B., 2016. Utilization of novel surfactant N-dodecyl-isopropanolamine as collector for efficient separation of quartz from hematite. Sep. Purif. Technol. 162, 188–194. https://doi.org/10.1016/j.seppur.2016.02.033

Liu, X., Xie, J., Huang, G., Li, C., 2017. Low-temperature performance of cationic collector undecyl propyl ether amine for ilmenite flotation. Miner. Eng. 114, 50–

56. https://doi.org/10.1016/j.mineng.2017.09.005

Liu, Y., Huang, G., Pan, Z., Wang, Y., Li, G., 2021. Synthesis of sodium polyacrylate copolymers as water-based dispersants for wet ultrafine grinding of cobalt aluminate particles. Colloids Surfaces A Physicochem. Eng. Asp. 610, 125553. https://doi.org/10.1016/j.colsurfa.2020.125553

Liu, Y., Lu, H., Poletto, M., Guo, X., Gong, X., 2017. Bulk flow properties of pulverized coal systems and the relationship between inter-particle forces and particle contacts. Powder Technol. 322, 226–240. https://doi.org/10.1016/j.powtec.2017.07.057

Locher, W.F., Seebach, H.M., 1972. Indus. Eng. Chem. Process Des. Develop 2 190.

Ma, S., Yang, J., Mo, W., Wang, G., Su, X., Yuan, C., 2010. The effect of grinding aids on laboratory grinding of a cassiterite-polymetallic sulfide ore. XXV Int. Miner. Process. Congr. 2010, IMPC 2010 2, 1001–1008.

Mao, Y., Wang, Z., Liu, W., Tian, P., 2022. Effect of TIPA/TEA combined grinding aid on the behavior of quartz flotation in DDA system. Powder Technol. 406, 117570. https://doi.org/10.1016/j.powtec.2022.117570

Melorie, A.K., Raj Kaushal, D., 2018. Experimental investigations of the effect of chemical additives on the rheological properties of highly concentrated iron ore slurries. KONA Powder Part. J. 2018, 186–199. https://doi.org/10.14356/kona.2018001

Mende, S., Stenger, F., Peukert, W., Schwedes, J., 2003. Mechanical production and stabilization of submicron particles in stirred media mills. Powder Technol. 132, 64–73. https://doi.org/10.1016/S0032-5910(03)00042-1

Mesa, D., Brito-Parada, P.R., 2019. Scale-up in froth flotation: A state-of-the-art review. Sep. Purif. Technol. 210, 950–962. https://doi.org/10.1016/j.seppur.2018.08.076

Miao, M., Bai, A., Jiang, B., Song, Y., Cui, S.W., Zhang, T., 2014. Characterisation of a novel water-soluble polysaccharide from Leuconostoc citreum SK24.002. Food Hydrocoll. 36, 265–272. https://doi.org/10.1016/j.foodhyd.2013.10.014

Mishra, R.K., Geissbuhler, D., Carmona, H.A., Wittel, F.K., Sawley, M.L., Weibel, M., Gallucci, E., Herrmann, H.J., Heinz, H., Flatt, R.J., 2015. En route to multi model scheme for clinker comminution with chemical grinding AIDS. Adv. Appl. Ceram. 114, 393–401. https://doi.org/10.1179/1743676115Y.0000000023

Mishra, R.K., Weibel, M., Müller, T., Heinz, H., Flatt, R.J., 2017. Energy-effective grinding of inorganic solids using organic additives. Chimia (Aarau). 71, 451–460. https://doi.org/10.2533/chimia.2017.451

Mohanty, A.K., Wu, F., Mincheva, R., Hakkarainen, M., Raquez, J.M., Mielewski, D.F., Narayan, R., Netravali, A.N., Misra, M., 2022. Sustainable polymers. Nat. Rev.

Methods Prim. 2. https://doi.org/10.1038/s43586-022-00124-8

Moran, C.J., Lodhia, S., Kunz, N.C., Huisingh, D., 2014. Sustainability in mining, minerals and energy: New processes, pathways and human interactions for a cautiously optimistic future. J. Clean. Prod. 84, 1–15. https://doi.org/10.1016/j.jclepro.2014.09.016

Morrell, S., 2009. Predicting the overall specific energy requirement of crushing, high pressure grinding roll and tumbling mill circuits. Miner. Eng. 22, 544–549. https://doi.org/10.1016/j.mineng.2009.01.005

Mudd, G.M., 2009. The Sustainability of Mining in Australia : Key Production Trends and Their Environmental Implications for the Future.

Mwale, A.H., Musonge, P., Fraser, D.M., 2005. The influence of particle size on energy consumption and water recovery in comminution and dewatering systems. Miner. Eng. 18, 915–926. https://doi.org/10.1016/j.mineng.2005.02.014

Nan, W., Ghadiri, M., Wang, Y., 2017. Analysis of powder rheometry of FT4: Effect of particle shape. Chem. Eng. Sci. 173, 374–383. https://doi.org/10.1016/j.ces.2017.08.004

Napier-Munn, T., 2015. Is progress in energy-efficient comminution doomed? Miner. Eng. 73, 1–6. https://doi.org/10.1016/j.mineng.2014.06.009

National Materials Advisory Board - Commission on Sociotechnical Systems, 1981. Comminution, DOE. Comminution and Energy Consumption: Report of the Committee on Comminution and Energy Consumption. Washington D.C.

Nguyen, M.T., Ziemski, M., Vink, S., 2014. Application of an exergy approach to understand energy demand of mine water management options. J. Clean. Prod. 84, 639–648. https://doi.org/10.1016/j.jclepro.2014.04.004

Noaparast, M., Rafiei, A., 2003. The effect of grinding aids on the work index values. pp. 1–6.

Nuorivaara, T., Serna-Guerrero, R., 2020. Unlocking the potential of sustainable chemicals in mineral processing: Improving sphalerite flotation using amphiphilic cellulose and frother mixtures. J. Clean. Prod. 261, 121143. https://doi.org/10.1016/j.jclepro.2020.121143

Ogonowski, S., Wołosiewicz-Głab, M., Ogonowski, Z., Foszcz, D., Pawełczyk, M., 2018. Comparison of wet and dry grinding in electromagnetic mill. Minerals 8, 1–19. https://doi.org/10.3390/min8040138

Orumwense, O.A., Forssberg, E., 1992. Superfine and Ultrafine Grinding A Literature Survey. Miner. Process. Extr. Metall. Rev. 11, 107–127. https://doi.org/10.1080/08827509208914216

Ozkan, A., Yekeler, M., Calkaya, M., 2009. Kinetics of fine wet grinding of zeolite in a steel ball mill in comparison to dry grinding. Int. J. Miner. Process. 90, 67–73. https://doi.org/10.1016/j.minpro.2008.10.006

Pommeret, A., Ricci, F., Schubert, K., 2022. Critical raw materials for the energy transition. Eur. Econ. Rev. 141, 1–24. https://doi.org/10.1016/j.euroecorev.2021.103991

Prziwara, P., Breitung-Faes, S., Kwade, A., 2019. Comparative study of the grinding aid effects for dry fine grinding of different materials. Miner. Eng. 144. https://doi.org/10.1016/j.mineng.2019.106030

Prziwara, P., Breitung-Faes, S., Kwade, A., 2018a. Impact of the powder flow behavior on continuous fine grinding in dry operated stirred media mills. Miner. Eng. 128, 215–223. https://doi.org/10.1016/j.mineng.2018.08.032

Prziwara, P., Breitung-Faes, S., Kwade, A., 2018b. Impact of grinding aids on dry grinding performance, bulk properties and surface energy. Adv. Powder Technol. 29, 416–425. https://doi.org/10.1016/j.apt.2017.11.029

Prziwara, P., Hamilton, L.D., Breitung-Faes, S., Kwade, A., 2018c. Impact of grinding aids and process parameters on dry stirred media milling. Powder Technol. 335, 114–123. https://doi.org/10.1016/j.powtec.2018.05.021

Prziwara, P., Kwade, A., 2020. Grinding aids for dry fine grinding processes – Part I: Mechanism of action and lab-scale grinding. Powder Technol. 375, 146–160. https://doi.org/10.1016/j.powtec.2020.07.038

Rajendran, N.P.B., Paramasivam, R., 1999. Analysis of the influence of grinding aids on the breakage process of calcite in media mills. Adv. Powder Technol. 10, 223–243. https://doi.org/10.1163/156855299X00316

Rajendran Nair, P.B., Paramasivam, R., 1999. Effect of grinding aids on the time-flow characteristics of the ground product from a batch ball mill. Powder Technol. 101, 31–42. https://doi.org/10.1016/S0032-5910(98)00121-1

Ranängen, H., Lindman, Å., 2017. A path towards sustainability for the Nordic mining industry. J. Clean. Prod. 151, 43–52. https://doi.org/10.1016/j.jclepro.2017.03.047

Rehbinder, P.A., Kalinkovaskaya, N.A., 1932. J Technol Phys. J Technol Phys 2, 726–755.

Rivas-Perez, R., Sotomayor-Moriano, J., Perez-Zuñiga, C.G., 2017. Adaptive Expert Generalized Predictive Multivariable Control of Seawater RO Desalination Plant for a Mineral Processing Facility. IFAC-PapersOnLine 50, 10244–10249. https://doi.org/10.1016/j.ifacol.2017.08.1284

Routray, S., Swain, R., 2019. Effect of Chemical Additives on Reduction in Mill Power During Continuous Grinding of Chromite Overburden Materials in a Tumbling

Mill: A Case Study. J. Inst. Eng. Ser. D 100, 123–128. https://doi.org/10.1007/s40033-018-0170-7

Schönert, K., 1996. The influence of particle bed configurations and confinements on particle breakage. Int. J. Miner. Process. 44–45, 1–16. https://doi.org/10.1016/0301-7516(95)00017-8

Semsari Parapari, P., Parian, M., Rosenkranz, J., 2020. Breakage process of mineral processing comminution machines – An approach to liberation. Adv. Powder Technol. 31, 3669–3685. https://doi.org/10.1016/j.apt.2020.08.005

Shi, H., Mohanty, R., Chakravarty, S., Cabiscol, R., Morgeneyer, M., Zetzener, H., Ooi, J.Y., Kwade, A., Luding, S., Magnanimo, V., 2018. Effect of particle size and cohesion on powder yielding and flow. KONA Powder Part. J. 2018, 226–250. https://doi.org/10.14356/kona.2018014

Shrimali, K., Miller, J.D., 2016. Polysaccharide Depressants for the Reverse Flotation of Iron Ore. Trans. Indian Inst. Met. 69, 83–95. https://doi.org/10.1007/s12666-015-0708-4

Singh, V., Dixit, P., Venugopal, R., Venkatesh, K.B., 2018. Ore Pretreatment Methods for Grinding: Journey and Prospects. Miner. Process. Extr. Metall. Rev. 40, 1–15. https://doi.org/10.1080/08827508.2018.1479697

SIP STRIM, 2019. Strategic Research and Innovation Roadmap for the Swedish Mining, Mineral and Metal Producing Industry.

Snow, R.H., Luckie, P.T., 1974. Annual Review of Size Reduction - 1973. Powder Technol. 10, 129–142.

Sohoni, S., Sridhar, R., Mandal, G., 1991. The effect of grinding aids on the fine grinding of limestone, quartz and Portland cement clinker. Powder Technol. 67, 277–286. https://doi.org/10.1016/0032-5910(91)80109-V

Solenis, 2016. Wet Grinding Aid in Hard Rock Mining Increases Recovery by 4 Percentage Points Zalta ™ Grinding Aid.

Somani, A., Nandi, T.K., Pal, S.K., Majumder, A.K., 2017. Pre-treatment of rocks prior to comminution – A critical review of present practices. Int. J. Min. Sci. Technol. 27, 339–348. https://doi.org/10.1016/j.ijmst.2017.01.013

Somasundaran, P., Lee, L.T., 1981. Polymer-Surfactant Interactions in Flotation of Quartz. Sep. Sci. Technol. 16, 1475–1490. https://doi.org/10.1080/01496398108058312

Sun, K., Nguyen, C. V, Nguyen, N.N., Nguyen, A. V, 2022. Flotation surface chemistry of water-soluble salt minerals : from experimental results to new perspectives. Adv. Colloid Interface Sci. 309, 102775. https://doi.org/10.1016/j.cis.2022.102775

Tohry, A., Dehghan, R., de Salles Leal Filho, L., Chehreh Chelgani, S., 2021. Tannin: An eco-friendly depressant for the green flotation separation of hematite from quartz. Miner. Eng. 168, 106917. https://doi.org/10.1016/j.mineng.2021.106917

Tong, Z., Liu, L., Yuan, Z., Liu, J., Lu, J., Li, L., 2021. The effect of comminution on surface roughness and wettability of graphite particles and their relation with flotation. Miner. Eng. 169, 106959. https://doi.org/10.1016/j.mineng.2021.106959

Toprak, N.A., Altun, O., Aydogan, N., Benzer, H., 2014. The influences and selection of grinding chemicals in cement grinding circuits. Constr. Build. Mater. 68, 199–205. https://doi.org/10.1016/j.conbuildmat.2014.06.079

Tucker, I.M., Corbett, J.C.W., Fatkin, J., Jack, R.O., Kaszuba, M., MacCreath, B., McNeil-Watson, F., 2015. Laser Doppler Electrophoresis applied to colloids and surfaces. Curr. Opin. Colloid Interface Sci. 20, 215–226. https://doi.org/10.1016/j.cocis.2015.07.001

Ulusoy, U., Yekeler, M., 2005. Correlation of the surface roughness of some industrial minerals with their wettability parameters. Chem. Eng. Process. Process Intensif. 44, 555–563. https://doi.org/10.1016/j.cep.2004.08.001

Uskoković, V., 2012. Dynamic Light Scattering Based Microelectrophoresis: Main Prospects and Limitations. J. Dispers. Sci. Technol. 33, 1762–1786. https://doi.org/10.1080/01932691.2011.625523

Valero, Alicia, Valero, Antonio, Calvo, G., Ortego, A., Ascaso, S., Palacios, J.L., 2018. Global material requirements for the energy transition. An exergy flow analysis of decarbonisation pathways. Energy 159, 1175–1184. https://doi.org/10.1016/j.energy.2018.06.149

Vieira, A.M., Peres, A.E.C., 2007. The effect of amine type, pH, and size range in the flotation of quartz. Miner. Eng. 20, 1008–1013. https://doi.org/10.1016/j.mineng.2007.03.013

Wang, Y., Li, C., Liu, P., Ahmed, Z., Xiao, P., Bai, X., 2010. Physical characterization of exopolysaccharide produced by Lactobacillus plantarum KF5 isolated from Tibet Kefir. Carbohydr. Polym. 82, 895–903. https://doi.org/10.1016/j.carbpol.2010.06.013

Weibel, M., Mishra, R.K., 2014a. Cement additives - Comprehensive understanding of grinding aids.

Weibel, M., Mishra, R.K., 2014b. Comprehensive understanding of grinding aids. ZKG Int. 67, 28–39.

Wills, B.., Finch, J.., 2016. Wills' Mineral Processing Technology, 8th ed.

Wu, L., Huang, Y., Wang, Z., Liu, L., 2010. Interaction and dispersion stability of alumina suspension with PAA in N,N'-dimethylformamide. J. Eur. Ceram. Soc.

30, 1327–1333. https://doi.org/10.1016/j.jeurceramsoc.2009.12.010

Xiao, X., Zhang, G., Feng, Q., Xiao, S., Huang, L., Zhao, X., Li, Z., 2012. The liberation effect of magnetite fine ground by vertical stirred mill and ball mill. Miner. Eng. 34, 63–69. https://doi.org/10.1016/j.mineng.2012.04.004

Xie, L., Wang, J., Lu, Q., Hu, W., Yang, D., Qiao, C., Peng, X., Peng, Q., Wang, T., Sun, W., Liu, Q., Zhang, H., Zeng, H., 2021. Surface interaction mechanisms in mineral flotation: Fundamentals, measurements, and perspectives. Adv. Colloid Interface Sci. 295, 102491. https://doi.org/10.1016/j.cis.2021.102491

Yang, A.., 1994. The Influence of Grinding Aids on the on the floatabilty of the fine casseterite. Fizykochem. Probl. Miner. 28, 37–46.

Yang, H., Plank, J., Sun, Z., 2019. Investigation on the optimal chemical structure of methacrylate ester based polycarboxylate superplasticizers to be used as cement grinding aid under laboratory conditions: Effect of anionicity, side chain length and dosage on grinding efficiency, mortar . Constr. Build. Mater. 224, 1018–1025. https://doi.org/10.1016/j.conbuildmat.2019.08.011

Yang, J., Li, G., Yang, W., Guan, J., 2022. Effect of Polycarboxylic Grinding Aid on Cement Chemistry and Properties. Polymers (Basel). 14. https://doi.org/10.3390/polym14183905

Yilmaz, M.T., İspirli, H., Taylan, O., Taşdemir, V., Sagdic, O., Dertli, E., 2021. Characterisation and functional roles of a highly branched dextran produced by a bee pollen isolate Leuconostoc mesenteroides BI-20. Food Biosci. https://doi.org/10.1016/j.fbio.2021.101330

Yoshioka, K., Sakai, E., Daimon, M., Kitahara, A., 1997. Role of steric hindrance in the performance of superplasticizers for concrete. J. Am. Ceram. Soc. 80, 2667–2671. https://doi.org/10.1111/j.1151-2916.1997.tb03169.x

Yun, H., Dong, L., Wang, W., Bing, Z., Xiangyun, L., 2018. Study on the flowability of TC4 Alloy Powder for 3D Printing, in: IOP Conference Series: Materials Science and Engineering. https://doi.org/10.1088/1757-899X/439/4/042006

Yusupov, T.., Kirillova, E.., 2010. Surfactants in fine ore grinding. J. Min. Sci. 46, 582–586.

Zhang, C., Wei, S., Hu, Y., Tang, H., Gao, J., Yin, Z., Guan, Q., 2018. Selective adsorption of tannic acid on calcite and implications for separation of fluorite minerals. J. Colloid Interface Sci. 512, 55–63. https://doi.org/10.1016/j.jcis.2017.10.043

Zhang, S., Huang, Z., Wang, H., Liu, R., Cheng, C., Shuai, S., Hu, Y., Guo, Z., Yu, X., He, G., Fu, W., 2021. Flotation performance of a novel Gemini collector for kaolinite at low temperature. Int. J. Min. Sci. Technol. 31, 1145–1152. https://doi.org/10.1016/j.ijmst.2021.09.001

Zhang, X., Han, Y., Kawatra, S.., 2020. Effects of Grinding Media on Grinding Products and Flotation Performance of Sulfide Ores. Miner. Process. Extr. Metall. Rev. 1–12. https://doi.org/10.1016/j.mineng.2019.106070

Zhang, X., Zhao, Z., Cui, Y., Liu, F., Huang, Z., Huang, Y., Zhang, R., Freeman, T., Lu, X., Pan, X., Tan, W., Wu, C., 2019. Effect of powder properties on the aerosolization performance of nanoporous mannitol particles as dry powder inhalation carriers. Powder Technol. 358, 46–54. https://doi.org/10.1016/j.powtec.2018.08.058

Zhang, Y., Fei, A., Li, D., 2016. Utilization of waste glycerin, industry lignin and cane molasses as grinding aids in blended cement. Constr. Build. Mater. 123, 785–791. https://doi.org/10.1016/j.conbuildmat.2016.07.034

Zhao, J., Wang, D., Wang, X., Liao, S., Lin, H., 2015. Ultrafine grinding of fly ash with grinding aids: Impact on particle characteristics of ultrafine fly ash and properties of blended cement containing ultrafine fly ash. Constr. Build. Mater. 78, 250–259. https://doi.org/10.1016/j.conbuildmat.2015.01.025

Zheng, J., Harris, C.C., Somasundaran, P., 1996. Role of Chemical Additives in Stirred Media Mill Grinding, in: 5th World Congress of Chemical Engineering - American Institute of Chemical Engineers.

Zhu, M., Zhang, Q., Xiao, X., Shi, B., 2022. A novel strategy for enhancing comprehensive properties of polyacrylate coating: Incorporation of highly dispersed zinc ions by using polyacrylic acid as carrier. Prog. Org. Coatings 162, 106596. https://doi.org/10.1016/j.porgcoat.2021.106596

Zhu, Y., Romain, C., Williams, C.K., 2016. Sustainable polymers from renewable resources. Nature 540, 354–362. https://doi.org/10.1038/nature21001

Zhu, Z., Yin, W., Wang, D., Sun, H., Chen, K., Yang, B., 2020. The role of surface roughness in the wettability and floatability of quartz particles. Appl. Surf. Sci. 527, 146799. https://doi.org/10.1016/j.apsusc.2020.146799

PART II – PAPERS

Paper I: A critical review on the mechanisms of chemical additives used in grinding and their effects on the downstream processes

Paper II: A comparative study on the effect of chemical additives on dry grinding of magnetite ore.

Paper III: Effects of chemical additives on rheological properties of dry ground ore - a comparative study.

Paper IV: Beneficial effects of a polysaccharide-based grinding aid on magnetite flotation: a green approach.

Paper V: Exploring the effect of a polyacrylic acid-based grinding aid on magnetite-quartz flotation separation.

Paper I

A critical review on the mechanisms of chemical additives used in grinding and their effects on the downstream processes.

V. Chipakwe, P. Semsari, T. Karlkvist, J. Rosenkranz, S. Chehreh Chelgani.

Journal of Materials Research and Technology, 9:4, 2020.

Available online at www.sciencedirect.com

jmr&t
Journal of Materials Research and Technology
www.jmrt.com.br

Review Article

A critical review on the mechanisms of chemical additives used in grinding and their effects on the downstream processes

*V. Chipakwe, P. Semsari, T. Karlkvist, J. Rosenkranz, S. Chehreh Chelgani**

Minerals and Metallurgical Engineering, Dept. of Civil, Environmental and Natural Resources Engineering, Luleå University of Technology, SE-971 87 Luleå, Sweden

ARTICLE INFO

Article history:
Received 30 March 2020
Accepted 20 May 2020
Available online 8 June 2020

Keywords:
Grinding aids
Dry grinding
Energy efficiency
Size reduction
Flowability

ABSTRACT

Grinding aids (GAs) have been an important advent in the comminution circuits. Over the last few decades, in order to address the high energy consumption and scarcity of potable water for mineral processing, chemical additives have become a promising alternative. Using GAs can have some advantages such as enhancing grinding efficiency, reducing water usage, improving material flowability, and narrowing the particle size distribution of the grinding products. A study on the effect of GAs on size reduction units is crucial for the beneficiation value chain of minerals and the impact on downstream processes. However, our understanding of the effects of these materials on the particle size reduction is quite limited. This article analyses the literature, which used GAs and provides a comprehensive review of their applications in the ore beneficiation processes. The outcomes of this investigation indicated that the current understanding on the mechanism of GA effects focuses only on their impacts on the product fineness and size distribution, and neglecting the aspect of energy expended and physicochemical environment. The application of GAs is mainly for rationalisation of energy where the type of reagent, pH, and ionic strength of the grinding environment is important. Gaps in knowledge of GAs are discussed in the context of addressing their use in the mineral industry, considering the mechanism of their effect, effect on grinding efficiency, and effect on the downstream processes. Addressing these gaps will pave the way for the application of GAs in improving size reduction efficiencies, which ultimately reduces environmental impacts.

Chelgani as an associate professor is working at the Lulea university of technology. Throughout collaborative works in mineral separation and metal extraction (industry and academia), he has gained a lot of experience in teaching, research, R&D, industrial teamwork and management. He has received the most prestigious awards in Canada and other countries (OGS, NSERC, Outstanding researcher & reviewer). He published more than 80 peer review articles and he is an editorial board member of some well-known journals within his research area.

* *Corresponding author.*
E-mail: saeed.chelgani@ltu.se (S.C. Chelgani).
https://doi.org/10.1016/j.jmrt.2020.05.080

1. Introduction

The term chemical additives or grinding aids (GAs) refers to any substance which results in increased grinding efficiency and reduction in power consumption when added to the mill charge (amounts not exceeding 0.25 wt.% of the feed) during grinding [1–3]. The use of grinding aids to increase mill throughput is quite common in the cement industry [2,4,5]. In mineral beneficiation, wet grinding is much preferred compared to dry grinding, but the growing scarcity of portable water poses a threat to mining activities, especially in arid regions. The use of GAs improves material flowability, which presents an opportunity for the application of dry grinding. This ultimately reduces the environmental impacts such as CO_2 emissions due to the energy intensive nature of grinding [6].

GAs range from organic (e.g. polyols, alcohols, esters, amines) to inorganic (e.g. calcium oxide, sodium silicate, sodium carbonate, sodium chloride) chemicals [7,8]. Despite the empirical evidence of the benefits for GAs in the cement industry, there is no agreed mechanism on their effects [2–4,7]. However, suggested mechanisms are mainly based on two principles; (1) The chemical-physical effect on the individual particle such as surface energy reduction (2) The effect on the particle arrangement and material flow properties [1,9–12].

To date, some studies on the effect of GAs on efficiency regarding power consumption, grindability, reduction ratio and mill operating parameters such as mill filling have been done [9,13–15]. Przwara et al. [14] investigated their effects on bulk properties such as particle size distribution, specific surface area, powder flowability, specific surface energy, and product fineness. GAs have been applied to address the problem of over-grinding and under-grinding (selective grinding) associated with poly-metallic sulphide ores due to their effect on producing a narrow particle side distribution [16,17]. Several investigations reported the improved material fluidity which allowed grinding at high solid concentrations (reducing the amount of processing water) [17–20]. Yusupov and Kirillova [21] reported that using GAs decreased amount of slime in the flotation feed compared to grinding without GA which is beneficial to froth flotation performance [22]. The reduction of excess fines by using GAs can also improve the dewatering processes such as thickening, decanting, filtration and tailings storage facility (TSF) draining and assists in water recycling [23]. Moreover, using GAs reduces energy consumption in downstream processes such as dewatering, classification, pumping due to improved flow properties [24,25].

Grinding, which is central in mineral processing to achieve particle size reduction and mineral liberation, is highly energy-intensive. It accounts for 50% of power consumption in a concentrator [26,27]. In general, grinding has poor energy efficiency and accounts for about 2-3% of the world generated electricity [28]. Due to the depleting resources, the processing of refractory ores is becoming common. Such processes require fine grinding or ultrafine grinding to liberate the valuable minerals from gangue material; thus, energy-efficient technologies and strategies are required [26,29]. Current efforts in addressing the high energy consumption and poor energy efficiency associated with grinding in the minerals industry can be divided into three strategies [11,28]:(1) Development of alternative equipment,(2) Development of alternative flowsheet configuration,(3) Alteration of material properties of ores.

Considerable investments have been made on the development of alternative equipment. It is reported that the use of stirred media mills and high pressure grinding rolls (HPGR) improved grinding efficiencies compared to the conventional tumbling mills – balls mills and rod mills [11,30,31]. The development of new approaches to mineral processing, such as geometallurgical approach, which provides a holistic mine-to-mill view, has made strides in addressing these challenges [28]. Investigations have shown the potential to improve grinding efficiencies by exploiting material properties of the ore such as thermal, electrical, magnetic, microwave and bulk properties [26,27]. Singh et al. [26] and Somani et al. [27] summarised the application of various pre-treatment processes which exploit these material properties such as microwave treatment, shock wave treatment, ultrasonic treatment, electrical disintegration, thermal, and chemical additives treatment. However, there has been little discussion about the industrial application of GAs despite empirical evidence presented in the cement industry [2–4,7].

Whilst some studies on the use, effects, and mechanism of GAs exists, few investigations in mineral beneficiation have addressed their applications. Hence, this article provides a literature review of the application, effects, and mechanism of grinding aids to develop an understanding of the current status, challenges, and prospects on the use of GAs for improving grinding efficiencies in the mineral industry.

2. Grinding aids

As mentioned, GAs can be grouped into organic or inorganic-based additives. However, they are mostly used as a mixture of various individual additives.

2.1. *Organic GAs*

The most common organic grinding aids used in the process industry are based on triethanolamine (TEA), triisopropanol amine (TIPA), n-methyl-diisopropanolamine (MDIPA), glycerine, poly-carboxylate ether (PCE), diethyl glycol (DEG) and propylene glycol (Table 1) [32]. These materials have a number of different functional groups. However, there is no clear understanding of the relationship between these functional groups and their observed effects [32]. Jeknavorian et al. [33] suggested that the polarity of GAs due to their functional groups (-OH, $-NH_2$) results in the electrostatic bonding with the covalent bonds on the fractured particles. This reduces the agglomeration of ground particles and consequently improves grinding efficiencies. Dombrowe et al. [34] suggested that polar molecules with asymmetrical arrangements were more effective than those with symmetrical arrangements. This is due to the better grinding performance of alcohol (asymmetrical) to glycols (symmetrical); however, this hypothesis failed to hold for the case of amines and alcohol. On the grinding of quartz, the use of alcohol resulted in the doubling of the specific sur-

Table 1 – Organic grinding aids used in various investigations.

Grinding aid	Dry or Wet	Material	Reference
Methanol	–	Quartz	[44]
Triethanol amine (TEA)	Dry	Quartzite	[10]
	Dry	Limestone	[5]
	Wet	Cassiterite	[36]
	Dry	Fly ash	[45]
Polyacrylamides (PAM)	Wet	Cassiterite	[17]
Triisopropanol amine (TIPA),	Dry	Fly ash	[45]
Oleic acid	–	Limestone-Zinc blend	[7]
	Wet	Limestone	[38]
Steric acid	–	Limestone	[7]
Sodium Oleate	–	Quartz	[7]
	Wet	Limestone	[38]
Caprylic acid	Dry	Chrome-ore	[7]
Marine oil	Dry	Chrome-ore	[7]
Polyacrylic acid (PAA)	Wet	Calcite	[9]
	Wet	Limestone	[38]
	Dry	Gypsum ore	[46]
Citric acid	Wet	Hematite ore	[47]
Sodium sulphonapthenate	Wet	Quartzite	[7]
Heptanoic acid (HepAc)	Dry	Limestone	[48]
Amyl-acetate	–	Quartz	[7]
Acetone	Dry	Cement clinker	[7]
Aryl-alkyl sulphonic acid (RDA)	–	Graphite	[7]

face area. This phenomenon expended more energy compared to grinding in water as a GA [3]. It has been reported that polar GAs are more effective in improving grindability compared to non-polar ones [3]. The operating pH environment is crucial in the application of GAs with non-ionic compounds containing $-O^-$ and $-OH$ functional groups, which are less sensitive to pH being preferred for industrial application [35]. Typically, the grinding efficiency increases with an increase in the molecular weight of the GAs, up to a maximum, and the efficiency drops [36,37]. Ma et al. [36] used polyacrylamides (PAM) in the laboratory grinding of cassiterite. They found that high molecular weight PAM improves the grindability of cassiterite more than their low molecular weight counterparts. Zheng et al. [38] reported the same outcomes when using polyacrylic acid (PAA) for limestone grinding. Prziwara et al. [14] used different organic GAs, heptanoic acid, (HepAc), triethanolamine (TEA), 1-Hexanol (HexOH) and diethylene glycol (DEG) with molar masses of 130.18, 149.19, 102.18 and 106.12 g/mol, respectively) for dry grinding of limestone and extrapolated the following effectiveness based on product fineness: Carboxylic acid > Amines > Alcohols > Glycols

2.2. *Inorganic grinding aids*

The most common inorganic GAs are presented in Table 2. Generally, multivalent inorganic salts have been found to increase grinding efficiency more than the monovalent ones. This has been attributed to the ability of multivalent ions to increase electrical repulsion between particles and promotes deagglomeration [7,39]. Kukolev and Melnishenko [40] reported an improvement in the grinding efficiency of magnesite ($MgCO_3$) when using sodium hydroxide as a GA. However, no effect yielded on dolomite ($MgCO_3.CaCO_3$). Somasundaran and Lin [41] later argued these findings after they observed improved grinding efficiency in their independent investigation on grinding of limestone ($CaCO_3$) with sodium hydroxide. The observations were attributed to the different degree of adsorption of sodium hydroxide on the respective mineral surfaces. Fuerstenau [3] examined the effect of aluminium chloride on grinding efficiency of quartz at different pH conditions where improvement was only materialized in the acidic to neutral conditions. Water was also considered as a GA to explain the better grinding efficiencies observed in wet grinding compared to dry grinding systems [3,39]. Fuerstenau [3] claimed this could be attributed to the reduction in the surface energy of wet grinding compared to dry grinding. Water reduces the cushioning effect during grinding; thus, allowing for un-dampened collision with grinding media, which leads to improving the grinding efficiency [3,39]. In other experiments reported, the use of non-polar liquids like carbon tetrachloride (CCl_4) and methyl-cyclohexane (as an organic GA) resulted in a lower yield of fineness compared to water [3]. The observed contradicting effects can be explained by the dispersion/flocculation effect of the particles [42] and the point of zero charges; the further away the better the effect [43]. Mallikarjunan et al. [43] improved grindability of calcite and lowered grindability of quartz by decreasing pH range from 8–4, and attributed it to their respective point of zero charges (10.5 for calcite and 2 for quartz).

3. Mechanisms

Grinding involves numerous and simultaneous sub-processes [3,7,53] which can be divided into (1) The transportation of material to the grinding zone (2) The loading or stressing of material leading to fracture (3) Prevention of agglomeration of the material (4) The transportation of the material away from the grinding zone. The application of GAs for grinding has been reported to affect some of these processes [10,14,19,32,53–55]. For understanding the mechanism of GAs

Table 2 – Inorganic grinding aids are used in various investigations.

Grinding aid	Dry or Wet	Material	Reference
Sodium hydroxide	Wet	Magnesite	[7]
	Wet	Limestone	[20]
	Wet	Iron ore concentrate	[49]
	–	Chromite ore	[50]
Sodium silicate	–	Clay slip	[7]
	Wet	Chromite ore	[50]
Sodium carbonate	–	Limestone	[38]
Carbon dioxide	–	Magnesite	[7]
	–	Dolomite	[7]
	–	Quartzite	[7]
Sodium chloride	–	Quartzite	[7]
	Wet	Chromite ore	[51]
Calcium oxide	Wet	Magnetite ore	[52]
	Wet	Iron ore	[24]
Calcium chloride	Wet	Magnetite ore	[52]
	Wet	Chromite ore	[50]
Aluminium chloride	–	Carbon black	[7]
	–	Graphite	[7]
	–	Talc	[7]
	Wet	Cassiterite	[17]
	Wet	Chromite ore	[51]
	Wet	Coal	[16]
Ferric sulphate	Wet	Cassiterite	[36]
Copper sulphate	–	Cassiterite	[29]
Ammonium carbonate	–	Mina	[7]
	–	Vermiculite	[7]
Sodium polymetaphosphate	–	Lead-zinc ore	[7]
	Dry	Talc	[15]
	–	Cassiterite	[29]
	Wet	Iron ore	[24]
	Wet	Chromite ore	[50]

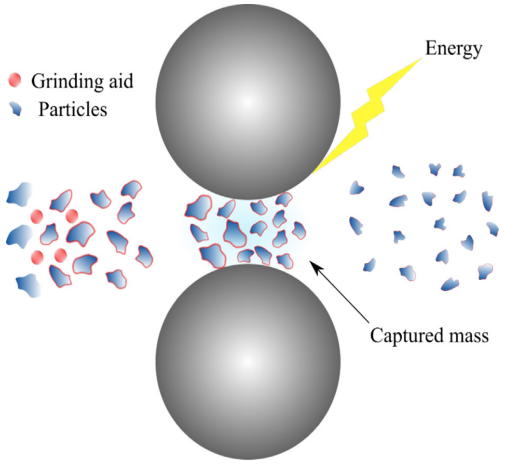

Fig. 1 – A schematic illustration of the particle capturing between grinding media in relation to the material flowability.

effectiveness, the grinding process can be simply described as a process that simultaneously involves the transportation and capturing of particles in the grinding zone and application of mechanical stress to yield breakage (Fig.1) [7,48,50].

The mechanisms of GA during grinding can be broadly divided into two groups (1) The alteration of surface and mechanical properties of individual particles such as surface energy (i.e. Rehbinder effect) and surface hardness; (2) The alteration of the particle arrangement and material flow characteristics by flocculation/ dispersion or the prevention of agglomeration or control of material flowability [1,3].

Although it is difficult to determine the mechanism of adsorption experimentally, it was reported that for all these proposed mechanisms, the adsorption of the GA onto the particle surface is a prerequisite [56]. This adsorption has been agreed to occur through the following ways; hydrogen bonding, especially for particles with near-neutral surface charges, chelating bonding with metal ions, hydrophobic bonding through the hydrocarbon tail, and electrostatic bonding [32,35].

3.1. *Surface energy*

The grinding process involves the application of mechanical stress for initiating and/or propagating a crack that results in fractures [7]. According to Griffith's theory of fracture mechanics, a successful fracture will occur if the loss in the elastic strain energy exceeds the increase in surface energy (i.e. the energy associated with the creation of new surfaces). This is the basis of Rehbinder's suggested mechanism that the reduction in the surface energy translates to the reduction in energy required for successful fracture, which promotes grinding [57].

Some studies have proven that application of GAs result in the reduction of the surface energy [14,55,57,58]. However, from a thermodynamic point of view, the energy associated with new surfaces is less than 1% of the input energy [7], which cannot account for the realised energy reduction in actual grinding. The mechanism assumes the existence of crack and ignores crack initiation, making pre-existing cracks a prerequisite for the effect of GAs [7]. On the other hand, Westwood and Goldheim [59] supported the effect of GAs on the surface and mechanical properties but questioned Rehbinder's explanation of the effect. They postulated that when GAs adsorbed on the particles, they immobilize the near-surface dislocations, which imparts brittleness; thus, resulting in improved grindability. These mechanisms assume that the material transport of GAs is faster than the crack propagation to allow for adsorption of GAs on the surface, which has been dismissed by other studies [35,39,60]. Schönert [60] found that the crack propagation velocities are significantly higher than the diffusion transport of GAs. Enustun et al. [16] dismissed these suggested mechanisms in their work were improved grinding efficiency of coal was reported at 43% solids concentration. However, no effect was reported at a lower density (16% solids) using the same ratio of coal to Aquard ™ (an ammonium chloride based GA). Besides such limitations to these proposed mechanisms, the explanations were followed in some other investigations [16,51,61]. Anoshin et al. [51] reported an increased degree of Cr^{3+} leaching from chromite with a factor greater than the reduction in surface area. They attribute the phenomena to inter-granular fracturing, which substantiates the effect of GAs on the fracture behaviour. Oettel and Husemann [62] found this speculative as they did not find direct evidence of the influence on fracture behaviour during communication of confined and unconfined particle beds of limestone using a single compressive load together with caproic acid. In a study on chromite ore, Camalan and Hoşten [61] reported an improved liberation after application of different GAs namely sodium oleate, potassium ethyl xanthate (PEX), sodium isopropyl xanthate (SIPX) and sodium lauryl dodecyl-sulphate (SLS) relative to the blank (without grinding aid). They related this improvement to the effect of the GAs on the fracture behaviour. Mishra et al. [32] performed molecular simulations to establish a correlation between experimental findings and the structure of the GA at the atomic scale. They did not succeed and concluded that at a molecular scale, the effect of GAs was to keep the cleaved surfaces apart rather than affecting crack propagation. The suggested mechanisms are likely to be relevant in a dominant abrasion process such as stirred media mill, which has a slower mechanism compared to fracture dominant process in the case of tumbling mills [16].

3.2. *Particle arrangement*

The material flowability in grinding is pivotal as it ensures the transportation of the material to and from the grinding zone. Mishra et al. [32] observed that N-methyl-diisopropanolamine (MDIPA) yielded the highest grinding efficiency (increase in surface area) compared to triisopropanol amine (TIPA) and triethanolamine (TEA). They ascribed it to the high dispersion of ground particles, which reduces agglomeration caused by MDIPA and consequently supporting the mechanism on particle arrangement (dispersion/ flocculation effect). Particle arrangement also depends on particle size, shape and concentration which affect the flow dynamics and particle breakage [63]. Several investigations have proven that the application of GAs alters the particle arrangement and flow properties [1,5,14,17,44,47,49,58]. The dispersion and flocculation effect is also supported by Somasundaran et al. [20]'s findings were the zeta potential of a particle decreases with the adsorption of oppositely charged surfactants. Vieira and Peres [49] researched on the grinding of iron ore concentrate using sodium hydroxide. Their work showed a strong correlation between grinding efficiency (quantified by surface area and specific power) and the degree of dispersion at varying pH and pulp density, which corroborates the mechanism on particle arrangement. Klimpel and Manfroy [1], suggested that GAs neutralise the particle charges. This reduces the particle-particle interaction and tendency of agglomeration and, therefore, improves material flowability. Weibel and Mishra [2] found agglomeration to be inversely proportional to grinding, which supports Klimpel and Manfroy [1] proposed mechanism. In the grinding of limestone with polyacrylic acid as a GA, Zheng et al. [20] observed a drop in the mill power draw and improved material transport. Rajendran and Paramasivam [12] investigated the effects of GAs on grinding efficiency and found a reduction in agglomeration accompanied by improved material flowability.

The theories based on surface and mechanical properties have failed to explain the effect of GAs in grinding. Therefore, it is the prevailing mechanism of effect is one based on the particle arrangement and material flow properties. The mechanism based on the material flow properties can be illustrated using Fig. 1. At low flowability (adding a low GA ratio), too much material is captured in the grinding zone relative to the stress-energy, which results in low grinding efficiency. At high flow-ability (using a high GA ratio), the material captured in the grinding zone is too low. Regardless of the stress-energy this results in the low efficiency, which suggests that an optimum flow-ability exists. Despite the lack of support on the surface and mechanical properties mechanism, the commonly reported reduction in the surface energy remains a point of discussion on its role in grinding when GAs adding to the process.

4. Grinding efficiency

Few studies have been conducted to investigate the effect of GAs on grinding efficiency. Grinding efficiency is mostly described in terms of mill throughput and specific energy consumption based on the final product. Kokolev [64] studied the effect of organosilicon (0.005 wt. %) in the context of wet grinding of alumina in a ball mill where the grinding time decreased four-fold compared to grinding without any additive. Similarly, Orlova [65] reported a four-fold decrease in grinding time in the wet grinding of zircon using TEA (0.2 wt.%). Melnik [66] discussed the results of the ball mill test where organosilicon (0.05 wt. %) was used in grinding of cement clinker, and the grinding time was reduced by 70% in comparison with the absence of GAs. Schneider [67] observed the same outcomes

where the grinding of cement clinker using glycol resulted in a 50% decrease in time for the same production.

During grinding, higher energy is required for further size reduction due to the significance of particle-particle interaction, which decreases grinding efficiency [10,48,53]. Grinding efficiency is mainly evaluated based on energy consumed per given mass of material as a function of time [39,68]. It is shown that GAs reduce energy consumption (Table 3). The reduction in the energy consumption increases by increasing GAs dosage to a maximum, after which further addition gives no effect [5,10,20]. During the grinding of calcite using polyacrylic acid as a GA, Choi et al. [9] observed 31.6% and 37.2% of energy reduction at 60 and 70 wt.% solids. This evidences that GAs are more effective at a high solid percentage. The reduction in energy consumption is attributed to the reduction in particle-particle interaction, which prevents agglomeration [9,14]. This is in agreement with Zheng et al. [20]'s comments that the reduction in energy consumption represents an improvement in the material flowability, which points to a reduction in particle-particle interaction. Zheng et al. [38], studied the grinding of limestone using polyacrylic acid and attributed the decrease in energy consumption based on the increased particle flocculation.

Various materials respond differently to GAs with some showing positive and negative effects or no response at all. This phenomena has been reported in many studies suggesting that GAs are solid-specific although there is no correlation of global surface chemical properties (such as functional groups, molar masses) with their effectiveness [2,70]. From rheology studies, the observations can be attributed to the varying degree of flow properties such as flow index, bulk density, internal friction factor and shearing cohesion [12].

5. Product properties

5.1. *Particle size distribution*

It has been observed that by increasing the GA dosage, the particle size distribution (PSD) gets narrower and shifts to the finer size range (Fig. 2) [5,10,15,45,48,58,71]. In a study on the grinding of cement using triethanolamine, Altun et al. [5] observed a coarser and wider particle size distribution in the blank compared to the run with the GA. Zhao et al. [45] reported a similar trend on the grinding of ultrafine fly ash using a blend of triethanolamine and ethylene glycol. Ma et al. [36] found that the use of polyacrylamide on the grinding of cassiterite polymetallic sulphide ore resulted in a narrow particle size distribution. Yusupov and Kirillova [21], reported the use of GA for controlling the particle size distribution by reducing slimes in the flotation feed, thus reducing the detrimental effects. The resulting narrow particle size distribution due to the use of GA can be attributed to the improved flowability. This allows all particles to be ground under an optimum particle-bed thickness. This supported Schönert's [72] finding that the particle size distribution became wider as the particle bed height increased. Przwara et al. [48]'s results also confirm this phenomenon when they compared the effect of diethyl glycol (DEG) (low flowability) and heptanoic acid (HepAc) (high flowability) on the particle size distribution of calcite where the latter gave a narrower and fine particle size distribution. Moothedath and Ahluwalia [73] attribute the phenomenon to the reduction of the abrasion component due to the use of GA. This promotes fine and course material generation due to the roundness of particles from the nipping. This nipping action inhibits further breakage, although it highly depends on the main breakage mechanism of the process. The higher the viscosity of the GA, the narrower the product particle size distribution [3].

5.2. *Specific surface area*

Specific surface area in the section, is defined as the surface area per unit mass which is a function of porosity, pore size distribution, shape, size, and roughness [75]. The effect of GA on the specific surface area (SSA) follows a similar profile as for the energy consumption. The SSA increases with an increase in dosage up to a maximum and starts decreasing (Fig. 3) [20,32,44]. This phenomenon of a decrease after an initial increase in the SSA is attributed to the agglomeration of particles [44]. A strong correlation was established between the SSA and the applied energy, confirming the significance of agglomeration as particle size decreases [49]. The use of GA increases the SSA without necessarily increasing the energy consumption (Table 4) [5,13,32,49]. The increase in the SSA at a given energy is attributed to the reduced particle-particle interaction due to enhanced dispersion of particles [37,44].

5.3. *Surface properties*

The grinding physico-chemical environment including the presence or absence of GAs affects material surface properties such as surface roughness, surface area, surface defects [21,76,77]. Yusupov and Kirillova [21] observed that during the fine grinding of a Norilsk Ore (a silicate ore) with oleic acid as a GA, less defects on the mineral structure were generated compared to grinding without the GA. The reduced defects can be attributed to the differences in the flowability which affects the captured mass (Fig. 1), this phenomenon consequently leads to more defects in case of low captured mass and high stress intensity. Moreover, several studies have shown that GAs increase the specific surface area compared to grinding without GAs [10,15]. This increase in the surface area can lead to increase in surface roughness based on Jaycock and Parfitt's relation where the surface roughness is directly proportional to the SSA for a given density and particle diameter [78].

6. Material flowability

It was well documented that the grinding efficiency can be improved by controlling the rheological or flow characteristics of the material [7,35,79]. These material flow characteristics are influenced mainly by the solids content, particle size distribution, and the chemical environment - flocculation/dispersion state [3,7,35]. Some other properties, such as particle shape, temperature, and shear rate (stirring) are also reported as effective features [35,79]. GAs improve material flowability by narrowing the particle size distribution,

Table 3 – Effect of grinding aids on energy consumption.

Grinding aid	Material	Reduction in power consumed (%)	Reference
Triethylamine (TEA)	Limestone	98.5	[10]
BMA-1923^{TM} (Amine based)	Feldspar	60.0	[69]
TIPA	Cement	20.6	[5]
Propylene glycol	Clinker	10.0	[13]
Sodium polyphosphate	Copper ore	15.7	[13]
Alcohol	Coal	2.37	[13]
Diethylamine (DEA)	Coal	1.05	[13]
Sodium polyphosphate	Talc	33.7	[15]
Sodium polycarboxylic acid	Talc	20.7	[15]
Polyacrylic acid	Calcite	37.2	[9]
Triethylamine (TEA)	Cement	17.34	[68]
Polyacrylic acid	Limestone	100	[20]
Aluminium chloride	Coal	25.0	[16]
Sodium silicate	Chromite	4.67	[50]

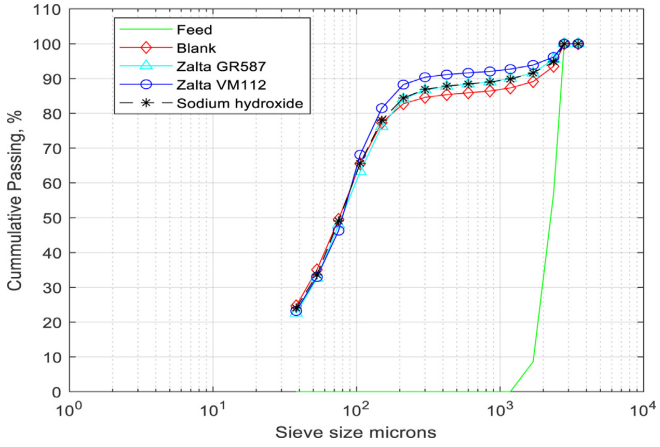

Fig. 2 – Effect of grinding aids on the particle size distribution [74].

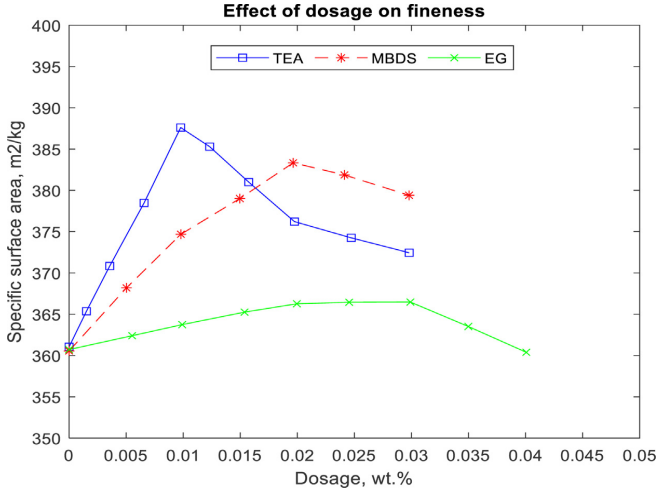

Fig. 3 – Effect of GA dosage on specific surface area. *TEA – triethanolamine, EG- Ethylene glycol, MDBS – Sorbitol based on [58].

Table 4 – Effect of GA on the specific surface area.

Grinding aid	Material	Specific surface area (cm^2/g)			Reference
		Without	With	% Change	
Triethylamine (TEA)	Cement	3520	3580	1.7	[32]
Triethylamine (TEA))	Limestone	–	–	34	[10]
Triethylamine (TEA)	Quartz	–	–	17.5	[10]
Triethylamine (TEA)	Clinker	–	–	54.0	[10]
TIPA	Cement	–	–	6.8	[5]
TEA: Ethylene glycol	Fly Ash	7500	8540	13.8	[45]
Sodium polyphosphate	Talc	3360	4030	19.9	[15]
Sodium polycarboxylic acid	Talc	3360	3830	14.0	[15]
TIPA:TEA:NaOH	Cement	–	–	10.6	[58]
Amine based blend	Cement	4512	4543	0.7	[68]
Triethylamine (TEA)	Cement	3950	3980	0.8	[55]

thus minimising the number of fines generated [9,35,48]. This improvement reduces material retention time in a mill; thus, increases the grinding efficiency [3,5,7,9,11,45]. The use of additives in grinding of metal powders also follows the principle of reducing abrasion thereby improving material flowability (tribology) where materials like graphite and molybdenum disulphide [80,81].

6.1. *Wet systems*

It is approved that viscosity influences grinding processes [49,79]. In wet grinding systems, a critical viscosity or slurry yield value exists, where the grinding efficiency starts decreasing due to high solids content and excessive fines [35,82]. According to Fuerstenau et al., [82] the grinding media starts centrifuging (stick to the mill walls) above this critical viscosity, which affects the cataracting and cascading motion in the case of tumbling mills. As such, GAs work by reducing the slurry yield point and eliminating the centrifuging effect [49,82,83]. A reduction in material flow properties normally results in the deviation from the Newtonian slurries (shear stress is directly proportional to the rate of shear) resulting in an increase in viscosity [3]. An increase in viscosity has been found to be inversely proportional to grinding efficiency [13,47]. GAs reduce the pulp viscosity, thus increasing material transport [13,37,49].

6.2. *Dry systems*

The particle-particle interaction increases by increasing grinding time leading to agglomeration, which in turn decreases material flowability [14,53]. Poor material flowability results in the accumulation of material in the mill, thus allowing for the re-agglomeration of ground particles [13]. These conditions are increased extensively during dry grinding. GAs change the grinding environment by neutralizing the surface charges on the particles, which reduces inter-particle interaction, thus fluidizing the material [1,5,50].

7. Grinding environment

As mentioned earlier, rheological properties affect the grinding efficiency, which depends mainly on the grinding environment. Grinding in liquids, particularly water, is generally believed to be more efficient compared to a dry system [3,7]. In the case of water, several researchers attributed this to the physicochemical interaction of water with a broken surface bond, which promotes crack propagation [60,84–86]. Grinding in organic liquids has been found to be more effective compared to water, although the economics of the application is prohibitive [3,67,84]. According to Engelhardt [87], alcohol resulted in less energy consumption for the same specific surface area compared to water in the grinding of quartz. The observations are attributed to the difference in surface tension and viscosity of the medium with alcohol having a lower surface tension [3,7]. GAs are influenced by the solids percentage, slurry pH, degree of mixing, and temperature [1,7,79].

The effect of GA depends on the dosage as well as the pH environment [7]. Gamal [88] showed a strong effect of pH on product fineness and grindability during the grinding of a quartz sample using sodium silicate, isoamyl alcohol, and ethylene glycol, respectively (Fig. 4). Ryncarz and Laskowski [89] correlated the observed effects to the zeta potential values of quartz in amine solutions where grinding efficiency was low at pH conditions close to the point of zero charge (PZC) values. Halasyamani et al. [42] investigated the effect of pH on the grinding of quartz and calcite with HCl and NaOH in a ball mill. The maximum grinding efficiency for quartz was at pH 7 and was attributed to the dispersion effect since its PZC was at pH 2. In a similar setup, Mallikarjunan et al. [43] confirmed an increase in surface area of calcite by decreasing pH from 8 to 4, whilst for quartz, the surface area decreased. Vieira and Peres [49] studied the effect of degree of dispersion on the regrinding of iron ore concentrate with sodium hydroxide. They reported an increase in the degree of dispersion from 3 to 28% with an increase in pulp pH from 7.3 to 10.This resulted in 17.4% decrease in the specific power consumption. Basically, this can be explained by the increase in dispersion of particles since the pH change is way from the point of zero charge given its 2.0 and 10.5 for quartz and calcite, respectively [3,90]. As such non-ionic chemicals that contain the –O and –OH functional groups are usually preferred in industry; as these are less sensitive to pH changes [35].

Dombrowe et al., [34] found no influence of temperature on the efficiency of using GAs in a tumbling mill. In

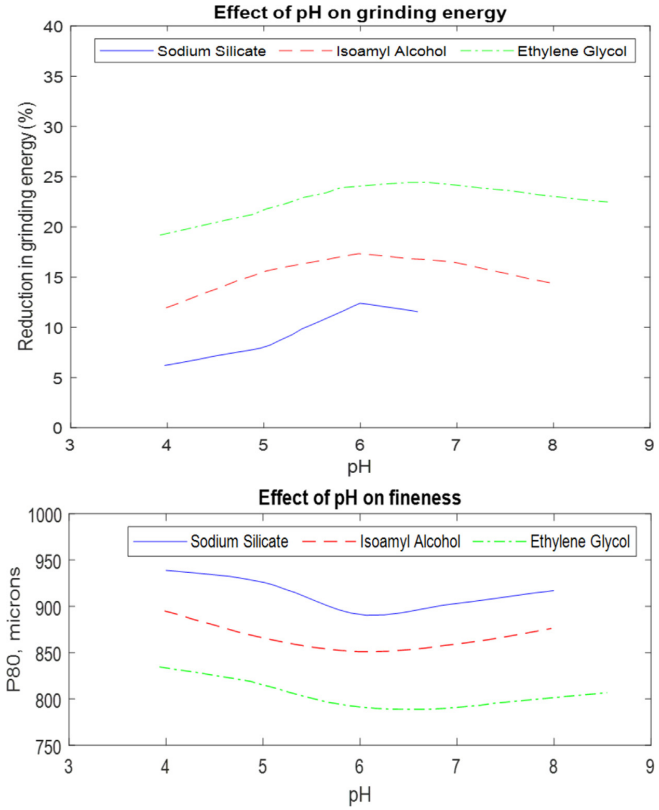

Fig. 4 – Effect of pH on product fineness and grinding energy for a quartz sample based on [88].

contrast, Scheibe et al. [91], showed a decrease in specific surface area and increase in agglomeration with an increase in temperature during ball milling of a cement clinker with trimethylamine as a GA. The effect of temperature is often overlooked in wet laboratory grinding considering the relatively lower and narrow temperatures experienced in the set ups. Many grinding aids used commercially can withstand grinding temperatures minimizing losses in GAs due to volatilization or decomposition [2]. It should be highlighted that temperature correlates with inter-molecular interaction which affect the adsorption strength of GAs on particle surface [2].

8. Process parameters

Prziwara et al., [48] gave a global overview on the effects of process parameters on the performance of GAs. They emphasized on the importance of mill "machine related parameters" as well as material properties. There is no published study on the effect of direct machine related parameters or grinding force (loading mechanism) on the efficiency of using GAs. However, few investigations addressed the stress conditions which are machine related factors [34,48,73,92]. Prziwara et al. [48], used a modern stirred media mill and they found that the efficiency in the presence of GAs depends on the stirrer tip speed but independent of the grinding media type.

8.1. *Mill feed and solids content*

In the grinding of a taconite ore with sodium hydroxide, Hartley et al. [93] reported an increase of grinding efficiency for a feed with a narrow (uniform) size compared to a feed with a wide range size. From their observations, the application of GAs is more effective on narrow PSD feed compared to the feed with a widespread PSD. It has been reported that GAs are more effective at a high slurry concentration or solids content [3,20,48]. In the grinding of calcite with polyacrylic acid, grinding efficiency was 31.61 and 37.27% for 60 and 70 wt. % solid percentage, respectively. This confirms that GAs are more effective at higher solid concentrations (Fig. 5). This observation is mainly attributed to the increase in material to media ratio resulting in the full utilization of grinding media [9,48].

8.2. *Grinding media*

The effect of GA on grinding media with a focus on the material and size was addressed in some investigations [2,48]. The use of GA in grinding reduces the coating of the grinding media, thereby reducing the cushioning effect of fines and pro-

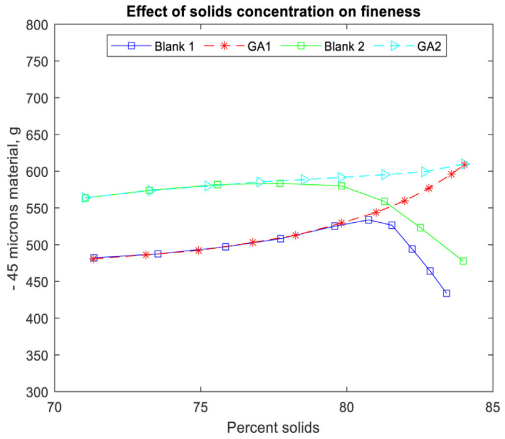

Fig. 5 – Effect of solids concentration on the product fineness of a tarconite ore using a polycarboxylate (XFS 4272) as a GA, where blank 1 and GA1 at a lower viscosity whilst, blank 2 and GA2 at a higher viscosity based on [3].

motes grinding impact [14]. The effect of GAs on the different grinding media, made by alumina, steel, and zirconia, utilizing grinding balls of different sizes with a density of 3.62, 7.86, and 6.07 kg/l, respectively was studied [48]. Regarding the GA choice, the grindability proved to be independent of the grinding media size and material. Based on the product fineness and specific energy, the alumina grinding media was found to be the best option as it resulted in less stress-energy with less energy (heat) dissipation due to its low density. It can be stated that as long as the critical size (a size that allows for minimum mass capturing based on particle size) is exceeded, the effect of material flowability (due to the use of GAs) becomes critical on mass capturing. The material of grinding media is believed to affect grinding due to properties such as surface roughness, which may influence flowability. However, no investigations have been reported [94]. The choice of material for grinding media is also important to ensure that the GAs do not corrode the media [21,37]. The use of oleic acid as a GA for fine quartz grinding by metallic balls showed no increase in grinding efficiency. This was attributed to the oleic acid-metal reaction, which used up the grinding aid due to side reactions reducing the amount of oleic acid available for grinding [21]. Routray and Swain [50] reported a beneficial effect on the wear of steel balls from the GAs-grinding media interaction. The use of sodium silicate, sodium hydroxide and sodium hexa-metaphosphate resulted in 0.37, 0.44 and 0.50% ball wear, respectively, compared to 0.55% observed for the blank (without GA). This observation can be attributed to the improved fluidity of the slurry which reduces the frictional wear on the grinding media [50].

8.3. *Shear rate*

Studies on the effect of stirrer speed on the application of GAs in the case of stirred media mills have been conducted by [48]. It was reported that the range 2–3 m/s was the optimum, whereas low speeds (1 m/s) and high speed (4 m/s) were less effective, showing the importance of optimum stress intensity. The use of heptanoic acid (high flowability) improved grindability for the low speeds (1 m/s) whereas diethylene glycol (low flowability) improved grindability for the high speed (4 m/s). Basically, the observation was explained using the particle capturing model with low speeds resulting in too low-stress intensity relative to the captured mass and vice versa, i.e. too much stress intensity relative to captured mass at high speeds resulting in high dissipation of energy as heat [48,95–98]. Grinding aids help in controlling the flowability to give the optimum mass capturing conditions.

8.4. *Dosage strategy*

A number of studies have been done to determine the effect of the GA dosage strategy in grinding, comparing continuous and once-off addition [16,48]. Although not conclusive, stage-wise addition has been reported to be more effective compared to single-stage addition [48]. At the onset of grinding the material is coarse (low specific surface area) with too much GA (high flowability) which is detrimental but rather continuous addition the total amount of GA increases with an increasing fineness (specific surface area) which ensures optimum flowability [16,48,83,93].

9. Downstream performances

Considering that grinding is one of the first steps in ore beneficiation, the application of GAs has to be economical and, most importantly, have no detrimental effects on the downstream processes. GAs such as sodium hexametaphosphate (SHMP) and sodium silicate (they are typically dispersant and depressant) are mainly used for complex minerals. The use of these GAs should be assessed since they are effective in flotation [24,35]. From an environmental point of view, sodium hexametaphosphate is harmful due to the phosphate group, which was reported in effluent water [35]. Sodium hydroxide is commonly used as a GA. It is primarily used as a dispersant for mineral oxides but also acts as a pH modifier, and as such, the downstream process pH should be considered [35,50]. Citric acid is a general-purpose dispersant for a number of minerals and is more effective at pH < 6, although it has a tendency of forming insoluble salts with Ca^{2+} ions and other metals which increases its consumption [35]. Some reported effects of GA on downstream processes are listed in Table 5.

Selective grinding of materials is a promising solution to problems of over-grinding/under-grinding and high energy consumption associated with the beneficiation of complex minerals such as cassiterite or polymetallic sulphides [16,29,36,100]. The concept of selective grinding recognizes that soft minerals have a slower grinding rate compared to brittle ones due to the effect that Tanaka [101], described it as the shielding effect [83,100]. The GAs increase the grinding rates of both minerals, which reduce the differences in the grinding rate [83,101]. The aspects are not well understood regarding the effect on individual grinding rates (i.e. the soft and hard mineral), and it is believed GAs equally increase the grinding rates of all components [83]. Depending on the

Table 5 – Downstream effects of grinding aids.

Grinding Aid	Effects	Reference
Calcium Oxide	2.9 % increase in dense media separation efficiency of magnetite (65.0–67.9 %)	[8]
ZALTA™	4 % increase of copper recovery through flotation by maintaining high throughput without comprising the mineral liberation	[99]
Benzyl arsenic acid	6.4 % increase in flotation recovery of cassiterite (51.6–58%)	[29]
Sodium hexa-metaphosphate	42 % decrease in flotation recovery of cassiterite (51.6 – 9.6%)	[29]
Hydroxylamine based GA	7% reduction in recycled fines in an air classifier underflow (22.6–15.5 %)	[68]
Ammonium chloride	Increased dissolution of chromite in HCl	[51]
Potassium ethyl xanthate (PEX)	6% increase in recovery of chromite ore	[61]

downstream process, the preferential grinding of the gangue is usually preferred for physical separation whilst the reverse is desired for chemical separation.

During grinding, fracture occurs either as intra-granular (within the particle itself) or inter-granular (along grain boundary) with both sufficient for size reduction. The latter is more beneficial for mineral liberation [7,61]. Anoshin et al. [51] conducted a study to understand the effect of inorganic GA on the structural properties of chromite. The observed increase in the dissolution in hydrochloric acid was more than the rate in the increase of the specific surface area after grinding with ammonium chloride. Although dissolution is related to the surface area, they attributed the differences in the rates to the effect of the GA. The observations suggest that GAs increase the degree of amorphisation of the mineral structure; thus, improving its dissolution [21,50,51]. Camalan and Hoşten [61] assessed the GAs' effect on promoting the liberation of chromite. In their work, they pre-treated chromite ore prior to a drop weight test and analysed the progenies using a scanning electron microscope and X-ray diffraction. They reported that the use of potassium ethyl xanthate enhanced liberation by promoting fracturing of particles along grain boundaries. The non-random liberation is attributed to the hydrolysis of the grain boundary due to the GA, thus resulting in its weakening [61].

The use of CaO as GA in the grinding of magnetite ore improved its recovery [52]. The authors observed a 67.9% recovery after using the GA and 65.0% for the run without GA in the heavy liquid separation giving a 2.9% increase. Enustun et al. [16] investigated the effect of Aquard ™, (an ammonium chloride-based GA) on the grinding of coal. The GA resulted in selective grinding of the inorganic matter (pyrite), which presents an opportunity of simplifying coal washing to a mere separation by size process [16]. This is all attributed to the preferential grinding effect of GA, which favours the grinding of gangue material and promoting the separation via gravity methods.

Toprak et al. [54] developed a GA specific model for an air classifier using different types of GAs. The model is based on Whiten's partition function [54], together with the relation between GA type and dosage with the model parameters.

$$E_{o\alpha} = C^{*}\left(\frac{\left(1+\beta^{*}\beta^{**}\frac{d}{d_{50c}}\right)^{*}(\exp(\alpha)-1)}{\exp\left(\alpha^{*}\beta^{*}\frac{d}{d_{50c}}\right)+\exp(\alpha)-2}\right)$$

where, $E_{o\alpha}$ is the actual efficiency to overflow, C is the fraction subjected to real classification, β (fish-hook) is a parameter that controls the rise of the curve in fine sizes, β^{*} is a parameter that represents the definition of d_{50c} (i.e. d_{50c} = d when E = 1/2C), d is the particle, and α is the corrected cut size i.e. sharpness of separation. GAs were found to mainly affect the β (fish-hook) and C (fraction subjected to real classification) parameters. This substantiates the finding reported in those studies that GAs result in the reduction of the fines recirculated back into the mill, which is often referred to as the bypass fraction [14,32,68]. Basically, this is explained by the effect of GA on the reduction of agglomeration which improves the feed dispersion and consequently improves classification [14,32,54,55,83].

Several investigations were carried out to address problems in the beneficiation of cassiterite using GAs [29,36,100]. In the study they wanted to ensure that the feed was not over-ground for the use of gravity methods and, at the same time, avoid under-grinding for the flotation feed. The use of benzyl arsenic acid improved grinding efficiency (i.e. energy consumption and narrow PSD) and flotation recoveries whilst SHMP only improved grinding efficiency but had low flotation recoveries. This observation is attributed to the depressant nature of SHMP, which reduces the floatability of cassiterite whilst benzyl arsenic acid acts as a collector [29,102].

10. Summary

In mineral beneficiation, wet grinding is much preferred compared to dry grinding, but the growing scarcity of potable water poses a threat to mining activities, especially in arid regions. For dry grinding, the high energy consumption remains the major problem coupled with low throughputs. This necessitates energy-efficient technologies and strategies. As such, the use of additives (grinding aids) in mineral processing can be considered as a promising alternative for reducing energy consumption. Chemicals that can be employed as GAs range from organic (such as polyols, alcohols, esters, amines) and inorganic (such as calcium oxide, sodium silicate, sodium carbonate, sodium chloride) with some also employed as modifiers, flocculants, surfactants, and dispersants in downstream processes.

1 GAs have some additional benefits besides reduction in energy consumption such as enhancing grinding efficiency, reducing water usage, improving material flowability, improved liberation, and narrowing the particle size distribution of the products. These effects can mainly improve grinding efficiencies under selected conditions. Thus, it

is necessary to understand and establish such conditions based on the mechanisms involved.

2 There is no established correlation between grinding efficiency and the GA's structure at the atomic scale. The wide range of chemicals, which act as GA, makes it difficult to relate the atomic structure to resulting effects.

3 The effectiveness of grinding aids depends on the GA type, dosage, grinding environment as well as various process parameters.

4 There is a lack of scientific understanding on the mechanism of GAs' effect in grinding processes. Surprisingly, the aspect of energy expended to characterise the effects is neglected, which is the basis of their application in the industry. Moreover, there is a lack of understanding on the effects of the physicochemical environment, which could explain the many contradicting effects of GAs reported. For addressing the lack in understanding on the mechanism of effect, the understanding of GA is required looking at properties such as the zeta potential, surface tension, pH ionic strength, temperature, and chemical composition are required. Another approach is required looking at the machine characteristics such as speed, size, mechanism of stress loading, and mill filling. A better understanding of the aspects will pave the way for the application of GAs as an energy-efficient technology, which ultimately reduces environmental impacts.

5 There is a general acceptance on the state of dispersion/flocculation and particle arrangement (flowability) as the effective mechanism, although no outright scientific explanation exists. To fill this gap in scientific knowledge, further studies on the effect on fracture behaviour (Rehbinder's effect) are required. A better understanding of the effect of GAs on fracture behaviour could open up the potential for improving mineral liberation. Most research work and industrial applications that exist in literature are in the cement industry and few in mineral industrial. Currently, few studies show some positive effects of GAs on classification and separation efficiency of downstream processes such as froth flotation together with some negative effects. The successful application of GA in beneficiation plants requires an understanding of possible effects on downstream processes.

Therefore, more research work is required in the application of GAs in the mineral industry to explore possible benefits.

Declaration of interests

The authors declare that they have no known competing financial interests or personal relationships that could have appeared to influence the work reported in this paper.

Acknowledgments

This study was conducted with the financial support of CAMM - Centre of Advanced Mining and Metallurgy, a Centre of Excellence at Luleå University of Technology, and by the SEESIMA project, a Kolarctic CBC (Cross-Border Collaboration) supported by the European Union, Russia, Norway, Finland and Sweden. Its contents are the sole responsibility of the authors at the Luleå University of Technology, and do not necessarily reflect the views of the European Union or the participating countries.

REFERENCES

[1] Klimpel RR, Manfroy W. Chemical grinding aids for increasing throughput in the wet grinding of ores. Ind Eng Chem Process Des Dev 1978;17:518–23, http://dx.doi.org/10.1021/i260068a022.

[2] Weibel M, Mishra RK. Cement additives - comprehensive understanding of grinding aids; 2014.

[3] Fuerstenau DW. Grinding aids. Kona Powder J 1995;13:5–18, http://dx.doi.org/10.14356/kona.1995006.

[4] Hao S, Liu B, Yan X. Review on research of cement grinding AIDS and certain problems. Key Eng Mater 2017;753, http://dx.doi.org/10.4028/www.scientific.net/KEM.753.295. KEM:295–299.

[5] Altun O, Benzer H, Toprak A, Enderle U. Utilization of grinding aids in dry horizontal stirred milling. Powder Technol 2015;286:610–5, http://dx.doi.org/10.1016/j.powtec.2015.09.001.

[6] Jeswiet J, Szekeres A. Energy consumption in mining comminution. Procedia CIRP 2016;48:140–5, http://dx.doi.org/10.1016/j.procir.2016.03.250. Elsevier B.V.

[7] El-Shall H, Somasundaran P. Physico-chemical aspects of grinding: a review of use of additives. Powder Technol 1984;38:275–93, http://dx.doi.org/10.1016/0032-5910(84)85009-3.

[8] Bhima, Rao R, Narasimhan KS, Rao TC. Effect of additives on grinding of magnetite ore. Miner Metall Process 1991;8:144–51.

[9] Choi H, Lee W, Kim DU, Kumar S, Kim SS, Chung HS, et al. Effect of grinding aids on the grinding energy consumed during grinding of calcite in a stirred ball mill. Miner Eng 2010;23:54–7, http://dx.doi.org/10.1016/j.mineng.2009.09.011.

[10] Csoke B, Racz A, Mucsi G. Grinding and flowing investigation on dry stirred ball milling in order to determine the influence of grinding aids. In: XXV International Mineral Processing Congress 2010, (IMPC) 2010 Proceedings Brisbane, QLD, Australia, Vol. 1. 2010. p. 629–36.

[11] Przwara P, Breitung-Faes S, Kwade A. Impact of the powder flow behavior on continuous fine grinding in dry operated stirred media mills. Miner Eng 2018;128:215–23, http://dx.doi.org/10.1016/j.mineng.2018.08.032.

[12] Rajendran Nair PB, Paramasivam R. Effect of grinding aids on the time-flow characteristics of the ground product from a batch ball mill. Powder Technol 1999;101:31–42, http://dx.doi.org/10.1016/S0032-5910(98)00121-1.

[13] Noaparast M, Rafiei A. The effect of grinding aids on the work index values; 2003. p. 1–6.

[14] Przwara P, Breitung-Faes S, Kwade A. Impact of grinding aids on dry grinding performance, bulk properties and surface energy. Adv Powder Technol 2018;29:416–25, http://dx.doi.org/10.1016/j.apt.2017.11.029.

[15] Diler K-B. The effect of additives on stirred media milling of talc. Powder Technol 2018;5:36–9, http://dx.doi.org/10.1016/S0032-5910(96)03236-6.

[16] Enustun BV, Liu DC, Markuszewski R, Lin KL. Use of a surfactant as a coal grinding additive. Coal Prep 1987;4:193–207, http://dx.doi.org/10.1080/07349348708945532.

[17] Ma S, Yang J, Mo W, Wang G, Su X, Yuan C. The effect of grinding aids on laboratory grinding of a

cassiterite-polymetallic sulfide ore. In: XXV International Mineral Processing Congress 2010, IMPC 2010. 2010, 2:1001–8.
[18] Han Y, Zhu Y, Wang Z, Tian Y. Effects of DA as a grinding aid on selective grinding of Low-grade bauxite. In: XXV International Mineral Processing Congress 2010, IMPC 2010. 2010, 1:781–9.
[19] Rajendran NPB, Paramasivam R. Analysis of the influence of grinding aids on the breakage process of calcite in media mills. Adv Powder Technol 1999;10:223–43, http://dx.doi.org/10.1163/156855299X00316.
[20] Zheng J, Harris CC, Somasundaran P. Role of chemical additives in stirred media Mill grinding. In: 5th World Congress of Chemical Engineering - American Institute of Chemical Engineers. 1996.
[21] Yusupov T, Kirillova E. Surfactants in fine ore grinding. J Min Sci 2010;46:582–6.
[22] Feng D, Aldrich C. A comparison of the flotation of ore from the Merensky Reef after wet and dry grinding. Int J Miner Process 2000;60:115–29, http://dx.doi.org/10.1016/S0301-7516(00)00010-7.
[23] Mwale AH, Musonge P, Fraser DM. The influence of particle size on energy consumption and water recovery in comminution and dewatering systems. Miner Eng 2005;18:915–26, http://dx.doi.org/10.1016/j.mineng.2005.02.014.
[24] Melorie AK, Raj Kaushal D. Experimental investigations of the effect of chemical additives on the rheological properties of highly concentrated iron ore slurries. Kona Powder J 2018;2018:186–99, http://dx.doi.org/10.14356/kona.2018001.
[25] Kotake N, Kuboki M, Kiya S, Kanda Y. Influence of dry and wet grinding conditions on fineness and shape of particle size distribution of product in a ball mill. Adv Powder Technol 2011;22:86–92, http://dx.doi.org/10.1016/j.apt.2010.03.015.
[26] Singh V, Dixit P, Venugopal R, Venkatesh KB. Ore pretreatment methods for grinding: journey and prospects. Miner Process Extr Metall Rev 2018;40:1–15, http://dx.doi.org/10.1080/08827508.2018.1479697.
[27] Somani A, Nandi TK, Pal SK, Majumder AK. Pre-treatment of rocks prior to comminution – a critical review of present practices. Int J Min Sci Technol 2017;27:339–48, http://dx.doi.org/10.1016/j.ijmst.2017.01.013.
[28] Napier-Munn T. Is progress in energy-efficient comminution doomed? Miner Eng 2015;73:1–6, http://dx.doi.org/10.1016/j.mineng.2014.06.009.
[29] Yang A. The influence of grinding aids on the on the floatabilty of the fine casseterite. Fizykochemiczne Problemy Mineralurgii 1994;28:37–46.
[30] Xiao X, Zhang G, Feng Q, Xiao S, Huang L, Zhao X, et al. The liberation effect of magnetite fine ground by vertical stirred mill and ball mill. Miner Eng 2012;34:63–9, http://dx.doi.org/10.1016/j.mineng.2012.04.004.
[31] Morrell S. Predicting the overall specific energy requirement of crushing, high pressure grinding roll and tumbling mill circuits. Miner Eng 2009;22:544–9, http://dx.doi.org/10.1016/j.mineng.2009.01.005.
[32] Mishra RK, Weibel M, Müller T, Heinz H, Flatt RJ. Energy-effective grinding of inorganic solids using organic additives. Chimia 2017;71:451–60, http://dx.doi.org/10.2533/chimia.2017.451.
[33] Jeknavorian A, Barry E, Serafi F. Determination of grinding aids in Portland cement by pyrolysis gas chromatography-mass spectrometry. Cem Concr Res 1998;28:1335–45.
[34] Dombrowe H, Hoffmann B, Scheibe W. Über wirkungsweise und einsatzmöglichkeiten von mahlhilfsmitteln. Zement-Kalk-Gips 1982;11:571–80.
[35] Klimpel RR. The selection of wet grinding chemical additives based on slurry rheology control. Powder Technol 1999;105:430–5, http://dx.doi.org/10.1016/S0032-5910(99)00169-2.
[36] Ma S, Yang J, Mo W, Wang G, Su X, Yuan C. The effect of grinding aids on laboratory grinding of a cassiterite-polymetallic sulfide ore. In: XXV International Mineral Processing Congress 2010, IMPC 2010. 2010, 2:1001–8.
[37] Lartiges B, Somasundaran P. Ultra fine grinding of yttria stabilized zirconia in polyacrylic acid solutions. Soc Min, Metall, Explor 1992;43:585–98.
[38] Zheng J, Harris CC, Somasundaran P. The effect of additives on stirred media milling of limestone. Powder Technol 1997;91:173–9, http://dx.doi.org/10.1016/S0032-5910(96)03236-6.
[39] Somasundaran P. Theories of grinding. In: Ceramics processing before firing; 1978. p. 105–23.
[40] Kukolev G, Melnishenko L. Fireproof Mater 1948;13:447.
[41] Somasundaran P, Lin IJ. Effect of the nature of environment on comminution processes. Ind Eng Chem Process Des Dev 1972;11:321–31, http://dx.doi.org/10.1021/i260043a001.
[42] Halasyamani P, Venkatachalam S, Mallikarjunan R. Influence of pH on the kinetics of comminution of quartz. Ind Eng Chem Process Des Dev 1968;7:79–83, http://dx.doi.org/10.1021/i260025a016.
[43] Mallikarjunan R, Pai K, Halasyamani P. The effect of some surface active reagents on the comminution of quartz and calcite. Transactions 1965:79–82.
[44] Hasegawa M, Kimata M, Shimane M, Shoji T, Tsuruta M. The effect of liquid additives on dry ultrafine grinding of quartz. Powder Technol 2000;114:145–51, http://dx.doi.org/10.1016/S0032-5910(00)00290-4.
[45] Zhao J, Wang D, Wang X, Liao S, Lin H. Ultrafine grinding of fly ash with grinding aids: impact on particle characteristics of ultrafine fly ash and properties of blended cement containing ultrafine fly ash. Constr Build Mater 2015;78:250–9, http://dx.doi.org/10.1016/j.conbuildmat.2015.01.025.
[46] Öksüzoğlu B, Uçurum M. An experimental study on the ultra-fine grinding of gypsum ore in a dry ball mill. Powder Technol 2016;291:186–92, http://dx.doi.org/10.1016/j.powtec.2015.12.027.
[47] Liang B, Zhao LB, Han MM, Zhang H, Zhang QF, Zheng WM, et al. The influences and the mechanism of action of sodium hexametaphosphate during micro fine particle of lean hematite ore of grinding operation. Appl Mech Mater 2014;641–642:469–73, http://dx.doi.org/10.4028/www.scientific.net/AMM.641-642.469.
[48] Prziwara P, Hamilton LD, Breitung-Faes S, Kwade A. Impact of grinding aids and process parameters on dry stirred media milling. Powder Technol 2018;335:114–23, http://dx.doi.org/10.1016/j.powtec.2018.05.021.
[49] Vieira MG, Peres AEC. Effect of rheology and dispersion degree on the regrinding of an iron ore concentrate. J Mater Res Technol 2013;2:332–9, http://dx.doi.org/10.1016/j.jmrt.2013.07.002.
[50] Routray S, Swain R. Effect of chemical additives on reduction in Mill power during continuous grinding of chromite overburden materials in a tumbling Mill: a case study. J Inst Eng (India): Ser D 2019;100:123–8, http://dx.doi.org/10.1007/s40033-018-0170-7.
[51] Anoshin G, Yusupov T, Razvorotneva L, Tsimbalist V, Solotchina E. Effect of additives of inorganic salts during

superfine grinding on physicochemical and structural properties of chromite. Phys Chem Bases Concentration 1994:84–7.
[52] Rao RB, Narasimhan KS, Rao TC. Effect of additives on grinding of magnetite ore. Miner Metall Process 1991;8:144–51, http://dx.doi.org/10.1007/bf03402947.
[53] Paramasivam R, Vedaraman R. Studies in additive grinding of minerals. Adv Powder Technol 1992;3:31–7, http://dx.doi.org/10.1016/S0921-8831(08)60686-X.
[54] Toprak NA, Altun O, Benzer AH. The effects of grinding aids on modelling of air classification of cement. Constr Build Mater 2018;160:564–73, http://dx.doi.org/10.1016/j.conbuildmat.2017.11.088.
[55] Katsioti M, Tsakiridis PE, Giannatos P, Tsibouki Z, Marinos J. Characterization of various cement grinding aids and their impact on grindability and cement performance. Constr Build Mater 2009;23:1954–9, http://dx.doi.org/10.1016/j.conbuildmat.2008.09.003.
[56] Snow RH, Luckie PT. Annual review of size reduction - 1973. Powder Technol 1974;10:129–42.
[57] Rehbinder PA, Kalinkovaskaya NA. J Technol Phys (USSR) 1932;2:726–55.
[58] Guo Y, Sun S. The effect on the performance of cement grinding aid components. J Mater, Process Des 2017;1:29–39, http://dx.doi.org/10.23977/jmpd.2017.11006.
[59] Westwood ARC, Goldheim DL. Mechanism for environmental control of drilling in MgO and CaF2 monocrystals. J Am Ceram Soc 1970;53:142–7, http://dx.doi.org/10.1111/j.1151-2916.1970.tb12056.x.
[60] Schönert K. Trans Soc Min Eng AIME 1972;252:21–6.
[61] Camalan M, Hoşten Ç. Assessment of grinding additives for promoting chromite liberation. Miner Eng 2019;136:18–35, http://dx.doi.org/10.1016/j.mineng.2019.03.004.
[62] Oettel W, Husemann K. The effect of a grinding aid on comminution of fine limestone particle beds with single compressive load. Int J Miner Process 2004;74:239–48, http://dx.doi.org/10.1016/j.minpro.2004.07.014.
[63] Nan W, Ghadiri M, Wang Y. Analysis of powder rheometry of FT4: effect of particle shape. Chem Eng Sci 2017;173:374–83, http://dx.doi.org/10.1016/j.ces.2017.08.004.
[64] Kokolev G. Refractories; 1968. p. 741–2.
[65] Orlova I. Ogneupory, 6; 1977. p. 38–44.
[66] Melnik M. Tsement, 35; 1969. p. 6.
[67] Schneider H. Zem-kalk-gips, 22; 1969. p. 193–201.
[68] Toprak NA, Altun O, Aydogan N, Benzer H. The influences and selection of grinding chemicals in cement grinding circuits. Constr Build Mater 2014;68:199–205, http://dx.doi.org/10.1016/j.conbuildmat.2014.06.079.
[69] Gokcen HS, Cayirli S, Ucbas Y, Kayaci K. The effect of grinding aids on dry micro fine grinding of feldspar. Int J Miner Process 2015;136:42–4, http://dx.doi.org/10.1016/j.minpro.2014.10.001.
[70] Przwara P, Breitung-Faes S, Kwade A. Comparative study of the grinding aid effects for dry fine grinding of different materials. Miner Eng 2019;144, http://dx.doi.org/10.1016/j.mineng.2019.106030.
[71] Choi H, Lee W, Kim S. Effect of grinding aids on the kinetics of fine grinding energy consumed of calcite powders by a stirred ball mill. Adv Powder Technol 2009;20:350–4, http://dx.doi.org/10.1016/j.apt.2009.01.002.
[72] Schönert K. The influence of particle bed configurations and confinements on particle breakage. Int J Miner Process 1996;44–45:1–16, http://dx.doi.org/10.1016/0301-7516(95)00017-8.
[73] Moothedath SK, Ahluwalia SC. Mechanism of action of grinding aids in comminution. Powder Technol 1992;71:229–37, http://dx.doi.org/10.1016/0032-5910(92)88029-H.
[74] Chipakwe V, Karlkvist T, Rosenkranz J, Chelgani SC. Study on effects of additives on dry grinding perfomance of magnetite. Conf Miner Eng 2020:39–47.
[75] Pionteck J, Pionteck J, Wypych G. Handbook of antistatics. ChemTec Publishing; 2007.
[76] Bruckard WJ, Sparrow GJ, Woodcock JT. A review of the effects of the grinding environment on the flotation of copper sulphides. Int J Miner Process 2011;100:1–13, http://dx.doi.org/10.1016/j.minpro.2011.04.001.
[77] Liu J, Long H, Corin KC, O'Connor CT. A study of the effect of grinding environment on the flotation of two copper sulphide ores. Miner Eng 2018;122:339–45, http://dx.doi.org/10.1016/j.mineng.2018.03.031.
[78] Jaycock MJ, Parfitt GD. The study of liquid interfaces. Chem Interfaces 1981:38–132.
[79] He M, Wang Y, Forssberg E. Slurry rheology in wet ultrafine grinding of industrial minerals: a review. Powder Technol 2004;147:94–112, http://dx.doi.org/10.1016/j.powtec.2004.09.032.
[80] Miao Q, Ding W, Fu D, Chen Z, Fu Y. Influence of graphite addition on bonding properties of abrasive layer of metal-bonded CBN wheel. Int J Adv Manuf Technol 2017;93:2675–84, http://dx.doi.org/10.1007/s00170-017-0714-2.
[81] Zhao B, Ding W, Kuang W, Fu Y. Microstructure and tribological property of self-lubrication CBN abrasive composites containing molybdenum disulfide. Ind Lubr Tribol 2019;71:712–7, http://dx.doi.org/10.1108/ILT-04-2019-0114.
[82] Fuerstenau DW, Venkataraman KS, Velamakanni BV. Effect of chemical additives on the dynamics of grinding media in wet ball milling grinding. Int J Miner Process 1985;15:251–67.
[83] Tucker P. The influence of pulp density on the selective grinding of ores. Int J Miner Process 1984;12:273–84, http://dx.doi.org/10.1016/0301-7516(84)90034-6.
[84] Lin I, Metzmager A. The influence of the environment on the comminution of quartz. Trans AIME 1968;241:412–8.
[85] Rose HE, Sullivan RM. Ball tube and rod mills; 1958.
[86] Somasundaran P, Fuerstenau DW. Preferential energy consumption in tumbling mills. AIME Trans 1963;226:132–7.
[87] Engelhardt W. Grindability and surface energy of solids. Nat Sci 1946;33:195–203.
[88] Gamal SA. Rationalization of energy consumption in the grinding of some ores by using additives. Mater Testing 2017;59:395–401.
[89] Ryncarz A, Laskowski J. Influence of flotation reagents on the wet grinding of quartz. Powder Technol 1977;18:179–85.
[90] Somasundaran P, Agar GE. The zero point of charge of calcite. J Colloid Interface Sci 1967;24:433–40, http://dx.doi.org/10.1016/0021-9797(67)90241-X.
[91] Scheibe W, Hoffmann B, Dombrowe H. Einige probleme des einsatzes von mahlhilfsmitteln in der zementindustrie. Cem Concr Res 1974;4:289–98.
[92] Deckers M, Stettner W. Effect of grinding aids with special consideration of the mill conditions. Aufbereitungs-Technik 1979;10:545–50.
[93] Hartley JN, Prisbrey KA, Wick OJ. Chemical additives for ore grinding: how effective are they? Eng Min J 1978;179:105–11.
[94] Farber BY, Knopjes L, Bedesi N. Advances in ceramic media for high energy milling applications. Miner Eng 2009;22:704–9, http://dx.doi.org/10.1016/j.mineng.2008.12.011.
[95] Kwade A. A stressing model for the description and optimization of grinding processes. Chem Eng Technol 2003;26:199–205, http://dx.doi.org/10.1002/ceat.200390029.
[96] Wang Y, Forssberg E, Sachweh J. Dry fine comminution in a stirred media mill - MaxxMill®. Int J Miner Process

2004;74:65–74, http://dx.doi.org/10.1016/j.minpro.2004.07.010.
[97] Burmeister C, Titscher L, Breitung-Faes S, Kwade A. Dry grinding in planetary ball mills: evaluation of a stressing model. Adv Powder Technol 2018;29:191–201, http://dx.doi.org/10.1016/j.apt.2017.11.001.
[98] Shi F, Morrison R, Cervellin A, Burns F, Musa F. Comparison of energy efficiency between ball mills and stirred mills in coarse grinding. Miner Eng 2009;22:673–80, http://dx.doi.org/10.1016/j.mineng.2008.12.002.
[99] Solenis. Wet grinding aid in hard rock mining increases recovery by 4 percentage points zalta™ grinding aid; 2016.
[100] Yang J, Shuai Z, Zhou W, Ma S. Grinding optimization of cassiterite-polymetallic sulfide ore. Minerals 2019;9, http://dx.doi.org/10.3390/min9020134.
[101] Tanaka T. Preferential grinding mechanism for binary solid mixture of components of different grindabilities and the critical size ratio of each component. Kagaku Kogaku 1962;26:792–9.
[102] Wang W. Non-ferrous metals; 1979. p. 22–9.

Paper II

A comparative study on the effect of chemical additives on dry grinding of magnetite ore.

V. Chipakwe, P. Semsari, T. Karlkvist, J. Rosenkranz, S. Chehreh Chelgani.

South African Journal of Chemical Engineering, 34, 2020.

South African Journal of Chemical Engineering 34 (2020) 135–141

Contents lists available at ScienceDirect

South African Journal of Chemical Engineering

journal homepage: www.elsevier.com/locate/sajce

Editorial

A comparative study on the effect of chemical additives on dry grinding of magnetite ore

V. Chipakwe, P. Semsari, T. Karlkvist, J. Rosenkranz, S Chehreh Chelgani*

Minerals and Metallurgical Engineering, Dept. of Civil, Environmental and Natural Resources Engineering, Luleå University of Technology, SE-971 87 Luleå, Sweden

ARTICLE INFO

Keywords:
Grinding aid
Energy consumption
Flowability
Dry grinding
Surface properties

ABSTRACT

Dry grinding as an alternative to wet grinding is one of Sweden's strategic research areas to promote dry beneficiation. However, dry grinding has remained unpopular due to its higher specific energy consumption (Ec), wider particle size distribution (PSD), difficult material handling, and purported effects on downstream processes. In this work, the effects of the new additives (Zalta™ GR20–587, Zalta™ VM1122, and Sodium hydroxide) employed as grinding aids (GA) on dry grinding and product characteristics of a magnetite ore were studied in light of possible downstream effects. The grinding efficiency of Magnetite increased after using GAs in comparison without the GAs; however, an optimal dosage exists for each of the chemical additives investigated. Comparing to grinding without GA, Zalta™ VM1122, a viscosity modifier was selected as the most effective GA where by using this GA; the Ec decreased by 31.1% from 18.0 to 12.4 kWh/t, the PSD became narrower and finer (the P_{80} decreasing from 181 to 142 μm), and the proportion of the particles (38–150 μm) increased from 52.5 to 58.3%. Zalta™ VM1122 resulted in increased surface roughness and minimum microstructural defects. Further, it was found that Zalta™ VM1122 resulted in similar zeta potentials and pH values for the product compared to grinding without GA. These comparable product properties are advantageous as they minimize any potential negative effects on all possible downstream processes such as flotation.

1. Introduction

Beneficiation of Magnetite as a source of iron, which is essential for the steel industry mainly involves comminution, magnetic separation and flotation to produce a concentrate which is further processed to produce iron and steel products. However, water scarcity is a big threat to mining activities, especially in arid regions like South Africa, Australia, Chile, and China (Chehreh Chelgani et al., 2019). Sweden as a leading producer of iron ore in Europe has set targets on improving resource efficiency and reduction of water usage in mining activities through dry beneficiation and looking for the possible strategies (SIP STRIM, 2019).

Due to the current processing of finely disseminated ores, grinding is a prerequisite to ensure size reduction and mineral liberation before any subsequent separation stage. As such, for any dry beneficiation techniques like classification, sorting, magnetic separation, gravity, or electrostatic separation, an efficient dry grinding process is required. Dry grinding has some merits, such as less wear of grinding media in comparison with wet grinding (Bruckard et al., 2011; Kanda et al., 1988; Koleini et al., 2012; Ogonowski et al., 2018). However, this process remains a challenge due to the higher energy consumption, i.e., about 20–25%, wider particle size distribution, difficult material handling, and purported effects on downstream processes (Chehreh Chelgani et al., 2019; Feng and Aldrich, 2000). Moreover, dry grinding is characterized by low material transport in the pneumatic and hydraulic pumping system resulting in lower throughputs (Feng and Aldrich, 2000; Kanda et al., 1988; Ogonowski et al., 2018). These problems become pronounced as grinding products get finer due to the increase in particle-particle interaction leading to agglomeration (Prziwara et al., 2018a). Using chemical additives (grinding aids: GA) in dry grinding is one promising alternative to address some of these limitations (Fuerstenau, 1995). GA refers to any substance added to the mill, which results in a grinding efficiency increment and energy consumption reduction during grinding (Their amounts should not exceed 0.25 wt.% of the material) (Fuerstenau, 1995; Klimpel and Manfroy, 1978). These GAs can either be inorganic or organic, although the latter is more common commercially (Chipakwe et al., 2020). GAs improve the material flow properties during dry grinding, which reduces material retention time in a mill; thus, it increases the grinding efficiency (El-Shall and Somasundaran, 1984; Fuerstenau, 1995; Prziwara et al., 2018a). This is attributed to the neutralising the surface charges on the particles, which reduces inter-particle interaction, and as

* Corresponding author.
E-mail address: saeed.chelgani@ltu.se (S.C. Chelgani).

https://doi.org/10.1016/j.sajce.2020.07.011
Received 31 March 2020; Received in revised form 17 June 2020; Accepted 22 July 2020
Available online 17 August 2020

a result, reducing agglomeration (Altun et al., 2015; Assaad and Issa, 2014). GAs also give a narrow particle size distribution (Ma et al., 2010). A narrow particle size distribution is beneficial for downstream processes such as classification, as it also reduces energy consumption (Kotake et al., 2011).

In efforts to understand the effectiveness of GAs, Mishra et al. (2017) carried out a simulation to relate the functional group to the grinding performance of cement clinker. Their findings were inconclusive as no correlation could be established. Prziwara et al. (2018a), (2018b) gave an overview of the influence of GAs on grinding performance, process parameters, surface properties, and material bulk properties during the grinding of limestone. Their findings indicated that process parameters, grinding aid type, dosage, and the material itself all influence on the grinding performance. Most literature on dry grinding with GAs is within the cement industry, focusing mainly on their effect on fineness, energy consumption, and product properties (setting time and compressive strength) (Altun et al., 2015; Guo and Sun, 2017). There has been little discussion about the application of GAs in dry grinding that addresses some of the above mentioned shortcomings. Despite some positive effects of GAs, many contradicting results exist in the literature, further complicating their application (Chipakwe et al., 2020). Moreover, a few studies have been explored the possible changes on the surface of minerals and the slurry in the presence of GAs. These parameters potentially can effect on separation efficiency; therefore, GAs with minimum negative effects on the downstream processes will be essential.

Accordingly, this study seeks to investigate the use of new GAs in dry grinding regarding energy reduction as well as their effects on product surface properties to improve dry grinding. The goal is to perform a comparative interpretation of the application and effects of GAs on dry grinding of magnetite ore (as one the most important ores within Sweden) and the resulting product surface properties. Three different industrial additives employed as GAs, at varying dosages, and compared with a blank condition (without GAs) as the reference case. The energy consumption, particle size distributions, zeta potential, and pH of the slurry from the dry ground products were assessed on the different conditions to determine their variations. Finally, the surface roughness was quantified using a combination of Brunauer – Emmett – Teller (BET) surface area, and the bulk density measurements together with optical microscopic images for microstructural analysis were considered. Outcomes of this investigation would be a step forward for filling the existing gap on improving the efficiency of dry processing and the application of GAs with negligible effects on the downstream processes.

2. Materials and methods

2.1. Materials

In this study a magnetite ore containing 54–57% (Fe_3O_4) was collected from LKAB's mine in Malmberget, Sweden. An XRD analysis was done using a D/MAX-2500 pc powder diffractometer equipped with Co-Kα (λ = 1.54 Å) for mineral identification. The XRD patterns showed that Magnetite is the dominant valuable mineral together with ilmenite, actinolite, albite, biotite, quartz, apatite, and diopside as gangue minerals (Fig. 1).

A randomized regular 3-level experimental design in duplicate was chosen for the three different GAs namely Zalta™ GR20–587 (Commercial GA) and Zalta™ VM1122 (Commercial viscosity aid) from Solenis (Sweden) as well as sodium hydroxide (analytical grade) from Kebo Lab (Sweden) together with three levels of dosages (0.03, 0.05, and 0.1 wt.%) (Table 1). The ore sample was initially crushed in a laboratory scale jaw crusher to minus 3.35 mm. Hartley et al. (1978) reported that GAs are more effective for more uniform particle size. Therefore, a narrow size range was selected in this study (size range of +1.00–3.35 mm). The sample was carefully split by a riffle splitter to reach the required mass range for the grinding experiments.

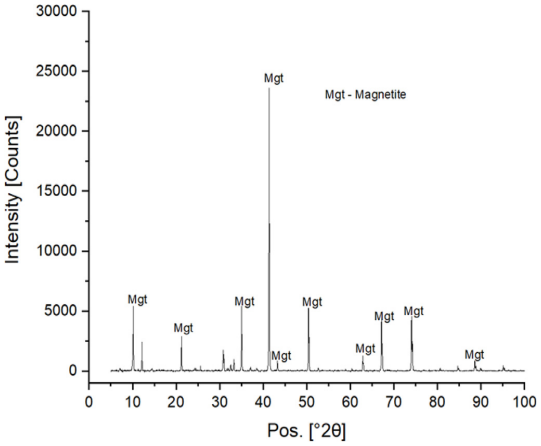

Fig. 1. XRD analysis of the magnetite ore.

Table 1
Chemicals employed as GAs.

Chemical and physical properties	Zalta™ GR20–587	Zalta™ VM1122	Sodium hydroxide
Description	Grinding aid	Viscosity aid	pH modifier
pH	8	4–7	14
Appearance	Aqueous solution	Liquid	Crystalline solid
Colour	Yellow	White	White
Boiling point °C	100	98.9 – 103.3	1388
Flash point °C	–	207	–
Water solubility	Soluble	–	Soluble
Dynamic viscosity (mPa.s)	150	2.0–3.0	0.997
Density at (g/cm^3)	1.20	1.06	2.13

*Physical properties at 20 °C.

2.2. Grinding tests

A 115 mm internal diameter CAPCO Jar mill was operated at 91% critical speed, with steel grinding media (graded charge: top-size 36 mm). The test procedure and parameters used were developed by Mwanga et al. (2017) to carter for a small amount of samples for batch grindability tests. The feed had a top size of 2.8 mm and a F_{80} of 2594 μm. The mill conditions were kept constant for all the runs. For the first run, the ball mill was run with the ore continuously for 30 min and the energy was read from an energy meter before and after the operation. The same conditions were applied in the grinding process with the GAs. The GAs were added in the supplied form (no solutions were prepared) just before the grinding procedure. No pre-treatment was done for representing the industrial-scale mill conditions of adsorbing the GAs during grinding. The grinding energy was determined using the work index according to Eq. (1).

$$W = 10.\ W_i\left(\frac{1}{\sqrt{P}} - \frac{1}{\sqrt{F}}\right) \quad (1)$$

Where: Wi: work index (kWh/t), W: grinding energy (kWh/t), P: 80% passing size of the mill product, in μm, F: 80% passing size of the mill feed, in μm (Bond, 1961). The ground material was collected after the grinding process and analysed for particle size distribution. The particle size was determined via a combination of dry and wet sieve analysis from which the P_{80} was determined. For measuring the pH of the

grinding environment, a pulp was prepared for the respective grinding products.

2.3. Characterisation of grinding products

2.3.1. Surface morphology analysis

Surface morphology analyses were performed based on microscopic analysis. Representative samples were collected, molded, and polished. Microscopic analyses were performed with a Zeiss Axioscope 7 optical microscopy. The analysis was carried out on +150 −1000 μm size fraction. The criterion for topology studies and the microstructural defects of the particle surfaces was based on randomly selected particle surfaces of the samples treated with and without GAs.

2.3.2. Surface roughness

Specific surface area (area per unit mass or volume) is a useful measurement for particle characterization and roughness. When a solid surface is exposed to a gas, e.g., nitrogen, the gas molecules are attracted and adsorb to the surface to form adsorbed layers. Under fixed conditions assuming a monolayer of molecules, the amount of adsorbed gas is proportional to the total surface area of the solid, which increases with increasing roughness (Allen, 1997). The surface area of the particles was measured by the BET technique, which characterises the surface roughness of particles. The surface roughness (R_S) values (dimensionless) was calculated using the following equation described by Jaycock and Parfitt (1981).

$$R_S = A_B \rho \left(\frac{D}{6}\right) \quad (2)$$

Where: A_B is the BET surface area measurement, ρ is the density of solid, and D is the average particle diameter. For each product ground with and without GAs, the BET specific area was measured by Micromeritics Flowsorb II 2300 instrument. In addition, the density of the selected materials was measured using an automated Micromeritics AccuPy II 1340 gas pycnometer.

2.4. Zeta potential measurement

The zeta potential measurements for the ground samples were carried out using a CAD ZetaCompact instrument. The principle of the instrument is based on micro-electrophoresis i.e., observation of particle motion under an electric field using a CCD camera. The image analysis is done by Zeta4 software based on Smoluchowski equation to evaluate the electrophoretic mobility data (Forbes et al., 2014). The suspension was prepared by adding 30 mg of a pure sample with −5 μm samples ground with various grinding conditions, deionized water, and

10^{-2} M KCl solution as the electrolyte. The suspension was stirred uniformly in a beaker to form a suspension containing 0.01 wt.%. The reported values are the mean calculated measurements.

3. Results and discussion

3.1. Energy consumption

Work index calculations (Fig. 2) indicate that the GAs results in a reduction in energy consumption for all the additives compared to the blank test (reference line). The extent of energy reduction is affected by both the type of grinding aid and the dosage. In terms of GA type, Zalta™ VM1122, sodium hydroxide, and Zalta™ GR20–587 had a 31.1%, 28.8%, and 26.6% reduction, respectively, compared to the blank sample. Considering dosages of 0.03 and 0.05 wt.%, sodium hydroxide is the most effective; however, the lowest work index (12.4 kWh/t) is reported for Zalta™ VM1122 at 0.1 wt.%.

The difference in the work index of the selected GAs can be attributed to the change in material flowability. As the flowability

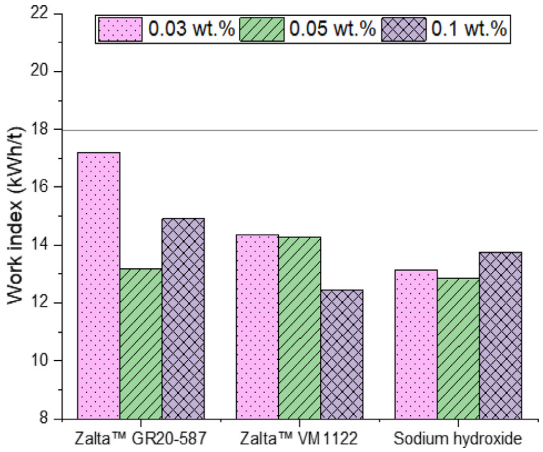

Fig. 2. Effect of grinding aids on work index.

increases to an optimum, the energy is transferred efficiently to allow for successful breakage of all particles, after which the efficiency drops again. In comparison with the blank test, the work index drops off when using sodium hydroxide and Zalta™ GR20–587, and interestingly starts to increase with dosage increment. The difference in the work index of the selected GAs can be attributed to the change in material flowability. As the flowability increases to an optimum, the energy is transferred efficiently to allow for the successful breakage of all particles, after which the efficiency drops again. In comparison with the blank test, the work index drops off when using sodium hydroxide and Zalta™ GR20–587, and interestingly starts to increase with dosage increment. This sudden increase in the work index after 0.05 wt.% dosage implies that an optimal improvement in flowability exists, which allows for effective particle breakage. High powder flowability affects particle capturing with particles more easily pushed out of the active grinding zone, resulting in poor size reduction (Przwara et al., 2018b; Schönert, 1996). Accordingly, in the case of high flowability, less mass is captured, resulting in less effective particle size reduction for the given energy and higher amounts of energy consumption per given mass.

3.2. Product fineness

The effect of GA types and its dosage on the product fineness was analyzed using a combination of dry and wet sieving as well as specific surface area measurements. All the used GAs result in an increased product fineness, expressed by the P_{80}, compared to the dry grinding without additive (reference line) (Fig. 3). Thereby, both the GA type and dosage affect product fineness. From the investigated dosage ranges, the finest product size was achieved by grinding with Zalta™ VM1122, followed by sodium hydroxide and, lastly, Zalta™ GR20–587. A decrease in product fineness was achieved for both sodium hydroxide and Zalta™ GR20–587, which is more drastic at high dosages. These results correspond to those of Gamal (2017) during wet grinding of quartz conditioned with various GAs separately, namely sodium silicate, isoamyl alcohol, and ethylene glycol ether in a ball mill. A similar trend, as observed for the work index, can be seen for fineness increment when raising the dosage to a maximum, which follows a sudden decrease of fineness for both sodium hydroxide and Zalta™ GR20–587.

3.3. Particle size distribution

The results (Fig. 4) indicate that the middling size fraction (+38 −150 μm) has the highest frequency within the particle size

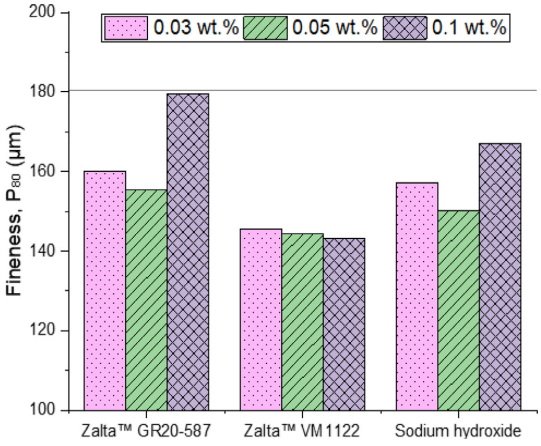

Fig. 3. Effect of grinding aids on product fineness.

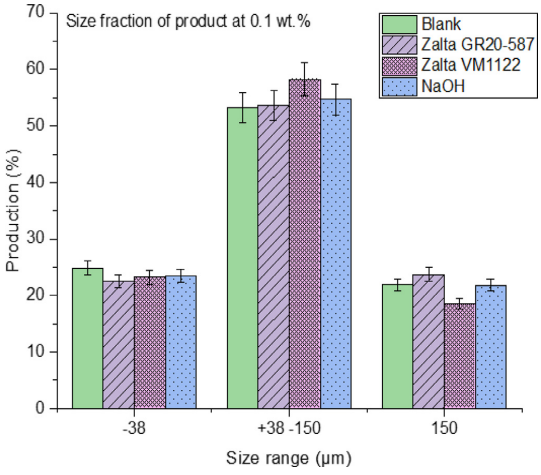

Fig. 4. Particle size distribution of products for different GAs.

distribution of dry ground samples, which can be considered as an optimum condition for downstream separation processes such as flotation. Grinding in the presence of Zalta™ VM1122 produces particle size distributions with 23.2; 58.8; and 18.5%, whereas the blank test results in 24.9; 53.2 and 21.9% for −38, +38 −150, and +150 µm size fractions, respectively. I.e., using GAs reduces the production of fine particles (−38 µm). This corroborates with Zhao et al., al.(2015)'s finding on the grinding of ultrafine fly ash in a ball mill using a blend of triethanolamine and ethylene glycol. The resulting narrow particle size distribution can be attributed to the improvement in flowability due to the use of GAs. This allows all particles to be ground under the optimum particle bed thickness. The differences in the particle size distribution between GAs can be attributed to the difference in material flowabilities. Differences in the flowability result in the various captured mass, which consequently has a selective impact on particle breakage behavior within a particle bed (Prziwara et al., 2018b). In the case of high captured mass and comparatively low-stress intensity, the particle breakage will be poor and will lead to excessive fines generation. Therefore, it strengthens the position that the best GA brings a balance on the captured mass and the stress intensity, which consequently will have a narrow particle size distribution – with no under or over-grinding.

These outcomes indicate a relationship between the physical properties of the chemicals (Table 1) and the observed energy reduction. Zalta™ VM1122, a polysaccharide, which illustrates to be the best GA, has a dynamic viscosity ranging from 2.0–3.0 compared to 150 and 0.997 mPa.s for Zalta™ GR20–587 and sodium hydroxide, respectively. Using the mass capturing concept by (Schönert, 1996), Zalta™ GR20–587 has too low flowability whilst sodium hydroxide has too high flowability. The respective densities of the GAs show a correlation with low density, resulting in improved grindability. These corroborate with Prziwara et al. (2018b)'s findings during the grinding of limestone. They found heptanoic acid (density = 0.918 kg/L) to be an effective GA compared to diethylene glycol (density = 1.12 kg/L). Studies have shown that the number of molecules per surface area influence flowability due to the thickness of the adsorbed layer (Prziwara et al., 2018a). It can be postulated GAs with a lower density that is larger volume relative to the mass results in a lower number of molecules, thus resulting in a thinner adsorption layer and reduced flowability. This can account for Zalta™ VM1122's superiority compared to sodium hydroxide (with lower dynamic viscosity).

3.4. Surface morphology

The surface roughness of Magnetite from using different GAs was determined quantitatively from BET measurements and qualitatively from optical microscope imaging. The density measurements with a pycnometer show that the magnetite sample had a bulk density of 4.48 gcm^{-3}. The GAs results in high surface roughness compared to the blank test except for Zalta™ GR20–587, compare Table 2. In general, for all size fraction, Zalta™ VM1122 indicates the highest specific surface area and surface roughness (Table 2). The differences in surface roughness for various GAs can be explained by the increase in surface area compared to the blank sample of each size fraction. Surface morphology affects the hydrophobicity, which finally affects the downstream separation processes, especially flotation separation. The resulting high surface roughness from the use of GAs improves the

Table 2
Specific surface area and roughness of magnetite particle ground by different grinding aids.

Size fraction (µm)	Arithmetic mean size (µm)	Sample type	Specific surface area (A_B) (m^2/g)	Surface roughness (R_S)
−106 + 75	90.5	Blank	0.677	45.667
		Zalta™ GR20–587	0.624	42.092
		Zalta™ VM1122	0.766	51.671
		NaOH	0.693	46.747
−75 + 53	64.0	Blank	0.690	32.915
		Zalta™ GR20–587	0.743	35.444
		Zalta™ VM1122	0.850	40.548
		NaOH	0.769	36.684
−53 + 38	45.5	Blank	0.885	30.014
		Zalta™ GR20–587	1.008	34.185
		Zalta™ VM1122	1.056	35.813
		NaOH	0.904	30.658

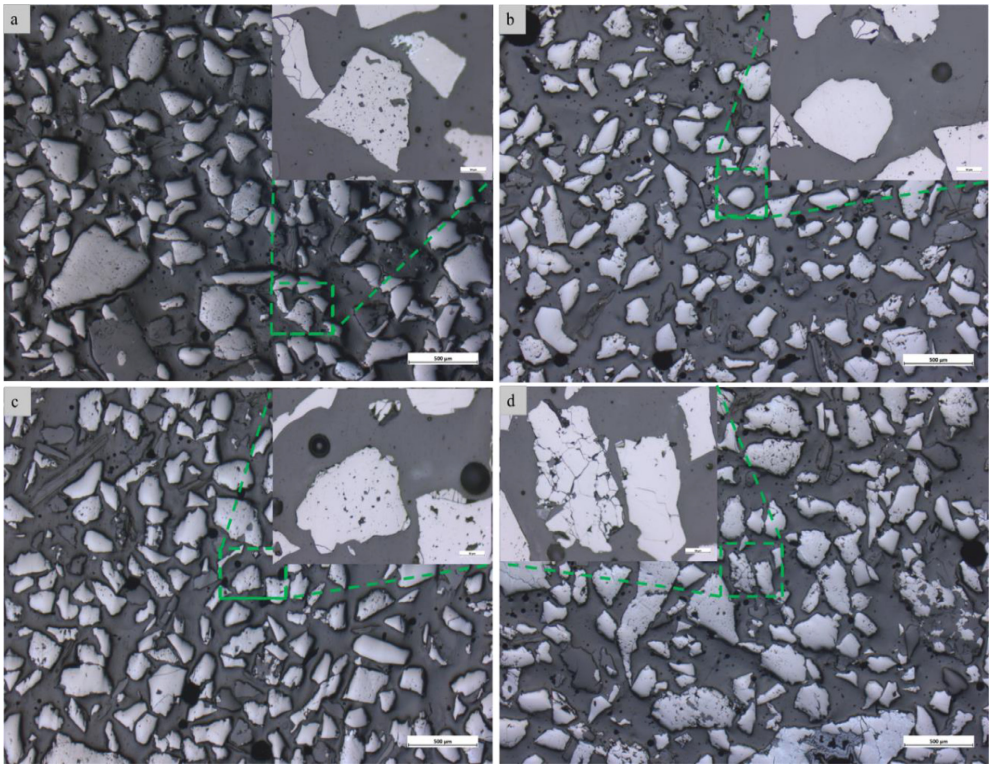

Fig. 5. Optical microscope images at 20X magnification for a) grinding without GA, b) grinding with Zalta™ GR20–587, c) grinding with Zalta™ VM1122, and d) grinding with sodium hydroxide all conditioned at 0.1 wt.% dosage.

flotation kinetics due to the improved particle-bubble attachment (Feng and Aldrich, 2000; Ahmed 2010; Hicyilmaz et al., 2006; Ulusoy and Yekeler, 2005). The topographies demonstrate the difference in the degree of microstructural defects with GAs, reducing the defects except for sodium hydroxide (Fig. 5). The other considerable observation is the degree of micro-defects on the surfaces for sodium hydroxide treated sample and the blank sample (Fig. 5). The resulting high surface roughness from the use of GAs improves the flotation kinetics (Feng and Aldrich, 2000; Hicyilmaz et al., 2006; Ulusoy and Yekeler, 2005). This could be attributed to the change in the particle shape, which is not within the scope of this study. Surface roughness was found to be more effective than shape in pyrite flotation of the ball and autogenous products (Ahmed, 2010; Hicyilmaz et al., 2006).

3.5. Zeta potentials

Zeta potentials are influenced by many factors, such as a crystalline structure (Carlson and Kawatra, 2013). The difference in zeta potentials can be attributed to the varying degree of hydration/hydroxylation due to the adsorption of the grinding aids on the particle surface. The high degree of hydration leads to high hydrogen bond formation, which in turn leads to oxygen atoms being less free and a reduction of the oxidation degree (Morimoto and Kittaka, 1973). Therefore, it would be essential to minimize zeta potential variation by adding GAs to the system for promoting possible reactions during flotation. Zeta potential measurements indicate that adding Zalta™ VM1122 generates the lowest difference compared to the blank test (Fig. 6). There is good agreement between zeta potential measurement (Fig. 6) and surface morphology results (Fig. 5) since using Zalta™ VM1122 generated the lowest microstructural defects and zeta potential variation. The observed minimum microstructural defects point to the optimum flowability that Zalta™ VM1122 imparts on the flow behavior.The adsorption of flotation reagents is controlled by the electrical double layer at the surface-water interface, and zeta potentials are key in ascertaining the adsorption conditions (Fuerstenau and Pradip, 2005). Therefore both the pH and zeta potential can either prevent enhancing flotation. In other words, using Zalta™ VM1122 results in similar zeta potential and pH with grinding without GAs; thus, minimizing the potential of negative.

From the pH values (Table 3), Zalta™ VM1122 shows the minimum change relative to the grinding without GA, which results in minimum effect on downstream processes. Sodium hydroxide has the maximum change, which is expected since it is a strong alkali pH modifier, followed by Zalta™ GR20–587. These results help to understand how GAs can affect surface properties since the pH has a direct impact on zeta potentials (Carlson and Kawatra, 2013). From a practical point of view, the addition of sodium hydroxide during grinding can serve as both grinding aid and pH regulator for minimizing any possible negative effects on the downstream processes.

4. Conclusions

The dry grinding of a uniform sized magnetite feed (−3.35 mm +1.0 mm) was carried out with three different GAs, namely Zalta™ GR20–587, Zalta™ VM1122, and sodium hydroxide, using a laboratory scale ball mill. Generally, assessments indicated that all selected additives had a positive effect on the product compared to grinding without grinding aids. The grinding tests showed that Zalta™ VM1122 resulted in the highest energy reduction, narrower particle size distribution, rough surfaces, minimum microstructural defects, minimum

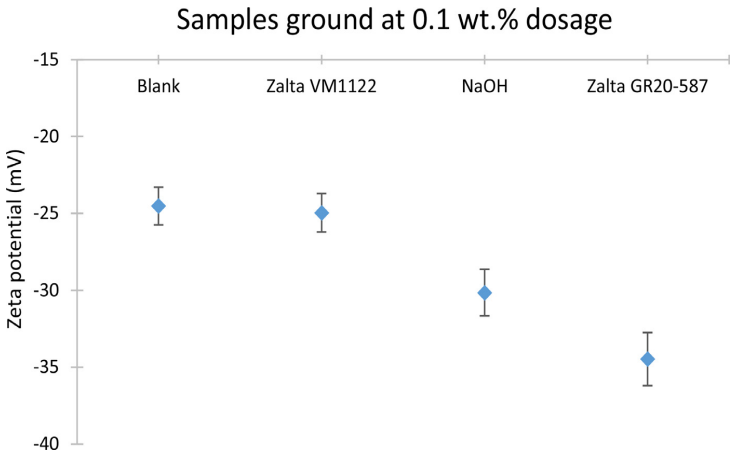

Fig. 6. Zeta potential measurement of magnetite ground with different GAs.

Table 3
pH variation of the ground products by different GA dosages.

Dosage, wt.%	Zalta™ GR20–587	Zalta™ VM1122	Sodium hydroxide
0	8.2	8.2	8.2
0.03	8.5	8.4	9.4
0.05	8.7	8.3	10.3
0.10	8.9	8.4	10.9

pH modification, and zeta potential variation. In general, the calculations from BET measurements showed that GAs results in rougher surfaces compared to the blank sample. The resulting high surface roughness from the use of GAs may improve the flotation kinetics. The samples ground with GAs showed less microstructural defects compared to the black samples, whereas this is not applicable for sodium hydroxide. Considering that Zalta™ VM1122 is a commercial viscosity modifier, these findings substantiate for the conceptual premise. In this regard, the main mechanism of GAs is based on the particle arrangement properties, although inconclusive to disprove other mechanisms. These outcomes indicated that chemicals employed as grinding aids as a mono-component and potentially mixtures could improve grinding efficiencies, which presents an opportunity for the application of dry grinding for water usage reduction in mineral processing.

Author statement

V. Chipakwe and S. Chehreh Chelgani conceived and designed the experiments; V. Chipakwe and P. Semsari performed the experiments; V. Chipakwe and S. Chehreh Chelgani analyzed the data and wrote the manuscript; T. Karlkvist and J. Rosenkranz helped to edit the language of the manuscript and provided some supervisions.

Declaration of Competing Interest

The authors declare that they have no known competing financial interests or personal relationships that could have appeared to influence the work reported in this paper.

Acknowledgments

This publication study was conducted with the financial support of the CAMM - Centre of Advanced Mining and Metallurgy, a Centre of Excellence at the Luleå University of Technology, and the SEESIMA project, a Kolarctic CBC (Cross-Border Collaboration) supported by the European Union, Russia, Norway, Finland, and Sweden. Its contents are the sole responsibility of the authors at the Luleå University of Technology and do not necessarily reflect the views of the European Union or the participating countries. The authors would also like to thank Solenis (Sweden) for providing some of the reagents used in this work.

References

Ahmed, M.M., 2010. Effect of comminution on particle shape and surface roughness and their relation to flotation process. Int. J. Mineral Process. 94, 180–191. https://doi.org/10.1016/j.minpro.2010.02.007.
Allen, T., 1997. Powder Sampling and Particle Size Measurement (Vol. 1). Chapman and Hall.
Altun, O., Benzer, H., Toprak, A., Enderle, U., 2015. Utilization of grinding aids in dry horizontal stirred milling. Powder Technol. 286, 610–615. https://doi.org/10.1016/j.powtec.2015.09.001.
Assaad, J.J., Issa, C.A., 2014. Effect of clinker grinding aids on flow of cement-based materials. Cement Concrete Res. 63, 1–11. https://doi.org/10.1016/j.cemconres.2014.04.006.
Bond, F.C., 1961. Crushing and Grinding Calculations. British Chem. Eng.
Bruckard, W.J., Sparrow, G.J., Woodcock, J.T., 2011. A review of the effects of the grinding environment on the flotation of copper sulphides. Int. J. Mineral Process. 100, 1–13. https://doi.org/10.1016/j.minpro.2011.04.001.
Carlson, J.J., Kawatra, S.K., 2013. Factors affecting zeta potential of iron oxides. Mineral Process. Extractive Metallurgy Rev. 34, 269–303. https://doi.org/10.1080/08827508.2011.604697.
Chelgani, S..., Parian, M., Parapari, P.S., Ghorbani, Y., Rosenkranz, J., 2019. A comparative study on the effects of dry and wet grinding on mineral flotation separation–a review. J. Mater. Res. Technol. 1–8. https://doi.org/10.1016/j.jmrt.2019.07.053.
Chipakwe, V., Semsari, P., Karlkvist, T., Rosenkranz, J., Chelgani, S.C., 2020. A critical review on the mechanisms of chemical additives used in grinding and their effects on the downstream processes. J. Mater. Res. Technol. 9, 8148–8162. https://doi.org/10.1016/j.jmrt.2020.05.080.
El-Shall, H., Somasundaran, P., 1984. Physico-chemical aspects of grinding: a review of use of additives. Powder Technol. 38, 275–293. https://doi.org/10.1016/0032-5910(84)85009-3.
Feng, D., Aldrich, C., 2000. A comparison of the flotation of ore from the Merensky Reef after wet and dry grinding. Int. J. Mineral Process. 60, 115–129. https://doi.org/10.1016/S0301-7516(00)00010-7.
Forbes, E., Davey, K.J., Smith, L., 2014. Decoupling rehology and slime coatings effect on the natural flotability of chalcopyrite in a clay-rich flotation pulp. Miner. Eng. 56, 136–144. https://doi.org/10.1016/j.mineng.2013.11.012.
Fuerstenau, D.W., 1995. Grinding Aids. KONA Powder Particle J. 13, 5–18. https://doi.org/10.14356/kona.1995006.
Fuerstenau, D.W., Pradip, 2005. Zeta potentials in the flotation of oxide and silicate minerals. Adv. Colloid Interface Sci. 114–115, 9–26. https://doi.org/10.1016/j.cis.2004.08.006.
Gamal, S.A., 2017. Rationalization of energy consumption in the grinding of some ores by using additives. Mater. Test. 59, 395–401.
Guo, Y., Sun, S., 2017. The Effect on the Performance of Cement Grinding Aid Components. J. Mater. Process. Des. 1, 29–39. https://doi.org/10.23977/jmpd.2017.11006.
Hartley, J.N., Prisbrey, K.A., Wick, O.J., 1978. Chemical Additives for Ore Grinding: how

Effective Are They? Eng. Mining J.
Hicyilmaz, C., Ulusoy, U., Bilgen, S., Yekeler, M., Akdogan, G., 2006. Response of rough and acute surfaces of pyrite with 3-D approach to the flotation. J. Mining Sci. 42, 393–402.
Jaycock, M.J., Parfitt, G.D., 1981. The study of liquid interfaces. Chem. Interfaces 38–132.
Kanda, Y., Abe, Y., Yamaguchi, M., Endo, C., 1988. A Fundamental Study of Dry and Wet Grinding from The Viewpoint of Breaking Strength. Powder Technol. 56, 57–62. https://doi.org/10.5188/ijsmer.7.195.
Klimpel, R.R., Manfroy, W., 1978. Chemical Grinding Aids for Increasing Throughput in the Wet Grinding of Ores. Ind. Eng. Chem. Process Des. Dev. 17, 518–523. https://doi.org/10.1021/i260068a022.
Koleini, S.M.J., Abdollahy, M., Soltani, F., 2012. Wet and dry grinding methods effect on the flotation of taknar Cu-Zn sulphide ore using a mixed collector. In: 26th International Mineral Processing Congress, IMPC 2012: Innovative Processing for Sustainable Growth - Conference Proceedings, pp. 5113–5119. https://doi.org/10.13140/2.1.3508.9606.
Kotake, N., Kuboki, M., Kiya, S., Kanda, Y., 2011. Influence of dry and wet grinding conditions on fineness and shape of particle size distribution of product in a ball mill. Adv. Powder Technol. 22, 86–92. https://doi.org/10.1016/j.apt.2010.03.015.
Ma, S., Yang, J., Mo, W., Wang, G., Su, X., Yuan, C., 2010. The effect of grinding aids on laboratory grinding of a cassiterite-polymetallic sulfide ore. In: XXV International Mineral Processing Congress 2010, IMPC 2010 2, pp. 1001–1008.
Mishra, R.K., Weibel, M., Müller, T., Heinz, H., Flatt, R.J., 2017. Energy-effective grinding of inorganic solids using organic additives. Chimia (Aarau) 71, 451–460. https://doi.org/10.2533/chimia.2017.451.
Morimoto, T., Kittaka, S., 1973. The Electrification of Iron Oxide in Water. Bull. Chem. Soc. Jpn. 46, 3040–3043. https://doi.org/10.1246/bcsj.46.3040.
Mwanga, A., Rosenkranz, J., Lamberg, P., 2017. Development and experimental validation of the Geometallurgical Comminution Test (GCT). Miner. Eng. 108, 109–114. https://doi.org/10.1016/j.mineng.2017.04.001.
Ogonowski, S., Wołosiewicz-Głab, M., Ogonowski, Z., Foszcz, D., Pawełczyk, M., 2018. Comparison of wet and dry grinding in electromagnetic mill. Minerals 8, 1–19. https://doi.org/10.3390/min8040138.
Przwara, P., Breitung-Faes, S., Kwade, A., 2018a. Impact of grinding aids on dry grinding performance, bulk properties and surface energy. Adv. Powder Technol. 29, 416–425. https://doi.org/10.1016/j.apt.2017.11.029.
Przwara, P., Hamilton, L.D., Breitung-Faes, S., Kwade, A., 2018b. Impact of grinding aids and process parameters on dry stirred media milling. Powder Technol. 335, 114–123. https://doi.org/10.1016/j.powtec.2018.05.021.
Schönert, K., 1996. The influence of particle bed configurations and confinements on particle breakage. Int. J. Mineral Process. 44–45, 1–16. https://doi.org/10.1016/0301-7516(95)00017-8.
SIP STRIM, 2019. Strategic Research and Innovation Roadmap for the Swedish Mining. Mineral Metal Prod. Ind.
Ulusoy, U., Yekeler, M., 2005. Correlation of the surface roughness of some industrial minerals with their wettability parameters. Chem. Eng. Process.: Process Intensif. 44, 555–563. https://doi.org/10.1016/j.cep.2004.08.001.
Zhao, J., Wang, D., Wang, X., Liao, S., Lin, H., 2015. Ultrafine grinding of fly ash with grinding aids: impact on particle characteristics of ultrafine fly ash and properties of blended cement containing ultrafine fly ash. Constr. Build. Mater. 78, 250–259. https://doi.org/10.1016/j.conbuildmat.2015.01.025.

Paper III

Effects of chemical additives on rheological properties of dry ground ore - a comparative study.

V. Chipakwe, C. Hulme-Smith, T. Karlkvist, J. Rosenkranz, S Chehreh Chelgani.

Mineral Processing And Extractive Metallurgy Review, 43:3, 2021.

Mineral Processing and Extractive Metallurgy Review
An International Journal

Volume 43
Included in this print edition
Number 3

Taylor & Francis
Taylor & Francis Group

Mineral Processing and Extractive Metallurgy Review
An International Journal

ISSN: (Print) (Online) Journal homepage: https://www.tandfonline.com/loi/gmpr20

Effects of Chemical Additives on Rheological Properties of Dry Ground Ore - a Comparative Study

Vitalis Chipakwe, Christopher Hulme-Smith, Tommy Karlkvist, Jan Rosenkranz & Saeed Chehreh Chelgani

To cite this article: Vitalis Chipakwe, Christopher Hulme-Smith, Tommy Karlkvist, Jan Rosenkranz & Saeed Chehreh Chelgani (2022) Effects of Chemical Additives on Rheological Properties of Dry Ground Ore - a Comparative Study, Mineral Processing and Extractive Metallurgy Review, 43:3, 380-389, DOI: 10.1080/08827508.2021.1890591

To link to this article: https://doi.org/10.1080/08827508.2021.1890591

Published online: 24 Feb 2021.

MINERAL PROCESSING AND EXTRACTIVE METALLURGY REVIEW
2022, VOL. 43, NO. 3, 380–389
https://doi.org/10.1080/08827508.2021.1890591

Taylor & Francis
Taylor & Francis Group

Effects of Chemical Additives on Rheological Properties of Dry Ground Ore - a Comparative Study

Vitalis Chipakwe [a], Christopher Hulme-Smith [b], Tommy Karlkvist [a], Jan Rosenkranz [a], and Saeed Chehreh Chelgani [a]

[a]Minerals and Metallurgical Engineering, Department of Civil, Environmental and Natural Resources Engineering, Luleå University of Technology, Luleå, Sweden; [b]Department of Materials Science and Engineering, KTH Royal Institute of Technology, Stockholm, Sweden

ABSTRACT

It is well documented that chemical additives (grinding aid "GA") during grinding can increase mill throughput, reduce water and energy consumption, narrow the particle size distribution of products, and improve material flowability. These advantages have been linked to their effects on the rheology, although there is a gap in understanding GA effectiveness mechanism on the flow properties. The present study aims to fill this gap using different GAs (Zalta™ GR20-587, Zalta™ VM1122, and sodium hydroxide) through batch grinding experiments of magnetite ore and addressing the mechanisms of their effects on the rheology by an FT4 Powder Rheometer as a unique system. Experimental results showed that GA improved grinding efficiency (energy consumption and product fineness), which were well-correlated with basic flow energy, specific energy, aerated basic flow energy, and aerated energy. Moreover, the rheometry measurement showed strong linear correlations between basic flow energy, specific energy, and the resulting work index when GAs was considered for grinding, which confirmed the effect of GA on ground particles' flowability. Zalta™ VM1122, a polysaccharide-based grinding aid, showed the best performance with 38.8% reduction of basic flow energy, 20.4% reduction of specific energy, 24.6% reduction of aerated basic flow energy, and 38.3% reduction of aerated energy. It also showed the strongest correlation between the grinding parameters and flow parameters ($r > 0.93$). The present investigation shows a strong indication that the predominant mechanism of GAs is based on the alteration of rheological properties and identify Zalta™ VM1122 as the best GA.

KEYWORDS

Energy; flowability; dry grinding; FT4 Powder Rheometer; grinding aid

1. Introduction

Grinding is an indispensable step in mineral processing to reduce particles' size and liberate minerals before they are subjected to further separation processes. Grinding is characterized by high energy consumption and low energy efficiency (~ 1%) (Cheng et al. 2019; Liu et al. 1989; Napier-Munn 2015). Moreover, grinding efficiency decreases as the particle size get finer due to the increase in the inter-particle forces by the electrostatic phenomenon (Choi, Lee and Kim 2009; Prziwara, Breitung-Faes and Kwade 2018a). As a solution, the use of chemical additives employed as grinding aids (GAs) in grinding circuits (mostly in the cement industry) significantly reduces the energy consumption (Ec), increases the throughput, improves classification, and enhances material flowability (Chipakwe et al. 2020a; Fuerstenau 1995; Hartley, Prisbrey and Wick 1978; Orumwense and Forssberg 1992; Singh et al. 2018; Toprak, Altun and Benzer 2018).

Although using GAs dates back to 1930, no agreed mechanism on their effect exists (Fuerstenau 1995; Hao, Liu and Yan 2017; Weibel and Mishra 2014). During grinding, the material flow plays a pivotal role in the product particles' properties (El-Shall and Somasundaran 1984; Fuerstenau 1995; He, Wang and Forssberg 2004). Some mechanisms have been proposed for the effect of GAs, which are mainly based on two principles, namely: the chemico-physical effect on individual particles such as the surface energy reduction (Rehbinder and Kalinkovaskaya 1932), and the effect on the particle arrangement and material flow properties (Klimpel and Manfroy 1978; Locher and Seebach 1972). In general, the impact of GAs on rheology is accepted as the main mechanism; however, no scientific knowledge substantiates this. All these scenarios have been emphasized the importance of flow characterization studies when GAs are considered.

There are several empirical techniques available for flow characteristics such as shear cell testers, angle of repose, bulk density, uniaxial compression test, Hall/Carnell method, tapped density, and bed collapse (Divya and Ganesh 2019; Hare et al. 2015; Leturia et al. 2014). These empirical techniques have poor reproducibility, sensitivity and are largely user-dependent. Previous studies on the influence of GAs on the flow behavior have been carried out using empirical techniques (Csoke, Racz and Mucsi 2010; Prziwara, Breitung-Faes and Kwade 2018b; Rajendran Nair and Paramasivam 1999). Recent advances in the automated powder rheometers have addressed these limitations and provide a correlation between these different empirical tests and dynamic, shear, and bulk properties (Freeman 2007; Hare et al. 2015; Leturia et al. 2014). Hao Shi et al. (2018) highlighted the importance of careful interpretation of these outputs from the automated powder rheometers.

To fill this gap, the FT4 Powder Rheometer as an advanced system can measure the flow behavior while the powder is in

CONTACT Vitalis Chipakwe vitalis.chipakwe@ltu.se; Saeed Chehreh Chelgani saeed.chelgani@ltu.se Minerals and Metallurgical Engineering, Department of Civil, Environmental and Natural Resources Engineering, Luleå University of Technology, Luleå SE-971 87, Sweden.

motion, which is more representative of the process conditions. In general, considering that flowability is not an inherent property and a single characteristic is inadequate. There is a need for a multivariate method that correlates results from different empirical tests, such as the FT4 Powder Rheometer. The stability and variable flow rate test method on the FT4 Powder Rheometer measures flow properties in a dynamic, constrained forced flow environment that closely simulates a grinding process in a tumbling mill.

For the first time, this investigation correlates the energy expended (grinding parameter) to flow indices. Most of the studies have focused mainly on particle properties such as fineness, specific surface area, surface energy, and particle size distribution as grinding parameters, not including energy reduction (Chipakwe et al. 2020a; Hasegawa et al. 2000). A recent investigation showed the effectiveness of additives as GAs during the dry grinding of magnetite and suggested that Zalta™ GR20-587, Zalta™ VM1122, and sodium hydroxide can reduce energy consumption compared to dry grinding without additive (Chipakwe et al. 2020b). This current study reports the findings on the characterization of dry ground magnetite ore flow properties using these additives. The ground materials in the presence of these GAs at varying dosages were characterized using the FT4 Powder Rheometer. This investigation aims to explore the probable mechanism for increasing the grinding efficiency by modifying rheological properties at a mesoscopic scale and correlating grinding performance with material flow properties using Pearson correlation analysis. These findings will provide a systematic way to design and optimize GAs.

2. Materials and methods

2.1. Materials and chemicals

For the study, a magnetite ore was received from LKAB (Luossavaara Kiirunavaara Aktiebolag), mine in Malmberget, Sweden. The sample contained magnetite of high purity (54–57% Fe_3O_4) (Figure 1), with quartz, ilmenite, actinolite, albite, biotite, apatite, and diopside as gangue minerals with a bulk density of 4.48 gcm^{-3}.

The sample was initially crushed in a laboratory scale jaw crusher to obtain the −2.8 + 1 mm size range and prepared for milling (Figure 2). A narrow feed of −2.8 + 1.0 mm was used as the mill feed to assess the grinding efficiency considering that GAs are more effective on a narrow feed size (Hartley, Prisbrey and Wick 1978). Zalta™ GR20-587 (Commercial GA) and Zalta™ VM1122 (Commercial viscosity aid) were obtained from Solenis (Sweden), and sodium hydroxide (NaOH, analytical reagent grade) was obtained from Kebo Lab (Sweden), Table 1.

2.2. Grinding tests

For the grinding experiments, a laboratory scale ball mill (CAPCO, UK) was used with the parameters summarized in Table 2. The GA dosages and variables' selection criteria were based on a randomized 3-level experimental design as described elsewhere (Chipakwe et al. 2020b) and mill parameters from the initial work of Mwanga et al. (2017). The procedure was developed for the Bond ball mill work index to carter for smaller amounts of sample (220 g) than conventional procedures.

In control tests, no additives were used (referred to as "reference test"), and for the other tests, one of the additives was combined with the ore at three different dosages. The mill conditions were kept constant for all the runs with replicates. The grinding performance was quantified in terms of energy consumption expressed as work index, material fineness, and the particle size distribution. The grinding products were subjected to particle size distribution after grinding. The recorded energy, together with the P_{80} from the PSDs were used to calculate the work index based on Bond's third theory, equation 1 (Bond 1961). Where is the work index (kWh/t), W is the energy input (kWh/t), while and are the 80% of the mill

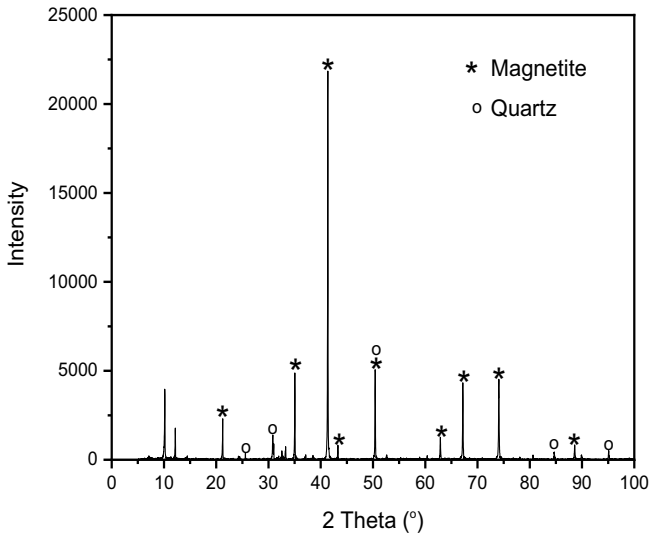

Figure 1. X-ray diffraction pattern of the magnetite ore.

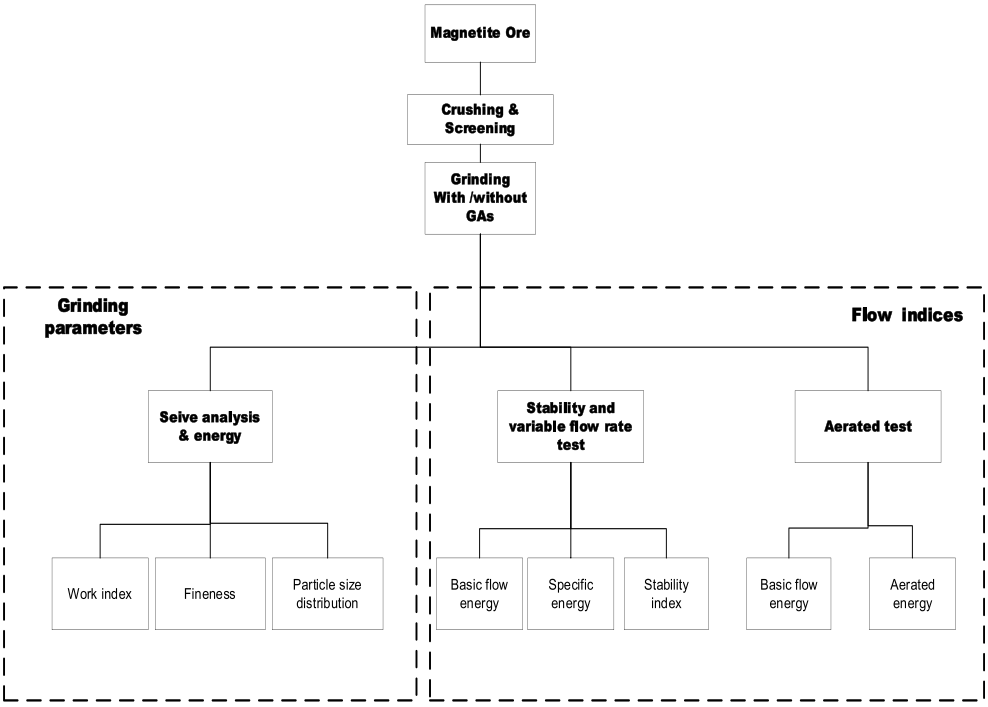

Figure 2. A simplified flow chart of the experiments.

Table 1. Chemical and physical properties of the grinding aids.

Chemical and physical properties	Zalta™ GR20-587	Zalta™ VM1122	Sodium hydroxide
Description	Grinding aid	Viscosity aid	pH modifier
Classification	Glycol-based	Polysaccharide-based	Alkaline
pH	8	4–7	14
Appearance	Aqueous solution	Liquid	Crystalline solid
Color	Yellow	White	White
Boiling point °C	100	98.9–103.3	1388
Flash point °C	-	207	-
Water solubility	Soluble	-	Soluble
Dynamic viscosity (mPa.s)	150	2.0–3.0	0.997
Density at 20°C (g/cm^3)	1.20	1.06	2.13

Table 2. Grinding parameters considered for the milling experiments.

CAPCO Jar mill	Ø 115 × 132 mm
Grinding media	Steel balls (graded 10–36 mm), 19 vol.% filling
Mill speed	114 rpm, 91% of critical speed
Mass of sample	220 g, ore:balls ratio – 0.16 w/w, top size < 2.8 mm
Grinding time	30 minutes

product and feed sizes (μm) respectively. The resulting products were prepared for analysis of flow characteristics using the FT4 Powder Rheometer (Figure 2).

$$W = 10.W_i\left(\frac{1}{\sqrt{P}} - \frac{1}{\sqrt{F}}\right) \quad (1)$$

2.3. Flow characterization

The ground material's flowability was measured by an FT4 Powder Rheometer (Freeman Technology Ltd, UK, now part of Micromeritics, USA). The instrument comprises a twisted blade, piston, or shear head, which can be rotated and moved axially in the sample whilst measuring the rotational and axial force. There are different modes, namely *stability and variable flow rate* test, shear test (rotational), and *aeration* test based on force, velocity, and torque. A 40 cm^3 volume of each ground sample was measured and pre-conditioned to homogenize the sample for rheometry. All test were carried out in 25 mm diameter glass vessels: a 25 cm^3 vessel for the *stability and variable flow rate* test, a 10 cm^3 vessel for the shear test, and a 35 cm^3 vessel for the *aeration* test (although the sample

volume for aeration tests was 25 cm^3), following the FT4 Powder Rheometer operating procedures (Leturia et al. 2014).

2.3.1. Stability and variable flow rate tests

The test procedure lowers a rotating blade into the powder at a defined axial and rotational speed and then bringing it up out of the powder at the same speed, measuring the torque and axial force at all times. The first seven test cycles use an axial speed of 100 mm/s blade tip speed to assess the constant blade motion's resistance. The remaining four cycles use decreasing axial speeds, starting at 100 mm/s and then 70, 40, and 10 mm/s, to measure the resistance's dependence on blade speed. In between each test cycle, the powder is conditioned (the blade moves through it in a pre-defined way) to remove the previous test's effect and restore the powder to a consistent starting condition. During both the downward and upward movement, the torque and axial force required to move the powder bed were measured and used for different calculations. This standard test produces data that are then used to determine: Basic Flowability Energy, BFE (energy required to move the blade downwards during the seventh test cycle), Specific Energy, SE (the energy required to move the blade out of the powder during the seventh cycle divided by the mass of the sample), Stability Index, SI (the ratio of the total energy consumed by the seventh test cycle to that consumed during the first test cycle), and Flow Rate Index, FRI (the ratio of the energy consumed during the cycle at a blade speed of 100 mm/s to that at 10 mm/s).

2.3.2. Aerated tests

An *aeration* test was also conducted on the different blends to assess the flow behavior in an aerated environment. Different airflow rates were used successively (0, 2, 4, 6, and 10 mm/s) from the cell's bottom. The blade's torque and axial forces are recorded during the blade's downward movement (tip speed = 100 mm/s) to give the total energy (TE) consumption. The successive increment of the airflow rate reduces the energy to give a minimum, which implies total fluidization of the bed. The corresponding total energy (TE) value gives the aerated energy (AE), while the reduction in energy as the airflow increases gives the aeration ratio (AR) (the ratio of the energy consumed during the test cycle with no airflow to the aeration energy). The basic flow energy in the aerated environment (A-BFE) is also determined.

2.4. Statistical analysis

All the measurements were performed in duplicate and based on a series of different batches, and the mean values are reported. Statistical analyses were conducted using analysis of variance (ANOVA) at a 95% significance level using Origin Pro 9.0 (OriginLab, USA. The association between the parameters was assessed using Pearson correlation "*r*" analysis. "*r*" is a linear factor determining relationships among variables to show their dependency. It ranges from −1 to +1. The sign of the r-value indicates the magnitude of a relationship, and its absolute value shows its strength.

3. Results

3.1. Grinding tests

Table 3 shows both grinding parameters and flow indices of the ground products from different blends. It can be observed that GAs reduce the number of coarse particles (+150 µm) for certain dosages compared to grinding without additives. The results showed interesting phenomena for sodium hydroxide and Zalta™ GR20-587 with an initial increase in grinding performance and a decrease after 0.05 wt. % dosage. It was shown that using an optimum grinding aid dosage makes it possible to reduce energy consumption and increase the product fineness. The observed phenomena point to an optimum dosage; thus, the flowability allows effective particle breakage. High GA dosages result in high flowability, which affects particles' capturing, with the particles being easily pushed out of the active grinding zone resulting in a poor grinding efficiency (Przwara, Breitung-Faes and Kwade 2018a; Schönert 1996; Chipakwe et al. 2020a). It was reported that grinding performance depends on the type and dosage of GAs while Zalta™ VM1122 showed the best performance in terms of reducing the work index and increasing the fineness production, followed by sodium hydroxide and lastly, Zalta™ GR20-587 (Chipakwe et al. 2020b).

3.2. Effect of GAs on flow properties

Flow characterization of different GAs and dosages were carried out using the *stability and variable flow rate* and *aeration* tests. The application of GAs generally improving flowability, as depicted in Figure 3. Both the stability and variable flow rate and aeration tests show that flowability increases with increasing GA dosage for the examined range.

Table 3. Effect of grinding aids on the grinding parameters and flow indices.

	Grinding parameters						Flow indices				
Condition	Dosage wt.%	Work index kWh/t	Fineness P_{80} µm	+150	Size range, µm −150 + 38	−38	BFE mJ	SE mJ/g	SI [-]	A-BFE mJ	AE mJ
Reference	0	18.0	181	21.9	53.2	24.9	1237	8.0	1.3	831	106.7
Zalta GR20-587	0.03	17.2	160	23.4	55.8	20.8	903	8.7	1.3	768	119.5
	0.05	13.2	156	25.0	53.6	21.4	458	7.4	0.4	855	109.0
	0.1	14.9	180	22.5	53.7	23.8	743	7.1	1.2	620	65.3
Zalta VM1122	0.03	14.4	146	24.7	56.7	18.6	961	9.3	1.1	985	107.2
	0.05	14.3	144	25.3	56.3	18.4	881	10.5	0.9	677	83.2
	0.1	12.4	143	23.2	58.3	18.5	757	6.4	1.4	627	65.8
Sodium hydroxide	0.03	13.2	157	24.5	55.0	20.5	886	8.0	1.5	670	98.8
	0.05	12.8	150	25.0	54.9	20.0	928	8.2	1.1	848	116.9
	0.1	13.8	167	23.5	54.7	21.8	980	6.9	1.0	516	62.9

3.2.1. Basic flow energy (BFE) and stability indices (SI)

The experimental results show that all grinding aids significantly reduce the BFE, which indicates improved flowability in the presence of GAs with varying magnitude depending on the type and dosage (Figure 4). The higher BFE for the reference test (indicated by dashed lines) compared to tests that included GAs indicates that the high resistance to flow is inherent in the ore powder. The BFE data for the different GAs with varying dosages shows both Zalta™ GR20-587 and sodium hydroxide have a similar profile of an initial decrease in BFE then sudden increase after 0.05 wt.% and 0.03 wt.%, respectively. Conversely, increasing the concentration of Zalta™ VM1122 results in improved flowability for the ranges investigated. Zalta™ GR20-587 reduces the flow energy requirement by 62.9% at 0.05 wt.% dosage, whereas Zalta™ VM1122 has a 38.8% reduction at 0.1 wt.% and sodium hydroxide gives a 28.3% reduction at 0.03 wt.% dosage. The stability indices (Figure 5) show that Zalta™ VM1122 results in higher stability compared to Zalta™ GR20-587 and sodium hydroxide. Generally, powders with a stability index between 0.9 and 1.1 can be considered normal stable powders (Bian et al. 2015). All the experiments show SI values out of this range except for the tests that used Zalta™ VM1122 at 0.05 wt.% (SI = 0.95). In general, all the experiments with Zalta™ GR20-587 and sodium hydroxide have low stability, which indicates high chances of segregation or disintegrating during flow (Freeman, Technology 2007). However, the samples that contained Zalta™ VM1122 (0.95–1.35) indicate the minimum deviation from the SI range, suggesting a low tendency to agglomerate compared to the other examined GAs.

The observed phenomena can be attributed to factors such as PSD, particle shapes, and bulk density (Liu et al. 2017). The different blends besides the PSD varied with GAs, which often resulted in a narrower PSD compared to the reference test (Table 3). Liu et al. (2017) used coal powders with different PSDs and showed that a small difference could significantly affect material flowability. The wide PSD had high isostatic tensile strength (a measure of cohesion) and compressibility,

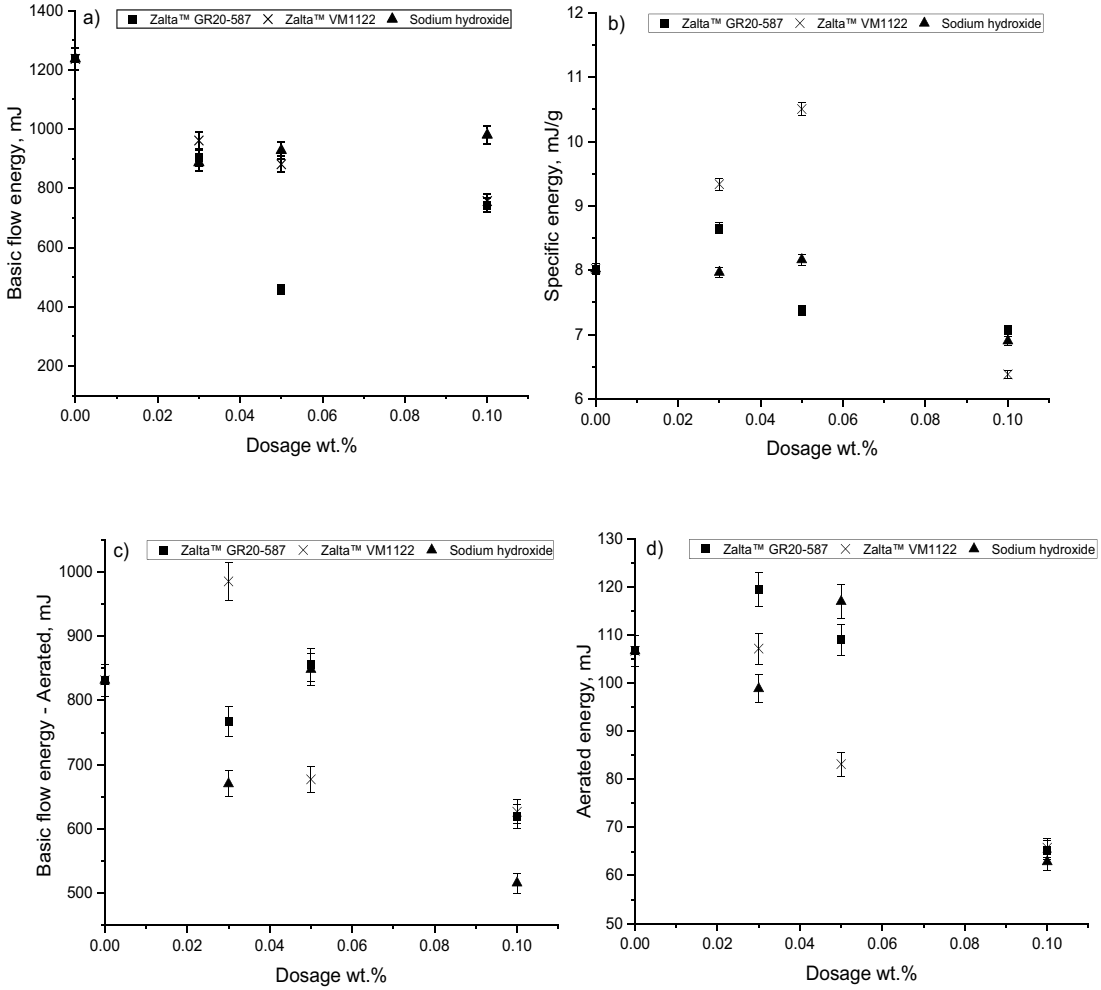

Figure 3. Effect of GAs on flow indexes a) Basic flow rate b) Specific energy c) Basic flow energy-aerated d) Aerated energy.

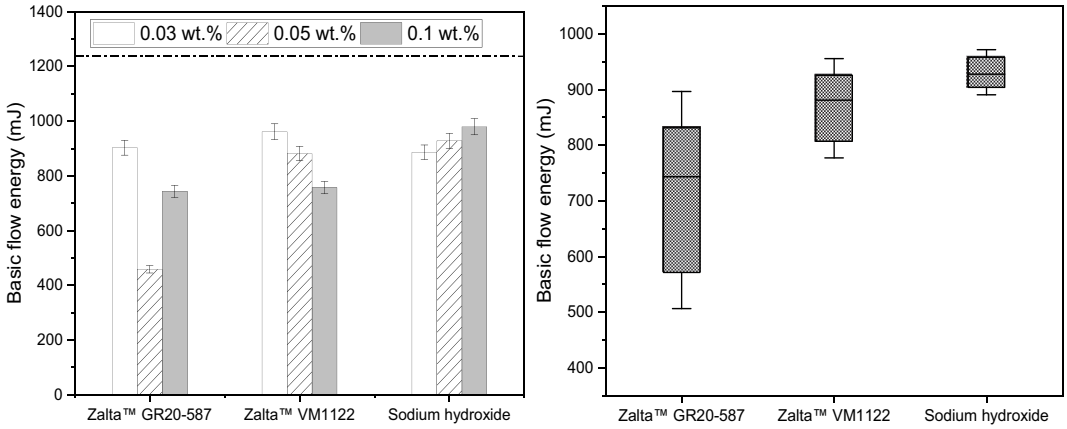

Figure 4. The basic flow energies for different GAs at varying concentrations.

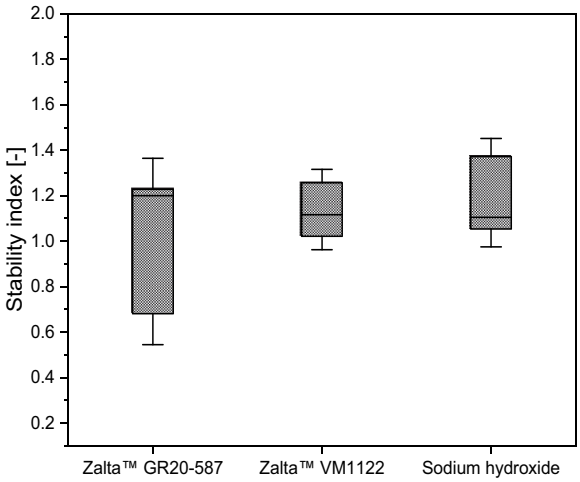

Figure 5. Variation of stability index for different GAs.

which gives a denser packing compared to a narrow PSD. Moreover, high packing density implies the bed's efficient packing, which means that high values of BFE will be needed to move the bed. In the *stability and variable flow rate* testing, the material's compressibility influences the measurements due to the blade's flow zone, which depends on the material bed. The narrow PSD (better uniform particle size) in samples that contain GAs can be linked with improved flowability (Yun et al. 2018). From these outcomes, it can be concluded that powders with GAs require less energy compared to grinding without GAs, which results in improving flowability.

3.2.2. Specific energy

Specific energy (SE) measures the powder flowability when it is unconfined or at low-stress levels (i.e., the blade lifting the powder during its upward movement). SE is an accurate measurement for assessing the influence of cohesive/adhesive forces from inter-particle interactions as opposed to compressibility for the BFE. Both BFE and SE depend on physical properties such as particle size, shape, and texture (Gnagne et al. 2017; Nan, Ghadiri and Wang 2017). Exploring the effect of GAs and their different concentrations on the SE values shows that the reference test's SE gives a value of 8.02 mJ/g, indicating that it has moderate cohesion forces (Figure 6). Zalta™ VM1122 demonstrated the lowest SE at 0.1 wt. % (6.38 mJ/g). The cohesion magnitude is only reduced at certain concentrations, and it is higher than the reference test for some concentrations. While Zalta™ GR20-587 decreases the SE with increasing concentration, Zalta™ VM1122 and sodium hydroxide give an increase at low concentrations but then a decrease with increasing dosage. The fact that the SE

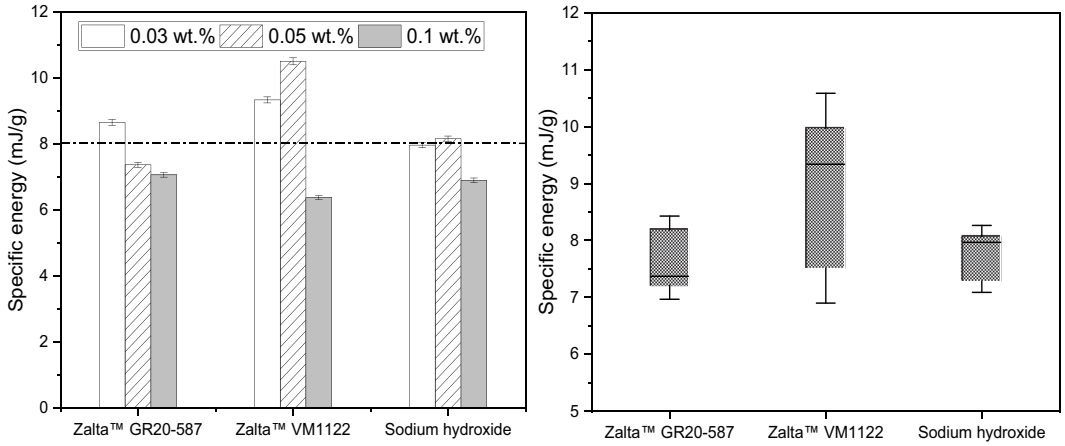

Figure 6. Influence of GAs on specific energy in different conditions.

decreases with an increase in the GA concentration, which agrees with findings that GAs reduce the inter-particle forces, decreases the degree of cohesion and improves flowability. These trends agree with reported results by other investigations, which documented a decrease in SE when reduced cohesion (Katsioti et al. 2009; Przwara, Breitung-Faes and Kwade 2018a).

3.3. Aerated tests

Considering that grinding is a dynamic process and, on the industrial scale, the dry milling process is airflow assisted, the *aeration* test is regarded adequate and informative for exploring the potential effects of GAs (Zhang et al. 2019). Generally, the GA experiments' A-BFE measurements are low compared to the reference test (except for Zalta™ VM1122 – 0.03 wt.%). This shows that using GAs can improve the powder's fluidization and facilitate transportation (Figure 7). Like the other energy measurements, A-BFE depends on cohesion, particle shape, texture, and density. In general, particles with more cohesive forces are difficult to fluidize (low AR and higher AE). For all the GAs, $2 < AR < 20$, which implies an average sensitivity to aeration, is typical of powders with moderate cohesion (Freeman, Technology 2013). (Table 4).

3.4. Correlating the flow properties and the grinding parameters

As discussed, all GAs reduce work index and increase product fineness during grinding, varying with GA type and dosage. Although the flow properties depend on several factors and are not an intrinsic property, some correlations have been established between the grinding parameters and flow indices. Pearson correlation assessments show that all samples' work index is well correlated to the BFE and SE when $r > 0.70$ (Figure 8). These indices reflect the ease of material movement (flowability) as the GAs reduce the cohesive forces. The linear correlation between the work index and BFE suggests that low BFE values would lower energy consumption. The SE also has a considerable correlation with the work index. This relationship implies that high SE values would result in lower energy consumption and finer particle size. These findings point out too high flowability in sodium hydroxide, affecting the efficacy concerning size reduction. By

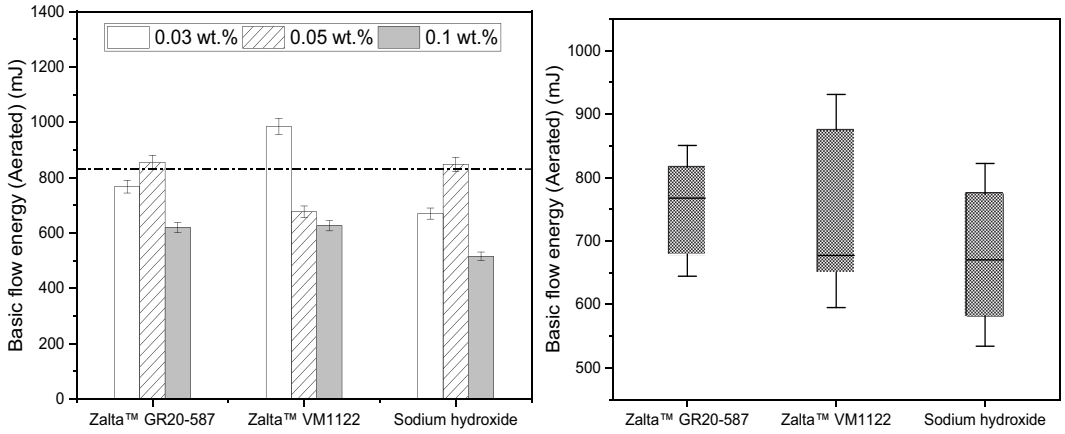

Figure 7. Influence of GAs on the aerated basic flow energy in different dosages.

Table 4. Aeration test results for various conditions in the presence and absence of GAs.

Type of grinding aid	Dosage (wt.%)	Aerated energy (mJ)	Aeration ratio
Reference	0	106.7	7.6
	0.03	119.5	6.4
Zalta™ GR20-584	0.05	109.0	7.9
	0.1	65.3	9.6
	0.03	107.2	9.4
Zalta™ VM1122	0.05	83.2	8.1
	0.1	65.8	9.6
	0.03	98.8	6.8
Sodium hydroxide	0.05	116.9	7.3
	0.1	62.9	8.4

considering the aeration test indices, significant correlations can be observed for work index and fineness with A-BFE and AE results, especially for the Zalta™ VM1122 case. This relation implies that the increase in fluidization results in improved transport, which also affects grindability.

4. Discussion

In general, all these outcomes demonstrate that flow properties influence the grinding process, which is evident from the grinding parameters (Table 3). Several studies have concluded that material transport (flowability) plays an important role in throughput and energy consumption in ball milling (He, Wang and Forssberg 2004; Orumwense and Forssberg 1992). As particle size decreases during grinding, particle-particle forces become more significant, leading to agglomeration and coating of grinding media, which reduces impact (Hasegawa et al. 2000; Prziwara, Breitung-Faes and Kwade 2018a; Sohoni, Sridhar and Mandal 1991). The grinding process can enhance by improving the grinding rate or reducing the agglomeration rate. The influence of grinding aids on BFE, SE, A-BFE, and AE has been illustrated, which are a measure of interparticle forces and are known to retard size reduction in comminution (Kojima and Elliott 2014, 2012; Prziwara, Breitung-Faes and Kwade 2018a). However, it is clear that an upper limit exists in

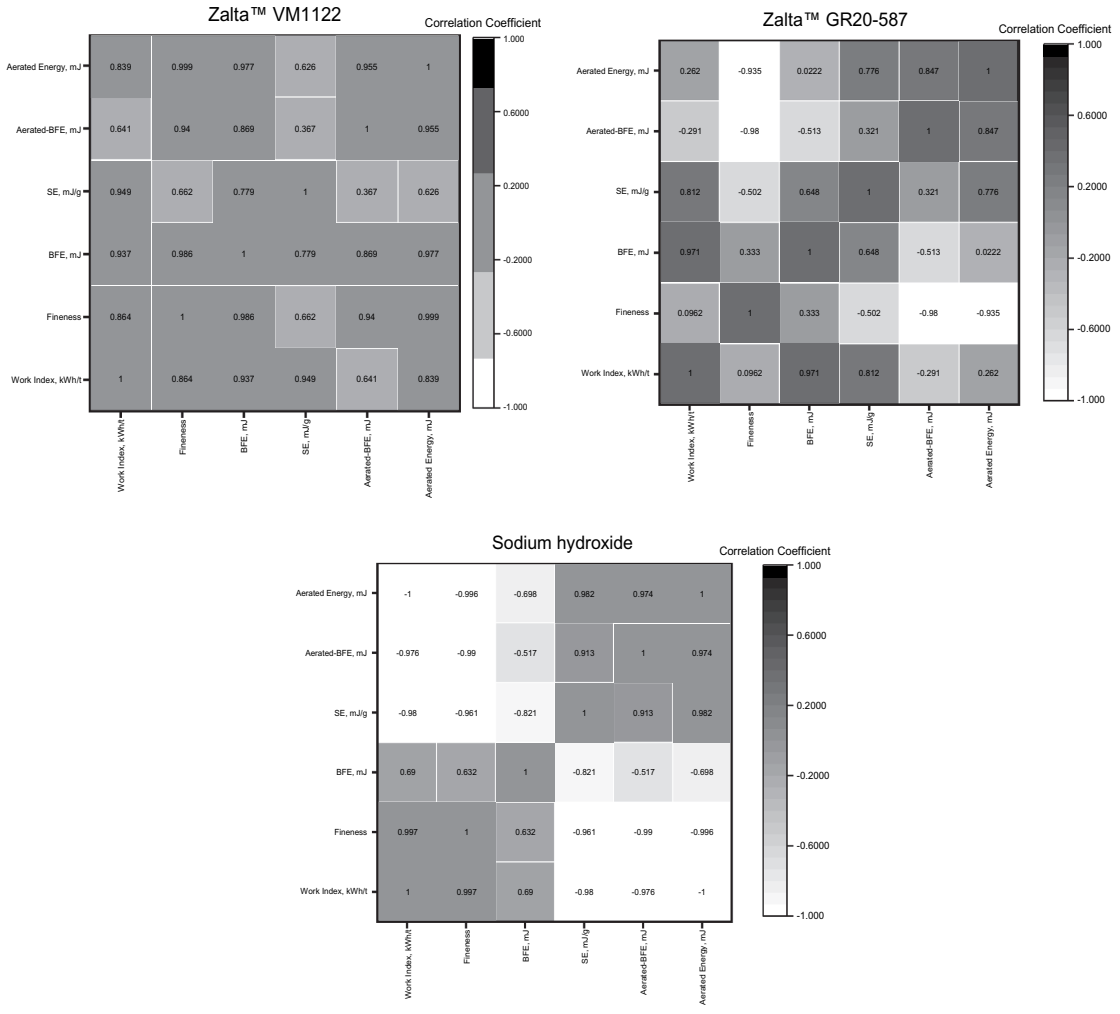

Figure 8. Pearson correlation of grinding parameters and flow properties.

terms of the GA concentration for each additive. This result agrees with established knowledge of grinding performance that an optimum dosage exists for each GA. It shows an optimum amount of GA molecules required to form the particle coating to ensure the neutralization of electrostatic charges.

Consequently, GA molecules continue to be beneficial as long as the inter-particle forces exist, after which negative effects start appearing (Liu et al. 1989). It appears that at higher dosages, the excess GA results in more packing and less compressibility, creating a large flow zone, increase volume fraction, and, consequently, high flow energy. On a mesoscopic scale, it can be agreed that grinding aids reduce particle-particle interactions by forming a film around the particles, and aiding flowability. This phenomenon confirms the noted difficulties in determining the optimum GA dosage as it depends on GA type, process conditions, particle surface properties, equally complex like determining flow properties. These facts generate a need for a particle scale based study that will investigate the influence on breakage mechanisms. The study's findings support the conceptual premise that the main mechanism of grinding aids is based on the material arrangement properties, although inconclusive to disprove other mechanisms. This term is supported by the good correlation between grinding efficiency (energy consumption and fineness) and the flow indices (BFE, SE, A-BFE and AE). The grinding efficiency increases by increasing flowability to a maximum, after which it starts to decrease.

Despite the obvious advantages of GAs in mineral processing, further work is still required to address some limitations. Considering that the processes supporting the improved grinding efficiency associated with GAs have no sound scientific backing, making trial and error the main criteria in the design and development of such chemistries. This fact generates a need for a particle scale based study together with molecular modeling that will investigate the influence on breakage mechanisms and link them to chemistries of the GAs. On the other hand, the application of GAs in mineral processing is limited by the high cost of the chemical additives making their economic justification difficult, although potential revenue can be saved. Research of cheaper alternatives such as Zalta™ VM1122 – a polysaccharide-based grinding aid containing dextrin, a starch derivative, presents an opportunity for a cheaper, biodegradable, and less toxic alternative for use in grinding circuits (Caballero et al 2003).

5. Conclusions

Results indicated that all the used chemical additives are satisfactorily effective grinding aids and resulted in improved material flowability compared to grinding without additives (in the examined dosage range). There exist an upper limit to the dosage at which GAs are beneficial for each additive. Zalta™ VM1122 results in a 38.8% reduction of the basic flow energy (BFE), 20.4% reduction of specific energy (SE), 24.6% reduction of the aerated basic flow energy (A-BFE), and 38.3% reduction of the aerated energy (AE). A significant correlation was found between grinding efficiency (including work index) and flow indices. Grinding aids increased grinding efficiency by altering the flow properties, i.e., decreased flow energy and cohesive forces. The predominant GA mechanism is based on the alteration of rheological properties.

Acknowledgments

This project is part of KO1030 SEESIMA, a Kolarctic CBC (Cross-Border Collaboration). This publication was produced with the European Union, Russia, Norway, Finland, and Sweden's financial support. Its contents are the sole responsibility of the authors at the Luleå University of Technology and do not necessarily reflect the European Union's views or the participating countries. This publication was also produced with CAMM's financial support - Center of Advanced Mining and Metallurgy as a center of excellence at the Luleå University of Technology. The authors are also grateful to Solenis for their help with the reagents used as grinding aids in this study.

Disclosure statement

No potential conflict of interest was reported by the author(s).

Funding

This work was supported by the KO1030 SEESIMA and the Centre for Advanced Mining and Metallurgy (CAMM) - LTU.

ORCID

Vitalis Chipakwe http://orcid.org/0000-0003-1676-8260
Christopher Hulme-Smith http://orcid.org/0000-0002-6339-4612
Saeed Chehreh Chelgani http://orcid.org/0000-0002-2265-6321

References

Bian, Q., S. Sittipod, A. Garg, and R. P. K. Ambrose. 2015. Bulk flow properties of hard and soft wheat flours. *Journal of Cereal Science* 63:88–94. doi:10.1016/j.jcs.2015.03.010.

Bond, F. C. 1961. Crushing and grinding calculations Brit. *Chemical Engineering*, (8).

Caballero, B., Trugo, L. C. and Finglas, P. M., 2003. *Encyclopedia of food sciences and nutrition*. Academic.

Cheng, F., Y. Feng, Q. Su, D. Wei, B. Wang, and Y. Huang. 2019. Practical strategy to produce ultrafine ceramic glaze: Introducing a polycarboxylate grinding aid to the grinding process. *Advanced Powder Technology* 30:1655–63. doi:10.1016/j.apt.2019.05.014.

Chipakwe, V., P. Semsari, T. Karlkvist, J. Rosenkranz, and S. C. Chelgani. 2020a. A critical review on the mechanisms of chemical additives used in grinding and their effects on the downstream processes. *Journal of Materials Research and Technology* 9:8148–62. doi:10.1016/j.jmrt.2020.05.080.

Chipakwe, V., P. Semsari, T. Karlkvist, J. Rosenkranz, and S. C. Chelgani. 2020b. A comparative study on the e ff ect of chemical additives on dry grinding of magnetite ore. *South African Journal of Chemical Engineering* 34:135–41. doi:10.1016/j.sajce.2020.07.011.

Choi, H., W. Lee, and S. Kim. 2009. Effect of grinding aids on the kinetics of fine grinding energy consumed of calcite powders by a stirred ball mill. *Advanced Powder Technology* 20:350–54. doi:10.1016/j.apt.2009.01.002.

Csoke, B., A. Racz, and G. Mucsi. 2010. Grinding and flowing investigation on dry stirred ball milling in order to determine the influence of grinding aids. In *XXV International Mineral Processing Congress 2010, (IMPC) 2010 Proceedings Brisbane, QLD*, 629–36. Australia.

Divya, S., and G. N. Ganesh. 2019. Characterization of powder flowability using FT4-powder rheometer. *Journal of Pharmaceutical Sciences and Research* 11:25–29. doi:10.3390/ecps2012-00825.

El-Shall, H., and P. Somasundaran. 1984. Mechanisms of grinding modification by chemical additives: Organic reagents. *Powder Technology* 38:267–73. doi:10.1016/0032-5910(84)85008-1.

Freeman, R. 2007. Measuring the flow properties of consolidated, conditioned and aerated powders - A comparative study using a powder rheometer and a rotational shear cell. *Powder Technology* 174:25–33. doi:10.1016/j.powtec.2006.10.016.

Freeman, Technology. 2007. Stability & variable flow rate method. *Work Instruction*.

Freeman, Technology. 2013. *Aeration method*.

Fuerstenau, D. W. 1995. Grinding Aids. *KONA Powder and Particle Journal* 13:5–18. doi:10.14356/kona.1995006.

Gnagne, E. H., J. Petit, C. Gaiani, J. Scher, and G. N. Amani. 2017. Characterisation of flow properties of foutou and foufou flours, staple foods in West Africa, using the FT4 powder rheometer. *Journal of Food Measurement and Characterization* 11:1128–36. doi:10.1007/s11694-017-9489-2.

Hao, S., B. Liu, and X. Yan. 2017. Review on research of cement grinding AIDS and certain problems. *Key Engineering Materials 753 KEM* 295–99. 10.4028/www.scientific.net/KEM.753.295 .

Hare, C., U. Zafar, M. Ghadiri, T. Freeman, J. Clayton, and M. J. Murtagh. 2015. Analysis of the dynamics of the FT4 powder rheometer. *Powder Technology* 285:123–27. doi:10.1016/j.powtec.2015.04.039.

Hartley, J. N., K. A. Prisbrey, and O. J. Wick. 1978. Chemical additives for ore grinding: How effective are they?. *Engineering and Mining Journal*. 179:10 105-111.

Hasegawa, M., M. Kimata, M. Shimane, T. Shoji, and M. Tsuruta. 2000. The effect of liquid additives on dry ultrafine grinding of quartz. *Powder Technology* 114:145–51. doi:10.1016/S0032-5910(00)00290-4.

He, M., Y. Wang, and E. Forssberg. 2004. Slurry rheology in wet ultrafine grinding of industrial minerals: A review. *Powder Technology* 147:94–112. doi:10.1016/j.powtec.2004.09.032.

Katsioti, M., P. E. Tsakiridis, P. Giannatos, Z. Tsibouki, and J. Marinos. 2009. Characterization of various cement grinding aids and their impact on grindability and cement performance. *Construction and Building Materials* 23:1954–59. doi:10.1016/j.conbuildmat.2008.09.003.

Klimpel, R. R., and W. Manfroy. 1978. Chemical grinding aids for increasing throughput in the wet grinding of ores. *Industrial and Engineering Chemistry Process Design and Development* 17:518–23. doi:10.1021/i260068a022.

Kojima, T., and J. A. Elliott. 2012. Incipient flow properties of two-component fine powder systems and their relationships with bulk density and particle contacts. *Powder Technology* 228:359–70. doi:10.1016/j.powtec.2012.05.052.

Kojima, T., and J. A. Elliott. 2014. A semi-empirical model relating flow properties to particle contacts in fine binary powder mixtures. *Powder Technology* 268:191–202. doi:10.1016/j.powtec.2014.08.013.

Leturia, M., M. Benali, S. Lagarde, I. Ronga, and K. Saleh. 2014. Characterization of flow properties of cohesive powders: A comparative study of traditional and new testing methods. *Powder Technology* 253:406–23. doi:10.1016/j.powtec.2013.11.045.

Liu, D. H., D. H. Birlingmair, L. E. Burkhart, and R. Markuszewski. 1989. Attrition grinding of coal in the presence of polymeric additives. *Coal Preparation* 6:195–206. doi:10.1080/07349348908960529.

Liu, Y., H. Lu, M. Poletto, X. Guo, and X. Gong. 2017. Bulk flow properties of pulverized coal systems and the relationship between inter-particle forces and particle contacts. *Powder Technology* 322:226–40. doi:10.1016/j.powtec.2017.07.057.

Locher, W. F., and H. M. Seebach. 1972. Influence of Adsoprtion Industrial Grinding. *Industrial & Engineering Chemistry Process Design and Development* 2:190. doi:10.1021/i260042a007.

Mwanga, A., Rosenkranz, J., Lamberg, P., 2017. Development and experimental validation of the Geometallurgical Comminution Test (GCT). *Miner. Eng.* 108:109–114. doi:10.1016/j.mineng.2017.04.001

Nan, W., M. Ghadiri, and Y. Wang. 2017. Analysis of powder rheometry of FT4: Effect of particle shape. *Chemical Engineering Science* 173:374–83. doi:10.1016/j.ces.2017.08.004.

Napier-Munn, T. 2015. Is progress in energy-efficient comminution doomed?. *Minerals Engineering* 73:1–6. doi:10.1016/j.mineng.2014.06.009.

Orumwense, O. A., and E. Forssberg. 1992. Superfine and ultrafine grinding a literature survey. *Mineral Processing and Extractive Metallurgy Review* 11:107–27. doi:10.1080/08827509208914216.

Prziwara, P., S. Breitung-Faes, and A. Kwade. 2018a. Impact of grinding aids on dry grinding performance, bulk properties and surface energy. *Advanced Powder Technology* 29:416–25. doi:10.1016/j.apt.2017.11.029.

Prziwara, P., S. Breitung-Faes, and A. Kwade. 2018b. Impact of the powder flow behavior on continuous fine grinding in dry operated stirred media mills. *Minerals Engineering* 128:215–23. doi:10.1016/j.mineng.2018.08.032.

Rajendran Nair, P. B., and R. Paramasivam. 1999. Effect of grinding aids on the time-flow characteristics of the ground product from a batch ball mill. *Powder Technology* 101:31–42. doi:10.1016/S0032-5910(98)00121-1.

Rehbinder, P. A., and N. A. Kalinkovaskaya. 1932. Decrease in the surface energy of solid bodies and the work of dispersion during formation of an adsorption layer. *Journal of Physics* (USSR) 2:726–755.

Schönert, K., 1996. The influence of particle bed configurations and confinements on particle breakage. *Int. J. Mineral Process.* 44–45, 1–16. doi:10.1016/0301–7516(95)00017–8

Shi, H., R. Mohanty, S. Chakravarty, R. Cabiscol, M. Morgeneyer, H. Zetzener, J. Y. Ooi, A. Kwade, S. Luding, and V. Magnanimo. 2018. Effect of particle size and cohesion on powder yielding and flow. *KONA Powder and Particle Journal* 2018:226–50. doi:10.14356/kona.2018014.

Singh, V., P. Dixit, R. Venugopal, and K. B. Venkatesh. 2018. Ore pretreatment methods for grinding: journey and prospects. *Mineral Processing and Extractive Metallurgy Review* 40:1–15. doi:10.1080/08827508.2018.1479697.

Sohoni, S., R. Sridhar, and G. Mandal. 1991. The effect of grinding aids on the fine grinding of limestone, quartz and Portland cement clinker. *Powder Technology* 67:277–86. doi:10.1016/0032-5910(91)80109-V.

Toprak, N. A., O. Altun, and A. H. Benzer. 2018. The effects of grinding aids on modelling of air classification of cement. *Construction and Building Materials* 160:564–73. doi:10.1016/j.conbuildmat.2017.11.088.

Weibel, M., and R. K. Mishra. 2014. Comprehensive understanding of grinding aids. *ZKG international (Deutsch-englische Ausgabe. 1995)*, (6). doi:10.1007/s00428-014-1656-9.

Yun, H., L. Dong, W. Wang, Z. Bing, and L. Xiangyun, 2018. Study on the flowability of TC4 alloy powder for 3D printing. In *IOP Conference Series: Materials Science and Engineering*. doi: 10.1088/1757-899X/439/4/042006.

Zhang, X., Z. Zhao, Y. Cui, F. Liu, Z. Huang, Y. Huang, R. Zhang, T. Freeman, X. Lu, X. Pan, et al. 2019. Effect of powder properties on the aerosolization performance of nanoporous mannitol particles as dry powder inhalation carriers. *Powder Technology* 358:46–54. doi:10.1016/j.powtec.2018.08.058.

Paper IV

Beneficial effects of a polysaccharide-based grinding aid on magnetite flotation: a green approach.

V. Chipakwe, T. Karlkvist, J. Rosenkranz, S Chehreh Chelgani.

Scientific reports, 12:6502, 2022.

scientific reports

Check for updates

OPEN

Beneficial effects of a polysaccharide-based grinding aid on magnetite flotation: a green approach

Vitalis Chipakwe✉, Tommy Karlkvist, Jan Rosenkranz & Saeed Chehreh Chelgani✉

Grinding is the most energy-intensive step in mineral beneficiation processes. The use of grinding aids (GAs) could be an innovative solution to reduce the high energy consumption associated with size reduction. Surprisingly, little is known about the effects of GAs on downstream mineral beneficiation processes, such as flotation separation. The use of ecofriendly GAs such as polysaccharide-based materials would help multiply the reduction of environmental issues in mineral processing plants. As a practical approach, this work explored the effects of a novel polysaccharide-based grinding aid (PGA) on magnetite's grinding and its reverse flotation. Batch grinding tests indicated that PGA improved grinding performance by reducing energy consumption, narrowing particle size distribution of products, and increasing their surface area compared to grinding without PGA. Flotation tests on pure samples illustrated that PGA has beneficial effects on magnetite depression (with negligible effect on quartz floatability) through reverse flotation separation. Flotation of the artificial mixture ground sample in the presence of PGA confirmed the benefits, giving a maximum Fe recovery and grade of 84.4 and 62.5%, respectively. In the absence of starch (depressant), PGA resulted in a separation efficiency of 56.1% compared to 43.7% without PGA. The PGA adsorption mechanism was mainly via physical interaction based on UV–vis spectra, zeta potential tests, Fourier transform infrared spectroscopy (FT-IR), and stability analyses. In general, the feasibility of using PGA, a natural green polymer, was beneficial for both grinding and reverse flotation separation performance.

Size reduction units (crushing and grinding) in cement and mineral processing plants consume up to 4% of the global electrical energy produced yearly[1]. Grinding, especially in a ball mill as the most popular grinding machine, is a fairly random process, and only 1–2% of the input energy serves to generate the required product sizes[2]. In the cement industry, the use of grinding aids (GAs) has been examined as a promising alternative to address these issues[3,4]. Chemical additives or GAs would be considered as any substance (less than 0.25 wt.%) added to the mill to reduce energy consumption[5–7]. GAs have been mostly examined in the cement industry and are still not widely practiced in mineral beneficiation plants. Based on the cement industry grinding process outcomes, GAs can improve grindability, reduce energy consumption, and increase specific surface area[8–12]. However, the grinding in cement plants is carried out in the last stage of production, and the reduction of the size is the initial step of mineral processing. Thus, the main concerns in the mineral processing plants include the high cost of GAs, potential contamination of the grinding products (purported negative effects on the downstream process), and environmental issues.

The design and selection of GAs are almost exclusively based on their grinding performance. Within the cement industry, many chemicals have been used as GAs. They range from pure chemicals such as triethanolamine (TEA) to more recently high-charge polymers[6,7,9,13]. Polymers are the most commercially existing GAs. They are mainly based on ethylene glycol, propylene glycol, triisopropanol amine (TIPA), triethanolamine (TEA), and tetraethylenepentamine (TEPA)[6,7,14]. Some of these GAs, such as TEPA (amine-based), are nonbiodegradable and raise environmental concerns[15]. Waste streams containing alkanolamines can increase the concentration of ammonia, nitrite, and nitrate, which could infiltrate the subsoils and water sources[15].

To address current environmental issues, a few investigations have been conducted on using ecofriendly benign materials as GAs. These studies have reported that natural polymers are advantageous because of their low cost, abundance, and nontoxicity. On the other hand, some investigations have explored the utilization of waste

Minerals and Metallurgical Engineering, Department of Civil, Environmental and Natural Resources Engineering, Luleå University of Technology, 971 87 Luleå, Sweden. ✉email: vitalis.chipakwe@ltu.se; saeed.chelgani@ltu.se

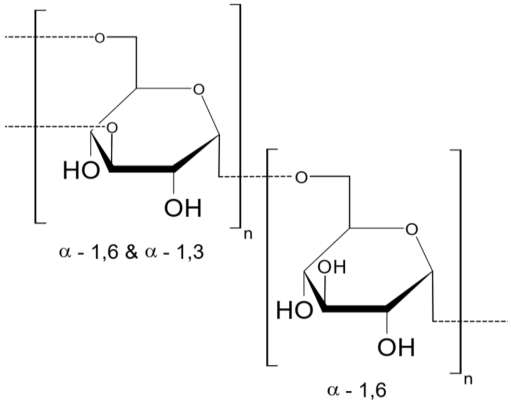

Figure 1. Typical chemical structure of a dextran.

Chemical	Description	Classification	Charge	Source
Zalta™ VM1122 (PGA)	Grinding aid	Polysaccharide-based	Non-ionic	Solenis
Lilaflot 822M	Collector	Ether-amine	Cationic	Nouryon
Starch	Depressant	Corn-starch	–	Merck
Sodium hydroxide	pH modifier	Alkaline	Neutral	Merck
Hydrochloric acid	pH modifier	Acidic	Neutral	Merck

Table 1. Materials used for various experiments.

streams from other industries such as waste cooking oil, glycerine, lignin, and cane molasses as GAs[16,17]. This has also been motivated by the high cost of triethanolamine-based GAs and the concepts of 'circular economy', which are emerging in the production of raw materials to reduce waste generation and reuse of 'waste' from other processes. Zhang et al.[17] demonstrated that a mixture of lignin, cane molasses, and waste glycerine could be used as GAs in cement production. Polysaccharide-based chemistries are a promising alternative to less toxic and cheaper reagent development options[18,19]. They are also organic polymers that are already used as depressants in flotation separation[20–23].

Since low environmental impact practices are in high demand within the mineral processing value chain[18,24], the best scenario would be the development of chemicals that improve grinding performance and ensure they do not have adverse impacts on downstream processes. Some studies have focused on the mineral industry with further discussion on downstream effects[25,26]; however, they were not in-depth. Understanding and controlling any GA-separation reagent interactions is critical to ensure that the required downstream process efficiency and integrity of the whole value chain are maintained. Such an understanding would be essential, particularly for flotation separation, where the separation could be efficient in the specific particle size range (mainly −100 + 25 µm)[27,28].

Previous studies demonstrated the benefits of polysaccharide-based GA (PGA) as a green chemical additive in improving mineral grinding performance[10] and material rheology[5]. However, the high cost and purported effects on downstream processes as a result of the potential synergistic interaction of the GAs and flotation reagents limit their applications. Moreover, their potential effects on the downstream beneficiation processes such as mineral flotation separation have not been addressed. This study aims to enhance the theoretical insights for using PGA on grinding magnetite and its possible effects on magnetite-quartz flotation separation as a strategic approach. While the new PGA—Zalta™ VM1122 is commercially available, this current work focuses on investigating the interaction of Zalta™ VM1122 with magnetite and flotation reagents through adsorption tests, stability measurements, Fourier transform infrared (FTIR) studies, and zeta potential measurements. Reverse flotation experiments on artificially mixed ore (magnetite + quartz) are presented. Flotation outcomes were used to evaluate the effect of PGA on the process recovery and grade and compare with conventional flotation (without GAs) as a benchmark.

Materials and methods

Chemicals. A polysaccharide-based grinding aid (PGA) with the trade name Zalta™ VM1122 was provided by Solenis (Sweden). PGA is a medium-molecular weight polysaccharide that mainly comprises dextran (Fig. 1). For all experiments, the PGA stock solution was freshly prepared daily to avoid any degradation. For the flotation tests, a collector, depressant, and pH modifiers were used (Table 1). Deionized water was used in all experiments unless otherwise noted.

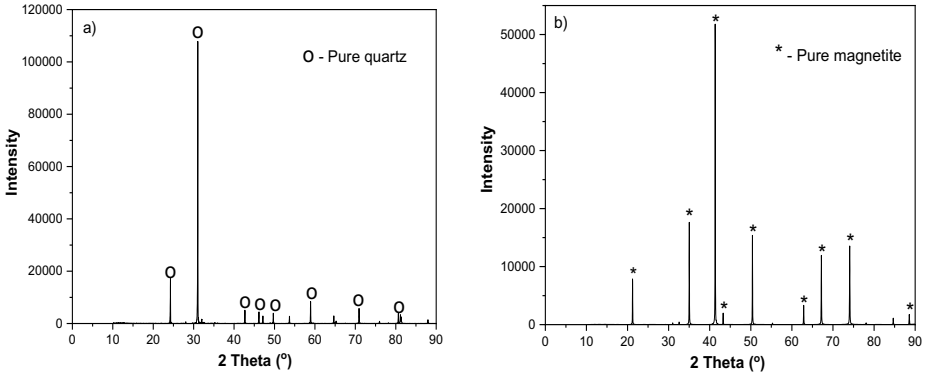

Figure 2. XRD pattern for the examined samples (**a**) pure quartz; (**b**) pure magnetite.

Minerals. For the experiments, a pure quartz sample (−2 mm) was obtained from VWR, Sweden (Fig. 2a). Magnetite ore from a mine in Malmberget, north of Sweden (Fig. 2b), was received from LKAB (Luossavaara Kiirunavaara Aktiebolag). Semi-quantitative X-ray diffraction (XRD) analyses shows > 99% SiO_2 for quartz and > 96% Fe_3O_4 for magnetite. Magnetite was crushed to −2.8 mm for grinding experiments using a laboratory jaw crusher to obtain mill feed. The pure minerals (magnetite and quartz) were ground using a laboratory ball mill to give −106 µm particle size for flotation and surface analyses. The resulting −106 + 38 µm fraction was used as flotation feed, while −38 µm material was further ground using a mortar and pestle to obtain −5 µm material for surface analyses.

Grinding. For the grinding experiments, a laboratory-scale ball mill (CAPCO, UK) of 115 mm internal diameter was operated at 91% critical speed, with steel grinding media (graded charge: top size 36 mm). In the control tests, no additives (referred to as 'reference') were used, and for the other experiments, PGA was combined with ore at three different concentrations (0.03, 0.05, and 0.1 wt.%). Mill conditions were kept constant for all runs and replicates. The particle size distribution (PSD) was determined using a combination of dry and wet sieve analysis using standard sieves and a RO-TAP® sieve shaker (model RX-29-10, W.S. Tyler, Mentor, OH, USA) from which the P_{80} was determined. Energy consumption was characterized using the work index according to Bond's Eqiuation[29]. Surface area was measured using the Brunner Emmet Teller (BET) technique by the Micromeritics Flowsorb II 2300 instrument, which characterizes the surface area of the particles using nitrogen gas. Furthermore, the surface area was used to calculate the surface roughness (R_S) values (dimensionless) using the following Eq. (1) described by Jaycock and Parfitt[30].

$$R_S = A_B \rho \left(\frac{D}{6} \right) \tag{1}$$

where A_B is the BET surface area measurement, ρ is the solid density, and D is the average particle diameter. Additionally, the density was measured using an automated Micromeritics AccuPyc II 1340 gas pycnometer. The same grinding protocol was used for the single minerals and the model ore to prepare the flotation feed. After grinding and sieving, the samples were thoroughly washed with dilute HCl solution (2%) to clean the particle surfaces.

Single mineral flotation. Single mineral flotation experiments for pure magnetite and quartz were performed using a mini flotation cell (Clausthal cell). In each flotation, 7.5 g of the sample (−106 + 38 µm) was added to the 150 cm^3 capacity with deionized water. Before the test was performed, the slurry was conditioned with a predetermined amount of PGA for 10 min. Subsequently, reagents (depressant and collector) were added to the suspension and conditioned for 10 (5 + 5) min. Caustic starch was used as a depressant. A fresh 1% alkaline starch solution (1:4 ratio) was prepared for each set of experiments. Lilaflot 822M, recommended and supplied by Nouryon (Sweden), was used as a cationic collector. The pH was adjusted by adding 1.0 M NaOH or 1.0 M HCl. The flotation was carried out for 2 min, scraping every 10 s. The froth products and tails were collected, weighed, dried, and recovery was calculated based on the dry weight. Each experiment was performed in duplicate and the average was reported.

Mixed mineral flotation. The mixed mineral flotation on the model ore was carried out using the same cell. The model ore consisted of 5.0 g magnetite and 2.5 g quartz (ratio 2:1). 7.5 g of the mixture (−106 + 38 µm) was used with deionized water was used for each test. The same procedure, such as the single mineral flotation, was also considered for the reverse flotation. The collector was fixed at 300 g/t, and the depressant was varied together with GAs. Conditioning was performed for 10 min followed by flotation for 2 min. The froth products and tails were collected, weighed, dried, and recovery was calculated based on the dry weight and chemical analyses using induction plasma (ICP OES). Each experiment was performed in duplicate and the average was reported. The separation efficiency (S.E) for each test was calculated using Eq. (2)[31]. Where *f*, *c*, and *t* are the feed,

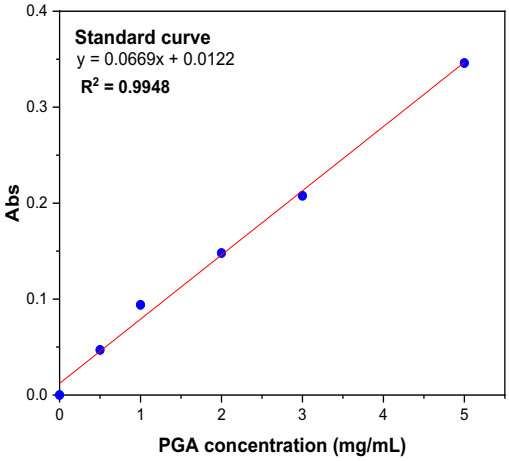

Figure 3. Standard curve of PGA adsorption.

concentrate, and tail grades of iron, respectively, a higher S.E value extrapolates a better separation efficiency of the process.

$$\text{S.E}(\%) = \frac{c(f-t)(c-f)(100-t)}{f(c-t)^2(100-f)} \times 100 \tag{2}$$

Zeta potential measurements. Zeta potentials of the samples were measured using a CAD ZetaCompact instrument. 20 mg of finely ground samples (−5 µm) was mixed with 50 ml of deionized water together with predetermined reagents in a beaker. The background electrolyte was a 10^{-2} M KCl solution. The pH was adjusted by using an HCl or NaOH solution. The mixture was stirred with a magnetic stirrer for 10 min and left to stand. The suspension supernatant was then transferred to an electrophoresis cell using a syringe. The particles in the suspension were illuminated by a laser and their electrophoresis was observed by a camera. Video analysis is done with Zeta4 software based on the Smoluchowski Eqiuation[32,33] to calculate the zeta potential from electrophoretic mobility data[34]. The reported result for each data point is an average of three measurements with different aliquots.

Adsorption measurements. Adsorption measurements to determine the amount of adsorbed PGA were carried out using the solution depletion method on the UV–VIS spectrometer (DU Series 730 – Beckman Coulter, USA). Standard solutions with PGA concentrations ranging from 0.5 to 5 mg/ml were used to obtain the calibration curve (Fig. 3). For the measurements, the maximum absorbance at 220 nm was used. 1.0 g of the sample (−106 + 38 µm) with 40 ml and the predetermined reagent concentration were added to a 100 ml flask. The suspension was stirred for 2 h at pH 10 and 20 ± 1 °C to ensure maximum adsorption. After vacuum filtration, the solution was passed through a 0.22 µm millipore membrane. The concentration of the remaining PGA in the solution was analyzed using UV absorbance at a wavelength of 220 nm. The measurements were corrected for the blanks and performed in triplicate. The concentration that was depleted from the solution was assumed to be adsorbed onto the surface of the sample particle. The adsorption density was calculated using Eq. (3);

$$Q_e = \frac{(C_1 - C_0)V}{m} \tag{3}$$

where Q_e is the amount of PGA (mg/g) adsorbed on the sample particle surface, C_0 and C_1 are the initial and final concentrations, i.e., before and after adsorption (mg/L), respectively. m is the mass (g) of the sample, and V is the volume (L) of the PGA solution. Furthermore, the experimental data for the adsorption isotherms were fitted to the Langmuir (Eq. 4) and Freundlich (Eq. 5) models:

$$Q_e = \frac{K_L C_e Q_0}{1 + K_L C_e} \tag{4}$$

$$Q_e = K_F C_e^{\frac{1}{n}} \tag{5}$$

where Q_e is the amount of PGA (mg/g) adsorbed, C_e is the equilibrium concentration of PGA. Q_m and K_L are Langmuir constants whilst K_F and $1/n$ are the Freundlich constants related to maximum monolayer adsorption capacity and energy of adsorption, respectively[35].

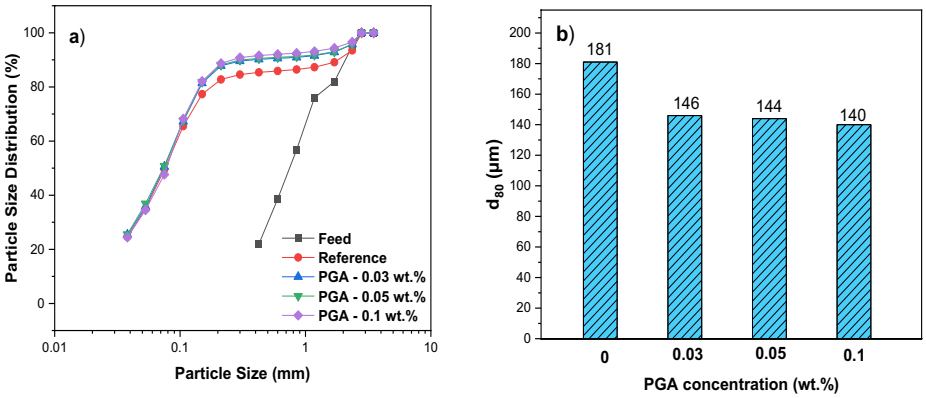

Figure 4. The particle size distribution and d80 of grinding products with and without PGA.

Stability measurements. Stability measurements of suspensions were performed using Turbiscan LAB EXPERT (Formulaction, France). Measurements were carried out to determine the behavior of coagulation and dispersion in the presence and absence of PGA. 50 mg of quartz and magnetite were added separately to 40 mL of deionized water. A predetermined amount of reagents was then added and stirred for 20 min at pH 10. 20 mL of suspension was transferred to a measuring vial and scanned at the height of 40 mm at 30° C. The suspension was scanned over 100 times in 60 min at 30 s intervals. The intensities of transmission (T) and backscattering (BS) of pulsed near-infrared light (λ = 880 nm) were recorded as a function of time. The data was then analyzed using TLab EXPERT 1.13 and Turbiscan Easy Soft software to calculate the Turbiscan Stability Index (TSI) Eq. (6). Where x_i is the average backscattering for a minute of measurement, x_{BS} is the average x_i, and n is the number of scans. The TSI coefficient values vary from 0 to 100, translating into an extremely stable to an unstable system[36,37].

$$TSI = \sqrt{\frac{\sum_{i=1}^{n}(x_i - X_{BS})^2}{n-1}} \tag{6}$$

FT-IR spectroscopy measurements. PGA characterization was performed using Fourier transform infrared (FTIR) spectroscopy with attenuated total reflection (ATR) attachment. The samples were ground to approximately −2 µm using an agate mortar and pestle. A 2.0 g mineral sample was treated with predetermined reagents and conditioned for 40 min at pH 10. The solid samples were thoroughly washed using deionized water. After washing and vacuum drying at 35 °C for 24 h, the samples were subjected to FTIR analysis. The samples were analyzed by diffuse reflectance (DR) and ATR-FTIR spectroscopy, using an IFS 66 V/S instrument and a Vertex 80v instrument, respectively (Bruker Optics, Ettlingen, Germany) under vacuum conditions (below 7 mbar), according to the protocol by András and Björn[38]. For diffuse reflectance measurements, powder from dry samples (ca. 10 mg) was mixed with infrared spectroscopy grade potassium bromide (KBr, Merck/Sigma-Aldrich, ca. 390 mg) and manually ground using an agate mortar and pestle until a homogeneous mixture was achieved. Spectra were recorded in the range of 400–4000 cm^{-1} at 4 cm^{-1} spectral resolution, and 128 scans were co-added, using pure KBr as the background under the same parameters. Spectra were processed using the built-in functions of OPUS (version 7, Bruker Optics, Ettlingen, Germany). Spectra were the first baseline corrected (64-point rubberband) over the entire spectral range, then vector normalized, and finally offset corrected. After these steps, no smoothing, derivatization, or other processing was applied. ATR measurements were done using a Bruker Platinum accessory with a diamond internal reflection element. Spectra were recorded in the range of 400–4000 cm^{-1} at 4 cm^{-1} spectral resolution, and 100 scans were recorded, using the empty diamond crystal as the background under the same parameters. The spectra were processed using the built-in functions of OPUS (version 7, Bruker Optics, Ettlingen, Germany) in the same way as the DR spectra.

Results and discussion

Grinding. Exploring the d_{80} of ground samples with and without PGA indicated that PGA (in various doses) could provide finer particles (Fig. 4). Further, the introduction of PGA (at 0.1 wt.%) reduced the particle size to a d_{80} = 140 µm compared to 181 µm for the reference, which translates to a finer product. Further size analyses of ground products (Table 2) revealed that the use of PGA could narrow their PSD, for example, the use of PGA (0.1 wt.%) resulted in 56.3% of particles being in + 38–106 µm, while without PGA, 51.2% of the particles were in this size range. This size range mostly favors flotation separation. In other words, the use of PGA could improve the grinding performance expressed by decreasing the distribution of ultrafine (−38 µm) and coarse particles (+ 106 µm) Table 2. Analysis of ground products showed that PGA (0.1%) generated a significantly higher specific surface area (0.89 m^2/g) than the reference (0.75 m^2/g). The high specific surface area also translated into a higher surface roughness (R_s) of 47.85 for PGA compared to 40.32 for the reference. Similar evidence of the

Size range (μm)	Reference	PGA (wt.%)		
	–	0.03	0.05	0.1
+ 106	23.9	21.1	20.0	20.5
+ 38 −106	51.2	54.2	54.7	56.3
−38	24.9	24.7	25.3	23.2
Energy consumption, Ec, (kWh/t)	18.0	14.4	14.3	12.4

Table 2. Summary of the grinding test with and without PGA (Ec expressed as work index).

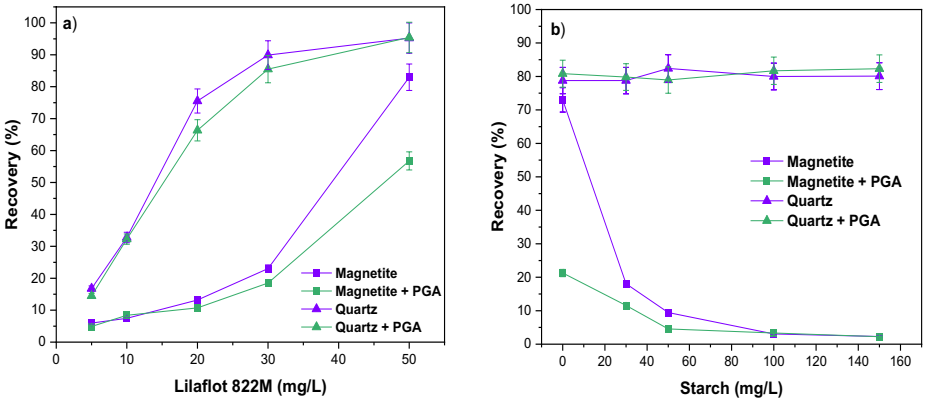

Figure 5. Single mineral flotation of magnetite and quartz as a function of (**a**) collector concentration in the presence and absence of 100 mg/L PGA at pH 10 and (**b**) depressant concentration in the presence and absence of 100 mg/L PGA at pH 10 and collector concentration of 50 mg/L.

increased surface area and surface roughness with the addition of GAs has been reported by Chipakwe et al.[10]. Evidently, PGA reduced the energy consumption with increasing concentration with a maximum reduction of 31.1% at 0.1 wt.% compared to the reference Table 2. In general, the grinding performance assessment indicated that PGA improved grinding efficiency compared to the reference (without PGA) based on the generation of new surfaces (higher specific surface area), lower energy consumption, and narrowing of the particle size distribution.

Flotation. *Single mineral.* Single mineral flotation experiments were carried out to assess the effect of Lilaflot 822M (collector) and starch (depressant) in the absence and presence of PGA (fixed dosage at 100 mg/L). Figure 5a presents the single mineral flotation performance for magnetite and quartz as a function of the collector. With an increase in Lilaflot 822M concentration, the recoveries of magnetite and quartz increased. As expected, the floatability of quartz for both conditions with and without PGA was markedly enhanced by increasing collector dosages (Lilaflot 822M is a silicate collector). In general, the floatability of quartz is comparable, although the presence of PGA resulted in lower floatability at lower collector concentrations. However, in high Lilaflot 822M concentrations, PGA indicated a significant effect on decreasing the floatability of magnetite compared to that of quartz. In other words, these findings suggested that PGA has a depressive effect on magnetite, which may be beneficial considering that magnetite depression is the key in reverse flotation separation. To further explore the impacts of PGA through additional experiments, the concentration of Lilaflot 822M (collector) was fixed at 50 mg/L, where quartz showed its highest floatability (recovery).

Furthermore, the floatability of magnetite and quartz as a depressant function with fixed collector and PGA doses was investigated (Fig. 5b). As anticipated, overly starch and PGA do not affect the floatability of quartz. The floatability of magnetite decreased significantly with increasing starch concentration, confirming the effectiveness of starch as a depressant. For the reference test, the floatability of magnetite continued to decrease with starch addition to a minimum of 2.3% at 100 mg/L. The depressing impact of PGA and reducing its floatability could be detected (Fig. 5b). A significant decrease in magnetite recovery to 21.3% without starch compared to 73.0% for the reference test could confirm the depressing effect of PGA. It can also be seen that the maximum depression effect of starch was observed at 100 mg /L, whilst with the addition of PGA, a comparable depression effect was achieved at 50 mg/L. Generally, single-mineral flotation tests indicated that increasing PGA has a favorable outcome in magnetite depression without changing quartz floatability.

Mixed mineral flotation. Subsequently, mixed mineral flotation experiments were carried out to assess the effect of PGA on the model ore (magnetite: quartz 2:1 mass ratio). Based on the results of the single mineral

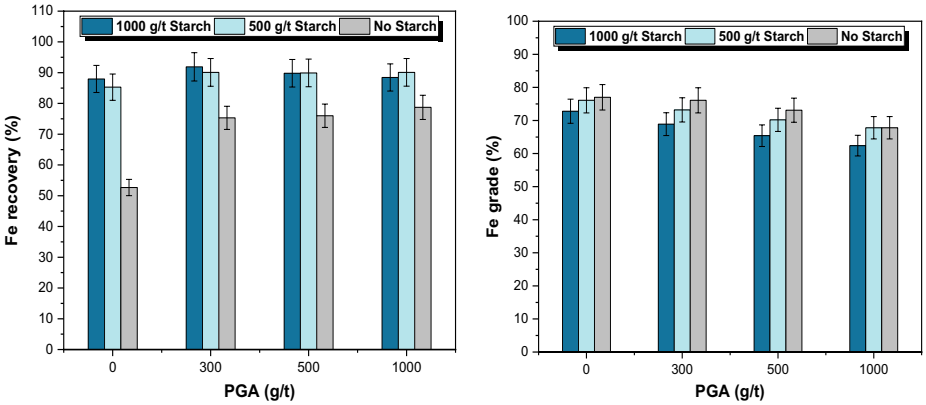

Figure 6. Effect of PGA and starch on magnetite flotation at a fixed amount of collector (300 g/t) at pH 10.

Separation efficiency (%)			
PGA (g/t)	No starch	500 (g/t) starch	1000 (g/t) starch
0	43.7	58.0	56.8
300	56.1	60.6	50.8
500	53.1	52.9	43.7
1000	47.0	48.5	37.6

Table 3. Variation of Separation Efficiency with and Without PGA and Starch.

flotation, 30 mg/L (which translates to 300 g/t) was considered for the doses of collector, while the starch and PGA dosages varied at pH 10. The variation in magnetite metallurgical recovery (as Fe) as a function of PGA and starch dosage was presented in Fig. 6. The results indicated that Fe recovery (magnetite hydrophilicity) improved by increasing PGA dosage in the absence of starch. However, the improvement was negligible after 300 g/t PGA. In the presence of starch, the recovery variations were insignificant. In other words, no obvious changes could be realized by increasing starch concentration from 500 to 1000 g/t. It could be translated as PGA improving grinding performance and reducing depressant consumption.

Higher Fe grades were reported in the absence of starch, although the recoveries are generally lower (Fig. 6). Therefore, the separation efficiency (SE) was calculated to better understand the interaction of PGA and starch and their resulting synergistic effects on separation (Table 3). Flotation outcomes indicated that PGA (in all dosages) could enhance the S.E in the absence of starch. 300 g/t PGA (in the absence of starch) provided results similar to those of 1000 g/t starch (in the absence of PGA). In general, the presence of both PGA and starch could improve the S.E compared to the reference conditions. It can be observed that high doses of both PGA and starch were not desirable. The highest S.E can be observed when starch and PGA were 50 and 300 g/t, respectively. The observed improvements in flotation separation corroborate findings reported elsewhere on the beneficial effects of a narrow particle size distribution[27,28] and surface roughness[39,40]. Besides the superior properties observed from using PGA, surface analyses were considered to assess PGA interaction with mineral surfaces.

Zeta potential measurements. Zeta potential measurements were carried out to further explore the interaction mechanism between PGA, Lilaflot 822M, and mineral particles to understand the observed flotation behavior. It is important to assess how these surfactants change the surface properties that affect the flotation behavior. Zeta potential measurement results indicated (Fig. 7) that the addition of PGA slightly affects the electrical charge on the surface of both quartz and magnetite implying a change in either solution or surface chemistry or both. These negligible effects could be due to the nonionic PGA composition. The zeta potentials for quartz decreased (absolute value) after PGA treatment. The evaluations illustrated that the zeta potentials decreased rapidly from 0 to 15 mg/L (PGA concentration) for both minerals, with quartz changing from −59.5 to −51.6 mV ($\Delta\zeta \sim +7.9$ mV) while magnetite changed from −44.9 to −35.6 mV ($\Delta\zeta \sim +9.3$ mV). The ζ measurements demonstrated that the addition of PGA to both minerals above 30 mg/L has almost no further effect in the investigated ranges. The addition of Lilaflot 822M to the treated minerals results in a behavior change to give more positive zeta potentials, especially for quartz. This illustrated that PGA had an insignificant effect on quartz, evident from the marked effect of Lilaflot 822M adsorption on the surface as a collector. A similar behavior could be observed with the addition of PGA, where the zeta potentials decreased with increasing PGA concentration. The relatively smaller change in magnetite zeta potentials, compared to quartz after Lilaflot 822M treatment, indicated that the presence of PGA reduced the interaction between Lilaflot 822M and magnetite. This highlighted that PGA adsorbed on magnetite rather than the quartz surface based on the collector impact.

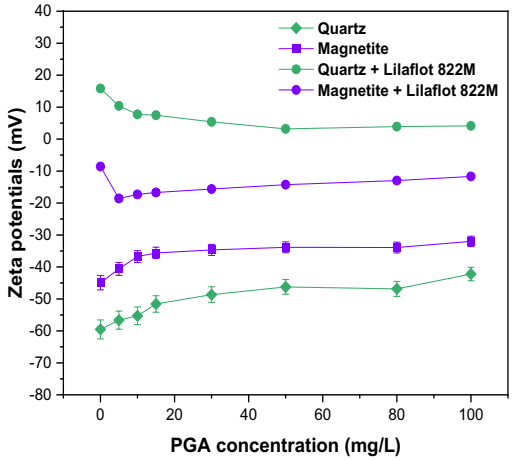

Figure 7. Zeta potentials at varying PGA concentration with fixed Lilaflot 822M (50 mg/L) and pH.

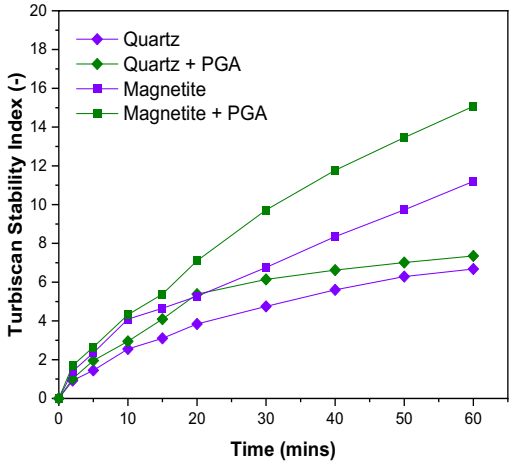

Figure 8. Stability of magnetite and quartz suspensions in the absence and presence of PGA (100 mg/L and pH 10).

Stability measurements. The Turbiscan stability index (TSI) assessments (Fig. 8) showed that treatment of both particle surfaces results in decreased stability compared to the reference (without PGA treatment). The observations are expected for any suspension, as the destabilization illustrated the effect of flocculation, coagulation, sedimentation, coalescence, and even a combination[36,37]. Figure 8 showed the destabilization kinetics of magnetite and quartz suspensions as a function of time. TSI values demonstrated that a relatively stable system was in agreement with the zeta potential results (Fig. 7) for both quartz and magnetite, which are all below −30 mV at pH 10, showing high stability[41,42]. The TSI values for magnetite are higher compared to those of quartz, generally showing less stability. After PGA treatment, the stability variation was more pronounced for magnetite compared to quartz for the total investigated time of 60 min. In other words, these outcomes suggested that the destabilizing effect of PGA was more pronounced on magnetite than on quartz, pointing to increased adsorption. This is consistent with the zeta potentials, which showed a higher absolute value for quartz relative to magnetite, indicating better suspension stability. When examining magnetite particles, the increase in TSI values (reduced dispersion) could help explain the depression effect of PGA, which might be due to aggregation/flocculation, thus hindering flotation. Similar observations have been reported in which polysaccharides interact with iron oxides from aggregations[43,44].

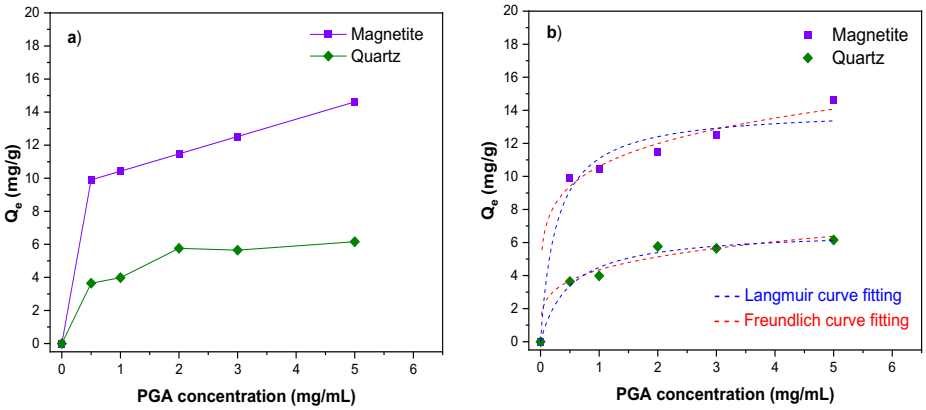

Figure 9. Adsorption of PGA as a function of initial concentration at pH 10.

Particles	Langmuir equation			Freundlich equation		
	Q_m	K_L	R^2	n	K_F	R^2
Magnetite	12.10	9×10^{-1}	0.9651	6.00	3.43	0.9085
Quartz	5.85	6.6×10^{-3}	0.9721	5.18	1.25	0.8506

Table 4. Langmuir and Freundlich parameters for PGA adsorption on magnetite and quartz.

Adsorption test. Figure 9a showed an increase in adsorbed PGA per unit mass of magnetite and quartz. Furthermore, it could be observed that the adsorption capacity of magnetite was more than double that of quartz. For magnetite, a trend of continued increase can be demonstrated based on the still high slope beyond 5 mg/ml, while for quartz, the curve started plateauing after 2 mg/ml. The adsorption isotherms of PGA in magnetite and quartz particles are shown in Fig. 9b. The results of the adsorption isotherms using the depletion method were fitted to the Langmuir (Eq. 2) and Freundlich (Eq. 3) models and are summarized in Table 4. The Langmuir model gave the best fit with R^2 of 0.9651 and 0.9721, whilst the Freundlich model had R^2 of 0.9085 and 0.8506 for magnetite and quartz, respectively. The trends observed in Fig. 9a were also supported by the calculated parameters from the Langmuir and Freundlich models (Table 4). The obtained parameters n and Q_m values (highlighted the strength and capacity of the adsorption, respectively) were higher for magnetite compared to quartz, which suggested that the adsorption of PGA on magnetite was much stronger. The findings from the adsorption studies showed that PGA fairly adsorbs on both magnetite and quartz, further confirming the effect of PGA on single-mineral flotation, possibly reducing the surface areas available for collector adsorption, especially for magnetite. These outcomes corroborated the zeta potentials and stability measurement findings that magnetite had a higher and stronger adsorption capability for PGA compared to that of quartz.

FTIR spectra analysis. FTIR was used to characterize the functional groups in PGA, which is mainly a dextran (Fig. 10). The main characteristic peaks showed a broad peak between 3000 and 3600 cm^{-1}, demonstrating a hydroxyl group[45,46]—OH stretching vibration and appearing at 3308 cm^{-1}. A distinct characteristic peak appeared at 2928 cm^{-1}, which was related to the C-H stretch vibration in the sugar ring[45,47]. Furthermore, the C–O stretching vibration was illustrated at 1643 cm^{-1}[48]. A peak emerged at 1346 cm^{-1} that could be assigned to the symmetric CH_3 bending[46]. Strong characteristic peaks emerged at 1006 cm^{-1} and 918 cm^{-1} in the region 950–1100 cm^{-1}, which was attributed to the C–O–C and C–O groups of polysaccharides[46]. The peak in the region 950–1100 cm^{-1} was due to the presence of the (1→6)- and (1→3)-linked α-D-glucose units, respectively[49,50].

The adsorption mechanism of PGA was investigated together with the collector on both magnetite and quartz surfaces. Figure 11a showed the spectra for pure quartz, quartz + PGA, quartz + PGA + Lilaflot 822M together with the respective pure reagents. For Lilaflot 822M, characteristic peaks emerged at 2964 cm^{-1}, 2869 cm^{-1}, which were attributed to the CH_2 stretching bond of the acyclic compounds[51]. The peak at 1587, 1464 and 653 cm^{-1} could be attributed to the bending of the NH_2 or NH bonds[51–53]. It is evident from Fig. 11a that the presence or absence of PGA on the quartz surface had no effect, as no observable change in the spectra exists. After treatment with Lilaflot 822M, a characteristic peak was observed on the quartz surface. After treatment of quartz with Lilaflot 822M, the characteristic peak of OH at 2964 cm^{-1} shifted to 2960 cm^{-1} as observed in quartz + PGA + Lilaflot 822M, which was consistent with the findings reported by Liu et al.[51]. Furthermore, the characteristic stretching of CH at 2869 cm^{-1} also changed to 2856 cm^{-1} after treatment. This indicated that Lilaflot 822M adsorbed onto the quartz surface through the OH and CH bonds. Compared to Lilaflot 822M, PGA did not show a characteristic peak and, given the water washing in the procedure, which meant that Lilaflot 822M adsorbed chemically and collaborated with the finding documented by Huang et al.[52] and Liu et al.[51] on the

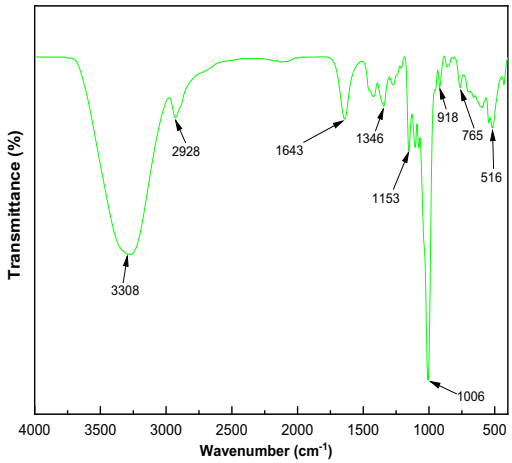

Figure 10. FT-IR spectra of the examined PGA using ATIR.

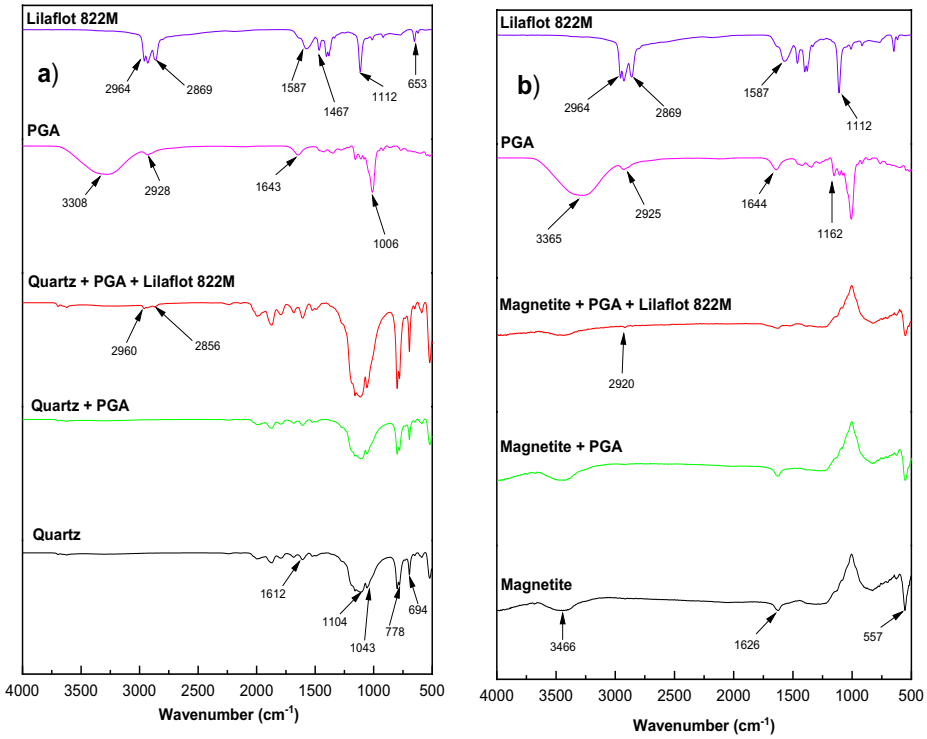

Figure 11. FTIR spectra of (**a**) quartz and (**b**) magnetite in the presence and absence of PGA and Lilaflot 822M (at 100 mg/L).

adsorption of amines on the quartz surface. In contrast, the absence of a characteristic PGA peak on the quartz surface suggested that PGA did not chemically adsorb on the quartz surface. This points to the slightly weak physisorption of PGA on the quartz surface.

The FTIR spectra for magnetite in the presence and absence of PGA and Lilaflot 822M (Fig. 11b) indicated that there was no characteristic peak in magnetite treated with PGA, and therefore there was no impact from PGA. Moreover, Lilaflot 822M had a negligible impact on the magnetite surface, evident from the relatively weak characteristic shifted peak at 2920 $cm^{-1.}$ Negligible characteristic peaks on magnetite meant weak adsorption,

especially compared to Lilaflot 822M adsorption on the quartz surface. The absence of a characteristic peak on magnetite in the presence of PGA suggested that PGA did not adsorb chemically but rather possibly a physical interaction. From the IR analysis, it can be said that for both quartz and magnetite PGAs, the interaction mechanism was not chemical. However, considering that the particles were subjected to thorough washing with water before analysis, the interaction could be physical and probably due to hydrogen bonding. Shrimali and Miller[22], in their concise review of the interaction of polysaccharides and iron ores, outline that polysaccharide adsorption may be due to hydrogen bonding, hydrophobic interaction, or chemical complexing (acid–base reaction). The hydrophobic interaction might play a major role in reducing the surface charge, allowing for flocculation/aggregation of the particles; thus, leading to magnetite depression. This is consistent with observations suggested that the mechanism of nonionic polymer adsorption would be due to the hydrophobic chain interaction leading to the bridging and/or charge neutralization[23,54,55].

Conclusions

In this study, a novel polysaccharide-based grinding aid was first used to improve grinding performance, and its secondary effects on reverse flotation of magnetite quartz from magnetite were explored. Empirical observations on batch dry grinding indicate that PGA improved grinding efficiency by reducing energy consumption, a narrower PSD, increased specific surface area, rougher surfaces, and a finer PSD. According to the single mineral flotation tests, PGA has a depressing effect (positive effects) on magnetite particles with a negligible effect on quartz particles. Through mixed mineral flotation separation (magnetite + quartz at 2:1) comparable results of 86% recovery and Fe grade of 62% could be achieved using PGA only without starch. For the best balance in recovery, grade and separation efficiency, 500 g/t starch could be recommended along with 300 g/t PGA. Based on UV–vis spectra, zeta potential tests, Fourier transform infrared spectroscopy (FT-IR), and stability measurements, the adsorption mechanism is mainly via physical interaction. In other words, the improved flotation separation efficiency in the presence of PGA could also be attributed to the narrowing of the particle size distribution and the increase in surface roughness. These results highlighted that the selection of suitable grinding aids (ecofriendly) could potentially reduce energy consumption (decrease CO_2 emissions), improve the distribution of suitable particles for downstream processes, and has no negative chemical impacts (even positive effects) on the separation stages.

Received: 16 February 2022; Accepted: 5 April 2022
Published online: 20 April 2022

References

1. Jeswiet, J. & Szekeres, A. Energy Consumption in Mining Comminution. *Procedia CIRP* **48**, 140–145 (2016).
2. Bouchard, J., Desbiens, A. & Poulin, É. Reducing the energy footprint of grinding circuits: the process control paradigm. *IFAC-PapersOnLine* **50**, 1163–1168 (2017).
3. Adewuyi, S. O., Ahmed, H. A. M. & Ahmed, H. M. A. Methods of ore pretreatment for comminution energy reduction. *Minerals* **10**, 1 (2020).
4. Singh, V., Dixit, P., Venugopal, R. & Venkatesh, K. B. Ore pretreatment methods for grinding: Journey and prospects. *Miner. Process. Extr. Metall. Rev.* **40**, 1–15 (2018).
5. Chipakwe, V., Hulme-Smith, C., Karlkvist, T., Rosenkranz, J. & Chelgani, S. C. Effects of chemical additives on rheological properties of dry ground Ore - A comparative study. *Miner. Process. Extr. Metall. Rev.* **00**, 1–10 (2021).
6. Chipakwe, V., Semsari, P., Karlkvist, T., Rosenkranz, J. & Chelgani, S. C. A critical review on the mechanisms of chemical additives used in grinding and their effects on the downstream processes. *J. Mater. Res. Technol.* **9**, 8148–8162 (2020).
7. Fuerstenau, D. W. Grinding Aids. *KONA Powder Part. J.* **13**, 5–18 (1995).
8. Assaad, J. J. Industrial versus Laboratory clinker processing using grinding AIDS (scale effect). *Adv. Mater. Sci. Eng.* **2015**, 1 (2015).
9. Cheng, F. *et al.* Practical strategy to produce ultrafine ceramic glaze: Introducing a polycarboxylate grinding aid to the grinding process. *Adv. Powder Technol.* **30**, 1655–1663 (2019).
10. Chipakwe, V., Semsari, P., Karlkvist, T., Rosenkranz, J. & Chelgani, S. C. A comparative study on the e ff ect of chemical additives on dry grinding of magnetite ore. *South Afr. J. Chem. Eng.* **34**, 135–141 (2020).
11. Mishra, R. K., Weibel, M., Müller, T., Heinz, H. & Flatt, R. J. Energy-effective grinding of inorganic solids using organic additives. *Chimia (Aarau).* **71**, 451–460 (2017).
12. Zhao, J., Wang, D., Yan, P. & Li, W. Comparison of grinding characteristics of converter steel slag with and without pretreatment and grinding aids. *Appl. Sci.* **6**, 1–15 (2016).
13. Weibel, M. & Mishra, R. K. Comprehensive understanding of grinding aids. *ZKG Int.* **67**, 28–39 (2014).
14. El-Shall, H. & Somasundaran, P. Mechanisms of grinding modification by chemical additives: Organic reagents. *Powder Technol.* **38**, 267–273 (1984).
15. Ervanne, H. & Hakanen, M. *Analysis of Cement Superplasticizers and Grinding Aids A Literature Survey. POSIVA* (2007).
16. Gao, X., Yang, Y. & Deng, H. Utilization of beet molasses as a grinding aid in blended cements. *Constr. Build. Mater.* **25**, 3782–3789 (2011).
17. Zhang, Y., Fei, A. & Li, D. Utilization of waste glycerin, industry lignin and cane molasses as grinding aids in blended cement. *Constr. Build. Mater.* **123**, 785–791 (2016).
18. Nuorivaara, T. & Serna-Guerrero, R. Unlocking the potential of sustainable chemicals in mineral processing: Improving sphalerite flotation using amphiphilic cellulose and frother mixtures. *J. Clean. Prod.* **261**, 121143 (2020).
19. Lapointe, M. & Barbeau, B. Understanding the roles and characterizing the intrinsic properties of synthetic vs natural polymers to improve clarification through interparticle Bridging: A review. *Sep. Purif. Technol.* **231**, 115893 (2020).
20. Deng, W., Xu, L., Tian, J., Hu, Y. & Han, Y. Flotation and adsorption of a new polysaccharide depressant on pyrite and talc in the presence of a pre-adsorbed xanthate collector. *Minerals* **7**, 1–14 (2017).
21. Filippov, L. O., Severov, V. V. & Filippova, I. V. An overview of the beneficiation of iron ores via reverse cationic flotation. *Int. J. Miner. Process.* **127**, 62–69 (2014).
22. Shrimali, K. & Miller, J. D. Polysaccharide Depressants for the Reverse Flotation of Iron Ore. *Trans. Indian Inst. Met.* **69**, 83–95 (2016).
23. Chimonyo, W., Fletcher, B. & Peng, Y. Starch chemical modification for selective flotation of copper sulphide minerals from carbonaceous material: A critical review. *Miner. Eng.* **156**, 1022 (2020).

24. Aznar-Sánchez, J. A., Velasco-Muñoz, J. F., Belmonte-Ureña, L. J. & Manzano-Agugliaro, F. Innovation and technology for sustainable mining activity: A worldwide research assessment. *J. Clean. Prod.* **221**, 38–54 (2019).
25. Bhima Rao, R., Narasimhan, K. S. & Rao, T. C. Effect of additives on grinding of magnetite ore. *Miner. Metall. Process.* **8**, 144–151 (1991).
26. Yang, A. The Influence of Grinding Aids on the on the floatabilty of the fine casseterite. *Fizykochem. Probl. Miner.* **28**, 37–46 (1994).
27. Chipakwe, V., Jolsterå, R. & Chelgani, S. C. Nanobubble-assisted flotation of apatite tailings: Insights on beneficiation options. *ACS Omega* https://doi.org/10.1021/acsomega.1c01551 (2021).
28. Chipakwe, V., Sand, A. & Chelgani, S. C. Nanobubble assisted flotation separation of complex Pb–Cu–Zn sulfide ore–assessment of process readiness. *Sep. Sci. Technol.* **00**, 1–8 (2021).
29. Bond, F. C. Crushing and Grinding Calculations. *Br. Chem. Eng.* **1**, 378–385 (1961).
30. Jaycock, M. J. & Parfitt, G. D. The study of liquid interfaces. *Chem. Interfaces* **1**, 38–132 (1981).
31. Tohry, A., Dehghan, R., Zarei, M. & Chelgani, S. C. Mechanism of humic acid adsorption as a flotation separation depressant on the complex silicates and hematite. *Miner. Eng.* **162**, 106736 (2021).
32. Yang, B. *et al.* Differential adsorption of hydrolytic polymaleic anhydride as an eco-friendly depressant for the selective flotation of apatite from dolomite. *Sep. Purif. Technol.* **256**, 1103 (2021).
33. Fu, Y. F. *et al.* New insights into the flotation responses of brucite and serpentine for different conditioning times: Surface dissolution behavior. *Int. J. Miner. Metall. Mater.* **28**, 1898–1907 (2021).
34. Hunter, R. *Zeta potential in colloid science: principles and applications*. (Academic press, 2013).
35. Zhang, C. *et al.* Selective adsorption of tannic acid on calcite and implications for separation of fluorite minerals. *J. Colloid Interface Sci.* **512**, 55–63 (2018).
36. Bastrzyk, A. & Feder-Kubis, J. Pyrrolidinium and morpholinium ionic liquids as a novel effective destabilising agent of mineral suspension. *Colloids Surfaces A Physicochem. Eng. Asp.* **557**, 58–65 (2018).
37. Ataie, M., Sutherland, K., Pakzad, L. & Fatehi, P. Experimental and modeling analysis of lignin derived polymer in flocculating aluminium oxide particles. *Sep. Purif. Technol.* **247**, 116944 (2020).
38. András, G. & Björn, S. Chemical Fingerprinting of Arabidopsis Using Fourier Transform Infrared (FT-IR) Spectroscopic Approaches. in *Arabidopsis Protocols. Methods in Molecular Biology (Methods and Protocols)* (ed. Sanchez-Serrano J., S. J.) 317–352 (2014). https://doi.org/10.1007/978-1-62703-580-4_18
39. Tong, Z. *et al.* The effect of comminution on surface roughness and wettability of graphite particles and their relation with flotation. *Miner. Eng.* **169**, 106959 (2021).
40. Zhu, Z. *et al.* The role of surface roughness in the wettability and floatability of quartz particles. *Appl. Surf. Sci.* **527**, 146799 (2020).
41. Uskoković, V. Dynamic light scattering based microelectrophoresis: Main prospects and limitations. *J. Dispers. Sci. Technol.* **33**, 1762–1786 (2012).
42. Tucker, I. M. *et al.* Laser Doppler electrophoresis applied to colloids and surfaces. *Curr. Opin. Colloid Interface Sci.* **20**, 215–226 (2015).
43. Tohry, A., Dehghan, R., de Salles Leal Filho, L. & Chehreh Chelgani, S. Tannin: An eco-friendly depressant for the green flotation separation of hematite from quartz. *Miner. Eng.* **168**, 106917 (2021).
44. Engwayu, J. & Pawlik, M. Adsorption of anionic polymers on hematite—a study of zeta potential distributions. *Miner. Eng.* **148**, 106225 (2020).
45. Yilmaz, M. T. *et al.* Characterisation and functional roles of a highly branched dextran produced by a bee pollen isolate Leuconostoc mesenteroides BI-20. *Food Biosci.* https://doi.org/10.1016/j.fbio.2021.101330 (2021).
46. İspirli, H. *et al.* Characterization of a glucansucrase from Lactobacillus reuteri E81 and production of malto-oligosaccharides. *Biocatal. Biotransform.* **37**, 421–430 (2019).
47. Kavitake, D., Devi, P. B., Singh, S. P. & Shetty, P. H. Characterization of a novel galactan produced by Weissella confusa KR780676 from an acidic fermented food. *Int. J. Biol. Macromol.* **86**, 681–689 (2016).
48. Wang, Y. *et al.* Physical characterization of exopolysaccharide produced by Lactobacillus plantarum KF5 isolated from Tibet Kefir. *Carbohydr. Polym.* **82**, 895–903 (2010).
49. Das, D. & Goyal, A. Characterization and biocompatibility of glucan: A safe food additive from probiotic Lactobacillus plantarum DM5. *J. Sci. Food Agric.* **94**, 683–690 (2014).
50. Miao, M. *et al.* Characterisation of a novel water-soluble polysaccharide from Leuconostoc citreum SK24.002. *Food Hydrocoll.* **36**, 265–272 (2014).
51. Liu, X., Xie, J., Huang, G. & Li, C. Low-temperature performance of cationic collector undecyl propyl ether amine for ilmenite flotation. *Miner. Eng.* **114**, 50–56 (2017).
52. Huang, Z. *et al.* Investigations on reverse cationic flotation of iron ore by using a Gemini surfactant: Ethane-1,2-bis(dimethyl-dodecyl-ammonium bromide). *Chem. Eng. J.* **257**, 218–228 (2014).
53. Liu, W., Liu, W., Wang, X., Wei, D. & Wang, B. Utilization of novel surfactant N-dodecyl-isopropanolamine as collector for efficient separation of quartz from hematite. *Sep. Purif. Technol.* **162**, 188–194 (2016).
54. Filippov, L. O., Houot, R. & Joussemet, R. Physicochemical mechanisms and ion flotation possibilities using columns for Cr6+ recovery from sulphuric solutions. *Int. J. Miner. Process.* **51**, 229–239 (1997).
55. Hanumantha Rao, K. & Forssberg, K. S. E. Mixed collector systems in flotation. *Int. J. Miner. Process.* **51**, 67–79 (1997).

Acknowledgements

This manuscript resulted from a project financially supported by CAMM, the Center of Advanced Mining and Metallurgy, as a center of excellence at the Luleå University of Technology. The authors also thank Solenis for their help with the reagents used as grinding aids in this study. The authors express their gratitude to Dr. Andras Gorzsas from Umeå University for assistance with FTIR analysis and fruitful discussions.

Author contributions

V.C. and S.C.C. were responsible for the Conceptualization, Design of experiments, Formal Analysis and Original draft; V.C. Performed the experiments; T.K. Reviewing and Editing, Data curation, Supervision. S.C.C. and J.R. provided the Resources, Reviewing and Editing, Data curation, Supervision

Funding

Open access funding provided by Lulea University of Technology.

Competing interests

The authors declare no competing interests.

Additional information

Correspondence and requests for materials should be addressed to V.C. or S.C.C.

Reprints and permissions information is available at www.nature.com/reprints.

Publisher's note Springer Nature remains neutral with regard to jurisdictional claims in published maps and institutional affiliations.

Paper V

Exploring the effect of a polyacrylic acid-based grinding aid on magnetite-quartz flotation separation.

V. Chipakwe, T. Karlkvist, J. Rosenkranz, S Chehreh Chelgani.

Separation and Purification Technology, 305:122530, 2022

Separation and Purification Technology 305 (2023) 122530

Contents lists available at ScienceDirect

Separation and Purification Technology

journal homepage: www.elsevier.com/locate/seppur

Exploring the effect of a polyacrylic acid-based grinding aid on magnetite-quartz flotation separation

Vitalis Chipakwe *, Tommy Karlkvist, Jan Rosenkranz, Saeed Chehreh Chelgani *

Minerals and Metallurgical Engineering, Department of Civil, Environmental and Natural Resources Engineering, Lulea University of Technology, SE-971 87 Lulea, Sweden

ARTICLE INFO

Keywords:
Grinding aid
Polymer
Polyacrylic acid
Flotation performance
Grinding
Pretreatment
Energy

ABSTRACT

It is well documented that the use of grinding aids (GAs) can reduce milling energy consumption. However, the impact of GAs on downstream processes must be addressed in view of complex processes such as froth flotation separation. This study investigates the effects of polyacrylic-based grinding aids (Zalta™ GR20-587: AAG) on the grinding performance and quartz flotation from magnetite. Various AAG dosages and conditions were examined. The grinding results showed lower energy consumption and a finer, more uniform product size with roughened surfaces for AAG compared to grinding without the grinding aid. Flotation tests of single pure minerals showed that AAG enhanced quartz collection with minimal effect on magnetite. Mixed mineral flotation showed that by using AAG, Fe recovery of 92.1 % and 64.5 % Fe grade could be achieved with a lower collector dosage of 100 g/t compared to 200 g/t in the absence of AAG. Zeta potentials and stability measurements showed that AAG shifts the potential, thus improving the stability and dispersion of the suspension. Adsorption tests illustrated that AAG adsorbed on both quartz and magnetite, the former having a higher capacity. FTIR indicated the physisorption interaction between AAG and the minerals. Therefore, the presence of AAG not only improved grinding efficiency but could potentially decrease the amount of collector required to achieve comparable metallurgical performance.

1. Introduction

Minerals' size reduction and liberation are associated with high energy consumption coupled with low efficiency [1–3]. Among many efforts to address these challenges, the use of grinding aids has been proposed as one of the potential solutions [4–6]. It is well documented that grinding aid (GA) can improve grinding performance, prevent agglomeration, generate narrow-size products, and reduce energy consumption [7–10]. Although understanding of the mechanism of the effect of these GAs remains unsatisfactory, there is a consensus that the adsorption of these chemical additives is a prerequisite for their applications [5,6]. It can be postulated that these chemicals will remain on the surface of the particles after milling.

Since size reduction is usually followed by the subsequent concentration or separation processes, it is paramount to ensure that the integrity and performance of these downstream processes are not compromised. Grinding as a step prior to the flotation separation process influences the surface properties of the particles, the solution/pulp chemistry, the surface chemistry, and even the crystal structure [11–15]. Ersoy et al. [16] investigated the effect of triethanolamine (TEA) and monoethyl glycol (MEG) (the most typical GAs) on the surface of calcium carbonate. Both GAs have been reported to adsorb on particle surfaces, resulting in changes in product properties, such as rheology, dispersion, and color properties [16]. Bulejko et al. [12] examined the effect of 0.1 wt% TEA in ultrafine wet grinding of corundum. TEA affected zeta potentials, turbidity, viscosity, and improved grinding performance. They considered only one TEA concentration (0.1 wt%) and reported relatively unstable suspensions based on zeta potentials and turbidity measurements [12]. Although several studies have discussed the effects of GAs on the final product (centered on the cement and aggregate industry, where grinding is usually the final step), few investigations have addressed their effects on products in view of downstream processes such as flotation [5,6]. In addition to the change in product properties during grinding, froth flotation involves using surfactants that can potentially interact with these grinding aids.

Polyacrylic acid (PAA) and its derivatives are widely used in mineral processing in different applications, as flocculants, dispersants, depressants, and viscosity modifiers [3,17–23]. Zhang et al. [21] examined

* Corresponding authors.
E-mail addresses: vitalis.chipakwe@ltu.se (V. Chipakwe), saeed.chelgani@ltu.se (S.C. Chelgani).

https://doi.org/10.1016/j.seppur.2022.122530
Received 29 August 2022; Received in revised form 10 October 2022; Accepted 29 October 2022
Available online 3 November 2022

the effect of PAA as a depressant in the flotation of calcite and fluorite. PAA was selectively adsorbed on calcite, selectively depressed, and improved fluorite recovery with sodium oleate at pH 7. Quezada et al. [24] reported that applying PAA could improve the sedimentation and storage of quartz, montmorillonite, and kaolinite flotation tailings. Through molecular dynamics simulation, PAA was reported to adsorb on quartz and clay mineral surfaces, ultimately preventing agglomeration of the tailings and allowing easy dewatering. Chen et al. [25], during the flotation separation of chalcopyrite and magnesium silicates with potassium xanthate (a collector) and gum Arabic (a depressant), found that the presence of a PAA-based polymer (sodium polyacrylate) improved the process. The synergism between sodium polyacrylate and gum Arabia allowed selective depression of magnesium silicate minerals, namely talc and serpentine. The improved flotation separation was attributed to the PAA dispersion effect in removing serpentine particles from the surface of the talc, which allowed gum Arabia to adsorb on the talc surface [25]. In size reduction units, using these GAs, such as PAA, makes it inevitable that these additives can directly or indirectly enter downstream separation processes, such as flotation. Froth flotation remains the most versatile separation technique, yet very complex, utilizing differences in natural or imparted wettability of the mineral surface [26–29]. In flotation, solution and surface chemistry are important in understanding the physicochemical processes occurring at the solid-water and the air–water interface [30,31].

GA polymers used primarily in solid–liquid separation units have been reported to enhance or depress flotation depending on their types, particle type, polymer concentration, and contact time [32]. From this detailed review of the literature, it is evident that more research is required in designing and selecting chemical additives used as GAs to ensure compatibility with the specifications of the product and downstream processes. Although some studies have been reported on polymer-surfactant interactions, mostly in flocculants, this study, as a practical approach, focuses on their interaction through GA-surfactant. This study first investigates the effect of a polyacrylic acid-based grinding aid (Zalta™ GR20-587: AAG) on the grinding performance and the surface of the ground particle. The effect of AAG on surface properties and pulp chemistry was then explored together with the resulting flotation behavior. The results of this study will aid in the development and selection of future multifunctional additives to further improve beneficiation performance.

2. Materials and methods

2.1. Materials

For the study, samples of pure quartz (99.9 % SiO_2) and magnetite (96.0 % Fe_3O_4) were obtained from VWR, Sweden (Fig. 1). For grinding experiments, a narrow particle size range of the mixture (−2.8 + 2 mm) was used as the grinding feed. The pure minerals were ground separately for flotation tests and subsequent surface analysis. From the resulting product, samples with a size fraction of −106 + 38 μm were used for flotation and adsorption tests. The −38 μm size fraction was further ground and used for subsequent surface analysis.

For all experiments, the anionic polyacrylic-based polymer (Zalta™ GR20-587: AAG) provided by Solenis with a typical chemical structure shown in Fig. 2 was used as GA. For grinding tests, AAG was used as received (aqueous form), and no stock solution was prepared to eliminate the effect of water. A cationic ether amine collector, Lilaflot 822 M, was obtained from Nouryon, Sweden. Analytical grade corn starch used as a magnetite depressant was purchased from Merck. Analytical grade HCl and NaOH (Merck) were prepared in an appropriate solution for pH adjustments.

2.2. Grinding test

A laboratory scale ball mill (CAPCO, UK) with a 115 mm internal diameter and a total volume of 1.4 L was used for the grinding experiments. The total grinding time of 30 min and the set parameters (19 vol % mill filling; 0.16 w/w feed: ball ratio; 10–36 mm graded steel balls) were predetermined as optimal for dry grinding in a natural atmosphere. Optimal parameters were adopted for all tests to reduce grinding energy, study the effect of GAs, and generate material for subsequent flotation tests. In the reference (blank), no additives were added, and for the other tests, AAG was combined with ore at three levels (300, 500, and 1000 g/t). The grinding products were subjected to particle size distribution (PSD) using a particle size analyzer (Mastersizer 3000, Malvern Instruments, UK), from which P_{80}, X_{10}, X_{50}, and X_{90} were determined. For a better assessment of the particle size distribution, the uniformity of the product was calculated using Eq. (1), which is a measure of the PSD

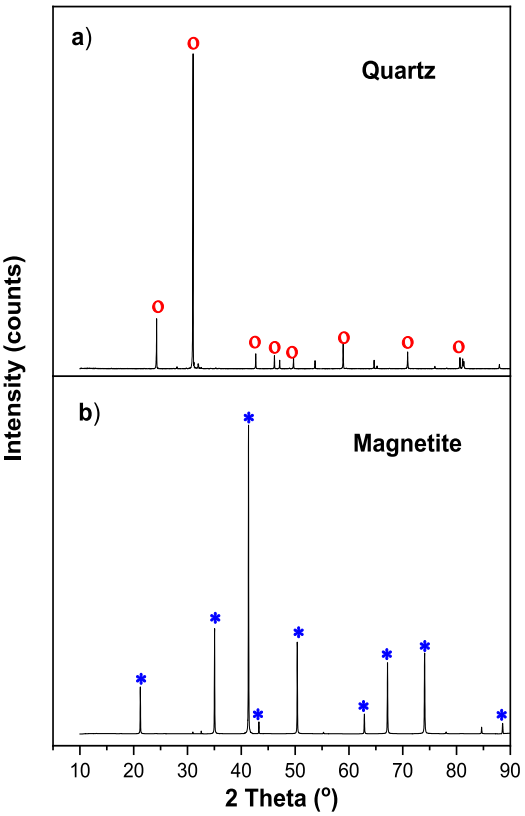

Fig. 1. XRD pattern for (a) pure quartz and (b) pure magnetite.

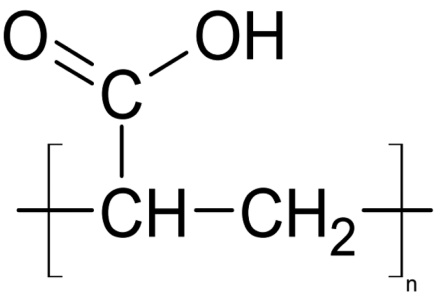

Fig. 2. Chemical structure of typical polyacrylic acid.

span. The smaller the value, the narrower the PSD [33,34].

$$Uniformity[-] = \frac{X_{90} - X_{10}}{X_{50}} \quad (1)$$

Here, X_{10}, X_{50}, and X_{90} are the diameters corresponding to 10, 50, and 90 vol% on a relative cumulative particle size distribution curve. Energy consumption was characterized using the work index according to the Bond equation (Eq. (2)) [35]. Where: Wi: work index (kWh/t), W: grinding energy (kWh/t), P: 80 % passing size of the mill product, in μm, F: 80 % passing size of the mill feed, in μm. The same grinding protocol was used for single minerals and the artificial mixture (magnetite: quartz 2:1). After grinding and wet sieving, the samples were thoroughly washed with a 2 % HCl solution to eliminate possible contamination the mineral surfaces.

$$W = 10.W_i\left(\frac{1}{\sqrt{P}} - \frac{1}{\sqrt{F}}\right) \quad (2)$$

2.3. Surface area and morphology

A sample was taken from the ground product for the surface area and morphology study. A Micromeritics Flowsorb II 2300 instrument was used to measure surface area based on the BET (Brunner Emmet Teller) method. Further, the surface roughness (R_S) was calculated using Eq. (3) [36].

$$R_S = A_B\rho\left(\frac{D}{6}\right) \quad (3)$$

where A_B is the BET surface area (m^2/g), ρ is the density of the sample, and D is the average particle diameter. Surface morphology under different grinding conditions was characterized by scanning electron microscopy (SEM). Secondary imaging (SE) was performed using the Zeiss Sigma 300 VP instrument (QanTmin).

2.4. Flotation test

Quartz and magnetite flotation tests were carried out using a 150 ml mini flotation cell (Clausthal cell, Germany) operated at 310 rpm and an airflow rate of 2 L/min. 7.5 g of the sample was added to the flotation cell with deionized water for each test. Before the flotation stage, the pulp was agitated with the required amount of AAG for 10 min to allow adsorption on the particle's surface. The required amount of depressant and collector was added to the pulp together with the corresponding pH adjustments for 10 min. An alkaline starch solution was prepared as a depressant together with Lilaflot 822 M as a collector. The total flotation time was 2 min, and afterward, the floats and sinks were collected, filtered, weighed, assayed, and recovery was calculated. In addition to single-pure mineral flotation, experiments were also carried out on the magnetite-quartz artificial mixture (at a 2:1 ratio). The selectivity S was calculated using equation (4) to assess the flotation performance under varying conditions. Where R_1 is the recovery of magnetite and R_2 is the recovery of quartz. A higher selectivity index S extrapolates better selectivity for the flotation separation [37,38].

$$S = R_1 - R_2 \quad (4)$$

2.5. Zeta potential measurements

The zeta potential measurements were carried out using the CAD ZetaCompact instrument (CAD Instruments, France). For the measurements, 20 mg of each mineral sample (−5 μm) was dispersed in 50 ml of potassium chloride solution (background electrolyte) together with predetermined reagents. The required pH adjustments were made using 0.1 M NaOH or HCl. Measurements were done in triplicate, and the average was reported.

2.6. Stability measurements

Stability measurements of the suspension were done using a turbidimeter (Turbiscan LAB Expert, Formulaction, France). The suspension (50 mg sample in 40 ml water) was mixed with varying reagent concentrations. Measurements were made using 20 ml aliquots and scanned at the height of 40 mm at 30° C. The measurements were conducted for 60 min at 30-second intervals. The light transmission and backscattering data obtained were used to calculate the Turbiscan stability index (TSI) (Eq. (5)). The values of the TSI coefficient range from 0 to 100 where the lower the stability of the value, the higher the suspension [22,39].

$$TSI = \sqrt{\frac{\sum_{i=1}^{n}(x_i - X_{BS})^2}{n-1}} \quad (5)$$

where x_i is the average backscattering for a measurement per minute, x_{BS} is the average x_i, and n is the number of scans.

2.7. Adsorption measurements

The adsorption of AAG on quartz and magnetite was measured using an ultra-violet visible spectrometer (DU Series 730 – Beckman Coulter, USA) at wavelength 210 nm in triplicate. For magnetite and quartz, 1.0 g particles were mixed with predetermined reagents at pH 10 in a 100 ml flask. To maximize adsorption, the mixture was stirred for 2 h. The adsorption capacity was calculated based on the depletion method using equation (6);

$$Q_e = \frac{(C_1 - C_0)V}{m} \quad (6)$$

where Q_e represents the adsorbed AAG on the sample particle surface in mg/g, C_0 and C_1 are the initial and residual AAG concentrations in mg/L, whilst V and m are AAG solution volume (L) and mass of mineral sample (g), respectively. The experimental data of the adsorption isotherm were fitted to the Langmuir (Eq. (7)), and Freundlich models (Eq. (8)) models, and the curve parameters are summarized in Table 4.

$$Q_e = \frac{K_L C_e Q_0}{1 + K_L C_e} \quad (7)$$

$$Q_e = K_F C_e^{\frac{1}{}} \quad (8)$$

where Q_e represents the amount of AAG (mg/g) adsorbed, C_e is the concentration of AAG at equilibrium. From Langmuir and Freundlich equations, the constants Q_m and K_L and K_F and $1/n$ respectively relate to the maximum adsorption capacity and the adsorption energy, respectively [40].

2.8. FT-IR measurements

FTIR spectra were obtained using an IFS 66 V/S instrument and a Vertex 80v instrument for diffuse reflectance (DR) and attenuated total reflectance (ATR), respectively (Bruker Optics, Ettlingen, Germany). For conditioning, 2.0 g pure samples were mixed with predetermined reagents (100 mg/L AAG and 50 mg/L Lilaflot 822 M) and conditioned for 40 min at pH 10. The solid samples were thoroughly washed with deionized water and dried at 35 °C for 24 h. The samples were mixed with potassium bromide. The scanning range was 400–4000 cm^{-1} at a resolution of 4 cm^{-1}.

3. Results and discussion

3.1. Grinding performance

To determine the optimal dose of GA to improve grinding perfor-

mance, a series of experiments using AAG were conducted. Grinding performance was first evaluated based on energy consumption (Ec) relative to the reference test (without AAG). The introduction of AAG decreases Ec to give a minimum of 16.69 kWh/t at 500 g/t compared to 19.41 kWh/t as reference (Table 1). Further the d_{80} of the product showed that 500 g/t is the optimal dosage with 184 μm whilst the reference had 207 μm (Table 1). The positive effect of grinding aids on improving product fineness has been observed in the literature [10,41–43]. The improvement in fineness points to better grinding due to improved material flowability resulting from the reduction in agglomeration [5,6,41,44,45]. In terms of uniformity, which generally measures PSD, the introduction of AAG results in a narrow PSD width (lower number uniformity). Furthermore, the specific surface area increases with the addition of AAG, with the highest of 0.6510 m^2/g at 500 g/t together with a corresponding maximum roughness of 0.3180 compared to 0.2389 for the reference (Table 1). The superior surface area result of the application of grinding aids compared to blank conditions has been widely reported in the literature [17,19]. Liu et al. 2021 [17], during cobalt aluminate using sodium polyacrylate, the specific surface area was greater (39.56 m^2/g) compared to the blank condition (20.18 m^2/g). In summary, the addition of an optimum amount of AAG improves the grinding performance evident from the reduction in Ec, the generation of new surfaces (higher SSA), and improved uniformity of the particles.

3.2. Surface morphology of ground products

Given downstream separation processes, the grinding stage goes beyond size reduction, as it involves a change in particle properties such as shape, roughness, and physicochemical properties [14,15]. These morphological characteristics have been shown to influence flotation performance [14,15,46]. SEM images were provided and analyzed to further characterize the effect of AAG on the morphological characteristic. Fig. 3 shows differences in the particle surface of the reference ground sample (Fig. 3a) compared to the ground in the presence of AAG at 1000 g/t (Fig. 3b), with the latter showing roughening of the surfaces. The reference particle shows smoother surfaces with some fragmented smaller particles on the surface. Smaller particles on the surface suggest an interparticle attraction that points to agglomeration tendencies in the absence of AAG. Similar findings have been reported in [41] on the effect of different grinding aids on fine dry grinding of calcite. SEM analysis of ground samples showed more agglomerates in the blank compared to particles with grinding aids [41]. Grinding mechanisms, such as abrasion and impact, have been reported to influence particle shape and roughness [14,47]. The observed roughening for AAG is consistent with the calculated roughness and the measured SSA, which is superior to the reference. The observed roughening could be attributed to the reduced contribution of abrasion due to the improved flowability with the introduction of AAG. Looking closely at the zoomed-out images, AAG generally resulted in a more uniform and overall finer particle size distribution than the reference, consistent with the findings from the Mastersizer particle analyzer.

Table 1
Effect of AAG on grinding performance and product (Ec expressed as work index).

Conditions	Ec (kWh/t)	D_{80} (μm)	Uniformity (–)	SSA (m^2/g)	Roughness (–)
Reference	19.41	207	2.056	0.4891	0.2389
300 g/t	17.28	187	1.848	0.5857	0.2861
500 g/t	16.69	184	1.797	0.6510	0.3180
1000 g/t	17.80	192	1.813	0.5628	0.2749

Table 2
Summary of the adsorption parameters of AAG on quartz and magnetite.

Mineral	Langmuir			Freundlich		
	Q_m	K_L	R^2	n	K_F	R^2
Quartz	3.45	0.718	0.9711	5.20	1.70	0.8851
Magnetite	3.19	0.315	0.9701	4.72	1.33	0.8365

3.3. Single mineral flotation

The flotation experiments were carried out on single minerals to study the effect of AAG in the ether-amine system (Lilaflot 822 M) for quartz and magnetite at pH 10 (Fig. 4a). The results demonstrated that by increasing the Lilaflot 822 M concentrate as a collector, both the quartz and magnetite recoveries increase, in addition to the absence or presence of AAG. Further analyses reveal that the addition of AAG increases the floatability of quartz and magnetite (Fig. 4a). The observed increase in the floatability of quartz in the presence of Lilaflot 822 M (an ether amine) corroborates with the literature findings showing amine's efficacy at pH 10 [48,49]. Quartz recovery reached a maximum of 90 % at 20 mg/L of the collector in the absence of AAG, while it would be 92 % at 10 mg/L of the collector in the presence of AAG. In other words, higher recoveries were achieved in the presence of AAG at a lower collector concentration. Similar behavior is observed for magnetite floatability, which at 20 mg/L collectors, its recovery increases from 15 to 80 % in the absence and presence of AAG, respectively. Generally, in both scenarios, the presence of AAG enhances the floatability of both quartz and magnetite.

In addition to the system, the effect of AAG on the floatability of quartz and magnetite in the presence of a depressant was investigated. Starch was utilized as a depressant to address the undesirable floatability of magnetite in the reverse flotation setup. The floatability was investigated at different starch concentrations at a fixed collector dosage of 20 mg/L and pH 10. As expected, a minimum effect was observed on quartz floatability with some decreases at concentrations above 80 mg/L (Fig. 4b). For the reference sample, starch was effective in depressing magnetite, giving the lowest floatability of 3 % at 50 mg/L starch concentration. In the presence of AAG, magnetite floatability was found to be quite high, with the lowest floatability of 2 % achieved only at 100 mg/L starch concentration. Evidently, the presence of AAG results in increased starch dosages. The single mineral flotation test showed that the application of AAG improved the collection of quartz and magnetite even at a lower collector dose. However, it was also observed that the addition of AAG increases the amount of depressant to counter the improved collection of magnetite. To gain a complete understanding of the behaviors observed in single mineral flotation, artificial mixtures were used in subsequent flotation tests.

3.4. Flotation of artificial mixture

Flotation tests on the artificial mixture were performed on the magnetite and quartz mixture with a mass ratio of 2:1 to determine the effect of improved quartz collection separation from magnetite. The flotation feed of the mixture had a Fe grade of 58.7 %. As shown in Fig. 5, the addition of AAG influences both recovery and grade. The result of the reference sample test shows that the recovery initially increases with increasing collector concentration to a maximum of 93.3 % at 200 g/t, after which it starts to decrease. Adding AAG improves recovery, especially at lower collector doses, supporting the findings from single-mineral flotation. At 500 g/t of AAG, a comparable maximum recovery of 92.1 % is achieved at a collector dose of 100 g/t. Adding AAG to all investigated collector concentrations, less than 200 g/t, results in higher recoveries than the reference sample. Fig. 5b agrees with the findings on the grades that increase with increasing collector and AAG concentrations. As in reverse flotation, the observed increase in

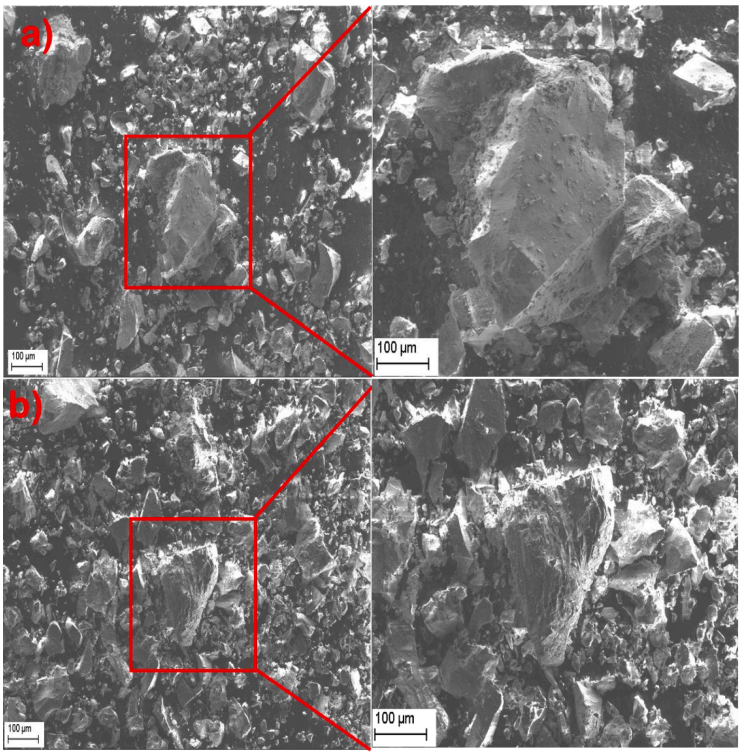

Fig. 3. SEM images showing the effect of AAG on the ground product (a) without AAG, (b) added 1000 g/t AAG.

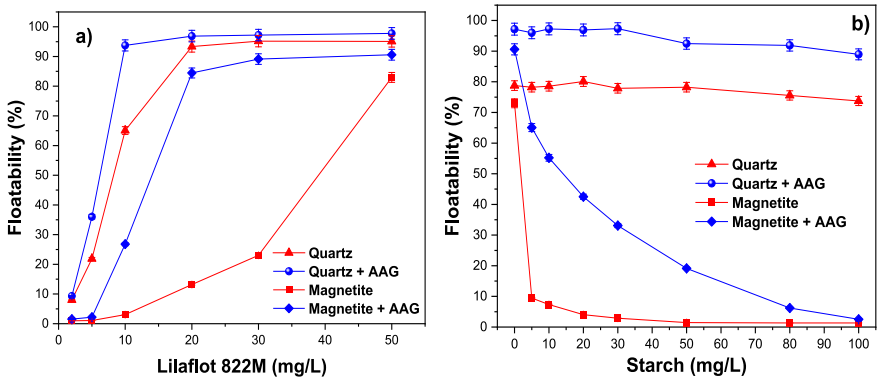

Fig. 4. Effect of AAG (100 mg/L) on magnetite and quartz single mineral flotation at pH 10 with varying (a) collector dosage and (b) depressant dosage (fixed collector – 20 mg/L).

grade is accompanied by a decrease in mass recovery, thus ultimately decreasing the metallurgical recovery.

Further evaluation of the selectivity of the process based on Eq. (4) is presented in Fig. 6. It can be observed that at lower collector dosages (below 300 g/t) the presence of AAG increases the process selectivity. However, it must be noted that above 300 g/t collector, the presence of AAG becomes detrimental to the process selectivity. For all scenarios, the best selectivity is reported between 200 and 300 g/t collector with a maximum of 76.2 % at 300 g/t AAG and 200 g/t collector. The results indicate that AAG enhances the collection of quartz and, to a lesser extent, the collection of magnetite. The selectivity variations at different AAG and collector dosages suggest synergistic interactions in the system. To better assess the observed effect of AAG on the separation of quartz from magnetite, surface analysis of the mineral surfaces was considered.

3.5. Zeta potential measurements

The effect of AAG on the colloidal stability of quartz and magnetite particles was carried out using zeta potentials from electrophoresis measurements. The change in zeta potential with varying AAG dosage at a fixed pH of 10 and 20 mg/L Lilaflot 822 M is presented in Fig. 7. For all conditions, it can be observed that the zeta potentials decreased (to a

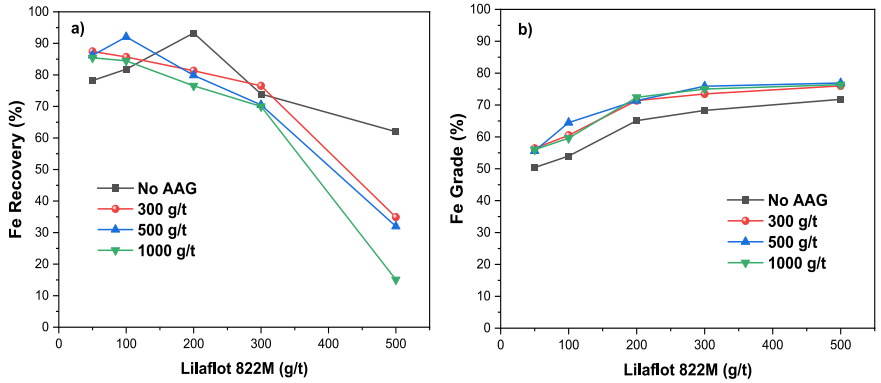

Fig. 5. Synergistic effect of AAG and collector on mixed mineral flotation (a) Fe recovery and (b) Fe grade.

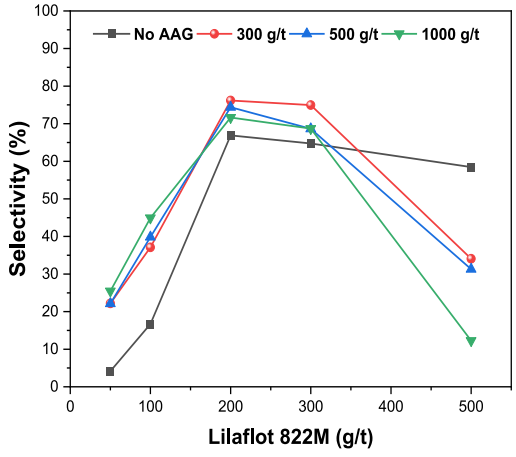

Fig. 6. Effect of AAG on selectivity with varying collector concentration.

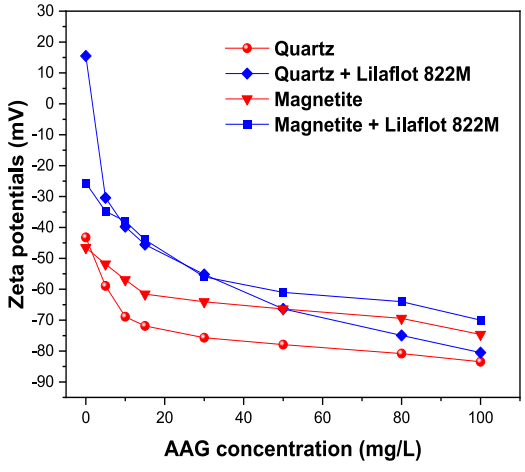

Fig. 7. Variation of zeta potentials at different concentrations of AAG at pH 10.

greater negative magnitude) when the AAG concentration was increased. For the reference test, quartz and magnetite have zeta potentials of −43.2 and −46.5 mV compared to −83.5 and −74.6 mV at 100 mg/L. The trend shows that the presence of AAG enhances the stability of the suspension regardless of the type of mineral. A similar shift in the zeta potentials is observed for both minerals as Lilaflot 822 M (a collector); however, the results show a more pronounced change for quartz, indicating increased adsorption of Lilaflot 822 M as a collector on its surface. From these observations, it could be considered that adding AAG results in an increased negative charge, especially on quartz, which could promote the interaction with the collector and improve its floatability.

3.6. Suspension stability measurements

To further understand the effect of AAG on mineral suspensions, stability studies were conducted based on the Turbiscan stability index. The variation in the Turbiscan stability index as a function of time with 100 mg/L AAG and pH 10 in quartz and magnetite suspensions is presented in Fig. 8. Similar behavior can be observed as the presence of AAG stabilizes the suspension (reduction in TSI), which corroborates the findings from the zeta potentials. The change is more pronounced for quartz than for magnetite surfaces. These findings corroborate the claim in the literature that PAA-derived polymers impart stability as a dispersant [50]. The observed decrease in stability also points to

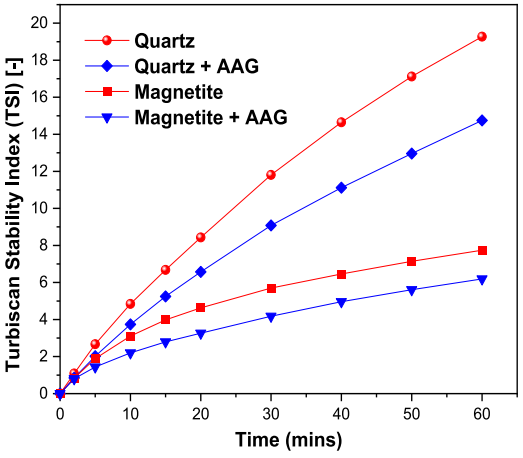

Fig. 8. Suspension stability of magnetite and quartz with and without AAG.

increased dispersibility with the introduction of AAG, which can also increase the quartz recovery.

3.7. Adsorption measurements

The flotation and suspension stability results showed a pronounced effect of AAG on quartz relative to magnetite. To better understand the phenomenon, adsorption measurements were performed on both mineral surfaces after treatment with varying concentrations of AAG at pH 10. Fig. 9 shows how the amount of AAG adsorbed per unit of mass increases with the AAG concentration. It is evident that quartz has a high adsorption capacity concerning magnetite in the investigated concentration. Furthermore, data fitting using the Langmuir and Freundlich models is summarized in Table 2. From the Langmuir model, the adsorption capacity (Q_m) is higher for quartz compared to magnetite, with 3.45 and 3.19, respectively. Similarly, the Freundlich model shows stronger adsorption (n) for quartz compared to magnetite, with 5.20 and 4.72, respectively. Langmuir has the best fit of the two models with an R^2 of 0.8851 compared to 0.8365 for the Freundlich model. These findings show that AAG adsorbs on both quartz and magnetite, supporting the observed effects on the flotation behavior. The superior adsorption of AAG on quartz compared to magnetite particles further explains its pronounced effect.

3.8. FTIR spectra analysis

The adsorption results showed that AAG has stronger adsorption on quartz surfaces than on magnetite surfaces. Fourier transform infrared (FTIR) spectra were performed to better understand the adsorption mechanism. Fig. 10 shows the spectra of bare and treated pure minerals of AAG, Lilaflot 822 M. For the collector (Lilaflot 822 M), characteristic peaks emerge at 2964 cm^{-1} and 2869 cm^{-1}, which are attributed to the CH_2 stretching bond of acyclic compounds [51]. Peaks at 1587, 1467, and 653 cm^{-1} can be attributed to the bending of the NH_2 or NH bonds [51–53]. A characteristic peak is observed at 1548 cm^{-1} and 1168 cm^{-1} for AAG, possibly due to the deprotonated C═O and C—O bond, respectively, since this was at pH 10 [54]. Fig. 10a shows that the surface of the introduction of AAG on the quartz mineral has no effect, and no new functional group is generated. The presence of Lilaflot 822 M is evident, with a characteristic peak showing. The characteristic OH peak at 2964 cm^{-1} changes to 2960 cm^{-1} as observed in quartz + AAG + Lilaflot 822 M, typical for an amine system [51]. A similar effect is observed for magnetite + AAG + Lilaflot 822 M with a characteristic peak from the introduction of the collector Fig. 10b. The CH peak at 2869 cm^{-1} also shifts to 2856 cm^{-1} and 2920 cm^{-1} for quartz and magnetite, respectively, after treatment. The spectra suggest a weaker Lilaflot 822 M-magnetite interaction than the Lilaflot 822 M-quartz interaction. The absence of a characteristic peak after treatment with AAG in both minerals implies that the interaction between AAG and the minerals is not chemical and thus physical adsorption.

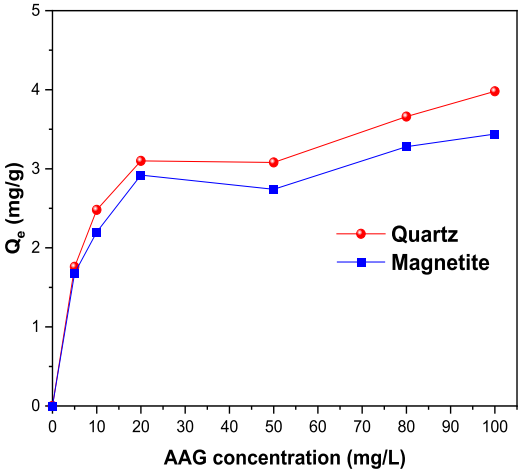

Fig. 9. Adsorption of AAG on quartz and magnetite at varying initial concentrations at pH 10.

Some interactions are evident from the observed behavior when AAG is added to both quartz and magnetite. The introduction of AAG markedly enhances the floatability of quartz with a minimal effect on magnetite. Mixed mineral flotation showed that at 500 g/t of AAG, a comparable maximum recovery of 92.1 % is achieved at a collector dose of 100 g/t. Surface analyses revealed that AAG adsorbs on mineral surfaces, increases the zeta potential (more negative), and increases the suspension stability. This is consistent with observations reported elsewhere suggesting that AAG increases dispersion and anionicity due to its anionic nature, thus increasing collector adsorption and ultimately improving flotation [32,54].

4. Conclusions

In this paper, the effect of AAG, a polyacrylic-based grinding aid, on the grinding and flotation separation behavior of a magnetite-quartz mixture was investigated. The grinding results illustrated that AAG improved the grinding efficacy at an optimum dosage and improved the product properties. The experimental results showed that the energy consumption decreased by 18 %, the specific surface area increased by 6 %, and the uniformity improved relative to the test without AAG (reference test). Further results from a single mineral flotation indicated that AAG could enhance the quartz collection, thus improving its floatability. The results of artificial mixture flotation revealed that under specific conditions of 500 g/t AAG, pH 10, 1000 g/t starch Fe recovery of 92.1 % and 64.5 % could be achieved with 100 g/t Lilaflot 822 M compared to the reference with a recovery of 93.0 % and 65.1 % grade at 200 g/t Lilaflot 822 M. The zeta potential measurement results showed a large negative shift for both quartz and magnetite; the former was more pronounced in the presence of AAG. The suspension stability results revealed that AAG results in a more stable suspension with improved dispersion compared to the reference test. The adsorption results showed superior adsorption of AAG on the quartz surface compared to magnetite. FTIR results illustrated that the adsorption mechanism of AAG on both quartz and magnetite was physical adsorption. In general, these results have addressed the long-standing question of the effect of polyacrylic-based grinding aids on the resulting products and subsequent flotation separation processes. The presence of AAG not only improved grinding efficiency but also could potentially decrease the amount of collector required to achieve comparable metallurgical performance. This paves the way for future research on the application of grinding aids in mineral processing with an approach to having grinding aids with a secondary beneficial function in view of downstream processes.

CRediT authorship contribution statement

Vitalis Chipakwe: Conceptualization, Data curation, Formal analysis, Investigation, Methodology, Visualization, Writing - original draft, Writing - review & editing. **Tommy Karlkvist:** Data curation, Supervision, Validation, Writing - review & editing. **Jan Rosenkranz:** Resources, Data curation, Supervision, Validation, Writing - review & editing. **Saeed Chehreh Chelgani:** Conceptualization, Formal analysis, Resources, Data curation, Supervision, Funding acquisition, Methodology, Visualization, Writing - original draft, Writing - review & editing.

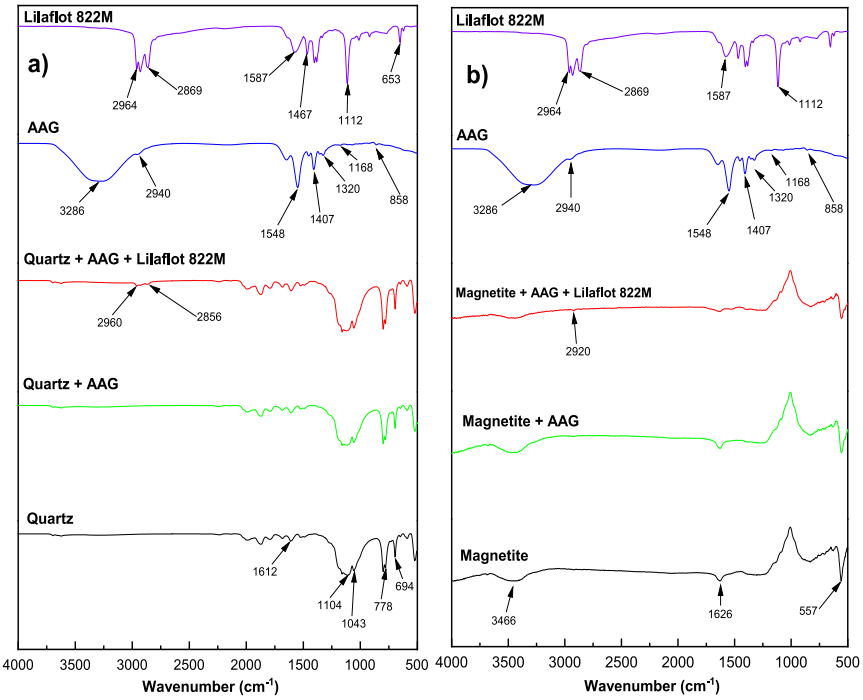

Fig. 10. FTIR spectra of AAG, Lilaflot 822 M, and bare minerals before and after treatment.

Declaration of Competing Interest

The authors declare that they have no known competing financial interests or personal relationships that could have appeared to influence the work reported in this paper.

Data availability

Data will be made available on request.

Acknowledgements

This manuscript resulted from a project financially supported by CAMM^2, the Center of Advanced Mining and Metallurgy, as a center of excellence at the Luleå University of Technology, and Vinnova for the RIO-MUN (Reverse flotation of iron oxide using magnetic, ultrasonic, nanobubble technology), project number: 2020-04835. The authors also thank Nouryon (Sweden) and Solenis for their help with the reagents used in this study.

References

[1] J. Jeswiet, A. Szekeres, Energy consumption in mining comminution, Proc. CIRP. 48 (2016) 140–145, https://doi.org/10.1016/j.procir.2016.03.250.
[2] T. Napier-Munn, Is progress in energy-efficient comminution doomed? Miner. Eng. 73 (2015) 1–6, https://doi.org/10.1016/j.mineng.2014.06.009.
[3] M. He, Y. Wang, E. Forssberg, Slurry rheology in wet ultrafine grinding of industrial minerals: a review, Powder Technol. 147 (2004) 94–112, https://doi.org/10.1016/j.powtec.2004.09.032.
[4] F. Cheng, Y. Feng, Q. Su, D. Wei, B. Wang, Y. Huang, Practical strategy to produce ultrafine ceramic glaze: introducing a polycarboxylate grinding aid to the grinding process, Adv. Powder Technol. 30 (2019) 1655–1663, https://doi.org/10.1016/j.apt.2019.05.014.
[5] V. Chipakwe, P. Semsari, T. Karlkvist, J. Rosenkranz, S.C. Chelgani, A critical review on the mechanisms of chemical additives used in grinding and their effects on the downstream processes, J. Mater. Res. Technol. 9 (2020) 8148–8162, https://doi.org/10.1016/j.jmrt.2020.05.080.
[6] P. Prziwara, A. Kwade, Grinding aids for dry fine grinding processes – Part I: Mechanism of action and lab-scale grinding, Powder Technol. 375 (2020) 146–160, https://doi.org/10.1016/j.powtec.2020.07.038.
[7] V. Chipakwe, T. Karlkvist, J. Rosenkranz, S.C. Chelgani, Beneficial effects of a polysaccharide-based grinding aid on magnetite flotation: a green approach, Sci. Rep. 12 (2022) 1–13, https://doi.org/10.1038/s41598-022-10304-x.
[8] V. Chipakwe, P. Semsari, T. Karlkvist, J. Rosenkranz, S.C. Chelgani, A comparative study on the e ff ect of chemical additives on dry grinding of magnetite ore, South African, J Chem. Eng. 34 (2020) 135–141, https://doi.org/10.1016/j.sajce.2020.07.011.
[9] K. Ohenoja, S. Breitung-Faes, P. Kinnunen, M. Illikainen, J. Saari, A. Kwade, J. Niinimäki, Ultrafine grinding of limestone with sodium polyacrylates as additives in ordinary portland cement mortar, Chem. Eng. Technol. 37 (2014) 787–794, https://doi.org/10.1002/ceat.201300707.
[10] P. Prziwara, S. Breitung-Faes, A. Kwade, Impact of grinding aids on dry grinding performance, bulk properties and surface energy, Adv. Powder Technol. 29 (2018) 416–425, https://doi.org/10.1016/j.apt.2017.11.029.
[11] S. Chelgani, M. Parian, P.S. Parapari, Y. Ghorbani, J. Rosenkranz, A comparative study on the effects of dry and wet grinding on mineral flotation separation–a review, J. Mater. Res. Technol. (2019) 1–8, https://doi.org/10.1016/j.jmrt.2019.07.053.
[12] P. Bulejko, N. Šuleková, J. Vlasák, R. Tuunila, T. Kinnarinen, T. Svěrák, A. Häkkinen, Ultrafine wet grinding of corundum in the presence of triethanolamine, Powder Technol. 395 (2022) 556–561, https://doi.org/10.1016/j.powtec.2021.09.079.
[13] S. Grano, The critical importance of the grinding environment on fine particle recovery in flotation, Miner. Eng. 22 (2009) 386–394, https://doi.org/10.1016/j.mineng.2008.10.008.
[14] Z. Tong, L. Liu, Z. Yuan, J. Liu, J. Lu, L. Li, The effect of comminution on surface roughness and wettability of graphite particles and their relation with flotation, Miner. Eng. 169 (2021) 106959, https://doi.org/10.1016/j.mineng.2021.106959.
[15] W.J. Bruckard, G.J. Sparrow, J.T. Woodcock, A review of the effects of the grinding environment on the flotation of copper sulphides, Int. J. Miner. Process. 100 (2011) 1–13, https://doi.org/10.1016/j.minpro.2011.04.001.
[16] O. Ersoy, D. Güler, M. Rençberoğlu, Effects of grinding aids used in grinding calcium carbonate (CACO3) filler on the properties of water-based interior paints, Coatings 12 (2022), https://doi.org/10.3390/coatings12010044.
[17] Y. Liu, G. Huang, Z. Pan, Y. Wang, G. Li, Synthesis of sodium polyacrylate copolymers as water-based dispersants for wet ultrafine grinding of cobalt aluminate particles, Colloids Surf. A Physicochem. Eng. Asp. 610 (2021) 125553, https://doi.org/10.1016/j.colsurfa.2020.125553.
[18] B. Yang, J. Liu, L. Wang, G. Ai, S. Ren, Enhanced collection of chalcopyrite by styrene-butyl acrylate polymer nanospheres in the presence of serpentine, Colloids

Surf. A Physicochem. Eng. Asp. 640 (2022) 128408, https://doi.org/10.1016/j.colsurfa.2022.128408.
[19] E. Kapeluszna, Ł. Kotwica, The effect of various grinding aids on the properties of cement and its compatibility with acrylate-based superplasticizer, Materials (Basel). 15 (2022), https://doi.org/10.3390/ma15020614.
[20] M. Lapointe, B. Barbeau, Understanding the roles and characterizing the intrinsic properties of synthetic vs. natural polymers to improve clarification through interparticle Bridging: a review, Sep. Purif. Technol. 231 (2020) 115893, https://doi.org/10.1016/j.seppur.2019.115893.
[21] C. Zhang, Y. Hu, W. Sun, J. Zhai, Z. Yin, Q. Guan, The effect of polyacrylic acid on the surface properties of calcite and fluorite aiming at their selective flotation, Physicochem. Probl. Miner. Process. 54 (2017) 868–877, https://doi.org/10.5277/ppmp1888.
[22] M. Ataie, K. Sutherland, L. Pakzad, P. Fatehi, Experimental and modeling analysis of lignin derived polymer in flocculating aluminium oxide particles, Sep. Purif. Technol. 247 (2020) 116944, https://doi.org/10.1016/j.seppur.2020.116944.
[23] M. He, Y. Wang, E. Forssberg, Parameter studies on the rheology of limestone slurries, Int. J. Miner. Process. 78 (2006) 63–77, https://doi.org/10.1016/j.minpro.2005.07.006.
[24] G.R. Quezada, E. Piceros, P. Robles, C. Moraga, E. Gálvez, S. Nieto, R.I. Jeldres, Polyacrylic acid to improve flotation tailings management: Understanding the chemical interactions through molecular dynamics, Metals (Basel). 11 (2021), https://doi.org/10.3390/met11060987.
[25] Z. Chen, Y. Wang, L. Luo, T. Peng, F. Guo, M. Zheng, Enhancing flotation separation of chalcopyrite and magnesium silicate minerals by surface synergism between PAAS and GA, Sci. Rep. 11 (2021) 1–16, https://doi.org/10.1038/s41598-021-85984-y.
[26] S. Zhang, Z. Huang, H. Wang, R. Liu, C. Cheng, S. Shuai, Y. Hu, Z. Guo, X. Yu, G. He, W. Fu, Flotation performance of a novel Gemini collector for kaolinite at low temperature, Int. J. Min. Sci. Technol. 31 (2021) 1145–1152, https://doi.org/10.1016/j.ijmst.2021.09.001.
[27] S. Shuai, Z. Huang, V.E. Burov, V.Z. Poilov, F. Li, H. Wang, R. Liu, S. Zhang, C. Cheng, W. Li, X. Yu, G. He, W. Fu, Selective separation of wolframite from calcite by froth flotation using a novel amidoxime surfactant: adsorption mechanism and DFT calculation, Miner. Eng. 185 (2022) 107716, https://doi.org/10.1016/j.mineng.2022.107716.
[28] Z. Huang, S. Shuai, V.E. Burov, V.Z. Poilov, F. Li, H. Wang, R. Liu, S. Zhang, C. Cheng, W. Li, X. Yu, G. He, W. Fu, Application of a new amidoxime surfactant in flotation separation of scheelite and calcite: adsorption mechanism and DFT calculation, J. Mol. Liq. 364 (2022) 120036, https://doi.org/10.1016/j.molliq.2022.120036.
[29] D. Mesa, P.R. Brito-Parada, Scale-up in froth flotation: a state-of-the-art review, Sep. Purif. Technol. 210 (2019) 950–962, https://doi.org/10.1016/j.seppur.2018.08.076.
[30] K. Sun, C.V. Nguyen, N.N. Nguyen, A.V. Nguyen, Flotation surface chemistry of water-soluble salt minerals : from experimental results to new perspectives, Adv. Colloid Interface Sci. 309 (2022) 102775, https://doi.org/10.1016/j.cis.2022.102775.
[31] L. Xie, J. Wang, Q. Lu, W. Hu, D. Yang, C. Qiao, X. Peng, Q. Peng, T. Wang, W. Sun, Q. Liu, H. Zhang, H. Zeng, Surface interaction mechanisms in mineral flotation: fundamentals, measurements, and perspectives, Adv. Colloid Interface Sci. 295 (2021) 102491, https://doi.org/10.1016/j.cis.2021.102491.
[32] P. Somasundaran, L.T. Lee, Polymer-surfactant interactions in flotation of quartz, Sep. Sci. Technol. 16 (1981) 1475–1490, https://doi.org/10.1080/01496398108058312.
[33] M. Hennemann, M. Gastl, T. Becker, Influence of particle size uniformity on the filter cake resistance of physically and chemically modified fine particles, Sep. Purif. Technol. 272 (2021) 118966, https://doi.org/10.1016/j.seppur.2021.118966.
[34] H. Choi, J. Lee, H. Hong, J. Gu, J. Lee, H. Yoon, J. Choi, Y. Jeong, J. Song, M. Kim, B. Ochirkhuyag, New evaluation method for the kinetic analysis of the grinding rate constant via the uniformity of particle size distribution during a grinding process, Powder Technol. 247 (2013) 44–46, https://doi.org/10.1016/j.powtec.2013.06.031.
[35] F.C. Bond, Crushing and grinding calculations, Br. Chem. Eng. 378–385 (1961).
[36] M.J. Jaycock, G.D. Parfitt, The study of liquid interfaces, Chem. Interfaces. (1981) 38–132.
[37] M. Fan, D. Tao, R. Honaker, Z. Luo, Nanobubble generation and its applications in froth flotation (part II): fundamental study and theoretical analysis, Min. Sci. Technol. 20 (2010) 159–177, https://doi.org/10.1016/S1674-5264(09)60179-4.
[38] V. Chipakwe, R. Jolsterå, S.C. Chelgani, Nanobubble-assisted flotation of apatite tailings: insights on beneficiation options, ACS Omega. (2021), https://doi.org/10.1021/acsomega.1c01551.
[39] A. Bastrzyk, J. Feder-Kubis, Pyrrolidinium and morpholinium ionic liquids as a novel effective destabilising agent of mineral suspension, Colloids Surf. A Physicochem. Eng. Asp. 557 (2018) 58–65, https://doi.org/10.1016/j.colsurfa.2018.05.002.
[40] C. Zhang, S. Wei, Y. Hu, H. Tang, J. Gao, Z. Yin, Q. Guan, Selective adsorption of tannic acid on calcite and implications for separation of fluorite minerals, J. Colloid Interface Sci. 512 (2018) 55–63, https://doi.org/10.1016/j.jcis.2017.10.043.
[41] S. Cayirli, Analysis of grinding aid performance effects on dry fine milling of calcite, Adv. Powder Technol. 33 (2022) 103446, https://doi.org/10.1016/j.apt.2022.103446.
[42] N.A. Toprak, O. Altun, A.H. Benzer, The effects of grinding aids on modelling of air classification of cement, Constr. Build. Mater. 160 (2018) 564–573, https://doi.org/10.1016/j.conbuildmat.2017.11.088.
[43] H.S. Gokcen, S. Cayirli, Y. Ucbas, K. Kayaci, The effect of grinding aids on dry micro fine grinding of feldspar, Int. J. Miner. Process. 136 (2015) 42–44, https://doi.org/10.1016/j.minpro.2014.10.001.
[44] D.W. Fuerstenau, Grinding Aids, KONA Powder Part. J. 13 (0) (1995) 5–18.
[45] V. Chipakwe, C. Hulme-Smith, T. Karlkvist, J. Rosenkranz, S.C. Chelgani, Effects of chemical additives on rheological properties of dry ground ore – a comparative study, Miner. Process. Extr. Metall. Rev. 00 (2021) 1–10, https://doi.org/10.1080/08827508.2021.1890591.
[46] M.M. Ahmed, Effect of comminution on particle shape and surface roughness and their relation to flotation process, Int. J. Miner. Process. 94 (2010) 180–191, https://doi.org/10.1016/j.minpro.2010.02.007.
[47] P. Semsari Parapari, M. Parian, J. Rosenkranz, Breakage process of mineral processing comminution machines – an approach to liberation, Adv. Powder Technol. 31 (2020) 3669–3685, https://doi.org/10.1016/j.apt.2020.08.005.
[48] A. Tohry, R. Dehghan, H. Mohammadi-Manesh, L. de S.L. Filho, S.C. Chelgani, Effect of ether mono amine collector on the cationic flotation of micaceous minerals—a comparative study, Sustain. 13 (2021) 1–13. doi:10.3390/su131911066.
[49] A.M. Vieira, A.E.C. Peres, The effect of amine type, pH, and size range in the flotation of quartz, Miner. Eng. 20 (2007) 1008–1013, https://doi.org/10.1016/j.mineng.2007.03.013.
[50] L. Wu, Y. Huang, Z. Wang, L. Liu, Interaction and dispersion stability of alumina suspension with PAA in N, N′-dimethylformamide, J. Eur. Ceram. Soc. 30 (2010) 1327–1333, https://doi.org/10.1016/j.jeurceramsoc.2009.12.010.
[51] X. Liu, J. Xie, G. Huang, C. Li, Low-temperature performance of cationic collector undecyl propyl ether amine for ilmenite flotation, Miner. Eng. 114 (2017) 50–56, https://doi.org/10.1016/j.mineng.2017.09.005.
[52] Z. Huang, H. Zhong, S. Wang, L. Xia, W. Zou, G. Liu, Investigations on reverse cationic flotation of iron ore by using a Gemini surfactant: Ethane-1,2-bis (dimethyl-dodecyl-ammonium bromide), Chem. Eng. J. 257 (2014) 218–228, https://doi.org/10.1016/j.cej.2014.07.057.
[53] W. Liu, W. Liu, X. Wang, D. Wei, B. Wang, Utilization of novel surfactant N-dodecyl-isopropanolamine as collector for efficient separation of quartz from hematite, Sep. Purif. Technol. 162 (2016) 188–194, https://doi.org/10.1016/j.seppur.2016.02.033.
[54] M. Zhu, Q. Zhang, X. Xiao, B. Shi, A novel strategy for enhancing comprehensive properties of polyacrylate coating: incorporation of highly dispersed zinc ions by using polyacrylic acid as carrier, Prog. Org. Coatings. 162 (2022) 106596, https://doi.org/10.1016/j.porgcoat.2021.106596.

Department of Civil, Environmental, and Natural Resources Engineering
Division of Minerals and Metallurgical Engineering

ISSN 1402-1544
ISBN 978-91-8048-217-2
ISBN 978-91-8048-218-9

Print: Lenanders Grafiska, 458273

LULEÅ
UNIVERSITY
OF TECHNOLOGY